University of Alberta

Heat and mass transfer in passively aerated compost

by

Shouhai Yu

A thesis submitted to the Faculty of Graduate Studies and Research
in partial fulfillment of the requirements for the degree of

Doctor of Philosophy

in

Bioresource and Food Engineering

Department of Agricultural, Food and Nutritional Science

Edmonton, Alberta
Spring 2007

Your file Votre référence
ISBN: 978-0-494-29775-9
Our file Notre référence
ISBN: 978-0-494-29775-9

Abstract

This work is the study of mathematical modeling of heat and mass transfer in passively aerated compost. Composting was studied in enclosed, passively aerated, cylindrical vessels. A smoke tracer flow meter was devised to measure airflow though the passively aerated compost. The total estimated pressure loss across the smoke tracer flow meter was 0.10 Pa, which had negligible influence on airflow measurement, and the responses of the flow meters were very linear in the calibration range ($R^2 = 0.98$). Compared with other flow meters used in similar experiments, the smoke tracer flow meter had the advantages of very low pressure loss, low cost, and robust performance under humid conditions.

An analytical model for the prediction of airflow rate in passively aerated compost was developed based on Darcy's law. The model related the physical characteristics (permeability) and temperature of the compost with the predicted air flow, and the compaction which occurs during composting was also taken into account in the application of the model. The calculated airflow values were not significantly different from the measured values ($p = 0.97$).

A novel mathematical model was proposed for the statistical comparison of temperature histories from composting trials, based on a modified Gompertz function that includes nonlinear, time-correlated effects. Methods were developed for the estimation of initial values for the model parameters. The model and methods were shown to be useful tools for the statistical comparison of time series temperature data in composting.

Microbial growth and the accompanying rate of substrate consumption were modeled using modified first-order kinetics. Microbial kinetic rate constants were found to follow a sigmoid relationship with free air space (FAS), with correlation coefficients (R^2) of 0.97 for the mesophilic stage and 0.96 for the thermophilic stage. Temperature histories and airflow measurements from an independent trial using compost with FAS of 0.57 were used to assess the model's performance. Simulation results indicate that the model could predict the general trend of temperature development. A plot of the residuals shows that the model is biased, however, possibly because many parameters in the model were not measured directly but instead were estimated from literature.

Acknowledgement

This thesis is a result of collective efforts.

I would like to thank my supervisor Dr. Jerry Leonard. His integral view on research, his deep insight into the problem, and his inspiring and thoughtful guidance and supervision, have made a deep impression on me. He could not even realize how much I have learned from him. I am really glad that I have come to get know Jerry in my life.

I would like to thank Dr. Grant Clark who kept an eye on the progress of my work and always was available when I needed his advises. The strict and extensive comments and discussions with Grant had a direct impact on the final form and quality of this thesis.

I would also like to thank other members of my PhD committee who monitored my work and took effort in reading and providing me with valuable comments on my work: Dr. John Feddes, Dr. Daryl McCartney. I thank you all.

I thank Dr. Peter Blenis, Department of Renewable Resources, for his help and insight with the statistical methods. I thank D. Martineau and Inka Ruotsalainen for help with the calibration of devised airflow meter, and Chris Ouellette for help with the electronics for my experiment.

This research has been supported and funded by Natural Sciences and Engineering Research Council of Canada and the Department of Agricultural, Food and Nutritional Science of the University of Alberta.

Especially, I would like to thank my family whose consistent support makes it possible for me to complete this work.

Table of contents

List of Tables

List of Figures

List of Symbols

[C]	Carbon concentration used in Monod expression, dry matter basis (kg kg_{dm}^{-1})
$[O_2]$	Oxygen concentration in air (kg_{O2} m^{-3})
$[O_2]_s$	Oxygen concentration (dissolved) in substrate (kg_{O2} kg_{dm}^{-1})
ΔP_d	Pressure loss due to change in pipe diameter (Pa)
ΔP_f	Pressure loss due to friction (Pa)
a	Maximum growth rate
A_i	Cross-sectional area of the unit air in the i^{th} layer of compost (m^2)
b	Maximum rate of increase
C	Carbon content in substrate, dry matter basis (kg kg_{dm}^{-1})
c_{nvs}	Specific heat of non-volatile solids (NVS) in the substrate (kJ (kg °C)$^{-1}$)
c_{vs}	Specific heat of volatile solids (VS) in the substrate (kJ (kg °C)$^{-1}$)
c_w	Specific heat of water (kJ (kg °C)$^{-1}$)
D	Diameter of pipe (m)
d	Indicator variable (0 or 1)
d_i	Depth in compost (m)
F	Mass flow rate of dry air (kg_{da} h^{-1}).
f	Friction factor (dimensionless)
FAS	Actual Free Air Space (0~1)
FAS_0	Measured initial Free Air Space (0~1)
f_C	Empirical conversion factor based on carbon content change
F_i	Net force on the air in the i^{th} layer (N)
g	Unit of acceleration due to earth's gravity (9.8m s^{-2})
h	Specific enthalpy of moist air (kJ kg_{da}^{-1})
h_∞	Maximum compressed state
h_i	Fraction of the initial thickness of i^{th} layer due to compaction effect
H_i	Height of the unit air in i^{th} layer of compost with cross-sectional area A_i (m)
i	Index number of the compost layer (dimensionless)
K	Permeability of the compost (m^2)
k^0_c	Initial estimate for the maximum cooling coefficient k_c

k^0_{hm}	Initial estimate for maximum heating coefficient k_{hm}
k^0_{ht}	Initial estimate for maximum heating coefficient k_{ht}
k_c	Maximum cooling coefficient
K_C	Half saturation constant of carbon ($kg_C\ kg_{dm}^{-1}$)
k_d	First-order rate constant for conversion of substrate dry matter to biomass (h^{-1})
k_{hm}	Maximum mesophilic heating coefficient
k_{ht}	Maximum thermophilic heating coefficient
K_L	Contraction-loss coefficient (dimensionless)
k_{max}	Maximum substrate degradation rate (h^{-1})
K_{O2}	Half saturation constant of O_2 content ($kg_{O2}\ kg_{dm}^{-1}$)
k_{temp}	Temperature correctionl coefficient for microbial growth
k_w	Moisture correction coefficient for microbial growth
L	Length of pipe between infra-red transducers (m)
m_{nvs}	Mass of non-volatile solid (kg)
MSE_c	Mean residual sum of squares for the simple model
MSE_i	Mean residual sum of squares for the complex model
m_{vs}	Mass of volatile solid (kg)
m_w	Mass of water (kg)
n	Specific volume ($m^3\ kg^{-1}$ dry air)
n	Number of observations.
n_{as}	Difference between specific volume of moist air at saturation and that of dry air ($m^3\ kg^{-1}$ dry air)
n_{da}	Specific volume of dry air ($m^3\ kg^{-1}$ dry air)
Q	Heat content of compost (kJ)
Q_{gen}	Bio-reaction heat production (kJ)
Q_{in}	Heat flow via intake air (kJ)
Q_{Latent}	Latent heat (kJ)
Q_{out}	Heat flow via exhaust air (kJ)
R	Gas constant ($8.315\ J\ K^{-1}\ mol^{-1}$)
S	Amount of substrate dry matter (kg_{dm})
T	Temperature (°C).
t	Time (s or h)

T_0	Temperature of ambient air (K)
T^0_c	Initial estimate for the cooling potential T_c
t^0_c	Initial estimate for the time of cooling inflection t_c
T^0_{hm}	Initial estimate for the heating potential T_{hm}
t^0_{hm}	Initial estimate for the time of heat inflection t_{hm}
T^0_{ht}	Initial estimate for the heating potential T_{ht}
t^0_{ht}	Initial estimate for the time of heat inflection t_{ht}
T_a	Ambient temperature
T_c	Cooling potential
t_c	Time when maximum cooling rate occurs
T_{hm}	Heating potential of the mesophilic stage
t_{hm}	Time when maximum mesophilic heating rate occurs
T_{ht}	Heating potential of the thermophilic stage
t_{ht}	Time when maximum thermophilic heating rate occurs
T_i	Temperature of the air in the i^{th} layer of compost (K)
t_m	Time of inflection
v	Average air velocity (m s^{-1})
V_a	Volumetric airflow rate (m^3 s^{-1})
V_i	Volume of air in the i^{th} layer of compost (m^3)
v_s	Speed of sound in air (m s^{-1})
w	Humidity ratio of air (0 to1)
W_s	Humidity ratio at saturation. Dimensionless ratio of the mass of water vapor to the mass of dry air in a cubic meter of air
X	Substrate biomass concentration (kg kg_{dm}^{-1})
$Y_{H/C}$	Heat yield from consumed substrate carbon (kJ kg_C^{-1})
$Y_{O2/S}$	Oxygen consumed during oxidization of substrate dry mass (kg_{O2} kg_S^{-1})
$Y_{W/S}$	Water yield from oxidation of substrate dry mass (kg_{H2O} kg_S^{-1})
$Y_{X/C}$	Biomass yield from consumption of substrate carbon (kg kg_C^{-1})
α	Flow regime correction factor (dimensionless)
β	Rate of volume reduction
Δh_0	Total compressible fraction
$\Delta P/\Delta y$	Pressure gradient through the compost (Pa m^{-1})

Δt	Time difference between signal drops at two infra-red transducers or times-of-flight between ultrasonic transceivers (s)
Δx	Direct distance between ultrasonic transceivers (m)
η	Fluid dynamic viscosity of the air ($m^2\ s^{-1}$)
θ	Relative angle between the ultrasonic beam and the mean direction of airflow
μ	Degree of saturation (dimensionless ratio, unity at saturation)
ν_c	Number of unknown parameters in the simple model
ν_i	Number of unknown parameters in the complex model
ρ	Density of fluid ($kg\ m^{-3}$)
ρ_0	Density of ambient air ($kg\ m^{-3}$)
ρ_i	Density of the air in the i^{th} layer ($kg\ m^{-3}$)
ρ_s	Initial bulk density of substrate ($kg\ m^{-3}$)
σ_i	Compressive stress at the i^{th} layer (kPa)
φ	Relative humidity (%)

Chapter 1 Introduction

1.1 Concept and evolution of composting techniques

Composting is generally defined as the biological decomposition of organic matter under controlled conditions (Haug, 1993; Epstein, 1997). It is a common technology believed to have been used since ancient times to recycle farm residuals, such as poultry manure and straw (Rynk, 1992). A "traditional" method of composting, which is still in use in the urban areas of the developing world, involves simply stacking the material in piles or pits to decompose over a long period, with little agitation and management (FAO, 2006). Anaerobic decomposition takes place under such conditions, since aerobic conditions cannot be maintained without turning or aeration, and this often results in the generation of offensive odors.

To improve efficiency and reduce odor generation, "rapid" composting methods have been developed to keep the process aerobic. "Aerobic" is generally taken to mean that oxygen concentration is maintained at >5% (Haug, 1993). The microorganisms that thrive under aerobic conditions and, in particular, aerobic thermophilic bacteria are the most efficient decomposers. Aerobic microbes grow faster than anaerobic ones and generate more heat as they digest organic matter, which is important in neutralizing many pathogens that might otherwise persist in compost. As a result, aerobic composting is usually adopted for organic material recycling in modern waste management. Hereafter in this study, "composting" is used to refer to aerobic composting.

Composting has found applications in many fields including municipal and agricultural waste management and bioremediation of environmental pollution. Research has indicated that the composting process and the use of mature compost also provides an inexpensive and technologically straightforward solution for managing hazardous industrial waste streams and for remedying soil contaminated with toxic organic compounds (e.g., solvents and pesticides) and inorganic compounds (e.g., toxic metals) (Civilini et al., 1996; Diaz et al., 1996; Miller and Clark, 1998). The addition of mature compost to contaminated soil accelerates microbial degradation of organic contaminants (Hupe et al., 1996), improves plant growth (Hoitink et al., 1996), and promotes plant establishment in toxic soils (EPA, 1997).

1.2 Current understanding of the composting process

Composting is a microbial process. The microorganisms needed for composting are normal flora of the natural environment. They are present in compost feedstock as well as in the water, air, and soil. The high diversity of microorganisms normally present makes it possible to maintain an active microbial population during the dynamic chemical and physical processes of composting, such as shifts in pH, temperature, water, organic matter, and nutrient availability.

Since heat is given off as a by-product of the microbial breakdown of organic material, the temperature of the substrate is a good indicator of microbial activity in the composting system and can be used to assess the progress of the decomposition. As a rule of thumb, a well-constructed aerobic composting system will heat up to

above 40°C within two to three days. A typical temperature curve for an unturned pile is shown in Figure 1.

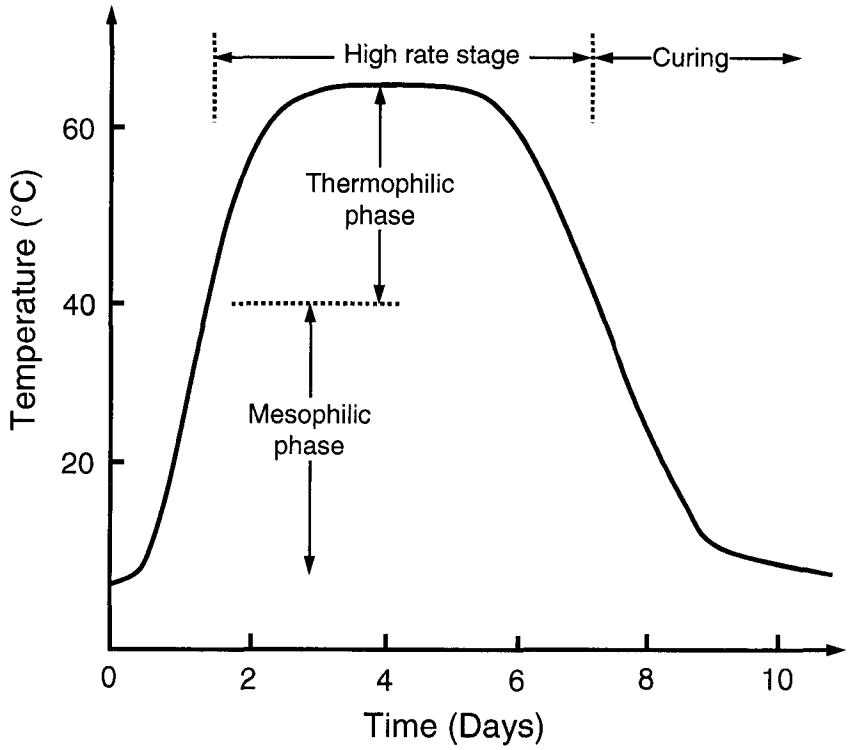

Figure 1-1 Schematic of typical temperature vs. time curve

Temperature plays a dual role in composting process. On one hand, it is the result (and therefore an indicator) of microbial activity. On the other hand, it is a selective agent in determining the microbial population present at any given stage of the composting process. At the start of composting, when the feedstock is mixed, the temperature of the substrate is usually close to that of ambient. The readily available organic substances in the feedstock, such as sugars, proteins, and fats, are rapidly consumed by the fastest growing mesophilic microorganisms. The heat released by the microbial activity begins to raise the temperature within the pile. When the temperature of the compost pile goes above 40°C, thermophiles (40-65°C) begin to

dominate and the composting proceeds to the second phase. Cellulose and other less biodegradable substances are broken down. Humic substances accumulate as decomposition proceeds. The thermophilic population continues generating more heat during decomposition of the remaining organic matter. The higher temperatures ensure rapid organic matter processing while simultaneously providing optimal conditions for the destruction of human and plant pathogens, as well as weed seeds. Temperature can remain high for days or weeks depending on the characteristics of the substrate and turning of the substrate is usually used to help keep the aerobic condition (Haug, 1993, p282).

When easily degradable organic material in the substrate is depleted, microbial activities are reduced. As a result, less heat is generated and the temperature of the composting pile declines gradually. The composting process comes to the curing phase in which the compost gradually comes to mature. The duration of the curing process varies from weeks to months. Although a plant growth bioassay is thought to be the best way to determine the maturity of the compost (Wang et al., 2004), a respiratory test (Gomez et al., 2006) can also be employed.

1.3 Microbial community dynamics during composting

During the first phase, mesophilic bacteria and fungi predominate. Most of these organisms can also be found in topsoil. The heat released by the microbial activity begins to raise the temperature within the pile. As the temperature of the compost pile reaches the 40°C thermophilic threshold, the activities of the mesophilic organisms cease, then vegetative cells and hyphae die and eventually lyse, until only heat resistant spores survive.

During the second phase, the thermophiles, comprising a number of bacterial species, actinomycetes, and fungi, begin to dominate the microbial community. The optimum temperature for these microorganisms is between 50 and 65 °C, and their activities terminate at 70 – 80 °C (Kutzner, 2000). *Bacillus spp.* and other facultative thermopiles survive this high-temperature process (Strom, 1995). The diversity of bacilli species is fairly high at temperatures from 50-55°C but decreases dramatically at 60°C or above. When conditions become unfavorable, bacilli survive by forming spores, which are ubiquitous in nature and become active whenever environmental conditions are favorable. At the highest compost temperatures, bacteria of the genus *Thermus* have been isolated (Beffa et al., 1996).

During the curing stage, the temperature declines again toward ambient, and the fungi and actinomycetes proliferate on the remaining, less degradable organic matter such as chitin, cellulose, and lignin (Kutzner, 2000).

1.4 Current status of compost modeling

Although the scientific basis of composting, including the fundamental principles of the physical, chemical, and biological aspects, has been understood, engineering design and operation of composting systems is still mostly based on trial and error, which is limited to specific substrate and pre-determined operational variable values such as pH, moisture content, aeration rate, and so on (Haug, 1993). Moreover, trial-and-error methodology can neither guarantee the robust design of an optimal configuration, nor can it be used for the real-time estimation of the progress and performance of a process. With an appropriate mathematical description of the composting process, however, such process monitoring and control can be achieved.

The basic strategy in the current practice of mathematical modeling of composting is to "couple empirically-derived substrate degradation kinetics with mass and energy balances" (Higgins and Walker, 2001). In a typical model, the description of the compost ecosystem is simplified and the parameters of microbial kinetics are determined by empirical estimations from experiments or from literature (Hamelers, 2004). The dynamic process model documented by Haug (1993), for example, and other studies reviewed by Mason (2006) were all based on the same approach. The application of this methodology is limited by measurement techniques and demanding experimental requirement, and so new methodologies stressing on fewer and identifiable model parameters is being explored by researchers (Hamelers, 2004).

1.5 Current modeling for passively aerated composting

Most composting models developed to date deal with forced aeration (Mason, 2006). Forced aeration systems have the advantage of high rate and good control of process variables, but generally involve large capital investments and operating costs, including maintenance and operator training (Haug, 1993). Passive aeration systems that rely on natural convection are more economical than active (i.e. forced) aeration systems in terms of initial capital investment, operation, maintenance, and operator training costs (Haug, 1993). Given an appropriate configuration, passive aeration can result in similar process rates (Fernandez and Sartaj, 1997) and compost quality (Solano et al., 2001). Passive systems can also be operated in cold climates (Lynch and Cherry, 1996a; McCartney and Eftoda, 2005).

In actively aerated systems, aeration typically takes place only during the high rate phase of the composting process which typically last one week to one month. Passive

aeration is used during the following curing phase, which usually lasts several months. Little attention however, has been paid to the curing phase even though this is an important part of the complete process (Haug, 1993). Good control of the curing process is necessary to guarantee a consistent end product of good quality, which is crucial for the potential application of compost in high value industries such as horticulture.

Mathematical descriptions of passively aerated systems are very limited, while mathematical models for actively aerated systems have been well documented (Haug, 1993). A typical mathematical model for an actively aerated compost system generally consists of a biodegradation model, which predicts the mass changes due to microbial activity, and a temperature model, which predicts the temperature profile developed in the compost bed. Modeling passively aerated systems also requires an airflow model which can predict the passive air movement through the compost bed, because aeration is not controlled by blowers or fans as in actively aerated systems. In passively aerated systems, however, the airflow rate is driven by natural convection, making it difficult to accurately estimate the supply of oxygen to the compost and the removal of excess heat and moisture without an appropriate mathematical model.

There are two published models of the airflow though passively aerated compost, and both were developed using similar methodology, i.e., analyzing the airflow based on the understanding of the fundamental mechanisms involved. The model proposed by Lynch and Cherry (1996b) treated compost as a porous medium and Darcy's law was employed to estimate the vertical velocity of air going through the compost pile.

Validation of the model was not demonstrated in the paper, however, possibly because of the difficulty of measuring airflow in actual windrow composting systems. Barrington et al. (2003) used least-squares regression to relate the Grashof number – the ratio of buoyancy to viscous forces – to the measured airflow rate in passively aerated compost, but no mechanistic explanation of the relationship was proposed. No further mathematical modeling effort on passively aerated compost has been reported since these two studies.

1.6 Research gaps and the scope of this research

The first challenge in the study of passively aerated composting is the measurement of airflow rate. Measuring the often low and highly variable flows in a passive aeration system is more challenging than measuring the forced airflow of an active system, especially in experimental or pilot-scale vessels of limited volume. The instrument used must be accurate at low flow rates, introduce very little pressure loss, remain effective and accurate over wide ranges of temperature and humidity, and be amenable to automation so as to effectively track fluctuations in the flow rate over time. As a research instrument, it should also be inexpensive and robust in laboratory and field environments.

A second challenge in the estimation of airflow rate in passively aerated composting systems is the development of a practical mathematical model that represents the natural convective movement of air, which is the driving force in such systems. The model should accurately portray the underlying physical processes and the values of the required input variables should be easy to measure. The model should be simple enough for practical application while still capturing the essence of the phenomenon.

As there is no steady, externally driven air flow through passively aerated compost, heat production is different at different locations in the compost bed and is strongly related to the airflow development. As a result, the microbial growth rates at different locations are also different, suggesting the need for a method to estimate the values of the microbial kinetic constants at different locations.

Although the ultimate goal of this work was to develop a general model which can be applied to any passively aerated composting system, a practical objective was to develop an empirical model suitable for a specific substrate, based on previously developed mathematical models of forced-aeration composting (Liang et al., 2004). Substrate free air space (FAS) was chosen as the primary variable for the empirical estimation of biodegradation kinetics in this work due to the significant effect of FAS on airflow development (Lynch and Cherry, 1996b; Barrington et al., 2003) and the important role of airflow in composting (Haug, 1993). A one factor (FAS) ANOVA experiment was designed and conducted to derive an empirical relationship between FAS and biodegradation kinetics (k_{max}). Full details of the experiment are provided in Chapter 5, but four levels of FAS were used in replicated vessels in which temperature was measured as an indicator of biological activity. Data from these experiments required the development of a statistical method test for significant difference among treatments.

The work discussed in this thesis was aimed to address the aforementioned issues and is presented in a paper format. Each chapter concentrates on one topic as listed below:

- Measurement of airflow in passively aerated compost systems

- A practical model to predict airflow development
- A rigorous way of significance test among treatments
- Empirical relationship between FAS and biodegradation kinetics (k_{max})

Chapter 1 provides a general literature review for this work. Chapter 2 deals with the measurement airflow in passively aerated compost systems. Chapter 3 describes an analytical model for the prediction of airflow velocity. A method of significance testing among treatments is proposed and discussed in Chapter 4. In Chapter 5 an empirical relationship between substrate FAS and biodegradation kinetics (k_{max}) is presented, and then used to simulate temperature development in a passively aerated compost system. All the conclusions are summarized in Chapter 6, together with recommendations for future work. Data used for this thesis and the source code for the numerical model and statistical analysis are printed in the appendices.

1.7 References

Beffa, T., M. Blanc, L. Marilley, J. Lott-Fischer, P.F. Lyon, and M. Aragno. 1996. Taxonomic and metabolic microbial diversity during composting, In: *The science of composting*. Bertoldi, M, P Sequi, B Lemmes, and T Papi eds. Blackie Academic & Professional. Bishopbriggs, Glasgow: pp. 149-61

Barrington, S., D. Choiniere, M. Trigui, and W. Knight. 2003. Compost convective airflow under passive aeration. *Bioresource technology*. 86 (3): 259-266

Civilini, M., C. Domenis, M. de Bertoldi, and N. Sebastianutto. 1996. Composting and selected microorganisms for bioremediation of contaminated materials. In: *The science of composting*. Bertoldi, M, P Sequi, B Lemmes, and T Papi eds. Blackie Academic & Professional. Bishopbriggs, Glasgow: pp884-891

Diaz, L.F., G.M. Savage, and C.G. Golucke. 1996. Stabilization of hazardous wastes through biotreatment. In: *The science of composting*. Bertoldi, M, P Sequi, B

Lemmes, and T Papi eds. Blackie Academic & Professional. Bishopbriggs, Glasgow: pp849-862

EPA (United States Environmental Protect Agency) 1997. Innovative uses of compost bioremediation and pollution prevention. EPA bulletin – EPA530-F-97-042. Washington, D.C.

Epstein, E. 1997. The science of composting. Lancaster, Pa.: Technomic Pub. Co. 487 p.

FAO. 2006. On-farm Composting Methods. http://www.fao.org/ag/agl/agll/compost/default.stm. Accessed Oct. 2006

Fernandez, L. and M. Sartaj. 1997. Comparative study of static pile composting using natural, forced and passive aeration methods. *Compost science & utilization* 5(4): 65-77

Gomez, R.B., F.V. Lima, and A.S. Ferrer. 2006. The use of respiration indices in the composting process: a review. *Waste management & research.* 24 (1): 37-47

Hamelers, H.V.M. 2004. Modeling composting kinetics: A review of approaches. *Reviews in environmental science & biotechnology.* 3(4):331-342

Haug, R.T. 1993. The Practical Handbook of Compost Engineering. Boca Raton. Lewis Publishers. 717 p

Higgins, C.W. and L.P. Walker. 2001. Validation of a new model for aerobic organic solids decomposition: simulations with substrate specific kinetics. *Process biochemistry.* 36(8-9): 875-884

Hoitink, H.A.J., A.G. Stone, and M.E. Grebus. 1996. Suppression of plant diseases by composts. In: *The science of composting.* Bertoldi, M, P Sequi, B Lemmes, and T Papi eds. Blackie Academic & Professional. Bishopbriggs, Glasgow: pp373-381

Hupe, K. J.C. Luth, J. Heerenklage, and R. Stegmann. 1996. Enhancement of the biological degradation of contaminated solids by compost addition In: *The science of composting.* Bertoldi, M, P Sequi, B Lemmes, and T Papi eds. Blackie Academic & Professional. Bishopbriggs, Glasgow: pp913-923

Kutzner, H.J. 2001. Microbiology of composting. In *Biotechnology*, Vol. 11c; Wiley: NY, pp 35–100.

Liang, Y., J.J. Leonard, J. Feddes, W.B. McGill. 2004. A simulation model of ammonia volatilization in composting. *Transactions of the ASAE* 47 (5): 1667-1680

Lynch, N.J. and R.S. Cherry. 1996a. Winter composting using the passively aerated windrow system. *Compost science & utilization* 4(3):44-52

Lynch, N.J. and R.S. Cherry. 1996b. Design of passively aerated compost piles: vertical air velocities between pipes. *Biotechnology progress* 12(5):624–629

Mason, I.G. 2006. Mathematical modelling of the composting process: A review. *Waste management.* 26(1): 3-21

McCartney, D. and G. Eftoda. 2005. Windrow composting of municipal biosolids in a cold climate. *Journal of environmental engineering and science.* 4(5): 341-352

Miller, F.C. and T. Clark. 1998. Literature Review and Position Paper on Composting as a Method of Remediating Petroleum Contaminated Soils. Final Report Submitted to Alberta Environmental Protection. Edmonton, AB

Rynk R. (Ed). 1992. On-Farm Composting Handbook. Northeast Regional Agricultural Engineering Service

Solano, M.L., F. Iriarte, P. Ciria, and M.J. Negro. 2001. Performance Characteristics of Three Aeration Systems in the Composting of Sheep Manure and Straw. *Journal of agricultural engineering research.* 79(3): 317-329.

Strom, P.F. 1985. Effect of temperature on bacterial species diversity in thermophilic solid-waste composting. *Applied and environmental microbiology.* 50(4):899-905

Wang, P., C.M. Changa, M.E. Watson, W.A. Dick, Y. Chen, and H.A.J. Hoitink. 2004. Maturity indices for composted dairy and pig manures. *Soil biology and biochemistry.* 36(5): 767-776.

Chapter 2 Airflow measurement in passively aerated compost [†]

2.1 Introduction

Composting is often used in waste management systems to treat organic material because of the high degradation rate, low odour generation, and efficient space utilization that can be achieved. Composting is a biological process that must be kept aerobic in order to realize these advantages. The aeration of compost promotes microbial activity by providing oxygen and removing carbon dioxide, ammonia, and excess moisture and heat (Haug 1993). Resistance to airflow varies with the airflow rate and material properties of the compost (Barrington et al. 2002; Veeken et al. 2002). In actively aerated systems, this resistance is overcome by a pump which draws or blows air through the compost, while in passively aerated systems the driving force is natural convection (Richard 1993; Fogiel et al. 1999).

Initial capital investment and operation, maintenance, and operator training costs are higher for active aeration systems as compared to passive aeration systems (Haug 1993). Passively aerated systems can provide the same process rate as active aeration systems (Fernandez and Sartaj 1997; Solano et al. 2001), and both types of system can operate all year, even in temperate climates (Lynch and Cherry 1995). The quality of compost produced by passive aeration is "remarkably similar" to the product of an active aeration system (Solano et al. 2001). Passive aeration can therefore be considered suitable not only for small-scale applications, but also as a

[†] A version of this chapter has been published as: Yu, Shouhai, O.G. Clark, J.J. Leonard. 2005. Airflow measurement in passively aerated compost. *Canadian Biosystems engineering*. 47(6):39-45

less expensive alternative to active aeration for large-scale processing (Lynch and Cherry 1995; Rynk 1992).

The primary difference between active and passive aeration systems, aside from cost, is that an active system generates a consistently high airflow rate. The airflow rate in a passive system is generally lower and more variable because it is driven by the heat from microbial activity. When microbial activity is low, at the start of the process, for instance, then the airflow rate is also low. This variable flow rate in passive aeration can be advantageous, conserving process heat and driving off less nitrogen from the compost. Passive aeration, as a result, is more energy efficient and has been shown to produce compost that is richer in nitrogen than actively aerated compost (Solano et al. 2001).

Measuring the potentially low and variable flows in a passive aeration system is more challenging than measuring the forced airflow of an active system, especially in experimental or pilot-scale vessels of limited volume. The instrument used must be accurate at low flow rates, introduce very little pressure loss, remain effective and accurate over wide ranges of temperature and humidity, and be amenable to automation so as to effectively track fluctuations in the flow rate. As a research instrument, it should also be inexpensive and robust in laboratory and field environments.

Perhaps because of the aforementioned challenges, there is less published literature about passively aerated composting systems than about actively aerated systems. Fogiel et al. (1999) measured the airflow at the inlet to a compost vessel using a thermal flow meter. Veeken et al. (2002) measured the exhaust flow with a thermal

flow meter. Barrington et al. (2003) measured the exhaust flow with an orifice plate. Orifice plates and thermal flow meters (or hot-wire anemometers) each have advantages and disadvantages. The orifice plate is the most commonly used flow sensor, but creates a large non-recoverable pressure loss due to turbulence around the plate (Foust 1980). Thermal meters have a low head loss but accurate measurements require knowledge of the temperature, thermal conductivity, and specific heat of the air current. The physical properties of compost exhaust air can vary substantially, since it is often saturated and the temperature can vary from 30 to 70°C, making the measurements taken with a thermal meter difficult to interpret (American Society of Heating, Refrigerating and Air-Conditioning Engineers (ASHRAE) 2001, Baker 1991). Both types of instrument are more accurate at high flow rates rather than at the low flow rates often encountered in passively aerated composting systems.

The objective of this study was to devise, test, and demonstrate an alternative instrument suitable for measuring airflow in passively aerated compost systems. Several possible methods were considered during preliminary work, including a hot-wire anemometer, a bubble meter, an ultrasonic airflow meter, and a smoke tracer airflow meter. The hotwire anemometer was considered because of its convenience and popularity, but was found to be too unstable at low flow rates. The bubble meter generated too much flow resistance, was finicky to operate, and was potentially difficult to automate. The smoke tracer and ultrasonic meters were therefore chosen for further development and comparison.

2.2 Materials and methods

2.2.1 Smoke tracer meter

Airflow can be measured by injecting a tracer element, such as smoke, into an air stream passing through a uniform conduit (a round pipe in this case) and using sensors to detect its passage at two points along the conduit. The apparent air speed (v) and volumetric airflow rate (Q) can thereby be calculated from the time interval between the arrival of the smoke at the first and the second detectors (Δt), the diameter of the pipe (D), and the distance between the two sensor pairs (L), according to Equations 1 and 2, respectively. This method causes negligible pressure drop or disturbance of the air stream.

$$v = \frac{L}{\Delta t} \tag{1}$$

$$Q = \frac{\pi}{4} D^2 \frac{L}{\Delta t} = \left(\frac{\pi \cdot D^2}{4} L \right) \frac{1}{\Delta t} \tag{2}$$

In this study, the chosen tracer element was sulphuric acid aerosol generated by a commercially available airflow tester (Flow Check, Draeger Canada Ltd., Mississauga, ON). The white aerosol smoke forms when moist air passes through the tester. The density of the aerosol varies with humidity of the air, but is of approximately neutral buoyancy and is carried in the air stream without influencing the flow pattern. Paired infra-red light-emitting diodes and photodetectors (QED123 and QSD123, Fairchild Semiconductor Corp., South Portland, ME) were installed at two points 200 mm apart in the walls of a 33-mm (inside diameter) polyvinyl chloride (PVC) pipe to detect the passage of the smoke (Figures 2-1 and 2-2).

Infrared technology has been widely applied and the transducer pairs are inexpensive and readily available. Smoke was injected into the inlet of the PVC pipe so that it was carried by the air current and passed the detectors sequentially. The smoke blocked the infra-red light beam as it passed between each transducer pair and reduced the output voltage signal from the detector (Figure 2-2).

2.2.2 Ultrasonic meter

A time-of-flight ultrasonic airflow meter was also constructed for use in this study (Brown 1991). A pair of ultrasonic transceivers (QK168, QKits Ltd., Kingston, ON) was installed in a PVC pipe as shown in Figure 2-3. Each transceiver can both send and receive ultrasonic signals. The time for the ultrasonic waves to travel from the upstream transceiver to the downstream one (t_1) can be calculated using Equation 3, and the time to travel the reverse path (t_2) using Equation 4. The effect of the air speed is proportional to the time difference (Δt) between the two flights (Equation 5), and the corresponding volumetric flow rate (Q) can be found using Equation 6.

$$t_1 = \frac{\Delta x}{v_s + v \cdot \cos\theta} \tag{3}$$

$$t_2 = \frac{\Delta x}{v_s - v \cdot \cos\theta} \tag{4}$$

$$\Delta t = t_2 - t_1 = \frac{\Delta x}{v_s - v \cdot \cos\theta} - \frac{\Delta x}{v_s + v \cdot \cos\theta} = \frac{\Delta x \cdot 2 \cdot v \cdot \cos\theta}{v_s^2 - v^2 \cdot \cos^2\theta} \cong \frac{\Delta x \cdot 2 \cdot v \cdot \cos\theta}{v_s^2} \tag{5}$$

$$V_a = \frac{\pi \cdot D^2}{4} \cdot v = \frac{\pi \cdot D^2}{4} \frac{\Delta t \cdot v_s^2}{2 \cdot \Delta x \cdot \cos\theta} = \frac{\pi \cdot D^2 \cdot v_s^2}{8 \cdot \Delta x \cdot \cos\theta} \Delta t \tag{6}$$

Since the speed of sound in air (v_s) is influenced by temperature, the flow meter is sensitive to temperature change. If the temperature of the measured air stream varies

substantially, then the speed of sound used in Equations 3–6 should be adjusted accordingly (Brown 1991, Reese 2000) by the use of Equation 7. That was not a concern in this study, where temperature of the inlet air stream measured with the ultrasonic meter in the experiment (about 15°C) varied by only a few degrees from the calibration temperature (about 20°C). According to Equation 7, a 5°C difference in temperature results in error of less than 1%.

$$v_s = 331.5 + 0.60 \cdot T \tag{7}$$

2.2.3 Calibration

The meters were calibrated in the laboratory and the sensitivity of the sensor circuits was adjusted in order to optimize their response. As shown in Fig.2-4, compressed lab air (550kPa) was filtered and warmed to ambient temperature before entering the calibration system. A precision mass flow controller (Mass-Flo®, 1179A24CS1BV, MKS Instrument, Wilmington, MA) was controlled by a computer to deliver the airflow (MKS Instruments 2002). A primary gas flow calibrator (DryCal®, DCL-H Rev. 1.08, Bios International Corporation, Butler, NJ) was used as the standard to determine the volumetric airflow rate during calibration (Middendorf et al. 2001) and as the basis for the computer control of the air delivery system. The corresponding output signals from the experimental airflow meter were logged automatically. After the data were conditioned offline to determine the measured airflow rates, linear regressions were performed to determine the relationship between the airflow rates measured by the primary gas flow calibrator and the experimental airflow meters (Equations 2 and 6). Two independent calibrations of the two meters were conducted

and each calibration was performed with duplication. Data from these two independent calibrations were pooled for subsequent regression analysis (Figure 2-5 and 2-6).

2.2.4 Pressure loss

Pressure loss across a flow meter is influenced by the effective diameter of the flow meter. For steady flow, pressure loss (ΔP_d) caused by a change in the diameter of a pipe, as in the smoke tracer flow meter, can be estimated with Equation 8, where K (contraction-loss coefficient) = 0.55 for a large reduction in diameter, v is the velocity in the conduit of smaller diameter, and α (flow regime correction factor) = 0.5 for laminar flow (Geankopolis 1993). The maximum speed recorded in this trial was 0.30 m s^{-1}. According to Equation 8, the pressure loss due to the diameter change from the compost vessel to the smoke tracer flow meter was about 0.06 Pa.

$$\Delta P_d = K_L \frac{v^2}{2\alpha} \tag{8}$$

The pressure drop due to friction losses in the tube of the smoke tracer meter (ΔP_f) was calculated using the Darcy-Weisbach equation (Equation 9), and was estimated to be approximately 0.04 Pa (Geankopolis 1993). The total estimated pressure loss across the smoke tracer flow meter was therefore about 0.10 Pa.

$$\Delta P_f = 2f\rho \frac{L}{D} v^2 \tag{9}$$

The ultrasonic airflow meter was installed in the walls of the existing air inlet pipe and did not appreciably disrupt the airflow, and so caused only negligible pressure loss.

2.2.5 Application

Both the smoke tracer and ultrasonic meters were used in a composting trial conducted in a passively aerated, cylindrical, polyethylene vessel, 0.9 m in height and 0.6 m in diameter (Figure 2-7). The vessel was insulated and an expanded metal floor was installed 0.10 m from the bottom of the vessel to create an aeration plenum. Fresh dairy manure was mixed with air-dried ground straw, sawdust, and woodchips to obtain a carbon to nitrogen ratio of 35:1 and a free air space of 70%. Carbon and nitrogen content in the substrate were analyzed (Norwest Labs, Edmonton, AB) before and after composting. The initial moisture content of the prepared mixture was 78% (wet basis). At the beginning of the experiment, the depth of the compost in the vessel was 0.50 m. During the trial, the outlet airflow rate was measured using the smoke tracer meter. The performance of ultrasonic devices is inhibited by high relative humidity, so the ultrasonic meter was used to measure the airflow rate only at the inlet.

2.3 Results and discussion

The responses of the flow meters were very linear in the calibration range, as indicated by the correlation coefficients (R^2) of 0.98 and 0.99 for the smoke tracer and ultrasonic flow meters, respectively (Figure 2-5 and 2-6). Despite its linear response, the measured output voltage from the ultrasonic meter changed very little with increasing flow rate, showing low sensitivity at low airflow rates. The smoke tracer flow meter, for its part, exhibited greater variation at high airflow rates than did the ultrasonic device. The relatively low sampling rate (about 6 Hz), limited by the slow clock speed of the computer used in the trial, was a major contributor to

this. At a relatively high airflow rate of 21 L min^{-1}, while the average measured flow rate was 20.4 L min^{-1} (SD = 5.3 L min^{-1}), the mean rounding error caused by the sampling rate would have been 8.3 L min^{-1}, or 41% of the flow rate. The mean rounding error in the measurement of the transport time for the aerosol is expected to be ½ of the sampling period, resulting in a systematic overestimate of the transport time and subsequent underestimate of the air flow rate. This source of error is inversely proportional to the sampling frequency, which could easily be greatly increased with current hardware.

The temperature history at different locations in the compost vessel and the flow rate of air through the compost vessel are shown in Figure 2-8 and 2-9, respectively, for the experimental trial. The temperature in the top layer of the compost (0.5m) followed a typical curve for composting, increasing exponentially to about 65°C during the first 30 h of the trial and then gradually declining to about 40°C over the remaining 150 h. The airflow rate followed the same general pattern (Figure 2-9), with a few hours lag time, increasing to a maximum at about 40 h and then gradually declining. This illustrates how buoyancy influenced the convective airflow through the vessel as air was warmed by microbial activity in the compost bed.

The vertical temperature gradient illustrated in Figure 2-8 was the result of heat and mass transfer processes in the compost. The airflow through the compost was unidirectional, as indicated in Figure 2-7, passing through the compost from bottom to top and removing heat, moisture, and other volatile compounds. While heat production during composting is almost completely derived from biological activity (Finstein and Morris, 1975), thermal energy is lost mainly as latent heat due to the

vaporization of water (VanderGheynst et al. 1997). When the relatively cool, dry ambient air was drawn into the bottom layer of compost (0.0 m), the resultant heat transfer kept the compost there at mesophilic temperatures. Upon reaching the middle layer (0.3 m), the air had already been warmed and moistened and, as a result, biological heat generation during the active composting phase was sufficient to maintain thermophilic temperatures. Upon reaching the top layer (0.5 m), the oxygen content in the airflow had been reduced by microbial activity in the lower layers (Ekinci et al. 2006) and carbon dioxide, ammonia and volatile organic concentrations had been increased. Microbial activity in the substrate was therefore inhibited, while the still unsaturated airflow continued to evaporate moisture from the substrate, shifting heat energy from sensible to latent form and depressing the temperature. The volumetric and dry mass flow rates at the vessel inlet and exhaust are compared in Table 2-1. Conversion from volumetric to equivalent dry mass flow rate was done using standard psychrometric relationships (Equations 10 and 11, ASHRAE 2001), based on the assumptions that exhaust air was saturated (100% relative humidity) and that the inlet and exhaust pressures were atmospheric (101.3 kPa).

$$v = v_{da} + \mu \cdot v_{as} \tag{10}$$

$$\mu = \varphi/(1+(1-\varphi)\cdot W_s/0.62198) \tag{11}$$

The average ambient relative humidity in the laboratory was 56.4% (SD = 5.7%) and the average ambient temperature was 23.3°C (SD = 2.2°C). The exhaust flow rate, measured with the smoke tracer flow meter, was consistently higher than the inlet flow rate, measured with the ultrasonic meter. The exhaust flow peaked at about 16 g dry air min^{-1} (g da min^{-1}) (19 L min^{-1}) and then declined to about 9 g da min^{-1} (9 L

min^{-1}) by the end of the trial. At the inlet, the measured flow peaked at about 11 g da min^{-1} (10 L min^{-1}) and then declined to about 7 g da min^{-1} (6 L min^{-1}). According to the stoichiometric analysis descibed by Haug (1993), more gas is expected in the exhaust since more CO_2 and NH_3 are generated during the oxidation of the substrate and the magnitude of the difference depends on the composition of the substrate and the final composted product (Haug 1993, pp 261-286). Nutrient balances in this study, based on analysis of the compost at the start and end of the trial (Table 2-2), illustrate the loss of carbon and nitrogen during composting and the potential difference this could make between inlet and exhaust airflow. The data shown are based on the concentrations of two composite samples before and after composting. Comprehensive material balances were not performed since this was beyond the scope of this study.

The smoke tracer flow meter appears to be best suited to laboratory studies of this kind when evaluated according to the criteria stated in the introduction. Unlike the ultrasonic meter, the smoke tracer meter is robust in the presence of high humidity, temperature, or pressure changes in the air stream. The smoke tracer meter accurately measures small changes in airflow at low flow rates and causes negligible pressure loss, especially if the inside diameter of the body of the flow meter is the same as that of the exhaust duct. In this study, the smoke injection and the determination of the exact time at which the voltage drops occurred at each sensor were done manually, but both of these operations could easily be automated at little cost to increase the accuracy of the measurements. The magnitude of the voltage change from the phototransistor that was used is reduced at higher temperatures, although the transit

time of the tracer smoke is not affected by air temperature. This change in sensitivity could be compensated for by adjusting the value of the variable resistor in series with the phototransistor (Figure 2-2). A modulated signal might also be used to minimize the effect of temperature change on the sensitivity of the circuit. The accuracy of output of the ultrasonic meter, by contrast, is affected by temperature change, as described previously. The simple components of the smoke tracer flow meter (Figure 2-1) made it easy to build and the cost was low compared with that of any available commercial air flow meter. Any general-purpose analogue-to-digital conversion module could be used as a data logging system. The ultrasonic meter, by comparison, requires much more complex components for the ultrasonic transmission and reception and cannot be connected to computer readily (Becker 2003). To adapt the smoke tracer flow meter for use with piles of compost or windrows, a flux chamber (Frechen et al. 2004) could be employed.

2.4 Summary and conclusions

A smoke tracer flow meter was devised to measure airflow though passively aerated compost. Compared with other flow meters used in similar experiments, the smoke tracer flow meter had the advantages of very low pressure loss, low cost, and robust performance under humid conditions. The device was proven in an actual experiment to effectively measure the flow rate of warm, moist exhaust air from passively aerated compost. Further work could be done to completely automate this device. By comparison, an ultrasonic airflow meter had better linear response ($R^2 = 0.99$) but was shown to be poorly suited to this kind of experimental work due to its low

sensitivity at low flow rates and high sensitivity to changes in temperature and humidity.

2.5 References

American Society of Heating, Refrigerating and Air-Conditioning Engineers (ASHRAE). 2001. Psychrometrics. In *Handbook of Fundamentals*, ed. ASHRAE, 6.1-6.17. Atlanta, GA: ASHRAE.

Baker, W.C. 1991. Thermal mass flowmeters and controllers. In *Flow measurement – Practical guides for measurement and control*, ed. D.W. Spitzer, 335-346. Research Triangle Park, NC: Instrument Society of America.

Barrington, S., D. Choinière, M. Trigui and W. Knight. 2002. Compost airflow resistance. *Biosystems Engineering*. 81(4): 433-441.

Barrington, S., D. Choinière, M. Trigui and W. Knight. 2003. Compost convective airflow under passive aeration. *Bioresource Technology*. 86(3): 259-266.

Becker J. 2003. *Everyday Practical Electronics*. January 2003. 44-51

Brown A.E. 1991. Ultrasonic flowmeters. In *Flow measurement - Practical guides for measurement and control*, ed. D.W. Spitzer, 415-442. Research Triangle Park, NC: Instrument Society of America.

Ekinci K., H.M. Keener, and D. Akbolat. 2006. Effects of feedstock, airflow rate, and recirculation ratio on performance of composting systems with air recirculation, *Bioresource Technology*. 97(7): 922-932

Fernandez, L., and M. Sartaj. 1997. Comparative study of static pile composting using natural, forced and passive aeration methods. *Compost Science and Utilization*. 5(4): 65-77.

Finstein M.S., and M.L. Morris. 1975. Microbiology of municipal solid waste composting. *Advances in Applied Microbiology*. 19: 113-151.

Fogiel, A.C., R.D. von Bernuth, F.C. Michel Jr., and T.L. Loudon. 1999. Experimental verification of the natural convective transfer of air through a dairy manure compost media. ASAE Paper No. 99-4053. St. Joseph, MI: ASAE.

Foust, A.S., L.A. Wenzel, C.W. Clump, L. Maus, and L.B. Andersen. 1980. *Principles of Unit Operations*, 560-562. New York, NY: John Wiley and Sons.

Frechen FB, M. Frey, M. Wett and C. Loser. 2004. Aerodynamic performance of a low-speed wind tunnel. *Water Science & Technology*. 50(4): 57-64.

Geankopolis, C.J. 1993. Design equations for laminar and turbulent flow in pipes. In *Transport Processes and Unit Operations*, 3rd edition, 83-100. Englewood Cliffs, NJ: Prentice Hall.

Haug, R.T. 1993. *The Practical Handbook of Compost Engineering*. Boca Raton, FL: Lewis Publishers.

Lynch, N.J., and R.S. Cherry. 1995. Design of passively aerated compost piles: Vertical air velocity between the pipes. *The Science of Composting*, ed. M. De Bertoldi, P. Sequi, B. Lemmes and T. Papi, 973-982. Glasgow, UK: Blackie Academic and Professional.

Middendorf P.J., D.L. MacIntosh, L.V. Tow, and P.L. Williams. 2001. Performance of electronic flow rate meters used for calibration of air sampling pumps. *American Industrial Hygiene Association Journal*. 62(4): 472-476.

MKS Instruments. 2002. *Bulletin* 1179A-6/02.

Reese, R.L. 2000. *University physics*. 553. Pacific Grove, CA: Brooks/Cole.

Richard, T.L. 1993. Municipal solid waste composting: Biological processing. *MSW Composting Fact Sheets*, No. 2. Ithaca, NY: Cornell Waste Management Institute.

Rynk, R. (ed.) 1992. *On-Farm Composting Handbook*. NRAES 54, 24-42. Ithaca, NY: Natural Resource, Agriculture, and Engineering Service.

Solano, M.L., F. Iriarte, P. Ciria, and M.J. Negro. 2001. Performance characteristics of three aeration systems in the composting of sheep manure and straw. *Journal of Agricultural Engineering Research*. 79(3): 317-329.

VanderGheynst, J. S., L. P Walker, and J.Y. Parlange. 1997. Energy Transport in a High-Solids Aerobic Degradation Process: Mathematical Modeling, Validation and Analysis. *Biotechnology Progress*. 13(3): 238-248.

Veeken, A., V. de Wilde, and B. Hamelers. 2002. Passively aerated composting of straw-rich pig manure: Effect of compost bed porosity. *Compost Science and Utilization*.10(2): 114-128.

Table 2-1. Airflow rates as measured at the inlet and outlet of the compost vessel

	Inlet flow rate[†] (Ultrasonic flow meter)				Outlet flow rate[‡] (Smoke tracer flow meter)					
Time	Volumetric basis		Dry mass basis		Volumetric basis		Dry mass basis		Temperature	Difference
h	L min^{-1}		g da min^{-1}[§]		L min^{-1}		g da min^{-1}		°C	g da min^{-1}
42	1.9	(1.9)	2.2	(2.2)	4.2	(0.2)	4.3	(0.2)	44	2.0
63	9.5	(1.9)	11.1	(2.2)	19.2	(3.7)	16.1	(3.1)	61	5.0
92	7.6	(1.1)	8.9	(1.3)	13.1	(2.0)	12.1	(1.8)	53	3.2
116	n.d.[¶]		n.d.		11.8	(1.1)	11.4	(1.0)	49	n.d.
176	5.7	(1.9)	6.7	(2.2)	8.5	(1.1)	8.8	(1.1)	42	2.1
225	5.7	(1.9)	6.7	(2.2)	9.8	(1.7)	10.5	(1.8)	37	3.8

[†] Mean value with SD in parentheses. Mean inlet air temperature was 23.3°C and mean relative humidity was 56.4%.

[‡] Mean value with SD in parentheses. Outlet air was assumed to be saturated.

[§] g da min^{-1} Grams of dry air equivalent per minute

[¶] n.d. No data

Table 2-2. Total carbon and nitrogen balance per vessel during composting

	Initial	Final	Difference	Produced gas †
	g	g	g	g da min^{-1} ‡
Carbon	3510	2470	1040	1.27
Nitrogen	195	140	55	0.022

† Assumed complete conversion of lost C to CO_2 and lost N to NH_3 during high rate stage (50–100 h).

‡ g da min^{-1} Grams of dry air equivalent per minute

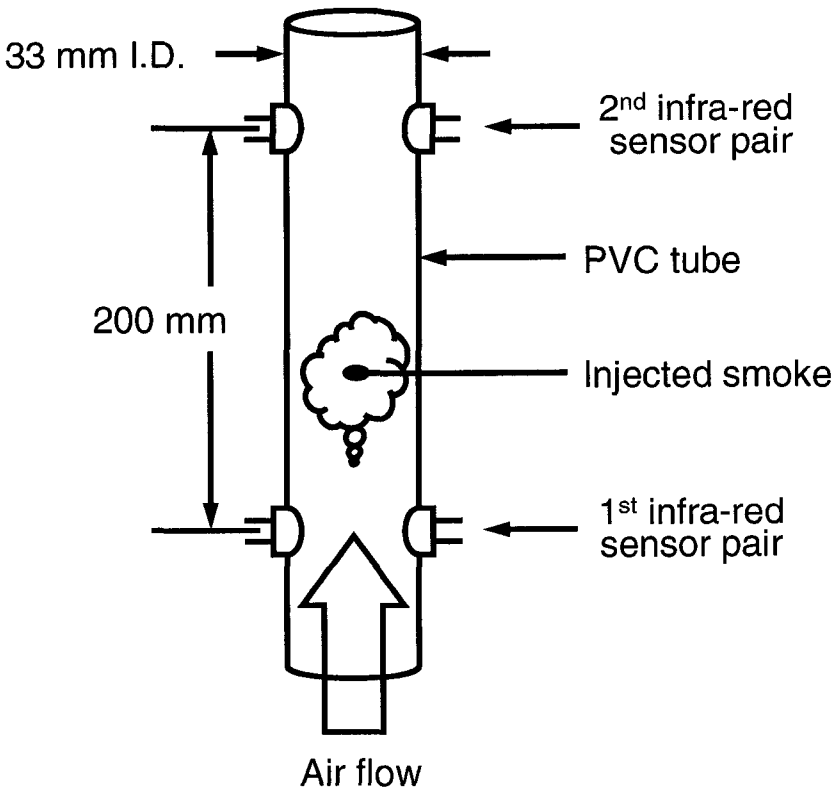

Figure 2-1. Schematic of the smoke tracer airflow meter

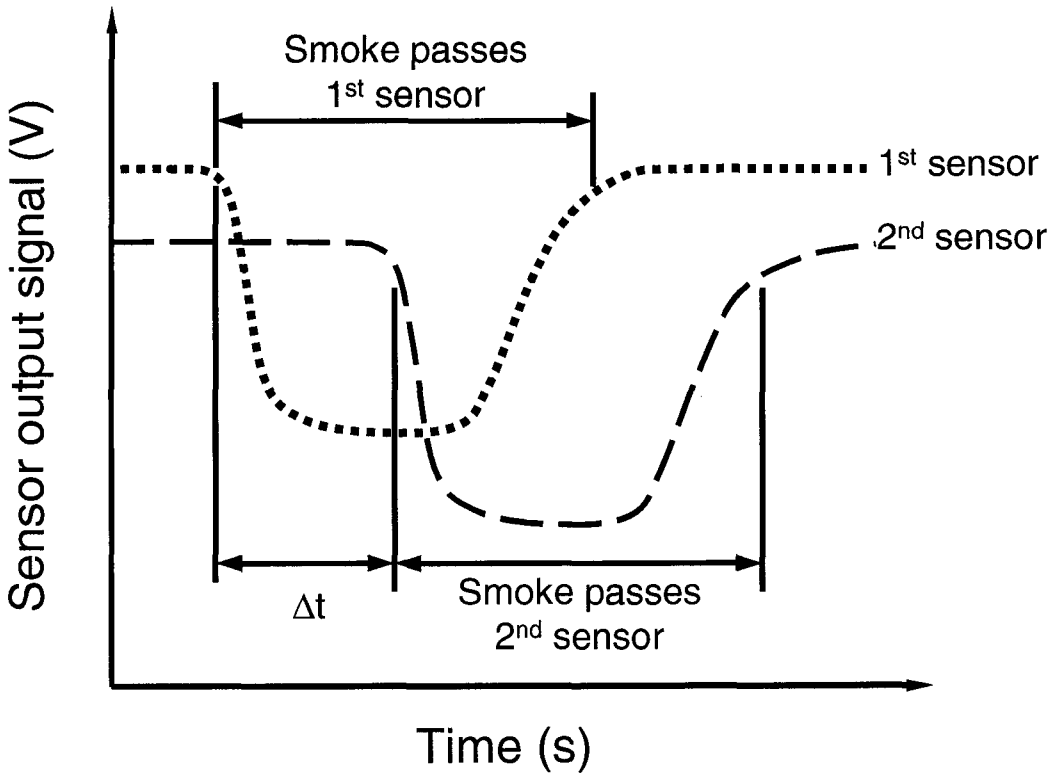

Figure 2-2. Theoretical shape of voltage signals from smoke tracer airflow meter

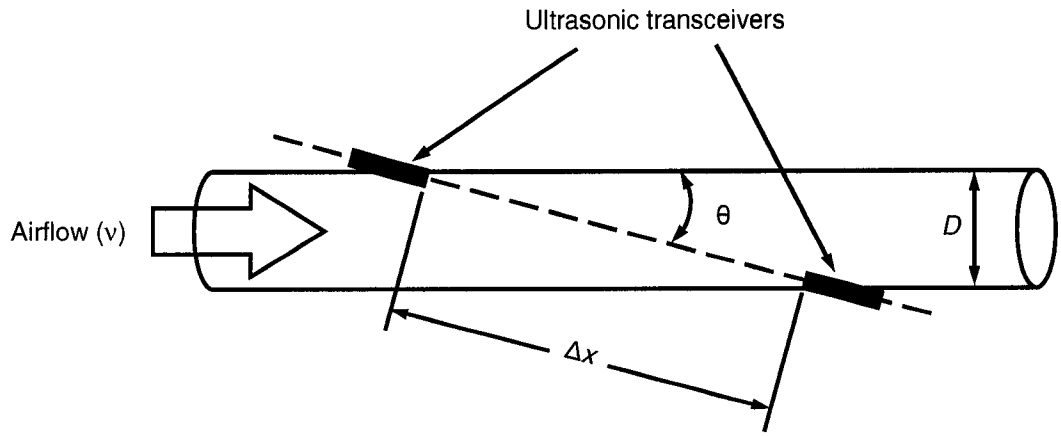

Figure 2-3. Schematic of the ultrasonic airflow meter

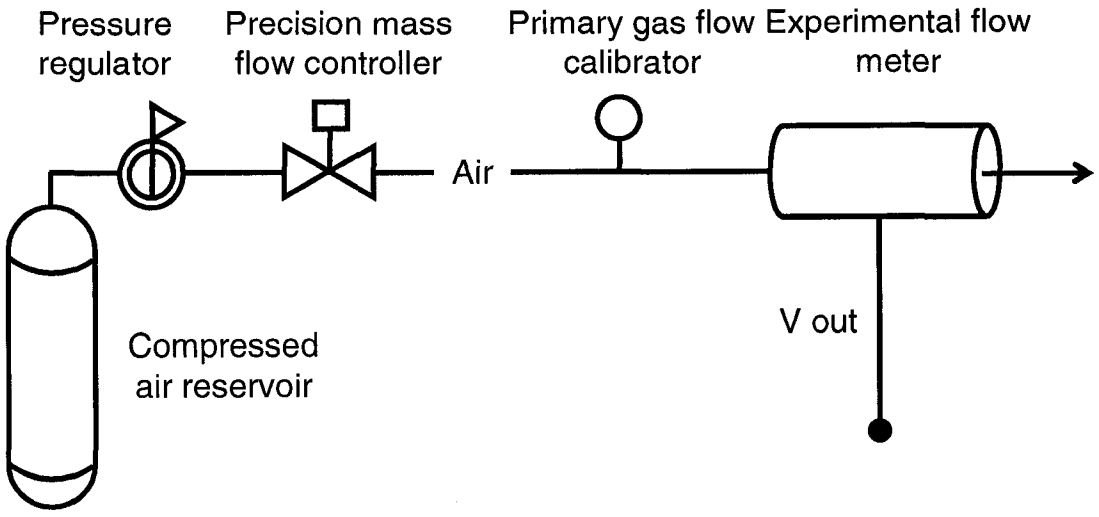

Figure 2-4. Schematic of the calibration system

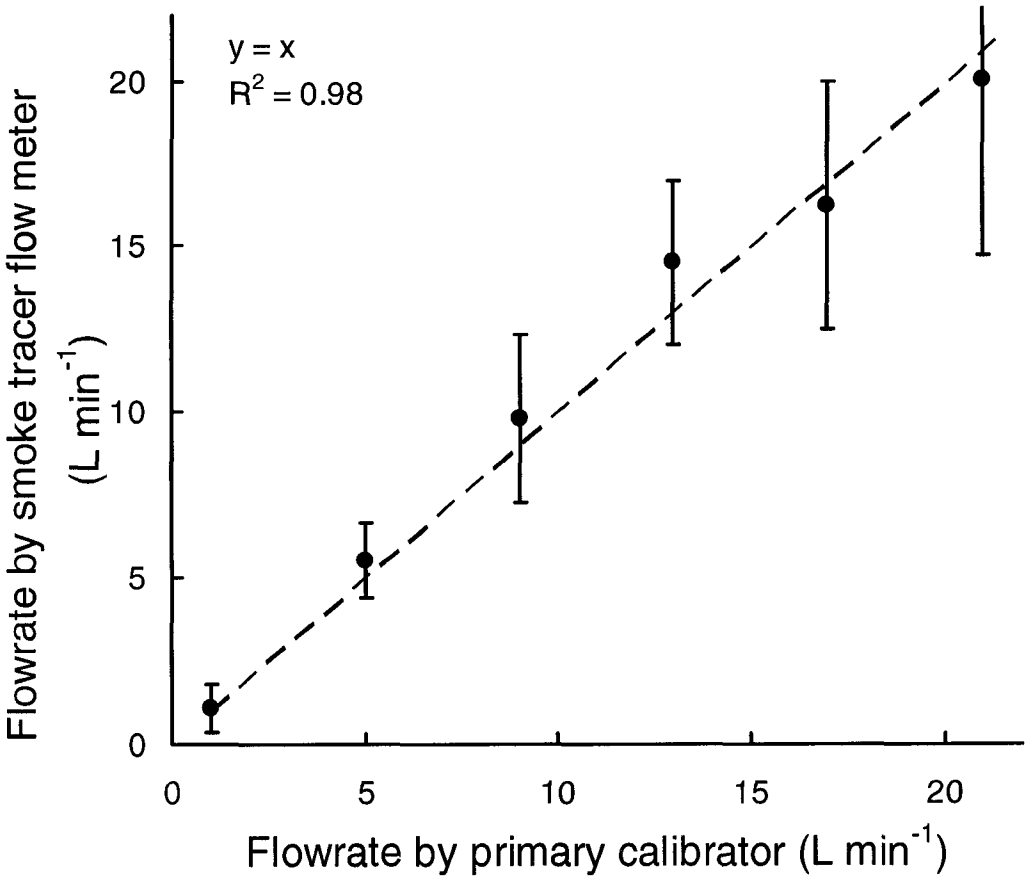

Figure 2-5. Calibration data for the smoke tracer airflow meter. Error bars indicate the standard error (n = 20).

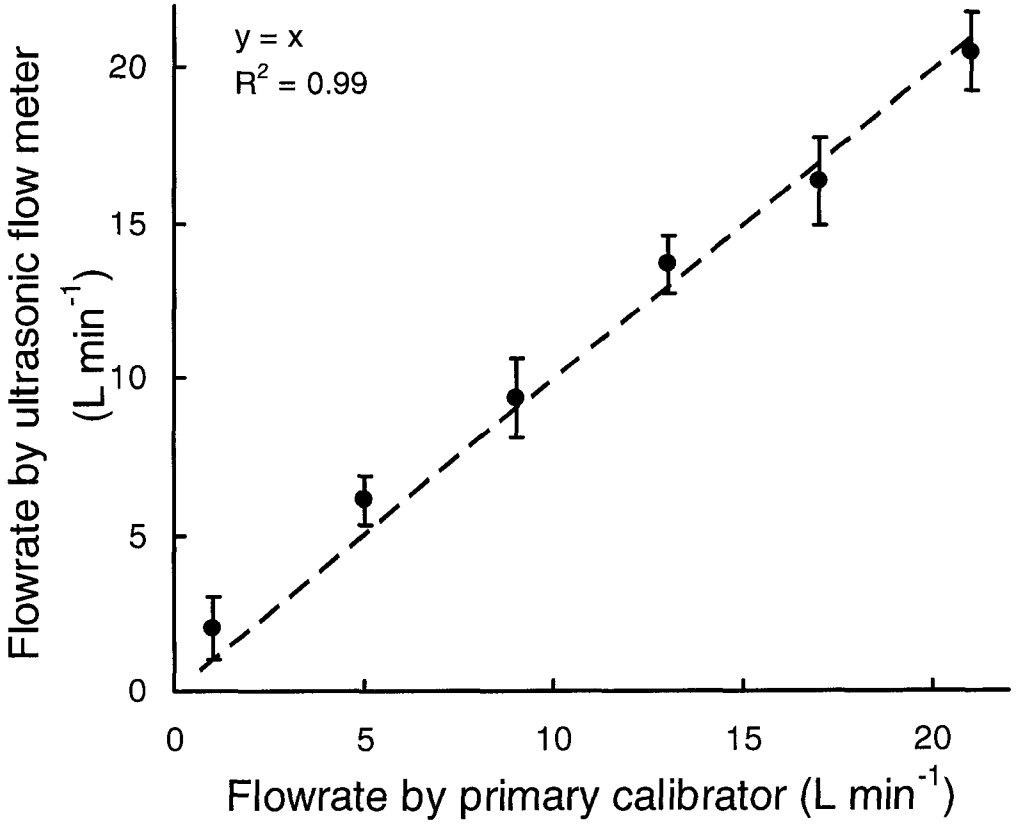

Figure 2-6. Calibration data for the ultrasonic airflow meter. Error bars indicate the standard error (n = 12).

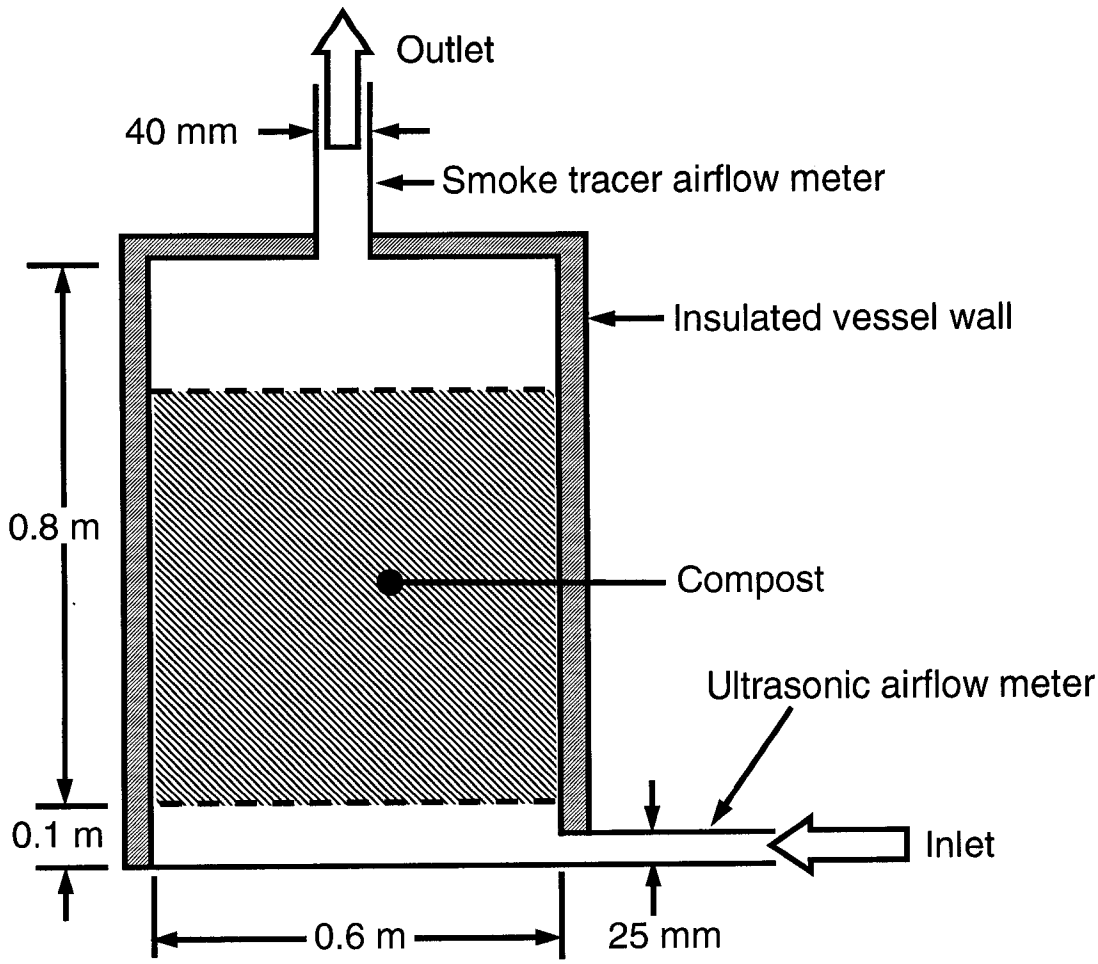

Figure 2-7. Schematic of passively aerated compost vessel

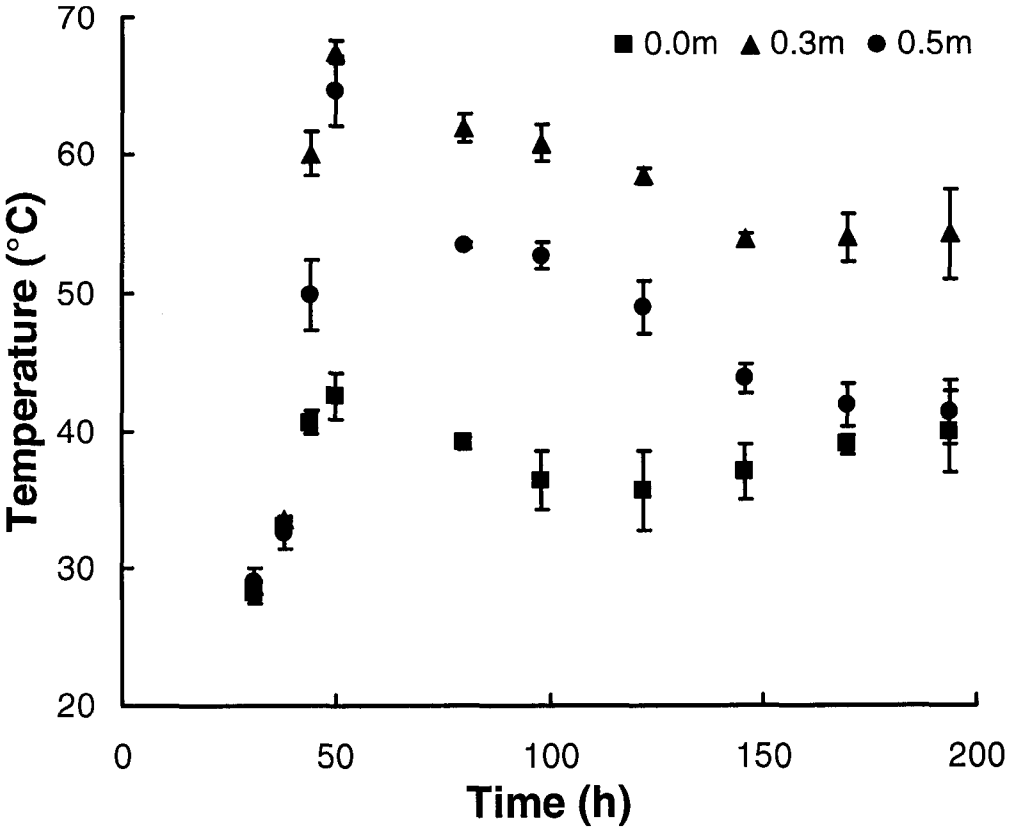

Figure 2-8. Temperature history at 0, 0.3, and 0.5 m from the bottom of the compost bed. Error bars indicate the standard error (n = 2).

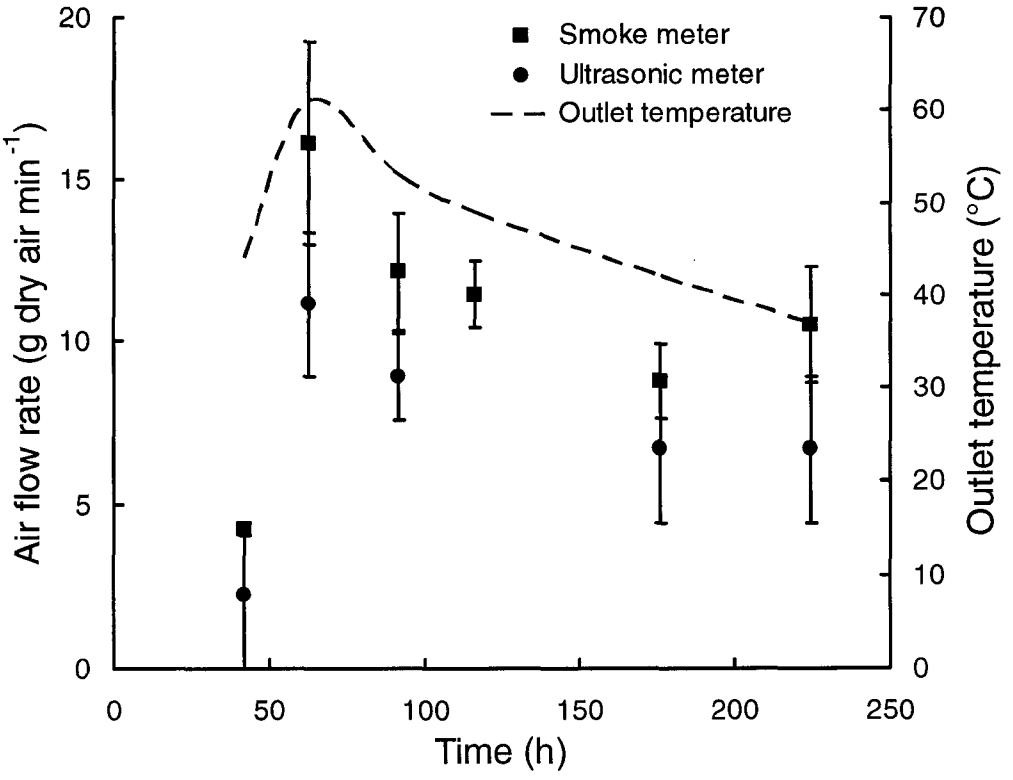

Figure 2-9. Air flow rate (equivalent mass of dry air) measured at the vessel inlet (ultrasonic meter) and outlet (smoke tracer meter). Dashed line indicates temperature at the top of the compost bed (outlet). Error bars indicate the standard error of 2 measurements for the ultrasonic flow meter (n = 2) and smoke tracer flow meter (n = 6).

Chapter 3 Mathematical model of vertical airflow [†]

3.1 Introduction

Composting is generally defined as the aerobic degradation of organic matter by microorganisms under controlled conditions. Aeration is critical in composting because it supplies oxygen, and removes carbon dioxide, excess heat and moisture from the compost (Haug, 1993, p261). The benefits of composting, e.g. high degradation rate, low odour generation, and efficient space utilization, cannot be achieved without appropriate aeration. Composting systems can be categorized into two types according to the aeration strategies employed: actively aerated systems and passively aerated systems. In actively aerated systems, mechanical means are used to draw or blow air through the compost, while in passively aerated systems the driving force is natural convection resulting from temperature differences (Fogiel *et al.*, 1999).

Passive aeration systems are more economical than active aeration systems in terms of initial capital investment, operation, maintenance, and operator training costs (Haug, 1993). Passive and forced aeration systems have been shown to result in similar process rates (Fernandez and Sartaj, 1997) and compost quality (Solano *et al.*, 2001), and both can be operated in cold climates (Lynch and Cherry, 1996a; McCartney and Eftoda, 2005).

[†] A version of this chapter has been submitted for publication as: Yu, Shouhai, O.G. Clark, J.J. Leonard. 2006. For the optimization of solid state fermentation: analytical model of vertical airflow. *Biosystems Engineering* (in review).

Mathematical descriptions of passively aerated compost systems, however, are very limited, probably due to the focus of the research interest. Actively aerated systems, however, have been well described mathematically (Haug, 1993). The lack of an adequate mathematical description of heat and mass transfer in passively aerated compost makes such systems difficult to predict and control. Effective system design and optimization is also difficult, which is a barrier to the adoption of passively aerated composting. One critical obstacle to modeling passively aerated systems is a mathematical description of airflow. In actively aerated systems, airflow rate is prescribed by pumps or fans. As a result, the supply of oxygen to the compost and the removal of carbon dioxide, ammonia, heat, and moisture can be estimated with reasonable accuracy. In passively aerated systems, however, the airflow rate is driven by natural convection. Natural convective airflow is difficult to estimate accurately without an appropriate mathematical model because it is often relatively small and highly variable (Yu *et al.*, 2005).

The more general problem of natural convection through porous media has been extensively studied in other areas of research, and this work has been well summarized by Nield and Bejan (1999). Attention has focused on specific configurations such as homogenous porous media adjacent to regular shaped heating sources (Nield and Bejan, 1999, chapter 5) or natural convection within enclosed porous media (Nield and Bejan, 1999, chapter 6, 7). Passively aerated composting, however, usually takes place in an open system with a very heterogeneous, self-heating substrate, making it very difficult to adopt any of the mature theories summarized by Nield and Bejan (1999).

An alternative is to start with a simple analysis to illustrate the mechanisms involved. Lynch and Cherry (1996b) proposed the first analytical model for the description of airflow through passively aerated compost, employing Darcy's law to estimate the vertical velocity of air through the porous compost pile. The model was based on the understanding that natural convection is driven by buoyancy derived from a temperature gradient. The influence of the substrate permeability was discussed in detail, and windrow geometry was included as a model parameter. Verification of the model was not demonstrated in the paper, however, possibly because of the difficulty of airflow measurement in actual windrow composting systems.

Barrington *et al.* (2003) took advantage of classical heat and mass transfer theory. The measured temperature and psychrometric properties of the air were used to calculate the Grashof number (Geankoplis, 1993), and a relationship between the Grashof number and the measured airflow rate was determined empirically using least-squared regression. The relationship between the Grashof number and the airflow rate was found to be linear or quadratic, depending on the structural characteristics of the substrate. No theoretical explanation of the nature of this relationship was proposed.

3.2 Objective

A practical mathematical model that can accurately predict the airflow development in passively aerated composting systems is required for system design and optimization. The model should accurately portray the underlying physical processes and the values of the input variables required to use the model should be easy to measure. The effect of compaction of the material on its permeability during composting should be

considered in the application of the model. The objective of this work was to derive such a model and to test it using experimental temperature and airflow data.

3.3 Model development

3.3.1 Physical model

The physical model used in this study consisted of dairy manure and straw composted in an enclosed, insulated, passively aerated composting vessel, 0.9 m in height and 0.6 m in diameter. An aeration plenum was created using an expanded metal floor installed 0.10 m from the bottom of the vessel. As demonstrated in previous work (Lynch and Cherry, 1996b; Barrington *et al.*, 2003), convective airflow is the primary mode of oxygen supply in passively aerated systems. The cylindrical physical model selected for this study embodies the key feature of convective airflow, which is the vertical movement of the air due to buoyancy.

3.3.2 Conceptual model

The compost bed in the vessel was considered to consist of layers, each having homogeneous physical and chemical properties (Figure 3-1). Microbial activity in each layer consumed oxygen (O_2) and released carbon dioxide (CO_2), heat, and moisture (H_2O). The airflow through the compost was considered to be uniform and unidirectional from bottom to top, removing heat, moisture, carbon dioxide, and volatile compounds.

The following assumptions were made for the development of the model equations:

1. Each layer was physically and chemically homogeneous in all respects.
2. Air was incompressible.

3. Air entered the bottom layer of compost uniformly, and airflow was uniform through each layer.
4. The mass flow rate of dry air was constant throughout the compost bed. The influence of oxygen consumption and carbon dioxide generation were negligible.
5. Air traveled through the compost bed in the vertical direction only.
6. The temperature of the air leaving each layer was the same as the substrate in that layer.

To be practical, a model should be able to predict the airflow rate given the values for a set of easy measurable input variables. Since natural convection derives from a temperature difference and air temperature can be easily measured compared with most other variables (Barrington *et al.*, 2003), temperature was incorporated into the model as an input. Other inputs included the permeability of the substrate, and the temperature and density of the ambient air. Based on the assumptions made in this work, the Ideal Gas Law and Archimedes' Principle were used to relate the temperature difference between the ambient air and the air in the compost bed to the buoyant force acting on the air. The derivation of this part of the model is detailed in the following section.

3.3.3 Analytical model of passive airflow: Fundamentals

In the simplest case, passive convection occurs when a fluid of constant viscosity and negligible compressibility is subjected to a temperature gradient. The creeping flow of an incompressible fluid through a porous medium (the compost) can be described by Darcy's law. Darcy's law is applicable when the Reynolds number (Re) is less than 1 (Equation 1) (Nield and Bejan, 1999).

$$\mathrm{Re} = \frac{\rho v \sqrt{K}}{\eta} \tag{1}$$

The buoyant force that drives the airflow is calculated using Archimedes' Principle: the buoyant force is equal to the weight of the displaced fluid. Given constant pressure, the change of volume of a unit of ideal gas is related to the change of temperature as shown in Equations 2 and 3:

$$\frac{V_0}{T_0} = \frac{V_i}{T_i} \tag{2}$$

$$V_0 = \frac{T_0}{T_i} V_i \tag{3}$$

The temperature of actively degrading compost is higher than ambient. In this model, the temperature of the air in the compost bed when it exits a given layer is assumed to be the same as that of the substrate in that layer, so that as a unit of air passes through the i^{th} layer in the compost it will undergo isobaric expansion from V_0 to V_i. The forces on this amount of air (Figure 3-2) are described by Equations 4-6.

$$F_{Bouyancy} = \rho_0 g V_i \tag{4}$$

$$G = \rho_0 g V_0 \tag{5}$$

$$F_i = F_{Buoyancy} - G = \rho_0 g (V_i - V_0) = \rho_0 g \left(1 - \frac{T_0}{T_i}\right) V_i \tag{6}$$

Compost can be viewed as a porous medium and Darcy's law is used to calculate average air velocity through the compost (Equation 7) for the sake of simplicity.

$$v = -\frac{K}{\eta} \frac{\Delta P}{\Delta y} \tag{7}$$

Assuming the volume of air in the i^{th} layer (V_i) has a height (H_i) that is the same as the thickness of the layer (Δy), and an effective cross-sectional area (A_i) that includes only that of the empty pore space in the compost, the pressure gradient over the thickness of the layer can be estimated from the net force distributed over the effective cross-sectional area (Equation 7.5). Substituting the last term in Equation 6 for F_i in Equation 7.5 and dividing the two sides of the equation by Δy (or the equivalent term H_i) gives Equation 8.

$$\Delta P = F_i / A_i \tag{7.5}$$

$$\frac{\Delta P}{\Delta y} = \left[\rho_0 g \left(1 - \frac{T_0}{T_i} \right) V_i \Big/ A_i \right] \Big/ H_i = \rho_0 g \left(1 - \frac{T_0}{T_i} \right) \tag{8}$$

Finally, substituting the simplified form of Equation 8 for the ratio denoting the pressure gradient in Equation 7 gives Equation 9.

$$v = -\frac{K}{\eta} \frac{\Delta P}{\Delta y} = -\frac{K}{\mu} \rho_0 g \left(1 - \frac{T_0}{T_i} \right) \tag{9}$$

3.3.4 Model inputs

To apply the proposed model (Equation 9), values for substrate permeability, air viscosity, temperature and density of ambient air, and temperature in the compost are required. The viscosity of air is well understood and well-developed theory can be readily employed to calculate the changing dynamic viscosity at different locations in the compost. The permeability of the composting material is a critical factor in the development of airflow, and the influence of substrate composition on the permeability is quite complex. A theoretical relationship between the geometry of the

substrate particles and the permeability of the substrate has been described elsewhere (Lynch and Cherry, 1996b). The application of this relationship is limited, however, since the measurement of the required parameters is not easy. Another approach is to use published results to estimate permeability, while also taking into account the effect of compaction. Since the determination of the permeability of the composting substrate was not the objective of this work, the latter approach was used, and is discussed further later in this paper. The temperature of the ambient air and the compost are convenient to measure. With measured values for the temperature and relatively humidity of the air, the density of the air can be calculated using psychrometric relationships (ASHRAE, 2001).

3.3.5 Changing substrate permeability: Compaction

As shown in Equation 9, the permeability of the substrate is required to predict the airflow rate. Neither the exact substrate permeability values nor the compaction of the compost were measured directly in this study. Instead, the permeability values were estimated from published results that relate measured values of bulk density, moisture content, and initial free air space. The effect of compaction was also considered in this estimate.

Firstly, the compressive stresses at different depths were calculated using Equation 10 (McCartney and Chen, 2000) from bulk density values measured using a pycnometer (Agnew *et al.*, 2003).

$$\sigma_i = \rho_s g d_i / 1000 \qquad (10)$$

Secondly, the resultant compaction at different depths was evaluated using Equation 11 (Das and Keener, 1997).

$$h_i = h_\infty + \Delta h_0 \cdot \exp(-\beta \cdot \sigma_i) \quad (11)$$

The result of Equation 11, h_i, gives the thickness of the i^{th} layer after compaction as a fraction of the initial thickness of the layer. The actual free air space (*FAS*) in the i^{th} layer (Equation 12) was then predicted using the initial free air space (FAS_0), measured with a pycnometer (Agnew *et al.*, 2003).

$$FAS = FAS_0 \cdot h_i \quad (12)$$

Richard *et al.* (2004) presented a relationship between FAS and the permeability of the substrate at different substrate moisture contents. This relationship was used to estimate permeability at different depths given the estimated FAS values from Equation 12 and the measured moisture content.

3.3.6 Verification of the proposed model: Experimental data

Verification of the model (Equation 9) was done using data from a composting trial. The trial was conducted in a passively aerated, insulated polyethylene vessel, with an aeration plenum under an expanded metal floor, an inlet pipe and an outlet pipe (Figure 3-1). The compost consisted of fresh dairy manure and bulking agents, i.e. wood chips, saw dust, and air-dried, ground straw. The mixture had a carbon to nitrogen ratio of 35:1, 57% free air space, a bulk density of 520 kg/m^3, and an initial moisture content of 76% (wet basis). At the beginning of the experiment, the depth of the compost in the vessel was 0.50 m. Temperatures at different positions above the

aeration plenum were recorded by an automated data logging system and the airflow rate was measured with smoke tracer and ultrasonic air flow meters (Yu *et al.*, 2005). The measured bulk density, initial moisture content, and free air space were used to estimate the permeability following the methodology discussed previously (Equations 10-12). The measured temperatures of the ambient air and the compost were used to predict the average air velocity using Equation 9. SAS 9.1 (SAS Inc., 2006) was used for statistical analysis and mixed model was employed for significant difference test of the calculated results and the measured data to evaluate the performance of the proposed model.

3.4 Results and discussion

The average ambient temperature was 23.3°C ± 2.2°C. The temperature histories at three locations in the compost are shown in Figure 3-3. Temperature histories in the middle of the compost followed a form typical of aerobic composting, increasing exponentially to more than 55°C and then gradually declining to about 40°C. The vertical temperature gradient in the compost (Figure 3-3) was the result of heat and mass transfer processes, which are strongly related to the local microbial activity in the substrate (Yu *et al.*, 2005). As described previously, the temperature of the air in the compost was assumed to be the same as measured substrate temperature (Figure 3-3).

The substrate permeability values were not measured directly but estimated using published results, as summarized previously. The measured initial bulk density was 520 kg/m^3, so that Equation 10 can be written as:

$$\sigma_i = 520 \times 9.8 \times d_i / 1000 \quad (13)$$

Substituting the depth values into Equation 13 gave the corresponding compressive forces.

The compressive force was substituted into Equation 11 together with coefficient values (h_∞, Δh_0, and β) estimated using the data reported by Das and Keener (1997), and the measured substrate moisture content (76%). These substitutions resulted in Equation 14, which was used to estimate the compression of each layer.

$$h_i = 0.586 + 0.141 \cdot \exp(-0.114 \cdot \sigma_i) \quad (14)$$

The free air space (*FAS*) at each layer after compaction was then calculated using the measured initial free air space ($FAS_0 = 0.57$) (Equation 12). Finally, the permeability of different depths was estimated using information presented by Richard *et al.* (2004, Figure 4) with the calculated free air space values and initial moisture content.

The measured and modeled airflow rates through the compost are shown in Figure 3-4. The measured airflow rate followed the general pattern of temperature change typical of composting (Figure 3-4), peaking at about 100 h and then gradually declining, illustrating the temperature-driven nature of the convective airflow. The peak airflow rate measured was 11.1 ± 5.1 mg dry air per s per kg initial dry matter (mg d.a. s^{-1} kg^{-1} i.d.m.). In comparison, Barrington *et al.* (2003) reported airflow rates from 1.5 to 0.7 mg d.a. s^{-1} kg^{-1} i.d.m. in passively aerated compost, and Liang *et al.* (2004) used a flow rate of 5.6 mg d.a. s^{-1} kg^{-1} i.d.m. in an actively aerated vessel. The calculated airflow rate followed a similar trend to, and was not significantly different from, the measured data ($p = 0.97$).

The assumptions under which this model was developed are very idealized: the air was assumed to be an Ideal Gas and the mass of the air was assumed to be constant through the compost bed. Phenomena such as the evaporation of moisture from the substrate and volatilization of the substrate, consumption of oxygen, and release of carbon dioxide by microbial activity were not considered. In reality, however, these processes do occur during composting, and further research is required to quantify and model their effect on convective airflow development.

Another possible improvement of the model would be to incorporate effects of drag on airflow, using a term such as the Dupuit-Forcheimer relationship (Richard *et al.*, 2004; Lage and Antohe 2000). The current use of Darcy's law, in which only viscous resistance to airflow is considered, is appropriate for the low-rate, laminar flows observed in small-scale, passively aerated systems. Larger-scale systems are more likely to develop higher flow rates, however, and resistance due to drag would become more dominant. Relationships based on the physical characteristics of the substrate might also be used to estimate airflow parameters such as permeability (Richard *et al.*, 2004; Ergun, 1952). Finally, the accurate measurement of the air velocity through the compost bed is required for the verification of any model. Measuring airflow in passively aerated compost is more challenging than in actively aerated systems, since the airflow is variable and is influenced by the microbial activity in the compost. As pointed out elsewhere (Yu *et al.*, 2005), the instrument used for such measurements must be effective and accurate over a wide range and introduce little pressure loss. Accurate airflow measurement in passively aerated compost is an area that must be

better developed in order to effectively validate models such as the one presented here.

The permeability of the substrate is another critical variable that must be accurately determined to improve the accuracy of models. Measurements of permeability have been done mainly under forced aeration (Das and Keener, 1997; Richard *et al.*, 2004). It is generally assumed that all the void space in the substrate is filled with air and that air is free to move through all of that space. As pointed out elsewhere, however, some void space in the composting substrate may not be available for air flow development (Eftoda and McCartney, 2004). Moreover, considering the heterogeneous and compressible nature of compost, it is very likely that some of the air in the void space does not move with the air flow. A model of such 'unsaturated' air flow might therefore be considered in further research to improve the prediction of average air velocity through compost.

3.5 Conclusions

In summary, passively aerated composting systems have proven to be more economical than active aeration systems while delivering similar performance, but mathematical descriptions of such systems are scarce, hindering the design and optimization of the process. A model was proposed to address a critical factor in modeling passively aerated systems: the airflow development. The model was developed to relate the physical characteristics and temperature of the compost with the predicted air flow, and the compaction which occurs during composting was also taken into account in the application of the model. The model was verified by using temperature histories from a passively aerated composting experiment to predict

airflow, and the calculated airflow values were not significantly different from measured values ($p = 0.97$).

3.6 References

Agnew J M; Leonard J J; Feddes J; Feng Y (2003) A modified air pycnometer for compost air volume and density determination. *Canadian biosystems engineering*, 45(6), 27-35

American Society of Heating, Refrigerating and Air-Conditioning Engineers (ASHRAE) (2001) Psychrometrics. In *Handbook of Fundamentals*, ed. ASHRAE, 6.1-6.17. Atlanta, GA: ASHRAE.

Barrington S; Choiniere D; Trigui M; Knight W (2003) Compost convective airflow under passive aeration. *Bioresource technology*, 86(3), 259-266

Das K; Keener H M (1997) Moisture effect on compaction and permeability in composts. *Journal of environmental engineering – ASCE*, 123(3), 275-281

Eftoda G; McCartney D (2004) Determining the critical bulking agent requirement for municipal biosolids composting. *Compost science & utilization*,12(3), 208-218

Ergun S (1952) Fluid flow through packed columns. Chem. Eng. Prog., 48, 89-94

Fernandez L; Sartaj M (1997) Comparative study of static pile composting using natural, forced and passive aeration methods. *Compost Science & Utilization*, 5(4), 65-77

Fogiel A C; von Bernuth R D; Michel F C Jr.; Louden T L (1999) Experimental verification of the natural convection transfer of air through a dairy manure compost media. *Proceedings of the International Meeting of the American Society of Agricultural Engineers*; ASAE, St. Joeseph, MI: 1999; ASAE paper no. 994053

Geankoplis C J (1993) Transport processes and unit operations. 3rd ed. Prentice Hall, Engelwood Cliffs, N.J. 921p

Haug R T (1993) The Practical Handbook of Compost Engineering. Boca Raton. Lewis Publishers. 717 p

Lage J L; Antohe B V (2000) Darcy's experiments and the deviation to nonlinear flow regime. *ASME J. Fluids Eng*, 122, 619-625

Lynch N J; Cherry R S (1996a) Winter composting using the passively aerated windrow system. *Compost Science & Utilization*, 4(3), 44-52

Lynch N J; Cherry R S (1996b) Design of passively aerated compost piles: vertical air velocities between pipes. *Biotechnology Progress*, 12(5), 624–629

McCartney D; Chen H T (2001) Using a biocell to measure effect of compressive settlement on free air space and microbial activity in windrow composting. *Compost science & utilization*, 9(4), 285-302

McCartney D; Eftoda G (2005) Windrow composting of municipal biosolids in a cold climate. *Journal of environmental engineering and science*, 4(5), 341-352

Nield D A; Bejan A (1999) Convection in porous media. 2nd ed. Springer, New York. 546p.

Richard T L; Veeken A H M; de Wilde V; Hamelers H V M (2004) Air-filled porosity and permeability relationships during solid-state fermentation. *Biotechnology progress*, 20(5), 1372-1381

Solano M L; Iriarte F; Ciria P; Negro M J (2001) Performance Characteristics of Three Aeration Systems in the Composting of Sheep Manure and Straw. *Journal of Agricultural Engineering Research*, 79(3), 317-329

Yu S; Clark O G; Leonard J J (2005) Airflow measurement in passively aerated compost. *Canadian biosystems engineering*, 47(6), 39–45

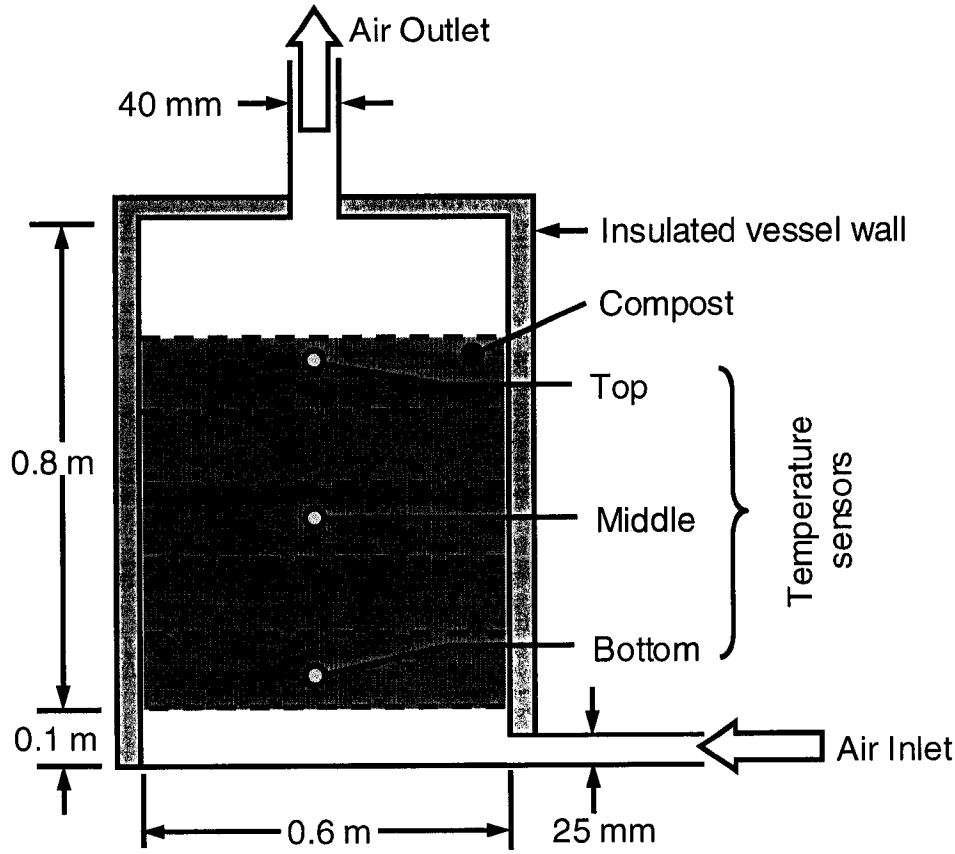

Figure 3-1. Schematic of the physical model of passively-aerated compost

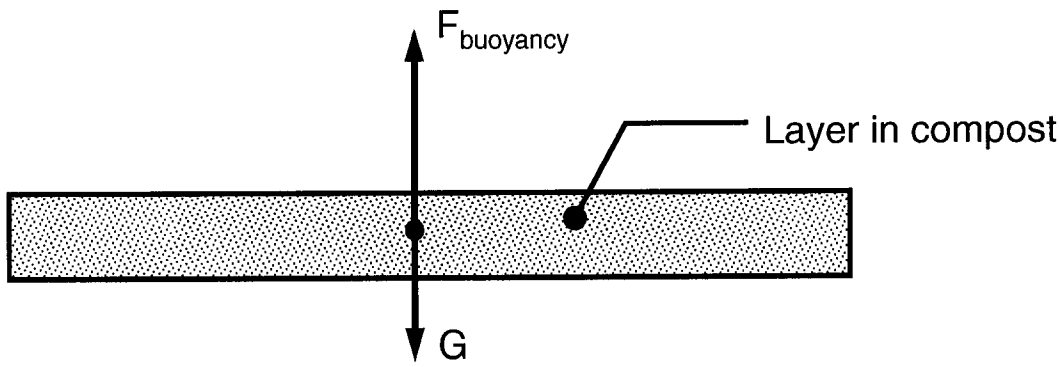

Figure 3-2. Schematic of the forces on the air in a single compost layer

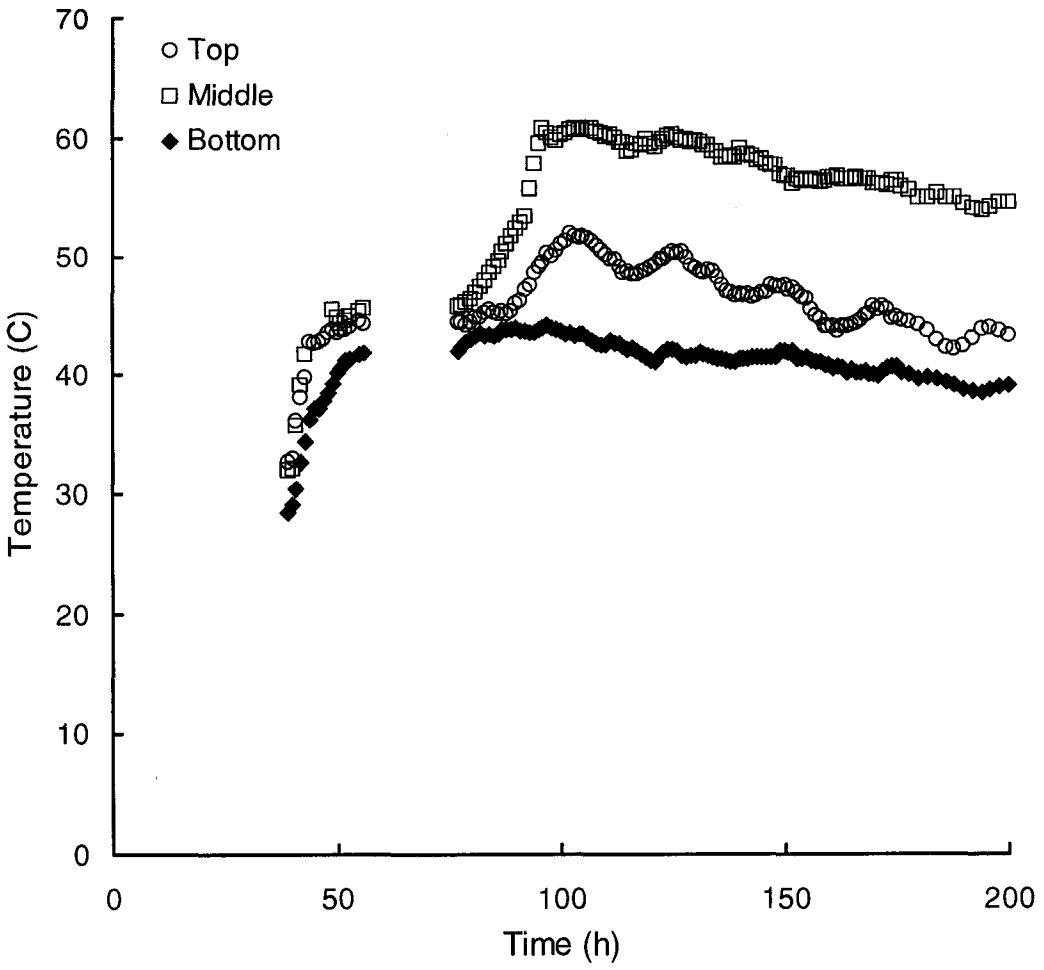

Figure 3-3. Temperature histories in the bottom, middle, and top of the compost bed

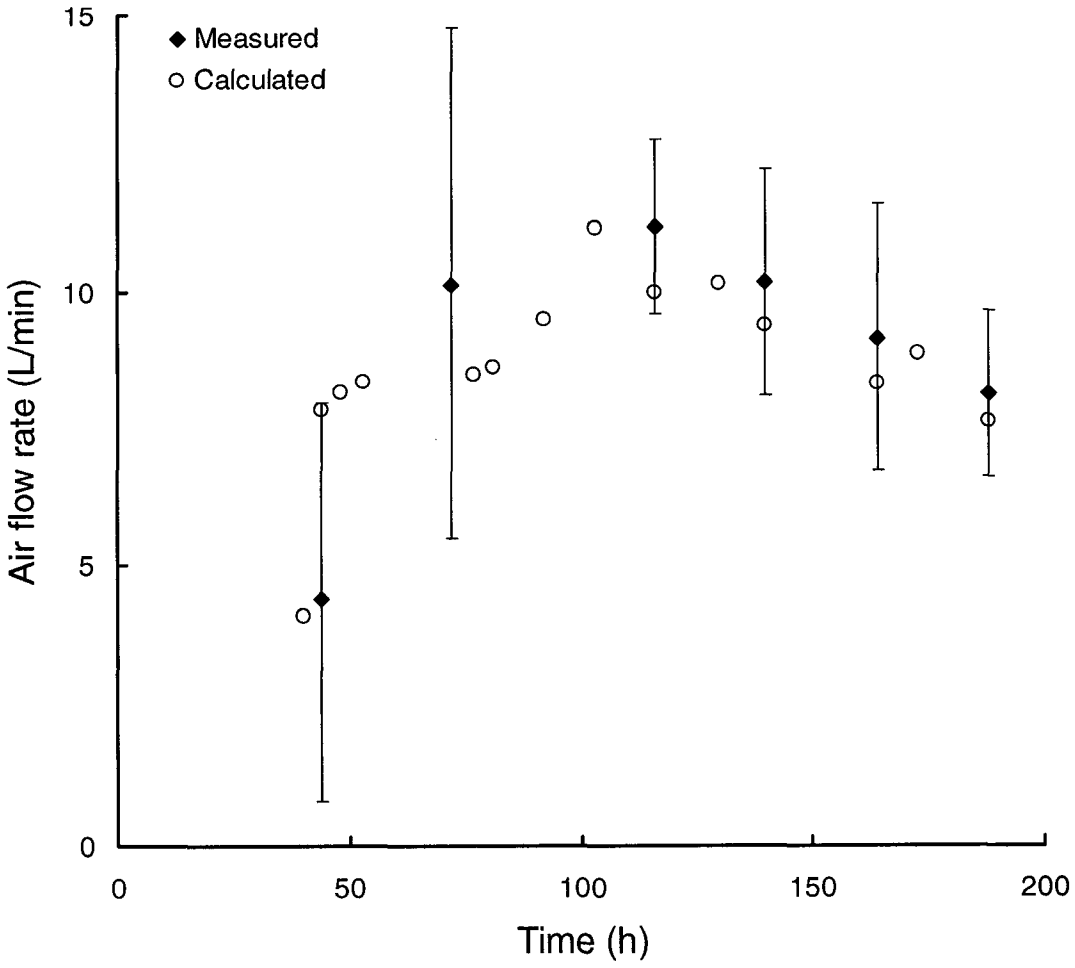

Figure 3-4. Measured and calculated air flow rates through the compost

Chapter 4 A statistical method for the analysis of nonlinear temperature time series from compost [†]

4.1 Introduction

Composting is the controlled, aerobic decomposition of organic matter by a consortium of microorganisms. It is a common technology believed to have been used since ancient times to recycle farm waste, such as animal manure and straw (Rynk, 1992). In addition to being an environmentally sustainable method of waste management, composting also has a potential role in solving various current environmental problems (EPA, 1997).

Heat production during composting is almost completely derived from biological activity (Finstein and Morris, 1975; Kutzner, 2001). The temperature of compost is an easily measured indicator of this biological activity because it changes in direct response to heat production. Temperature can therefore be used to assess the progress of decomposition and thus the performance of a composting system. Compost temperature is often used as the observed variable in process control, and to distinguish the effects of different experimental treatments in research.

The composting process is inherently variable, and so statistical analysis of the compost temperature measurements is used to detect the effect of various influencing factors. As in any statistical analysis, two fundamental questions need to be addressed to ensure that meaningful inferences are drawn from compost temperature data: (a)

[†] A version of this chapter has been submitted for publication as: Yu, Shouhai, O.G. Clark, J.J. Leonard. 2006. A statistical method for the analysis of nonlinear temperature time series from compost. *Bioresource Technology* (in review).

What is an appropriate mathematical model to describe the data? (b) How can the significance of any differences among different datasets be rigorously determined? Meaningful statistical analysis of compost temperature time series, as with any data, must be based on an adequate mathematical model (Judge et al., 1988). Composting is a highly time-correlated, auto-correlated, nonlinear process, and a compost temperature time series typically reflects this. Since temperature change in composting is nonlinear with respect to time, a nonlinear mathematical model should be used as the basis for statistical analysis. To date, however, the statistical methods used in the analysis of compost temperature data have generally been based on essentially linear mathematical models. To the best knowledge of the authors, the use of a nonlinear model in this context has never been reported.

In the past, Student's t-test and analysis of variance (ANOVA) have been typical choices for the statistical analysis of compost temperature data, but neither method takes time effects into account. Generally, only the mean temperature over the whole experiment period (Liang et al., 2003; Zhu et al., 2004) or the mean temperatures during certain periods (Schloss et al., 2000) are compared. The averaging of the temperature time series in this way collapses the information it contains into a single thermodynamic index, and this can be misleading. For example, the overall means of the four curves shown in Figure 4-1 are the same for the time period 0 to t. The inference that would be drawn from such a characterization of these very different curves would be that they do not differ statistically from one another.

The complete temperature time series of a composting trial contains not just coarse thermodynamic indicators, but detailed microbial kinetic information. The

temperature signal responds sensitively to microbial dynamics because the rate of change of the compost temperature results directly from microbial heat production. This time-correlated, auto-correlated, nonlinear information can be extracted from the temperature data using an appropriate mathematical model. Statistical methods in which the data are treated as instances of categorical variables are not satisfactory for this purpose, nor are those based on linear mathematical models. Fortunately, many nonlinear functions can now be easily implemented in statistical analysis (Freund and Littell, 2000), and an appropriate choice for describing compost temperature time series is discussed in this article.

Nonlinear functions can be fit to datasets using algorithms which are available in common statistical packages such as SAS®. When such curve-fitting algorithms are used, however, special care must be taken in determining the initial values because they can radically impact the fit of the model. A poor starting point can result in a divergent or incorrect solution (Motulsky and Ransnas, 1987). It is also important to be able to objectively quantify the goodness-of-fit of the resulting model in order to determine its utility as compared to other possible models. Methods for achieving these goals are presented later in this article.

A final critical requirement, as mentioned previously, is that a method must be available to determine the significance of any differences between datasets once an appropriate mathematical model has been fitted to them. This is the second major theme in this work.

4.2 Objectives

Meaningful statistical inference must be based on adequate and appropriate mathematical models of the data being examined. Compost temperature time series are non-linear, time-correlated, and auto-correlated, and a mathematical function with similar properties is therefore required to represent them. The first major objective of this work is to define such a function. A method of fitting the function to data using SAS® (Freund and Littell, 2000) is also discussed, as are the determination of initial values and tests for goodness-of-fit. Since the ultimate goal of statistical analysis is to determine the significance of any differences among datasets, a second major objective is to develop a method for the rigorous statistical comparison of different instances of the mathematical model after it has been fit to different datasets. The application of these methods is demonstrated through the analysis of two temperature time series from passively aerated composting trials.

4.3 Methods

4.3.1 What is an appropriate model for the temperature time series?

The temperature time series of aerobic composting (Epstein, 1997; Haug, 1993) is typically similar in form to the classical microbial population growth curve (Shuler and Kargi, 1992) (Figure 4-2). Considering the similarity of the shape and the underlying generative mechanism, the mathematical description of microbial growth may be used as a reference for the development of a function to describe the temperature time series in composting. Many functions, such as the logistic, Gompertz, Richards, and Weibull functions, have been widely used to describe

microbial growth (Zeide, 1993). The Gompertz equation (Equation 1) was selected as the basis for this work because it is simple and requires relatively few parameters, while its descriptive power is still comparable to other logistic functions (Winsor, 1932),

$$f(t) = a \cdot e^{-e^{-b \cdot (t - t_m)}} \tag{1}$$

The Gompertz equation can be used to model the first four phases of classical microbiological growth as shown in Figure 4-2(a) (Bratchell et al., 1989). In this function, the maximum rate of increase, b, occurs at the time of inflection, t_m, where the value of the function is a/e, about one-third of the maximum, a.

The Gompertz model, as with most mathematical depictions of microbial dynamics, depicts only the first four phases of the growth curve. Little attention has been paid to the development of a model describing the overall growth curve which includes decay. In composting, however, the complete processing of the feedstock into the final product involves the accelerating, decelerating, stationary, and decaying phases of microbial dynamics. Description of the entire temperature curve therefore necessitates a more sophisticated description than a simple Gompertz model. Numerous species of microorganism are present in a composting pile and the microbial variety and density change with temperature and nutrition (Epstein, 1997). It is reasonable, therefore, that a more complete description of microbial dynamics would include several concurrent growth and decay curves corresponding to the major microbial cohorts. This idea is further supported by the marked transition from the mesophilic to the thermophilic stages that is commonly observed during studies of high-rate composting (Sundberg et

al., 2004). The plateau in the example temperature time series used here (Figure 4-2(b)) reflects this typical transition. To adequately illustrate this phenomenon, a model must distinguish between mesophilic and thermophilic microbial activity.

The proposed model, therefore, is based on the understanding that compost temperature responds to heat production from the growth and decay of different microbial cohorts in the compost. The compost is assumed to be at ambient temperature when the composting process starts. Growth of mesophilic microbes is rapid during the initial, high-rate composting stage, heat is generated, and the compost temperature rises. Mesophilic microbial population declines as the temperature of the compost reaches about 40°C, and thermophilic microbes begin to dominate. A discontinuity is often seen in the temperature during this transition from mesophilic to thermophilic cohorts (Epstein, 1997). Finally, the microbes exhaust the easily available nutrient sources in the compost and their populations begin to decline. Heat production drops off and a drop in temperature follows.

The proposed model of this typical compost temperature time series is shown in Equation 2:

$$T(t) = T_a + T_{hm} \cdot e^{-e^{-k_{hm} \cdot (t - t_{hm})}} + T_{ht} \cdot e^{-e^{-k_{ht} \cdot (t - t_{ht})}} - T_c \cdot e^{-e^{-k_c \cdot (t - t_c)}} \quad (2)$$

T_a Ambient temperature

T_{hm} Heating potential of the mesophilic stage

T_{ht} Heating potential of the thermophilic stage

T_c Cooling potential

t_{hm} Time when maximum mesophilic heating rate occurs

t_{ht} Time when maximum thermophilic heating rate occurs

t_c Time when maximum cooling rate occurs

k_{hm} Maximum mesophilic heating coefficient

k_{ht} Maximum thermophilic heating coefficient

k_c Maximum cooling coefficient

The first term in Equation 2, T_a, provides a "base-line" corresponding to the start temperature of compost, which is assumed here to be the same as the ambient and end temperatures. The second term (T_{hm}·exp[-exp(-k_{hm}(t-t_{hm}))]) describes the temperature increase due to the accumulation of heat from mesophilic microbial activity in the compost pile. The third term (T_{ht}·exp[-exp(-k_{ht}(t-t_{ht}))]) describes the temperature increase due to heat generated by thermophilic microbial activity. The fourth term (T_c·exp[-exp(-k_c(t-t_c))]) represents the temperature decline during microbial decay. In this context, T_{hm} is the maximum temperature increase above ambient in the compost pile during the mesophilic stage and T_{ht} is the maximum temperature increase above the mesophilic plateau during the thermophilic stage. T_c is the difference between the combined maximum temperature and the ambient temperature, indicating the magnitude of the temperature drop from the time of maximum activity to compost maturity.

The curve described by Equation 2 is shown in Figure 4-3. Given appropriate parameter values, this function is very representative of the typical temperature time series shown in Figure 4-2 (b). Kinetic information, such as the maximum intensity of mesophilic and thermophilic activity, the rate of increase of microbial activity through the mesophilic and thermophilic stages, and the duration of these stages, are all

reflected in the parameters of the model. The function (Equation 2) can therefore flexibly represent a wide variety of temperature time series. It cannot describe temperature time series that include re-heating or mixing events, although additional terms could be included to accommodate such events.

4.3.2 How to fit the model to data: Determination of initial parameter values

To solve a nonlinear equation like Equation 2, initial estimates of the parameter values are required. A good choice of initial values is critical since a poor starting point can result in divergence or a wrong solution (Motulsky and Ransnas, 1987). Although no algorithm is currently available in SAS® to help select good starting values (Freund and Littell, 2000), it is possible, in practice, to objectively select initial parameters values.

As illustrated in Figure 4-3, the part of the function corresponding to mesophilic heating can be approximated by Equation 3 because the third (T_{ht}·exp[-exp(-k_{ht}(t-t_{ht}))]) and the fourth (T_c·exp[-exp(-k_c(t-t_c))]) terms in Equation 2 have small values during this stage. A reasonable initial estimate for the coefficient T_{hm} (T_{hm}^0) is the asymptote of the second term in Equation 2, which is the difference between ambient temperature and the highest temperature during the mesophilic heating stage.

$$T_1(t) = T_a + T_{hm} \cdot e^{-e^{-k_{hm} \cdot (t - t_{hm})}} \qquad (3)$$

Equation 3 can be log-transformed twice to linearize its form, as demonstrated in Equations 4 through 7. The original temperature data can then be transformed using the left sides of Equation 7 to generate a new dataset on Y_{hm}. The slope (k_{hm}^0) of the resulting line can be used as an initial estimate for the mesophilic heating coefficient

(k_{hm}), and the offset on the time axis (t_{hm}^0) as an initial estimate for the time of heat inflection (t_{hm}).

$$\ln(T_1(t)-T_a)=\ln\left(T_{hm}\cdot e^{-e^{-k_{hm}\cdot(t-t_{hm})}}\right)=\ln T_{hm}-e^{-k_{hm}\cdot(t-t_{hm})} \tag{4}$$

$$-(\ln(T_1(t)-T_a)-\ln T_h)=-\ln\frac{T_1(t)-T_a}{T_h}=e^{-k_h\cdot(t-t_h)} \tag{5}$$

$$\ln\left(-\ln\frac{T_1(t)-T_a}{T_{hm}}\right)=\ln e^{-k_{hm}\cdot(t-t_{hm})}=-k_{hm}\cdot(t-t_{hm}) \tag{6}$$

$$\ln\left(-\ln\frac{T_1(t)-T_a}{T_{hm}^0}\right)=-k_{hm}^0\cdot(t-t_{hm}^0) \tag{7}$$

$$Y_{hm}=-k_{hm}^0\cdot(t-t_{hm}^0) \tag{8}$$

T_{hm}^0 Initial estimate for the heating potential T_{hm}

k_{hm}^0 Initial estimate for maximum heating coefficient k_{hm}

t_{hm}^0 Initial estimate for the time of heat inflection t_{hm}

Similarly, the thermophilic heating stage can be approximated by Equation 9 since, during this stage, the second term in Equation 2 has approached its asymptote (T_{hm}) and can be approximated by a constant, and the value of the fourth term in Equation 2 is still negligible. A reasonable initial estimate for the coefficient T_{ht} (T_{ht}^0) is the asymptote of the third term in Equation 2, which is the difference between the maximum temperatures during the thermophilic and mesophilic heating stages. Equation 9 can be linearized by two log-transformations to obtain Equation 11. The

original temperature data can then be transformed using the left side of Equation 10 to generate a new dataset on Y_{ht} and find initial estimates of k_{ht} and t_{ht}.

$$T_2(t) = T_a + T_{hm} + T_{ht} \cdot e^{-e^{-k_{ht} \cdot (t - t_{ht})}} \tag{9}$$

$$\ln\left(-\ln\frac{T_2(t) - T_a - T_{hm}^0}{T_{ht}^0}\right) = -k_{ht}^0 \cdot \left(t - t_{ht}^0\right) \tag{10}$$

$$Y_{ht} = -k_{ht}^0 \cdot \left(t - t_{ht}^0\right) \tag{11}$$

T_{ht}^0 Initial estimate for the heating potential T_{ht}

k_{ht}^0 Initial estimate for maximum heating coefficient k_{ht}

t_{ht}^0 Initial estimate for the time of heat inflection t_{ht}

The decay stage of the function can be approximated by Equation 12 because both heating terms in Equation 2 have by this time approached their asymptotes, T_{hm} and T_{ht}, and can be approximated by constants. The initial value of the coefficient T_c (T_c^0) can be estimated by summing T_{hm}^0 and T_{ht}^0, which is the difference between the combined maximum and ambient temperatures. Equation 12 can be linearized by two log-transformations to obtain Equation 14. The original temperature data can then be transformed using the left side of Equation 13 to generate a new dataset on Y_c and find initial estimates of k_c and t_c.

$$T_3(t) = T_a + T_{hm} + T_{ht} - T_c \cdot e^{-e^{-k_c \cdot (t - t_c)}} \tag{12}$$

$$\ln\left(-\ln\frac{T_a + T_{hm}^0 + T_{ht}^0 - T_3(t)}{T_c^0}\right) = -k_c^0 \cdot \left(t - t_c^0\right) \tag{13}$$

$$Y_c = -k_c^0 \cdot \left(t - t_c^0\right) \tag{14}$$

T_c^0 Initial estimate for the cooling potential T_c

k_c^0 Initial estimate for the maximum cooling coefficient k_c

t_c^0 Initial estimate for the time of cooling inflection t_c

To illustrate this method, the transformation of data from a temperature sensor at the bottom of a passively aerated composting vessel (Figures 4-3 and 4-4 (a)) and its subsequent linear regression (Figure 4-5 (b), (c), and (d)) were used to obtain initial estimates of k_{hm}, t_{hm}, k_{ht}, t_{ht}, k_c, and t_c (Equation 15 – 17):

$$-0.2606 \cdot t + 10.419 = -k_{hm}^0 \cdot \left(t - t_{hm}^0\right) \tag{15}$$

$$-0.0949 \cdot t + 7.1437 = -k_{ht}^0 \cdot \left(t - t_{ht}^0\right) \tag{16}$$

$$-0.0069 \cdot t + 1.7837 = -k_c^0 \cdot \left(t - t_c^0\right) \tag{17}$$

4.3.3 Why trust the model? Tests of goodness-of-fit and normality

The goodness-of-fit of the model can be evaluated using the R-squared (R^2) statistic, which is a popular indicator of goodness-of-fit in regression analysis. Although not given directly in the NLIN procedure of SAS®, R^2 can be calculated from the variance statistics that are reported for the regression (Freund and Littell, 2000). Referring to the nonlinear regression results for the temperature data used in the previous example (Table 4-2), R^2 can be calculated using Equation 18.

$$R^2 = \frac{SS_{Model}}{SS_{Total}} = \frac{217587}{217615} \times 100\% \cong 99.99\% \tag{18}$$

Deviance, which is the average deviation of the residuals from zero, is another important indicator of the goodness-of-fit of a nonlinear model. A residual is the difference between the measured and modeled values for a given data point. Student's

t-test is used to evaluate a given model based on deviance, with the null hypothesis that the overall mean of the residuals does not differ significantly from zero ($\mu_0 = 0$), given the chosen α value. If the resulting *p* value of the test is greater than α, then the null hypothesis is accepted, meaning that the modeled values closely approximate the observed values. Rejection of the null hypothesis implies that the modeled values do not closely approximate the observed values, and the model should be improved accordingly.

A normality test of the residuals is also necessary when testing goodness-of-fit, since the above methods are based on the assumption of normally distributed residual values. A non-normal distribution of the residuals could be caused by outliers in the observed data, in which case the outlying values might be removed from the data. If there is a lack of normality that is not due to outliers, then adequacy of the model needs to be re-assessed and the model may be need to be modified to include other factors.

4.3.4 How to test rigorously for differences among datasets

Once the mathematical model is chosen, fitted to the data, and tested for goodness-of-fit, the next step is to test for significant differences among treatments. A statistical procedure based on the extra sums of squares principle can be used to test the significance of any differences between the models as they have been fitted to the temperature time series (Draper and Smith, 1966). In this procedure, the data are analyzed in two different ways and the analyses are compared. In the first analysis, a single, combined model (Equation 2) is fitted to all of the data, including all of the temperature time series to be compared. In essence, the temperature measurements are

treated as though they were all derived from a single population of data. The result of this first, combined analysis is a single mathematical function fitted to all the data. The differences (residuals) between the experimental data and the corresponding points on the fitted curve are calculated. The sum of the squared residuals is calculated as a measure of the variation not accounted for by the combined model. The sum is then divided by the number of degrees of freedom of the combined model used to obtain the mean sum of square error (MSE_c). In the second analysis, individual models, of the same general form, are fitted to each of the temperature time series by calculating a separate set of model parameter values for each, under the assumption that each temperature time series is derived from a different population of data. The result of this second, individual analysis is, therefore, a set of several fitted mathematical functions, one corresponding to each of the different time series. The combined sum of the squared residuals of all these several individual models is calculated and divided by the combined degrees of freedom to obtain the MSE_i. An F test can then be performed based on the two mean sums of squares (Equation 19).

$$F = \frac{\dfrac{MSE_c - MSE_i}{\nu_i - \nu_c}}{\dfrac{MSE_i}{n - \nu_i}} \text{ with } df = \nu_i - \nu_c,\ n - \nu_i \qquad (19)$$

MSE_c Mean residual sum of squares for the simple model

MSE_i Mean residual sum of squares for the complex model

ν_c Number of unknown parameters in the simple model

ν_i Number of unknown parameters in the complex model

n Number of observations.

The null hypothesis in this test is that there is no difference between the two sums. If the p value corresponding to the calculated F value is greater than the selected α, then the null hypothesis is accepted. If this is the case, then there is no significant difference between the ability of the combined and individual models to describe the variability of the observed data. Neither the models nor the datasets that they describe can be considered different from one another. If the null hypothesis is rejected, however, then the fitting of individual models to the datasets is shown to significantly increase the ability of the models to capture the variation in the observed data. In other words, the datasets as represented by the models can be considered to be significantly different from one another. The same methodology can also be used to perform pair-wise comparison of temperature time series for a more detailed analysis of any differences.

4.4 Results

4.4.1 An example of how this works: Experimental data for model calibration

An in-vessel composting experiment was conducted using passive aeration, a description of which is published elsewhere (Yu et al., 2005). Temperatures at different positions above the aeration plenum (Figure 4-3) were recorded by an automated data logging system. The NLIN procedure in SAS® (Freund and Littell, 2000) was used to perform the curve fitting, and the program was written as shown in Appendix I.

The temperature time series from two locations in the compost vessels and the corresponding fitted curves are shown in Figure 4-5 (e). The temperature time series

followed a form typical of aerobic composting, increasing exponentially to about 65°C, including the commonly-observed transition between the mesophilic and thermophilic stages, and then gradually declining to about 40°C. The proposed function (Equation 2) was fitted to these data using initial values determined as shown in Figure 4-5 (b), (c), and (d). The results of the curve fitting process are summarized in Table 4-1.

4.4.2 Test of goodness-of-fit and normality

The results of the test of deviance (Table 4-3) show that the overall means of the residuals were zero, meaning the fitted model passed through the observed values well. The residuals of the model of the bottom temperature time series were normally distributed (Table 4-3), while those for the middle layer were not, implying the need for careful examination of the dataset and cautious application of the fitted model. Figure 4-5 (f) shows that there were a few outliers (grey points) that skewed the residual distribution. The removal of the outliers makes the distribution of the residuals return to normality.

4.4.3 Test of difference among datasets

Equation 2 was used as a combined model for all of the experimental data, and an individual model was constructed as shown in Equation 20.

$$\begin{aligned} T(t) &= T_a \\ &+ (T_{hm1} + d \cdot dT_{hm2}) \cdot e^{-e^{-(k_{hm1} + d \cdot dk_{hm2}) \cdot [t - (t_{hm1} + d \cdot dt_{hm2})]}} \\ &+ (T_{ht1} + d \cdot dT_{ht2}) \cdot e^{-e^{-(k_{ht1} + d \cdot dk_{ht2}) \cdot [t - (t_{ht1} + d \cdot dt_{ht2})]}} \\ &- (T_{c1} + d \cdot dT_{c2}) \cdot e^{-e^{-(k_{c1} + d \cdot dk_{c2}) \cdot [t - (t_{c1} + d \cdot dt_{c2})]}} \end{aligned} \quad (20)$$

d Indicator variable (0 or 1)

In the first, combined analysis, all of the data are considered to be from one population, and the model (Equation 2) is fit accordingly. In the second, individual analysis, the data from each of two temperature sensors are considered to be distinct, and a model is fit separately to each of the two datasets. Here, an indicator variable is used to distinguish the parameter values corresponding to the two different datasets. For parameter values corresponding to data from the bottom sensor (Figure 4-5), the indicator variable d is assigned the value 0, while for parameter values corresponding to temperature data from the middle sensor the indicator variable is set to 1. The implementation of this test in SAS® is shown in Appendix II. A summary of the ANOVA table associated with the regressions is shown in Table 4-4 and the calculation of the F value is shown below (Equation 21).

$$F = \frac{\frac{MSE_s - MSE_c}{v_c - v_s}}{\frac{MSE_c}{n - v_c}} = \frac{\frac{56.0085 - 0.3234}{18 - 8}}{\frac{0.3234}{254 - 18}} \cong 4061 \text{ with } df = 10, 236 \qquad (21)$$

When the two analyses in this test are compared the null hypothesis is rejected ($p \leq 0.0001$), and the two datasets are shown to be significantly different. This is to say that it is advantageous to fit a model separately to each of the two temperature time series, instead of fitting only one model to all of the temperature data.

4.5 Conclusions

In conclusion, the proposed nonlinear mathematical model can be used for characterizing the highly time-correlated, autocorrelated temperature time series typical of composting. The implementation of a nonlinear curve fitting procedure

using SAS® was elaborated, together with methods for the objective determination of initial model parameter values and tests of goodness-of-fit. Furthermore, a method was described for rigorously testing the significance of differences among temperature time series modeled in this way. The usefulness of these methods was demonstrated by fitting models to different temperature time series from a composting experiment and then testing for significant differences between them.

The mathematical model can be fit to any temperature time series of the general form shown in Figure 4-2 (b). With appropriate modification, it could also be fit to temperature time series that include re-heating events. The model cannot, however, accommodate discontinuous data such as those from compost trials that involve turning and/or re-mixing.

It is speculated that the fitted coefficients of the proposed equation (Equation 2) might be useful indicators of the interaction between microbial activity and feedstock properties (e.g., carbon:nitrogen ratio and free air space), as expressed indirectly though temperature. Further research is required, however, to establish the relationship between the parameter values and physical quantities. Based on this understanding, a novel way of characterizing the physical process of composting might be developed.

The authors do not claim that Equation 2 is the only nonlinear equation appropriate for describing a compost temperature time series, but firmly maintain that the time-correlated information contained in such a temperature time series should not be ignored.

4.6 References

Bratchell, N., Gibson, A.M., Truman, M., Kelly, T.M., Roberts, T.A., 1989. Predicting microbial-growth – the consequences of quantity of data. International Journal of Food Microbiology. 8, 47–58.

Draper, N.R., Smith, H., 1966. Applied regression analysis. Wiley: NY.

EPA (Environmental Protect Agency), 1997. Innovative uses of compost bioremediation and pollution prevention. EPA bulletin – EPA530-F-97-042.

Epstein, E., 1997. The science of composting; Technomic Pub. Co.: Lancaster, PA.

Finstein, M.S., Morris, M.L., 1975. Microbiology of municipal solid waste composting. Advance in Applied Microbiology. 19, 113–151.

Freund, R.J., Littell, R.C., 2000. SAS system for regression. SAS Institute: Cary; N.C.

Haug, R.T., 1993. The practical handbook of compost engineering. Lewis Publishers: Boca Raton.

Judge, G.G., Hill, R.C., Griffiths, W.E., H Lütkepohl, H., Lee T.C., 1988. Introduction to the theory and practice of econometrics. 2nd Ed.; Wiley: NY.

Kutzner, H.J., 2001. Microbiology of composting. In Biotechnology, Vol. 11c; Wiley: NY, pp 35–100.

Liang, C., Das, K.C., McClendon, R.W., 2003. The influence of temperature and moisture contents regimes on the aerobic microbial activity of a biosolids composting blend. *Bioresource Technology*. 86(2), 131–137.

Motulsky, H.J., Ransnas, L.A.,1987. Fitting curves to data using nonlinear-regression - a practical and nonmathematical review. Faseb Journal. 1, 365–374.

Rynk, R., 1992. On-farm composting handbook. Northeast Regional Agricultural Engineering Service: Ithaca, NY.

Schloss, P.D., Chaves, B., Walker, L.P., 2000. The use of the analysis of variance to assess the influence of mixing during composting. Process Biochemistry. 35, 675–684.

Shuler, M.L., Kargi, F., 1992. Bioprocess engineering: basic concepts. Prentice Hall: Englewood Cliffs, NJ.

Sundberg, C., Smars, S., Jonsson, H., 2004. Low pH as an inhibiting factor in the transition from mesophilic to thermophilic phase in composting. Bioresource Technology. 95, 145–150.

Winsor, C.P., 1932. The Gompertz curve as a growth curve. Proceedings of the National Academy of Sciences of the United States of America. 18, 1–8.

Yu, S., Clark, G, Leonard, J., 2005. Airflow measurement in passively aerated compost. Canadian biosystems engineering. 47, 39–45.

Zeide, B., 1993. Analysis of growth equations. Forest Science. 39, 594–616.

Zhu, N.W., Deng, C.Y., Xiong, Y.Z., Qian, H.Y., 2004. Performance characteristics of three aeration systems in the swine manure composting. Bioresource Technology. 95, 319–326.

Table 4-1. Summary of regression results from SAS

Data	T_{hm}	T_{ht}	T_c	k_{hm}	k_{ht}	k_c	t_{hm}	t_{ht}	t_c
Bottom	30.0	2.1	23.4	0.1727	0.3983	0.0051	37.3	79.4	91.7
Middle	25.9	16.2	9.5	0.3057	0.1813	0.0257	38.5	88.1	137.3

Table 4-2. Analysis of variance for the regression of temperature data from the bottom compost layer

Source	DF	Sum of Squares	Mean Square	F value	Pr > F
Model	5	217587	43517.3	189585	<.0001
Error	125	28.7	0.2295		
Uncorrected Total	130	217615			

Table 4-3. Results of statistical analysis of the distribution of residuals

Data	$\mu_0 = 0$	Normality
Bottom	$p = 0.9887$	$p = 0.7362$
Middle	$p = 0.7847$	$p = 0.0090$

Table 4-4. Analysis of variance for the regression of combined and individual models

Source	DF	Sum of Squares	Mean Square	F value	Pr > F
Combined model	8	583786	72973.3	1302.9	<.0001
Error	246	13778.1	56.0085		
Uncorrected Total	254	597564			
Individual model	18	597488	33193.8	102630	<.0001
Error	236	76.3298	0.3234		
Uncorrected Total	254	597564			

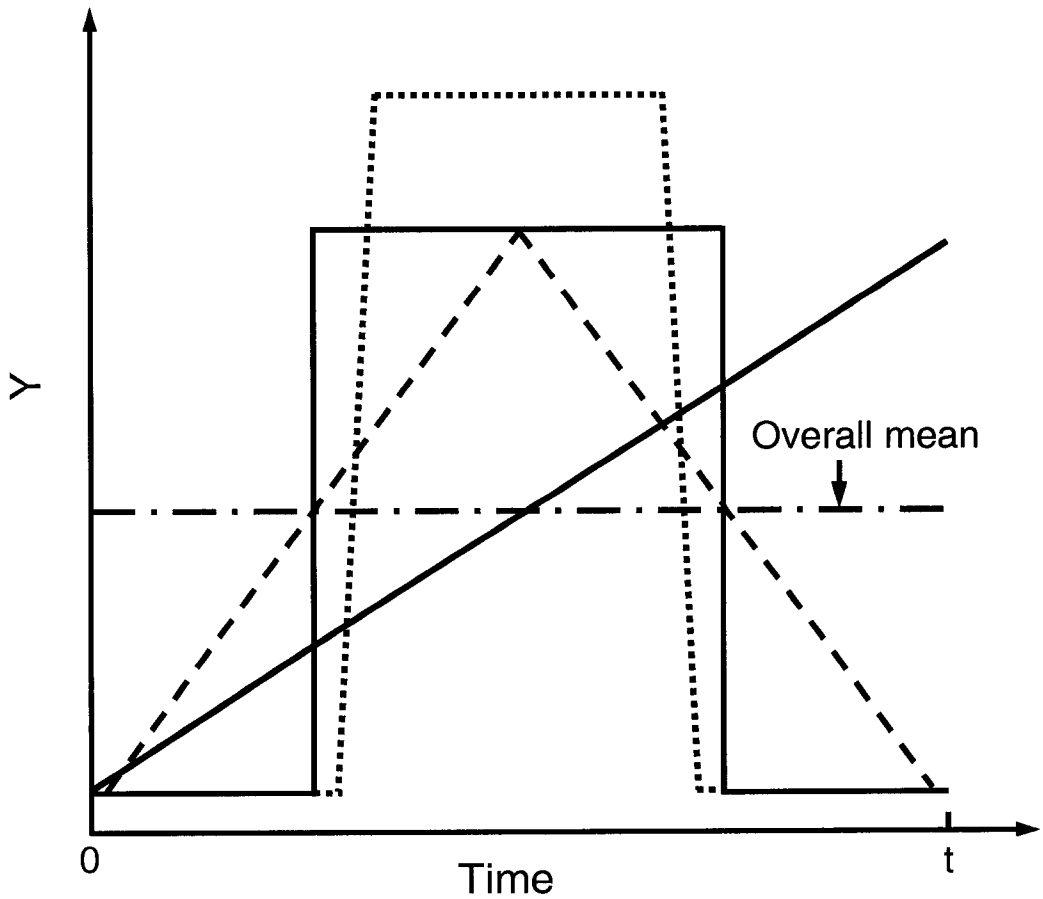

Figure 4-1. Overall means of differently shaped curves

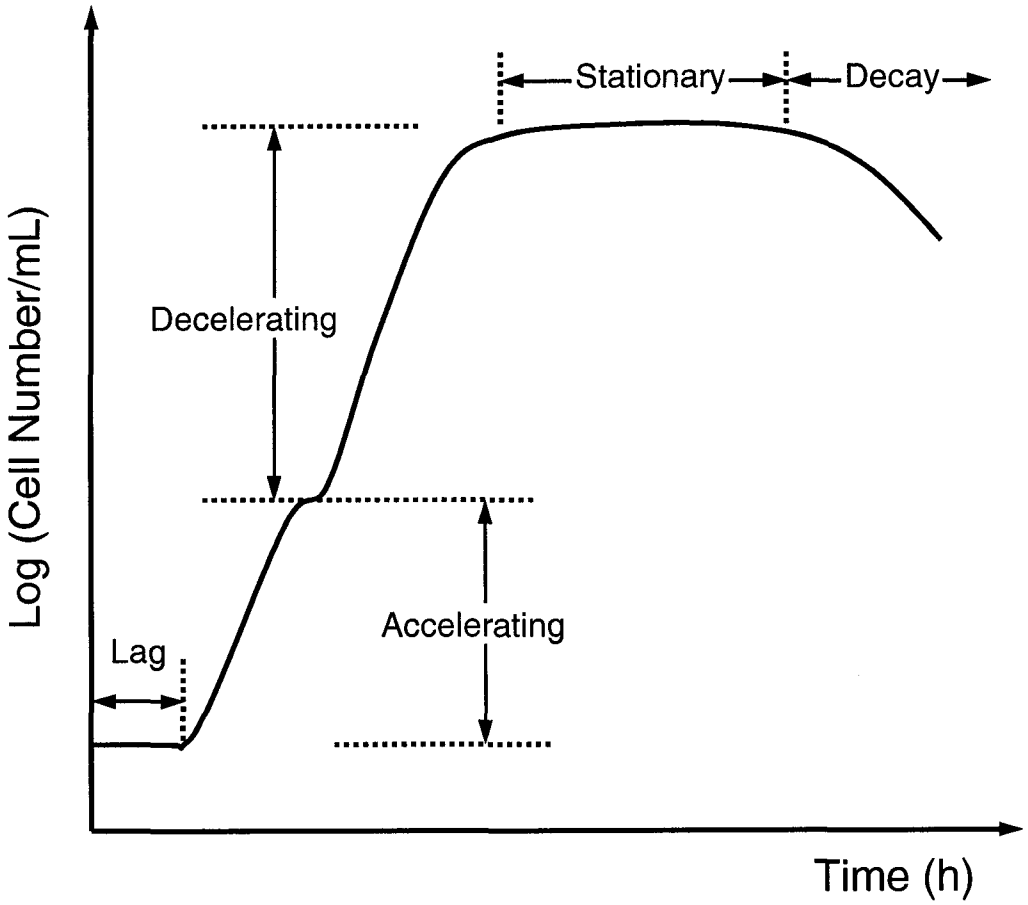

Figure 4-2 (a). Schematic of a typical microbial growth curve

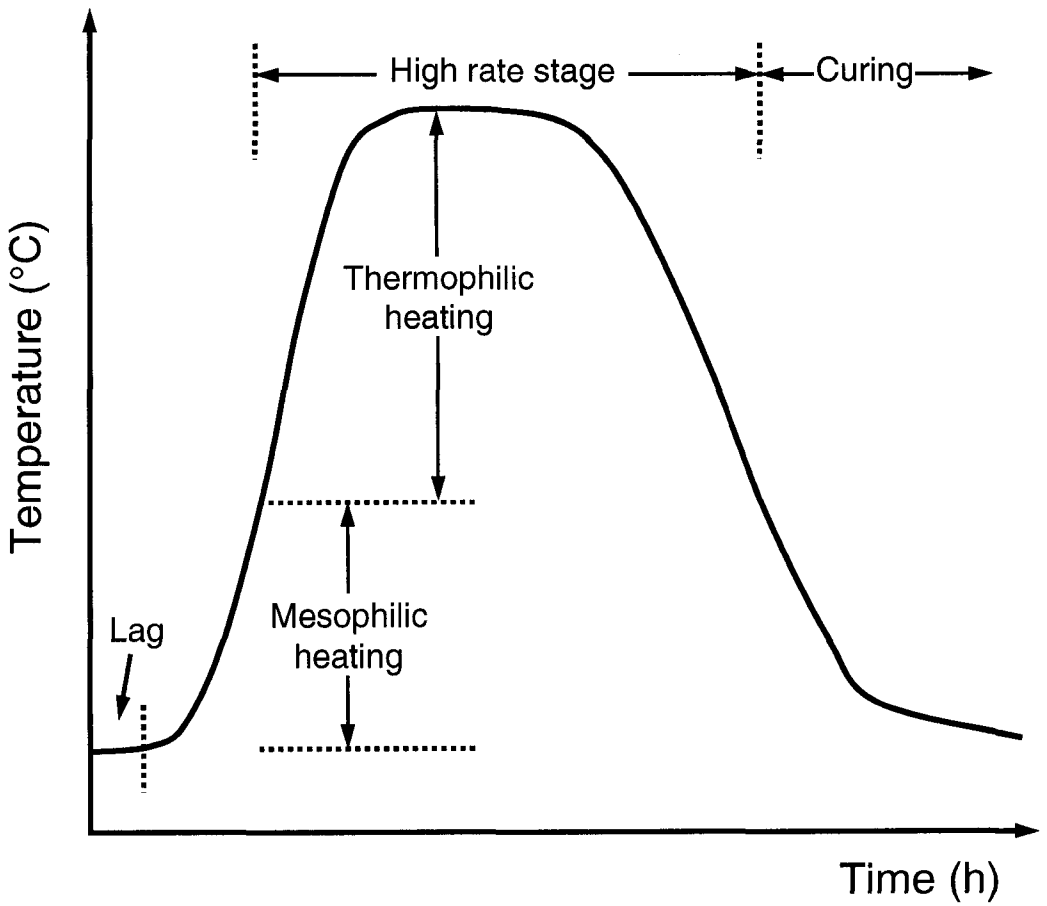

Figure 4-2 (b). Schematic of a typical composting temperature time series

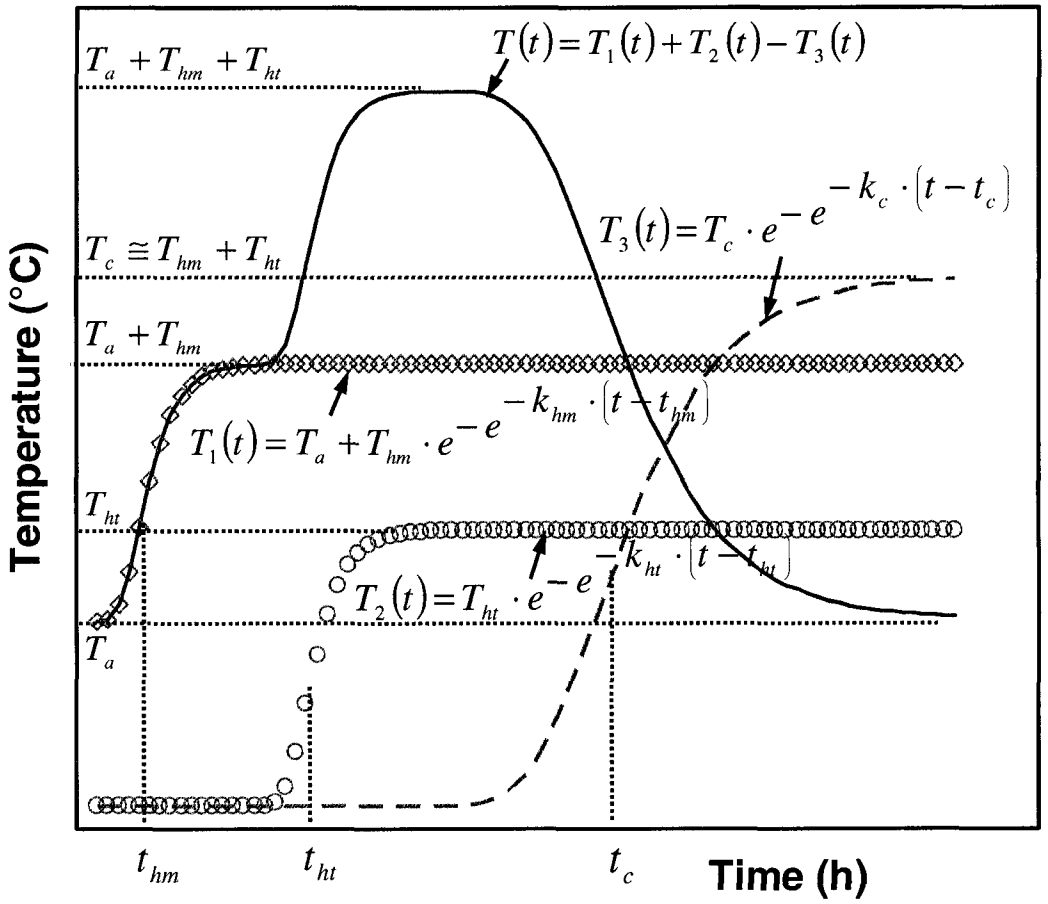

Figure 4-3. Characteristics of proposed function

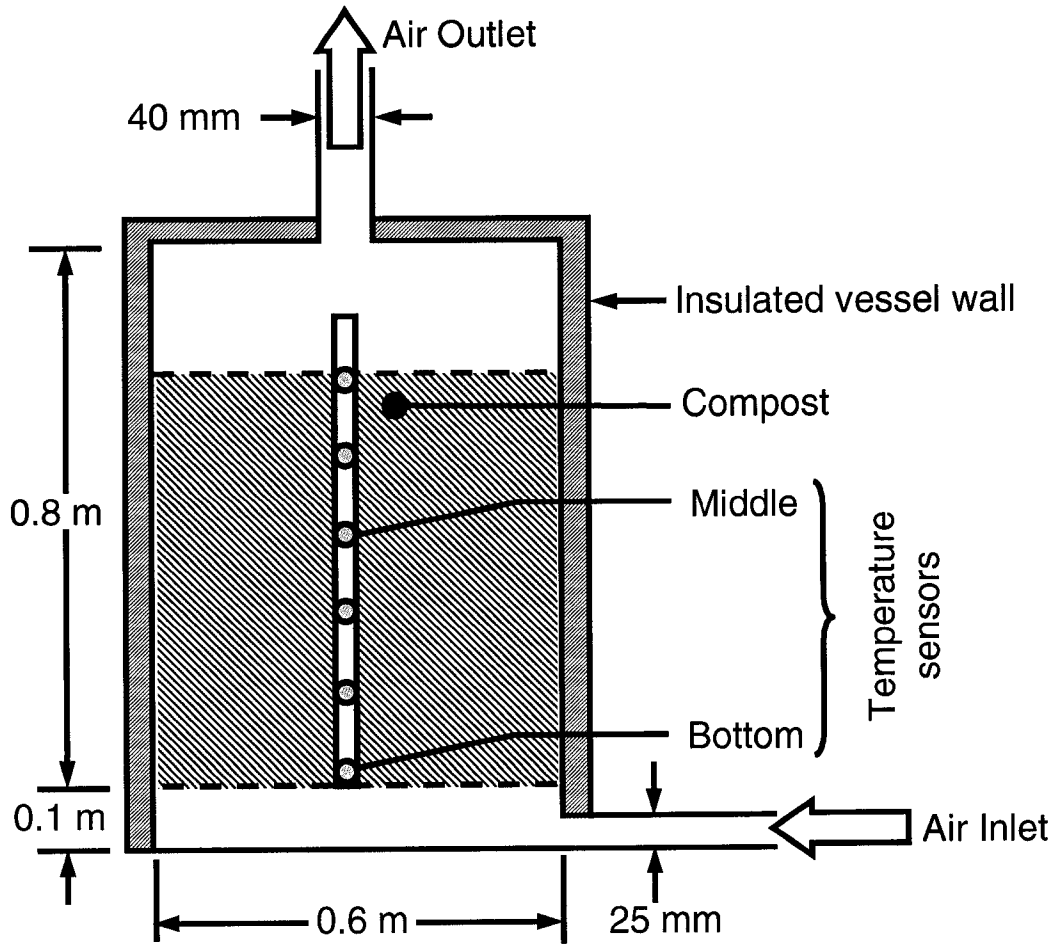

Figure 4-4. Schematic of passively aerated compost vessel

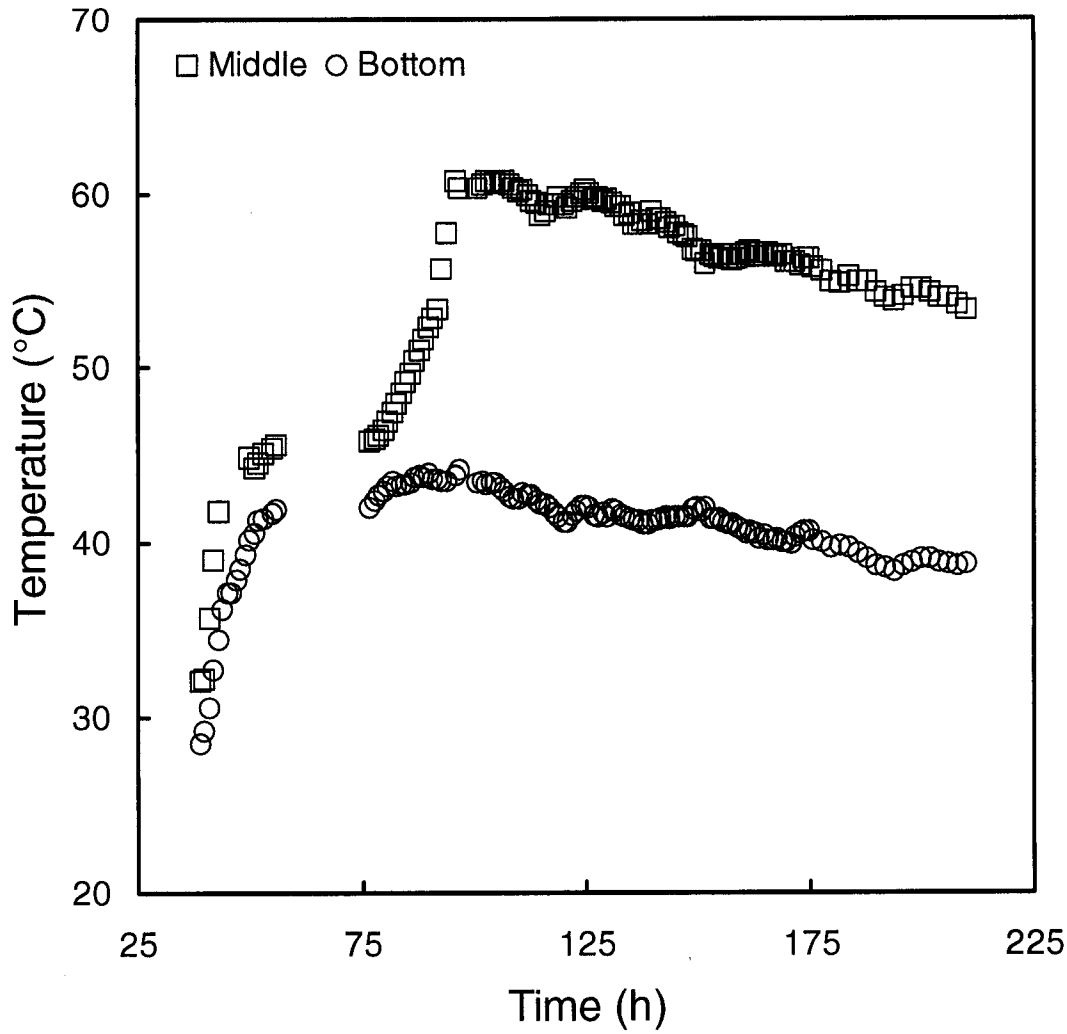

Figure 4-5 (a). Temperature time series of passively aerated compost (experimental data)

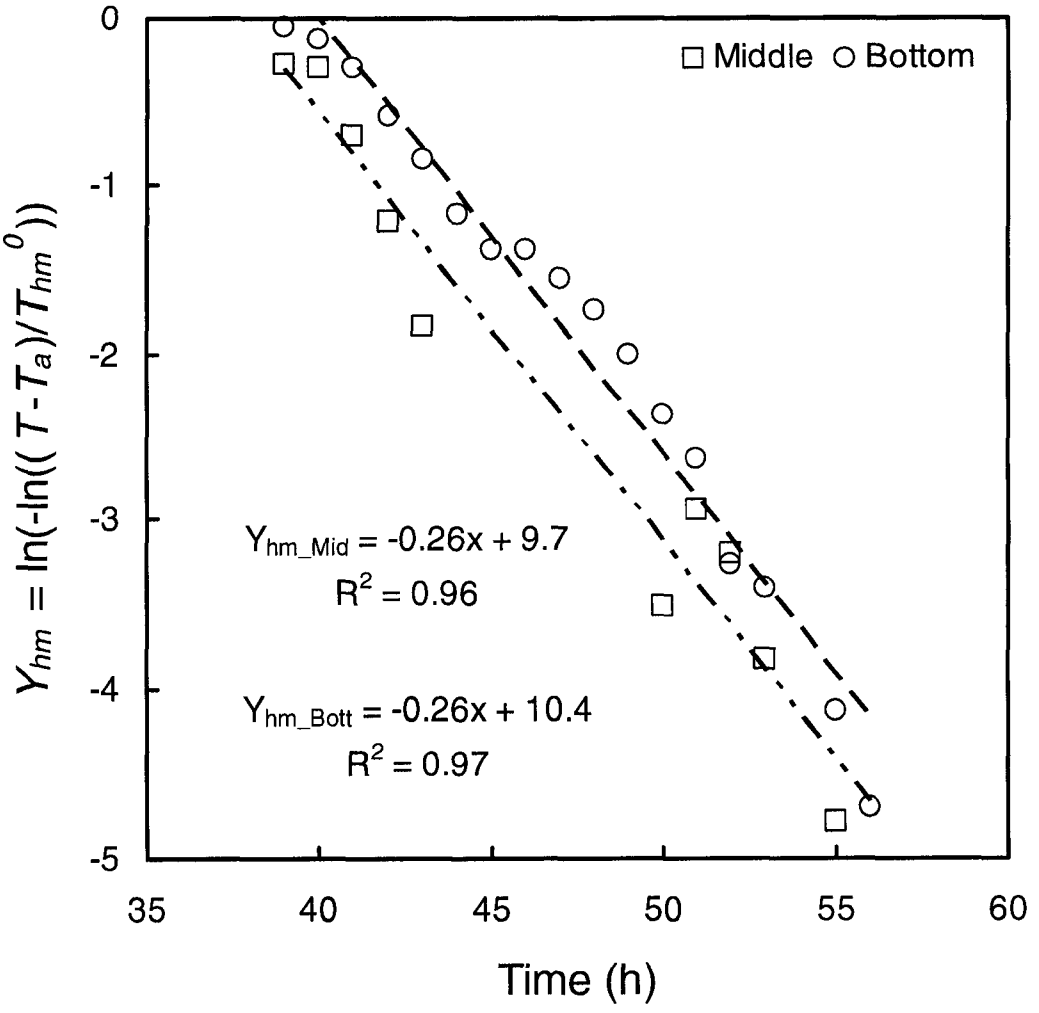

Figure 4-5 (b). Determination of initial parameter values for the mesophilic heating term

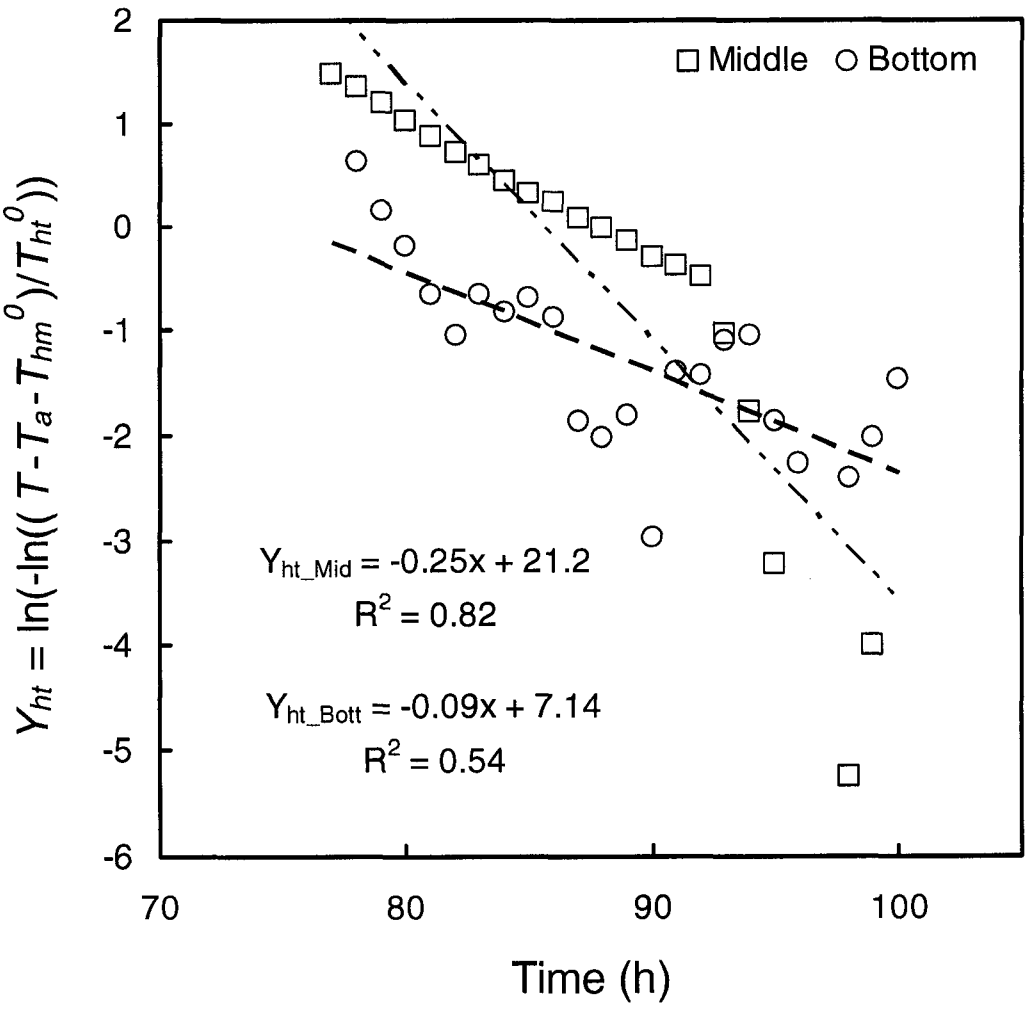

Figure 4-5 (c). Determination of initial parameter values for the thermophilic heating term

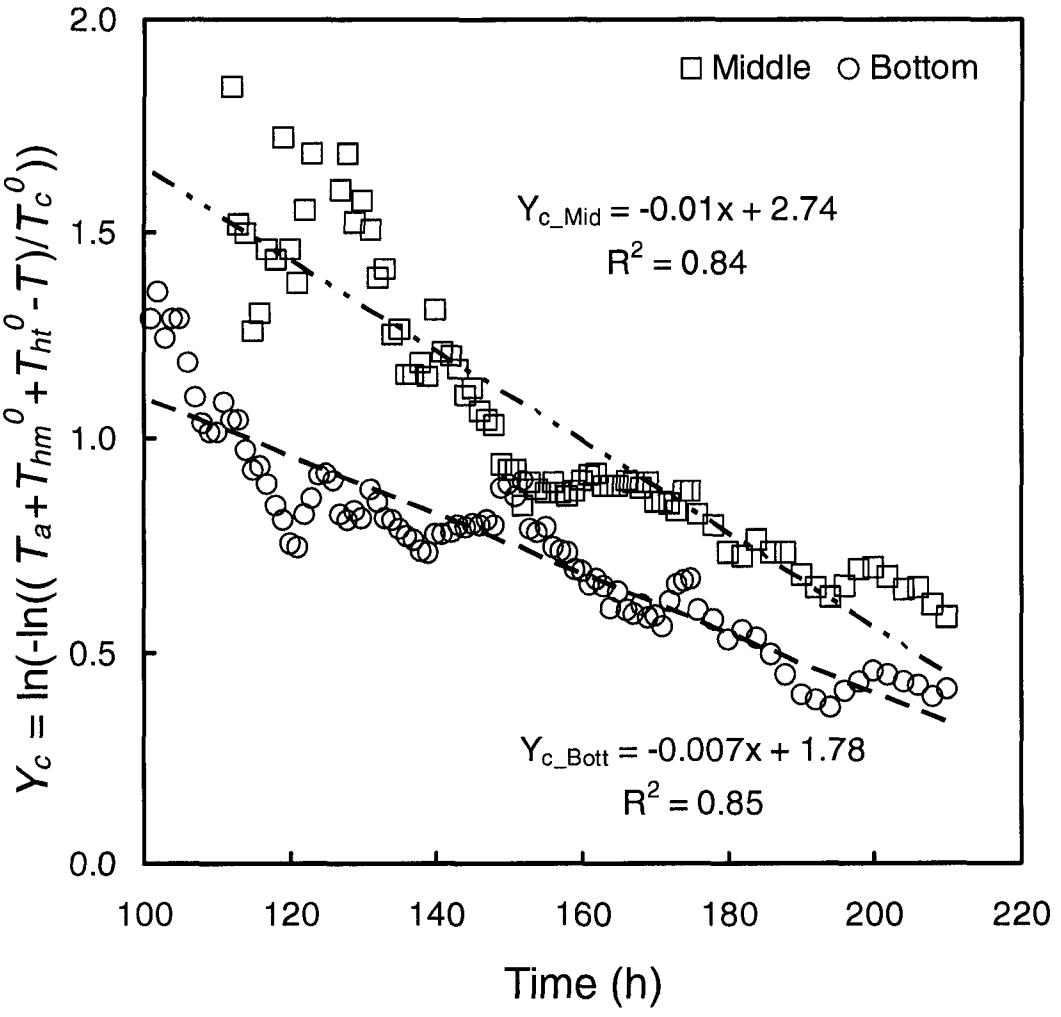

Figure 4-5 (d). Determination of initial parameter values for the cooling term

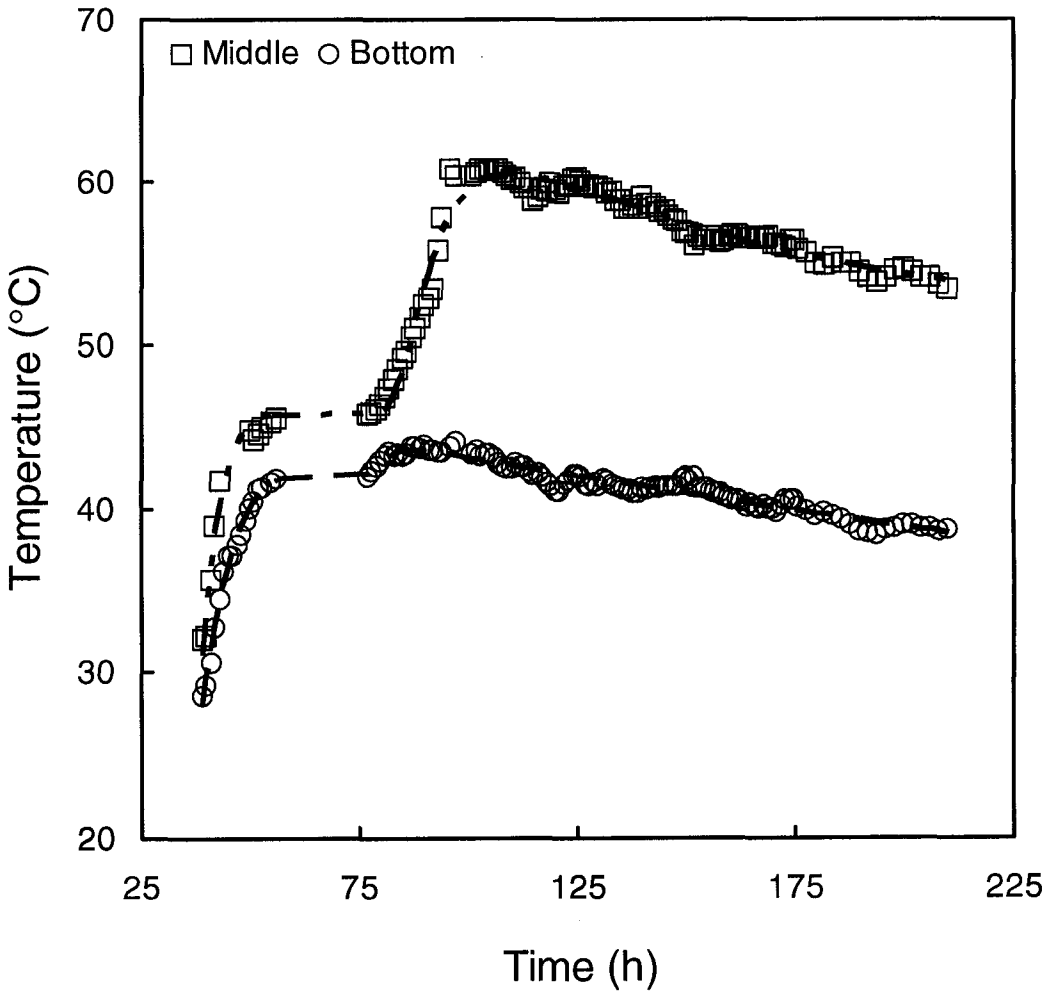

Figure 4-5 (e). Regressed curves for temperature time series from passively aerated compost

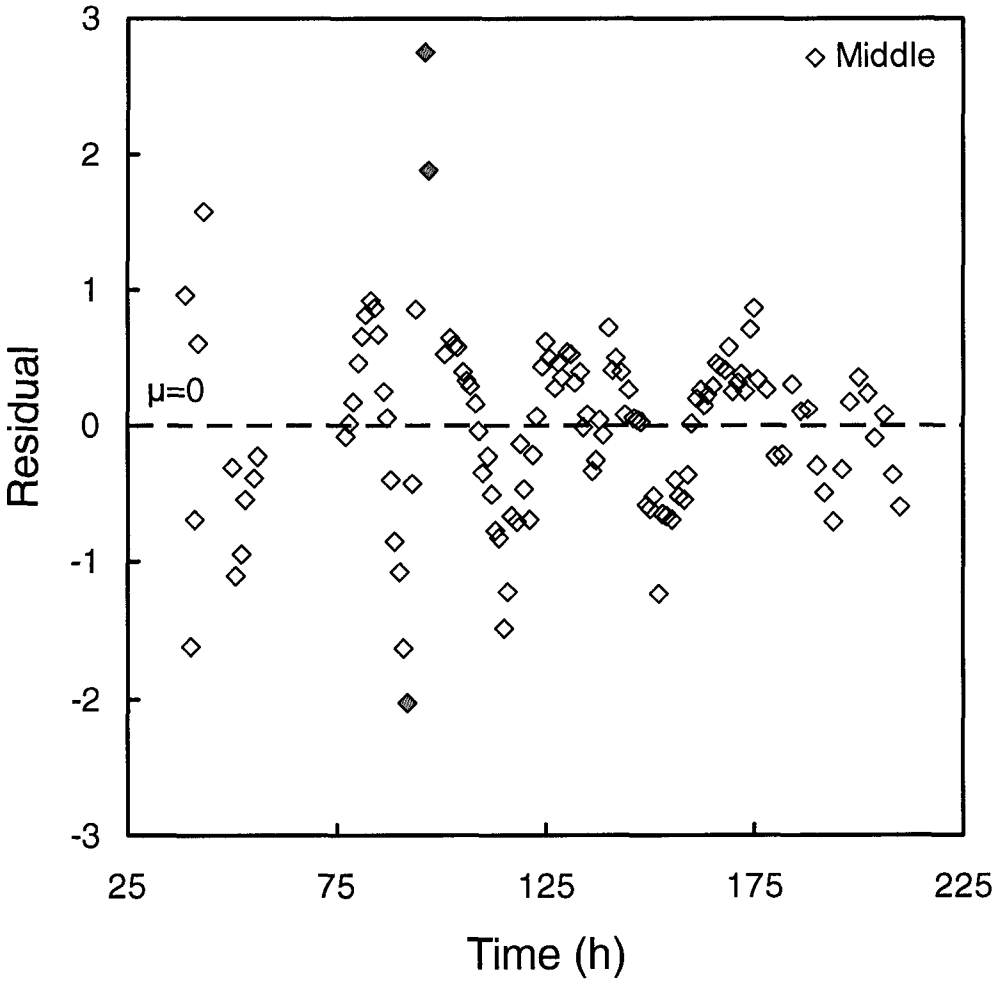

Figure 4-5 (f). Residual of regressed curve for temperature time series at middle layer

Chapter 5 Influence of free air space on microbial kinetics in passively aerated compost [†]

5.1 Introduction

Composting is gaining acceptance as an environmentally sustainable method of managing and recycling organic material. Mathematical models of composting are being developed for the purpose of improving our understanding of, predicting, and optimizing the composting process. Most composting models developed to date are for large scale processes with active aeration (Mason 2006). Actively aerated systems are often promoted as having the advantage of high processing rate and good control of process variables. Given an appropriate configuration, however, passive aeration can result in similar process rates (Fernandez and Sartaj, 1997), end product quality (Solano *et al.* 2001), and lower nitrogen loss compared with active aeration (Solano *et al.* 2001). It has been demonstrated that passive systems can be operated in cold climates, dispelling another common concern (Lynch and Cherry 1996a, McCartney and Eftoda 2005). Passive aeration systems also require less capital investment and operating costs are lower than for active aeration systems (Haug 1993). Passively aerated composting can therefore be a good alternative for processing organic residuals not only on small farms (De Bertoldi *et al.* 1985), but also for large-scale systems.

[†] Part of this chapter has been published as: Yu, Shouhai, O. Grant Clark, Jerry J. Leonard, Daryl M. McCartney. 2006. A mathematical model for passively aerated compost. In: *Proceedings of the International Conference ORBIT 2006*, Eckhard Kraft. eds, Weimar, Germany. pp 233-243.

Passive aeration is also an important consideration in composting systems that employ active aeration, since in such operations forced aeration is usually only used during the high rate phase, which typically lasts only one week to one month. After the active phase is complete, the compost generally is left to cure for several months, and only passive aeration takes place during this curing phase. Little attention has been paid to this curing phase even though it is an important part of the complete process (Haug 1993). Neglect of the curing phase of composting might partly contribute to the huge variation in compost quality between facilities.

The lack of an adequate mathematical description of the heat and mass transfer within passively aerated compost makes these systems difficult to predict and control. System design and optimization is also impossible, which is a barrier to the adoption of passively aerated composting. One critical challenge to modeling passively aerated systems is the lack of an adequate mathematical description of airflow. In actively aerated systems, air movement is mechanically driven at constant and predetermined rates by pumps or fans. As a result, the supply of oxygen to the compost and the removal of excess heat and moisture can be estimated with reasonable accuracy. In passively aerated systems, however, the airflow is driven by buoyancy, and its estimation is a challenging task that is crucial to the development of a complete model of the system. Lynch and Cherry (1996b) proposed the first analytical model for the description of the airflow though passively aerated windrow, in which Darcy's law was employed to estimate the vertical velocity of air going through the compost bed. The applicability of the model was not demonstrated, however, possibly because of the difficulty of measuring airflow and other model parameters in actual windrows.

Barrington *et al.* (2003) proposed the use of empirical relationships between the Grashof number and the measured airflow rate for the purpose of predicting airflow in passively aerated compost. The lack of theoretical explanation of the nature of such relationships limits the optimization of this methodology in practical applications.

A model relating the physical characteristics and temperature of the substrate with the measured air flow through passively aerated compost was developed and described elsewhere (Yu *et al.* 2006). The model was intended to predict the convective airflow resulting from the heat generated by the microbial activity in the compost. The effect of compaction on the permeability of the compost, although not directly included in the model, was also considered in its application. The model was verified using measured airflow and temperature time series data from a passively aerated composting experiment as inputs, and the predicted airflow was compared with measured values (Yu *et al.* 2006).

Another important factor is the estimation of microbial kinetics (i.e. degradation rate) in passively aerated compost. Microbial kinetics has been recognized as the most decisive variable in mathematical models of composting processes (Mason 2006, Hamelers 2004). As noted by Stombaugh and Nokes (1996) however, microbial kinetics in compost can vary among positions even in actively aerated compost, where the supply of oxygen can be more directly controlled. Microbial kinetics is likely to vary even more in a passively aerated composting system where there is no steady, externally driven air flow.

The ultimate goal of this work is to provide a general model which can be applied to any passively aerated composting systems, but a practical short-term objective is to

develop an empirical model suitable for a specific substrate. This more conservative approach is commonly adopted by most modelers in the composting field (Mason 2006) because knowledge of the microbiology involved in composting is still very limited, so that general relationships cannot yet be extrapolated from particular instances. As summarized by Mason (2006), a suitable model of composting can be achieved by combining empirical microbial kinetics from experiments with theoretical heat and mass balances. The work presented here illustrates how a novel empirical relationship between microbial kinetic coefficients and substrate FAS can be used in a numerical model to predict heat production and temperature at different locations in the compost bed. The degradation of the substrate carbon and the removal of moisture are the related mass transfer processes that were considered in the model.

5.2 Model description

5.2.1 Physical model

The selection of physical model was based on the following criteria: (a) the model should include all necessary components to reflect the fundamental characteristics of various passively aerated composting systems; (b) the model should be simple enough to represent only the very basic principles of interest and should minimize extraneous factors; (c) the variables of interest in the model should be easily measured.

In a passively aerated system, vertical airflow (Fogiel *et al.* 1999) and vertical temperature profile (Fernandes *et al.* 1994, Yu *et al.* 2005a) are the most fundamental characteristics. The physical model used to study the process consisted of dairy manure and straw composted in an enclosed, passively aerated composting vessel

(Figure 5-1). The insulated vessel was 0.9 m in height and 0.6 m in diameter with an expanded metal floor installed 0.10 m from the bottom to create an aeration plenum. The cylindrical vessel selected for the study embodied the fundamental features of passive convective airflow. Convection is the driving force for oxygen supply in passively aerated systems, and is characterized by the vertical movement of air due to buoyancy. Actual measurements of vertical airflow in passively aerated, in-vessel composting are also practical (Barrington *et al.* 2003, Yu *et al.* 2005a).

5.2.2 Conceptual model

The compost bed in the vessel was considered to consist of layers, each having homogeneous physical and chemical properties (Figure 5-1). Microbial activity in each layer was considered to consume oxygen (O_2) and organic matter (represented by carbon) from the substrate, and to release only carbon dioxide (CO_2), moisture (H_2O), and heat. The airflow through the compost was considered to be uniform and unidirectional from bottom to top, delivering oxygen and removing excess moisture, CO_2, and heat.

The following assumptions were made in the development of the model:

1. Each layer was physically and chemically homogeneous.
2. Microbial metabolism in each layer was limited by the availability of carbon, oxygen, and water.
3. Air was incompressible.
4. Air traveled through the compost bed in the vertical direction only.
5. Airflow was uniform through each layer.

6. The mass flow rate of dry air was constant vertically throughout the compost bed. This is to say that the consumption of oxygen and generation of carbon dioxide had a negligible contribution to the volume of air.
7. The temperature of the air stream was the same as the compost in each layer immediately after entering that layer.

The complete mathematical model of the mass and heat transfer within the passively aerated compost includes (Figure 5-2): (a) a biodegradation model to predict the mass changes due to microbial activity, including organic matter (represented by carbon), moisture, and oxygen content; (b) a temperature model to predict the temperature profile developed in the compost bed; and (c) an airflow model, to predict the passive air movement through the compost bed.

Inputs to the biodegradation model included the initial chemical and physical properties of the feedstock, such as carbon content, water content, bulk density, and FAS. As heat production in composting is almost completely derived from biological activity (Kutzner 2001), the temperature profile was determined using the heat output from the biodegradation model. Since the temperature model was directly verifiable using temperature measurements from experiments, the performance of the biodegradation model could be verified indirectly at the same time because of the strong correlation between temperature model and biodegradation model. Temperature is a more practical indicator variable than the oxygen uptake rate which, although a more direct indicator of aerobic microbial activity, is more difficult to measure (Paletski and Young 1995).

The numerical model proposed by Yu *et al.* (2006) was adapted to allow the estimation of airflow given the temperature in the compost bed, which is related to microbial activity and the basic properties of the substrate (e.g., permeability, mass, and specific heat capacity). The change in FAS due to compaction, although not explicitly calculated in this model, was estimated based on published data and taken into account in the application of the model (Das and Keener 1997, Richard *et al.* 2004). The model was conceived to be iterative in its execution, since airflow supplies oxygen while removing heat and moisture from the substrate, and this in turn impacts microbial activity (biodegradation and heat production) in the substrate. Therefore, a strong feedback loop exists among the airflow, temperature, and biodegradation models (Figure 5-2).

5.2.3 Mathematical model

5.2.3.1 Biodegradation model

The biodegradation model was based on the mathematical model of Liang *et al.* (2004), which was extended to incorporate the adjustment of microbial kinetics at each layer. The parameters in the biodegradation model were estimated and modified based on literature (Haug 1993, Stombaugh and Nokes 1996, Liang *et al.* 2004, Mason 2006). A first-order biodegradation model was used for the microbial growth at each layer:

$$\left(\frac{dX}{dt}\right)_i = k_{d,i} X_i \qquad (1)$$

The growth rate of microbes (dX/dt) at different positions (i^{th} layer) is represented as being proportional (k_d) to the population size, which is represented by biomass (X). The rate of substrate decomposition, expressed by the change of carbon content, was determined by:

$$\frac{dC_i}{dt} = \frac{1}{Y_{X/C_i}} \frac{dX}{dt} \tag{2}$$

The rate of change in carbon content in the substrate (dC/dt) at different positions (i^{th} layer) was estimated from the change in the microbial population (dX/dt) using a biomass yield coefficient ($Y_{X/C}$), i.e., the yield of biomass per unit mass of substrate carbon consumed. The strong correlation between changes in carbon content and microbial biomass is commonly employed in microbial growth models (Liang *et al.* 2004, Komilis 2006). For simplicity, therefore, only carbon content was calculated in this exercise. Validation of the carbon mass balance was considered to be outside the scope of this study. Following a similar rationale, an empirical constant was used to estimate the total amount of substrate consumed from the predicted change in carbon content (Liang *et al.* 2004) (Equation 3).

$$\frac{dS_i}{dt} = \frac{dX}{dt} \Big/ f_c \tag{3}$$

The concept of first-order kinetics is based on the general observation of nutrient-limited microbial growth in natural environments (Alexander 1999, Adams 2003, p198) and the use of a simple first-order rate constant is a common choice for modeling practice in composting (Haug 1993, Mason 2006). Since the first-order model does not consider the phenomenon of self limiting growth and carbon and

oxygen concentration levels in the substrate, the rate constant has to be multiplied by various adjusting coefficients, discussed below.

5.2.3.2 Adjustment of first-order rate coefficient

The rate coefficient in the first-order degradation model (Equation 1) was adjusted to account for the effect of temperature, moisture, oxygen and bioavailability of carbon (Haug 1993, pp. 395-402). A Monod-type (Monod 1949) expression was selected for this (Equation 3).

$$k_{d,i} = k_{d,\max,i} \frac{[C_i]}{K_C + [C_i]} \frac{[O_2]_S}{K_{O_2} + [O_2]_S} k_{temp} k_w \qquad (4)$$

The first-order growth rate (k_d) at different layers (i^{th} layer) is estimated by adjusting the maximum first-order growth rate ($k_{d,max}$) with a nutrient limiting factor, which is expressed in terms of carbon availability ($[C]/(K_C + [C])$), oxygen availability ($[O_2]/(K_{O2} + [O_2])$), and the influences of temperature (k_{temp}), and substrate moisture content (k_w). K_C and K_{O2} are half saturation constants of carbon and oxygen in the substrate.

Most composting models employ one function, linear or non-linear, to describe the effects of temperature (k_{temp}) over the whole composting process (Haug 1993, Mason 2006). Composting begins with a mesophilic stage, generally progresses through a thermophilic stage, and cools down to mesophilic stage during the curing phase (Haug 1993, Epstein 1997, Kutzner 2001, Ryckeboer *et al.* 2003). A lag in temperature change is commonly observed during the transition from the mesophilic to the thermophilic stages (Stombaugh and Nokes 1996, Seki 2000, Sundberg *et al.* 2004). Since mesophilic and thermophilic microbes have different responses to temperature

(Ryckeboer *et al.* 2003, Madigan and Martinko 2006), different termperature response curves are required for the two groups, for better description of the microbial activity. Simplified linear functions similar to that used by Liang *et al.* (2004) and Stombaugh and Nokes (1996) were employed to calculate the correctional coefficient (k_{temp}) (Figure 5-3). For mesophilic bacteria, active from about 0°C to 55 °C (Ryckeboer *et al.* 2003), the effect of temperature was estimated by:

$$k_{temp}^{meso} = \begin{cases} 0.033 \times T & 0 \le T \le 30 \\ 1.0 & 30 \le T \le 40 \\ -0.067 \times T + 3.667 & 40 \le T \le 55 \end{cases} \quad (5)$$

For thermophilic bacteria, active from about 40°C to 75°C, the effect of temperature was estimated by:

$$k_{temp}^{thermo} = \begin{cases} 0.10 \times T - 4.0 & 40 \le T \le 50 \\ 1.0 & 50 \le T \le 55 \\ -0.05 \times T + 3.75 & 55 \le T \le 75 \end{cases} \quad (6)$$

The effect of moisture (k_w) was estimated by:

$$k_w = \begin{cases} 0.0 & MC < 0.2 \\ 5.0 \times MC - 1.0 & 0.2 < MC < 0.4 \\ 1.0 & 0.4 < MC \end{cases} \quad (7)$$

where MC is the decimal, wet basis moisture content of the substrate.

The value of k_{max} was estimated by the analysis of temperature histories from the composting trial by fitting the sum of two additive, sigmoid, asymptotic growth curves and a decay curve to the temperature histories (Yu *et al.* 2005b). The fitted parameters were thereafter used to estimate microbial kinetic coefficients in this model. This method is more convenient than many that have been used previously (Haug 1993,

Mason 2006) because it is easier to measure temperature than oxygen uptake rate. Moreover, the oxygen uptake rate reflects mostly the activity of aerobic bacteria (Gomez *et al.* 2006), but not all microbes in compost are aerobic (Ryckeboer *et al.* 2003). Heat production, on the other hand, is a good indictor of the overall activity of all microbes in the compost bed, and temperature change in compost is related to heat production from all microbial activity. Furthermore, heat production rate has been used in a similar fashion to quantify microbial metabolic rate in soil (Barros *et al.* 2004), activated sludge (Aulenta *et al.* 2002), and wastewater (Daverio 2003). Nevertheless, more effort is needed to verify a rigorous relationship between the rate of change of temperature and microbial kinetics during composting since the change of temperature is also influenced by the mass and specific heat of the substrate, and convective and conductive heat loss.

5.2.3.3 Mass changes

The mass changes of oxygen and moisture in the substrate were estimated based on the principle of mass conservation, although the estimates were not validated experimentally. The mass change of the oxygen content in the compost was estimated by:

$$\frac{d[O_2]}{dt} = Y_{X/S}\frac{dS_i}{dt} + \frac{F}{\rho}\left([O_2]_{in} - [O_2]_{out}\right) \quad (8)$$

The estimation of oxygen content was done by an overall mass balance analysis of oxygen content in the inlet ($[O_2]_{in}$) and outlet ($[O_2]_{out}$) air, and the oxygen consumed by microbial activity in each layer of the compost bed. Oxygen consumed by microbes is commonly estimated indirectly from the substrate degradation (*dS/dt*) multiplied by

a microbial yield factor ($Y_{X/S}$). The concentration of oxygen in air ($[O_2]_{in}$) is volumetric, and the volume of air going though each layer of compost was estimated by the mass airflow rate (F) and the density of the air (ρ), which was calculated based on psychrometric relationships (ASHRAE 2005) from the temperature and humidity ratio of the air.

The change in moisture content was similarly estimated by an overall mass balance analysis of water content in the inlet (w_{in}) and outlet (w_{out}) air, and the water generated from microbial activity (Equation 9).

$$\frac{dW}{dt} = Y_{W/S}\frac{dS_i}{dt} + F \cdot (w_{in} - w_{out}) \tag{9}$$

Water generated by microbes is commonly estimated by yield ($Y_{W/S}$) from substrate degradation (dS/dt). The total mass of water carried away by the air during unit time period can be estimated by the airflow rate (F) times the difference in the humidity ratio between the inlet (w_{in}) and outlet (w_{out}). An effort was made to measure the change in air humidity during composting using commercially available integrated circuit humidity sensors (HIH-3610-003, Honeywell Sensing and Control, Freeport, IL, USA), but no meaningful conclusions could be drawn due to the poor performance of the sensors in the harsh conditions in the compost bed. As a result, the moisture removal from each layer was estimated based on current understanding and well-accepted assumptions.

The evaporation of water from substrate is driven by the difference between the vapor pressure and the partial pressure of the water (Alberty and Silbey 2000, p192), and the

vapor pressure is proportional to $\exp(-Q_{Latent}/RT)$ (Alberty and Silbey 2000, p185), which can be approximated using a Taylor series expansion (Adams 2003, p569):

$$\exp\left(-\frac{Q_{Latent}}{RT}\right) \approx 1 - \frac{Q_{Latent}}{RT} \tag{10}$$

Substituting an approximation of the latent heat (Haug 1993, p424) into Equation 10 gives:

$$\exp\left(-\frac{Q_{Latent}}{RT}\right) \approx 1.068 - \frac{113.0}{T} \tag{11}$$

where T is temperature in K. As a result, saturated vapor pressure can be considered as approximately proportional to the reciprocal of temperature, which can be easily measured. The amount of water picked up by the air in each layer was therefore assumed to be proportional to the difference between the reciprocal of temperature in that layer and the reciprocal of ambient temperature. To quantify the amount of water picked up in each layer, the total amount of water (m_w^{total}) removed by the air was calculated first using measured ambient temperature and relative humidity values, and the temperature of the exit air, which was assumed to be saturated (Haug 1993, Mason 2006). Then, the difference between the reciprocal of temperature at each (i^{th}) layer (T_i) and the reciprocal of ambient temperature ($T_{ambient}$) was calculated as $\Delta(1/T)_i = 1/T_{ambient} - 1/T_i$, the sum of which was $\Sigma\,\Delta(1/T)_i = \Delta(1/T)_{total} =$. The cumulative amount of water removed from a given (i^{th}) layer as the air exited was then estimated by $m_w^i = m_w^{total} \times \Delta(1/T)_i / \Delta(1/T)_{total}$.

5.2.3.4 Heat balance

The heat balance was based on the principle of conservation of energy, but was not validated experimentally. The heat balance of each layer in the compost can be expressed by:

$$\frac{dQ_i}{dt} = \frac{dQ_{gen}}{dt} - \left(\frac{dQ_{out}}{dt} - \frac{dQ_{in}}{dt} \right) \tag{12}$$

$$\frac{dQ_{gen}}{dt} = Y_{H/C} \frac{dC_i}{dt} \tag{13}$$

$$\frac{dQ_{out}}{dt} - \frac{dQ_{in}}{dt} = F \cdot (h_{out} - h_{in}) \tag{14}$$

The heat balance at a given (i^{th}) layer is the net result of biological heat production (dQ_{gen}/dt) minus the latent and sensible heat carried away by the airflow ($dQ_{out}/dt - dQ_{in}/dt$), as shown in Equation 12. The bioreactor in the physical model was well insulated, and radial measurements showed that there was no significant difference between the temperature in the middle and that 2 cm away from the wall. As a result, conductive heat through bioreactor walls and radiative heat loss were ignored for the sake of simplicity. Biological heat production (dQ_{gen}/dt) was assumed to be proportionately related by the heat conversion factor $Y_{H/C}$ to the substrate consumption rate, as represented by the change of carbon content (dC/dt) - (Equation 13). The heat conversion factor is an empirical value depending on the chemical and microbiological characteristics of the substrate. To calculate heat removal by the airflow, psychrometric equations (ASHRAE, 2005) were used to calculate the enthalpy of the input (h_{in}) and output (h_{out}) air (Equation 14), including the

temperature and humidity of the input air, the temperature and humidity of the exit air, and the latent heat of evaporated water from substrate.

The overall heat content was calculated for the compost from the heat content of the volatile substrate, non-volatile substrate, and water. The temperature change in each layer was then calculated:

$$\frac{dT_i}{dt} = \frac{1}{c_{VS} \cdot m_{VS} + c_{nvs} \cdot m_{nvs} + c_w \cdot m_w} \frac{dQ_i}{dt} \tag{15}$$

The water content (m_w) was determined as per Thompson *et al.* (2002). As water is the major part of the substrate (75% wet based), and the specific heat capacity of water is much higher than those of the other two items (Table 5-1), water content plays the dominant role in substrate temperature change. The actual values for volatile solid (m_{vs}), and non-volatile solid (m_{nvs}) were therefore not measured in this study. Instead, an empirical value of the content of volatile solid (i.e., 95% of initial dry matter) was used based on other studies (Liang *et al.* 2004; Alvarez *et al.* 2006). Non-volatile mass was estimated according to this ratio and assumed to be constant throughout the composting process. The specific heat capacity of water (c_w) is well-documented, and the values for the specific heat capacity of the volatile solids (c_{vs}) and non-volatile solids (c_{nvs}) were taken from literature (Liang *et al.* 2004) (Table 5-1).

5.3 Experimental data

The significance of FAS in composting has long been recognized (Haug 1993) and the influence of FAS on the quality of passively aerated composting has been reported (Veekeen *et al.* 2002). However, the quantitative relationship between FAS and the microbial kinetics in passively aerated compost has not been investigated. To address

this, experiments were conducted using compost with the same chemical properties but four different FAS values (0.45, 0.52, 0.57, and 0.65), achieved by adding different amount of woodchips.

The experiment was conducted in enclosed, well-insulated, passively aerated, cylindrical vessels. The compost used in the trial consisted of fresh dairy (*Bos taurus*) manure, softwood lumber chips (*Picea glauca*), pine wood saw dust (*Pinus contorta*), and air-dried, ground canola straw (*Brassica napus*). The mixture was designed to have a carbon-to-nitrogen ratio of 35:1 and initial moisture content of 76% (wet basis). The FAS of the mixture was determined with a pycnometer developed by Agnew *et al.* (2003), and average of 3 measurements was used to represent the FAS value for each treatment. At the beginning of the experiment, the depth of the compost in the vessel was 0.50 m. Integrated-circuit temperature sensors (LM35DZ, National Semiconductor Corporation, Santa Clara, CA) were deployed in the middle of the bioreactor, at positions of 0, 100, 200, 300, 400, and 500 mm from the bottom of the mixture (Figure 5-1). All temperature sensors were connected to a data acquisition system for automatic data logging with an interval of one hour. Airflow rates were measured at the inlet and outlet of each bioreactor three times a day at approximately 8 hour intervals. The outlet airflow rate was measured using a smoke tracer meter and the inlet airflow with an ultrasonic meter (Yu *et al.* 2005a). Each treatment was replicated twice, and measurements from the two replicates were averaged to represent each treatment.

Data from this one factor experimental design were analyzed by ANOVA to derive an empirical relationship between FAS and biodegradation kinetics (k_{max}). Previous

research has directly related biodegradation kinetics to temperature (Nielsen and Berthelsen 2002, Richard and Walker 2006) and oxygen consumption (Cronje *et al.* 2004). Substrate FAS was chosen as the primary variable for the empirical estimation of biodegradation kinetics in this study because FAS has a significant effect on airflow development in passively aerated compost (Lynch and Cherry 1996b, Barrington *et al.* 2003) and airflow is strongly related to oxygen supply and temperature development (Haug 1993).

Temperature histories from different positions from three treatments (i.e., FAS values of 0.45, 0.52, and 0.65) were analyzed using previously developed methods (Yu et al. 2005b) to obtain k_{max} values for the mesophilic and thermophilic ranges for each position. The k_{max} values were then regressed against FAS and the resultant regression function was used to estimate k_{max} for arbitrary values of FAS during simulation. The performance of the model was validated against temperature histories and airflow measurements from an independent treatment from the same experiment (i.e., FAS value of 0.57).

5.4 Results and discussion

Although the experimental data from this study were insufficient to estimate the relationship between k_{max} and FAS at very low and very high values of FAS, it is speculated that it might be described by a sigmoid function similar to those used to relate microbial kinetic factors with other environmental variables, such as moisture content (Haug 1993, p355, 398, 400). After removing possible outliers based on the 1.5 inter-quantile range criteria (Montgomery and Runger 2002, p207), the following

relationships were derived for use in this study (Figure 5-4): for mesophiles, active from about 0°C to 55 °C, k_{max} was estimated by:

$$k_{\max}^{meso} = 0.01 + 0.90 \times \exp(-\exp(-15.0 \times (FAS - 0.53))) \quad R^2 = 0.97 \qquad (16)$$

For thermophiles, active from about 40°C to 75 °C, k_{max} was estimated by:

$$k_{\max}^{thermo} = 0.01 + 0.70 \times \exp(-\exp(-12.3 \times (FAS - 0.55))) \quad R^2 = 0.96 \qquad (17)$$

As shown in Figure 5-4, k_{max} values are higher in the mesophilic phase than the thermophilic phase, meaning that the activity of mesophiles is higher than that of thermophiles. This agrees with the results reported by Sundberg *et al.* (2004). The easily degradable organic substances in the feedstock, such as sugar, protein, and fat, help to maintain the high activity of mesophiles at the beginning of the composting process. When the thermophilic phase is reached, readily available substances have been exhausted and, together with the inhibitive effect of lower substrate pH (Sundberg *et al.* 2004), the activity of thermopiles is therefore restrained.

The temperature histories at two locations in the compost with FAS value 0.57, which were used as an independent test for the assessment of model performance, are shown in Figure 5-5. The temperature in the middle of the compost (Middle) followed a form typical of aerobic composting, increasing exponentially to above 55°C and then gradually declining to about 40°C. Temperatures at the other position (Top), however, remained below 55°C, which is the optimal temperature for thermophilic microbes. This vertical temperature difference was assumed to be the result of local differences in microbial activity and the related heat and mass transfer processes in the compost (Yu *et al.* 2005a).

Simulation results, also shown in Figure 5-5, indicate that the model could predict the general trend of temperature development. The difference between the predicted and measured temperature histories was analyzed statistically using the method described by Yu *et al.* (2005b). *F*-values for the test of significance were 1026 for the middle and 485 for the top, both resulting in *p*-values less than 0.01, which means there are significant differences between the measured data and predicted values. Figure 5-6 shows that the residuals are not randomly distributed and are correlated with time, suggesting the model used for prediction is biased, possibly because many parameters in the model were not measured directly. Many microbial kinetics parameters required by the biodegradation model, such as the correctional coefficients for temperature and moisture, and the half-saturation coefficients for carbon and oxygen, were estimated based on literature. All these factors together affect the degradation rate constant k_d (Equation 4), which has been recognized as the most decisive variable in compost models (Mason 2006), for a small change in k_d can significantly change the shape of predicted curve (Adams 2003, p198).

The limited precision of the thermodynamic parameters required by the temperature model might also have contributed to the biased prediction. For example, as commonly done in similar studies, a single heat yield coefficient from literature was used in this study. Heat released by microbes, however, is different among different species and strains (Barros *et al.* 2004). Heat yield coefficients should therefore be different at different phases, e.g., relatively small during the mesophilic phase and relatively large during the thermophilic phase. By the use of one heat yield coefficient, heat production during the mesophilic phase might be over-estimated, resulting in a

shorter lag period, and under-estimated during the thermophilic stage, leading lower predicted temperatures. Further research is required to develop a more rigorous methodology to obtain the required parameter values so as to improve the accuracy of models.

The effect of compaction of the substrate was considered, as described elsewhere (Yu *et al.* 2006). From the measured initial bulk density and FAS values, the compressive stresses at different positions were calculated (McCartney and Chen 2000).

$$\sigma_i = \rho_s g d_i / 1000 \tag{18}$$

The resultant compaction at different depths was then estimated (Das and Keener 1997).

$$h_i = h_\infty + \Delta h_0 \cdot \exp(-\beta \cdot \sigma_i) \tag{19}$$

In this context, h_i, is the fraction of the initial thickness of the i^{th} layer after compaction, and h_∞, Δh_0, and β are coefficients estimated from data published by Das and Keener (1997). The actual *FAS* in the i^{th} layer after compaction was predicted by

$$FAS = FAS_0 \cdot h_i \tag{20}$$

Substituting the actual FAS value into the relationship developed by Richard *et al.* (2004), the permeability of the substrate was estimated and used in the airflow model. Substituting the corresponding FAS values into Equation 16 and 17, the maximum degradation rate, k_{max}, was obtained and used in the biodegradation model.

The measured and predicted airflow rates through the compost are shown in Figure 5-7. The measured airflow rate followed a pattern similar to the compost temperature. Measured airflow data obtained using both instruments increased to a maximum at about 100 h and then gradually declined, illustrating the temperature-driven nature of

the convective airflow through the compost. The calculated mass airflow rates through the compost followed the temperature history, and showed good agreement with the measured data ($p = 0.97$). The airflow model and suggestions for its improvement have been discussed elsewhere (Yu *et al.* 2006).

As with any composting model (Mason 2006), the applicability of the model described here is limited by a lack of knowledge of combining the process dynamics at the micro level with the process dynamics at larger scales. Composting is a process in which microbiology plays a critical role. Due to the inherently complex nature of large-scale microbiological systems, especially on heterogeneous substrates, composting models at present cannot be used as predictive tools applicable to all substrates; they are rather more useful as research tools. For a composting system with a consistent feedstock, however, the use of the model proposed in this study could help the operator manage the system by providing a good estimate of the progress and performance of the process.

Equation 16 and 17 were developed for use only with the feedstock and vessel in this study. Although direct application of these relationships to other scenarios is unlikely to be successful, the method of estimating microbial kinetics via the analysis of temperature histories from preliminary compost trials is recommended. Simulation results from this study do demonstrate that temperature histories from composting can be useful in the assessment of microbial kinetics. Such an approach is also economical in terms of instrumentation and the frequency of monitoring. Further research is required, however, to fully develop the relationship between temperature and microbial kinetics.

5.5 Summary and conclusion

Composting was studied in an enclosed, passively aerated, cylindrical vessel to investigate the quantitative relationship between FAS and the microbial kinetics in passively aerated compost. Based on this experimental system, a numerical model was developed in which the compost bed was considered to consist of layered elements, each being physically and chemically homogeneous. The microbial activity in each layer was represented in order to predict oxygen consumption and the release of water and heat. The resulting temperature changes, the subsequent convection of air, and the removal of moisture and heat through the layers were represented.

Microbial growth and substrate consumption rates were described using modified first-order kinetics, which were adjusted for each layer based on an innovative, non-linear, statistical analysis of temperature histories recorded at different positions in the compost bed from three treatments (i.e., FAS values of 0.45, 0.52, and 0.65). Temperature histories and airflow measurements from the treatment with FAS value 0.57 were used as an independent test for the assessment of model performance. For mesophilic bacteria, active from about 0°C to 55 °C, the empirical relationships between k_{max} and FAS developed in this study was:

$$k_{\max}^{meso} = 0.01 + 0.90 \times \exp(-\exp(-15.0 \times (FAS - 0.53))) \qquad R^2 = 0.97$$

For thermophilic bacteria, active from about 40°C to 75 °C, the empirical relationships between k_{max} and FAS developed in this study was:

$$k_{\max}^{thermo} = 0.01 + 0.70 \times \exp(-\exp(-12.3 \times (FAS - 0.55))) \qquad R^2 = 0.96$$

Simulation results indicate that the model could predict the general trend of temperature development. Statistical test and residual plot show that the model used

for prediction is biased, possibly because many parameters in the model were not measured directly. Results from this study could help to further develop the understanding of the relationships between various parameters, and models similar to this one could eventually be useful in the design, optimization, and management of passively aerated composting facilities.

5.6 References

Adams RA. 2003. Calculus: a complete course. 5th ed. Pearson Education Canada Inc., Toronto, Ontario.

Agnew JM, JJ Leonard, J Feddes, Y Feng. 2003. A modified air pycnometer for compost air volume and density determination. *Canadian-Biosystems-Engineering*. 45(6): 27-35

Alberty RA, RJ Silbey. 2000. Physical chemistry. 3rd Ed. New York: Wiley. 969 p.

Alexander M. 1999. Biodegradation and bioremediation. 2nd ed. San Diego: Academic Press, 453 p.

Alvarez R, S Villca, G Liden. 2006. Biogas production from llama and cow manure at high altitude. *Biomass & Bioenergy*. 30(1): 66-75

American Society of Heating, Refrigerating and Air-Conditioning Engineers (ASHRAE). 2005. Psychrometrics. In *Handbook of Fundamentals*, ed. ASHRAE, 6.1-6.17. Atlanta, GA: ASHRAE.

Aulenta F, C Bassani, J Ligthart, M Majone, A Tilche. 2002. Calorimetry: a tool for assessing microbial activity under aerobic and anoxic conditions. *Water research*. 36(5): 1297-1305

Barrington S, D Choiniere, M Trigui, W Knight. 2003. Compost convective airflow under passive aeration. *Bioresource technology* 86 (3): 259-266

Barros N, M Gallego, S Feijoo. 2004. Calculation of the specific rate of catabolic activity (A_c) from the heat flow rate of soil microbial reactions measured by calorimetry: significance and applications. *Chemistry & Biodiversity* 1(10): 1560-1568

Cronje AL, Turner C, Williams AG, Barker AJ, Guy S. 2004. The respiration rate of composting pig manure. *Compost Science & Utilization* 12(2): 119-129

Das K and H.M. Keener. 1997. Moisture Effect on Compaction and Permeability in Composts. *Journal of Environmental Engineering*123 (3): 275-281

Daverio E. 2003. Calorimetric assessment of activity in WWTP biomass. *Water science and technology*. 48(3): 31-38

De Bertoldi M, G Vallini, A Pera and F Zucconi. 1985. Technological aspects of composting including modelling and microbiology. In: J K R Gasser, Editor, *Composting of Agricultural and Other Wastes*, Elsevier Applied Science Publishers, London. p27-41.

Epstein E. 1997. The science of composting. Lancaster, Pa.: Technomic Pub. Co. 487 p.

Fernandes L, W Zhan, NK Patni and PY Jui. 1994 Temperature distribution and variation in passively aerated static compost piles. *Transactions of the ASAE* 48, 257–263.

Fernandez L and M Sartaj. 1997. Comparative study of static pile composting using natural, forced and passive aeration methods. *Compost science & utilization* 5 (4): 65-77

Fogiel AC, RD von Bernuth, FC Michel Jr, TL Loudon. 1999. Experimental Verification of the Natural Convective Transfer of Air Through a Dairy Manure Compost Media. ASAE. Paper No. 99-4053. Am. Soc. Agric. Engrs., St. Joseph, MI

Fry JC. 1988. Determination of biomass. In Methods in aquatic bacteriology. edited by B Austin. Wiley, Chichester, New York. p27-72

Gomez RB, Lima FV, Ferrer AS. 2006. The use of respiration indices in the composting process: a review. *Waste management & research*. 24(1): 37-47

Hamelers HVM. 2004. Modeling composting kinetics: A review of approaches. *Reviews in Environmental Science & Bio/Technology*. 3: 331–342

Haug RT. (1993) The Practical Handbook of Compost Engineering. Boca Raton. Lewis Publishers. 717 p

Komilis DP. 2006. A kinetic analysis of solid waste composting at optimal conditions. *Waste management.* 26(1): 82-91

Kutzner HJ. 2001. Microbiology of composting. In Biotechnology, Vol. 11c; Wiley: NY, pp 35–100.

Liang Y, JJ Leonard, J Feddes, WB McGill. 2004. A simulation model of ammonia volatilization in composting. *Transactions of the ASAE* 47 (5): 1667-1680

Lynch NJ and RS Cherry. 1996a. Winter composting using the passively aerated windrow system. *Compost Science & Utilization* 4(3):44-52

Lynch NJ and RS Cherry. 1996b. Design of passively aerated compost piles: vertical air velocities between pipes. *Biotechnology Progress* 12(5):624–629

Madigan MT and Martinko JM. 2006. Brock biology of microorganisms.11th ed. Pearson Prentice Hall. Upper Saddle River, NJ.

Mason IG. 2006. Mathematical modelling of the composting process: A review. *Waste Management* 26 (1): 3-21

McCartney D and HT Chen. 2001. Using a biocell to measure effect of compressive settlement on free air space and microbial activity in windrow composting. *Compost science & utilization* 9 (4): 285-302

McCartney D and G Eftoda. 2005. Windrow composting of municipal biosolids in a cold climate. *Journal of environmental engineering and science* 4 (5): 341-352

Monod J. 1949. The growth of bacterial cultures. *Annual Review of Microbiology.* 3, 371–394

Montgomery DC, GC Runger. 2002. Applied statistics and probability for engineers. 3rd ed. New York: Wiley, 706 p.

Nielsen H, Berthelsen L. 2002. A model for temperature dependency of thermophilic composting process rate. *Compost science & utilization.* 10(3): 249-257

Paletski WT and JC Young. 1995. Stability measurement of biosolids compost by aerobic respirometry. *Compost science & utilization.* 3, 16–24

Richard TL; AHM Veeken; V de Wilde, HVM Hamelers. 2004. Air-filled porosity and permeability relationships during solid-state fermentation. Biotechnology progress 20 (5): 1372-1381

Richard TL, Walker LP. 2006. Modeling the temperature kinetics of aerobic solid-state biodegradation. *Biotechnology progress*. 22(1): 70-77

Ryckeboer JR, J Mergaert, K Vaes, S Klammer, D de Clercq, J Coosemans, H Insam, J Swings. 2003. A survey of bacteria and fungi occurring during composting and self-heating processes. *Annals of Microbiology*. 53(4), 349-410.

Seki H. 2000. Stochastic modeling of composting processes with batch operation by the Fokker-Planck equation. *Transactions of the ASAE*.43 (1): 169-179

Solano ML, F Iriarte, P Ciria, MJ Negro. 2001. Performance Characteristics of Three Aeration Systems in the Composting of Sheep Manure and Straw. *Journal of Agricultural Engineering Research* 79 (3): 317-329.

Stombaugh DP and SE Nokes. 1996. Development of a biologically based aerobic composting simulation model. *Transactions of the ASAE*. 39 (1): 239-250

Sundberg, C., Smars, S., Jonsson, H., 2004. Low pH as an inhibiting factor in the transition from mesophilic to thermophilic phase in composting. *Bioresource Technology*. 95, 145–150

Thompson WH, PB Leege, PD Millner, ME Watson. 2002. Test methods for the examination of composting and compost. Composting Council Research and Education Foundation, Washington, D.C. USDA.

Veeken A, de Wilde V, Hamelers B. 2002. Passively aerated composting of straw-rich pig manure: Effect of compost bed porosity. *Compost science & utilization* 10 (2): 114-128

Yu S, G Clark, J Leonard. 2005a. Airflow measurement in passively aerated compost. *Canadian Biosystem engineering* 47(6):39-45.

Yu S, G Clark, J Leonard. 2005b. Analysis of temperature history in passively aerated compost. 2005 ASAE Pacific Northwest Regional Meeting, Lethbridge, AB, Canada. Paper No: PNW05-1013

Yu S, G Clark, J Leonard. 2006. Airflow in passively aerated compost. CSBE/SCGAB 2006 Annual Conference, Edmonton, AB, Canada. Paper No: 06-113

Table 5-1. Parameter values used in simulation

	Parameter	Units	Default	Reference
Microbial kinetics values	$Y_{X/C}$	$kg_X\ kg_C^{-1}$	0.35	Stombaugh and Nokes 1997
	$Y_{W/S}$	$kg_{H2O}\ kg_S^{-1}$	0.63	Stombaugh and Nokes 1997
	$Y_{X/S}$	$kg_{O2}\ kg_S^{-1}$	1.370	Stombaugh and Nokes 1997
	$Y_{H/S}$	kJ kg_S^{-1}	19,100	Stombaugh and Nokes 1997
	K_C	kg kg_{dm}^{-1}	0.15	Liang *et al.* 2004
	K_{O2}	kg kg_{dm}^{-1}	0.00003	Liang *et al.* 2004
Thermodynamic values	c_s	kJ (kg °C)$^{-1}$	1.480	Stombaugh and Nokes 1997
	c_{nvs}	kJ (kg °C)$^{-1}$	0.840	Stombaugh and Nokes 1997
	c_w	kJ (kg °C)$^{-1}$	4.187	Haug 1993
	c_a	kJ (kg °C)$^{-1}$	1.013	Haug 1993
	ρ	$kg_{da}\ m^{-3}$ air	1.286	Haug 1993

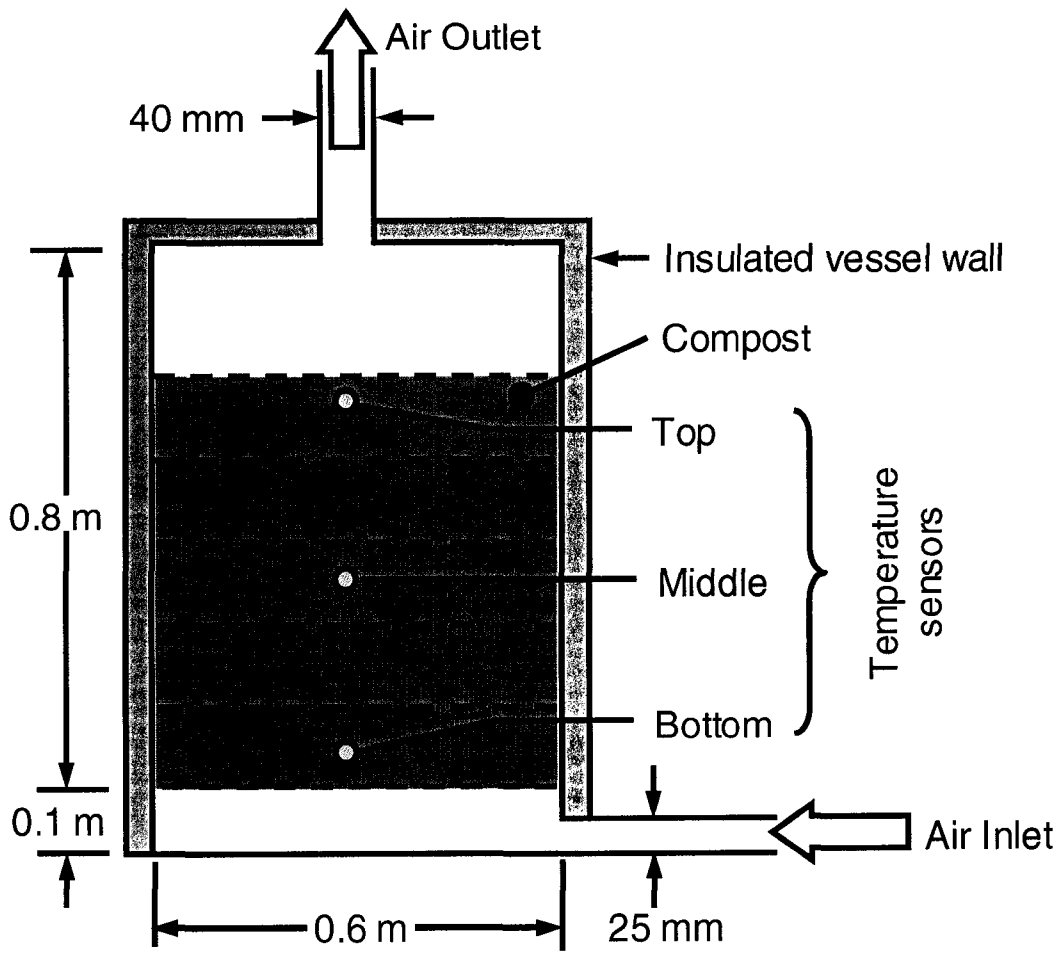

Figure 5-1. Schematic of the physical model used in this study

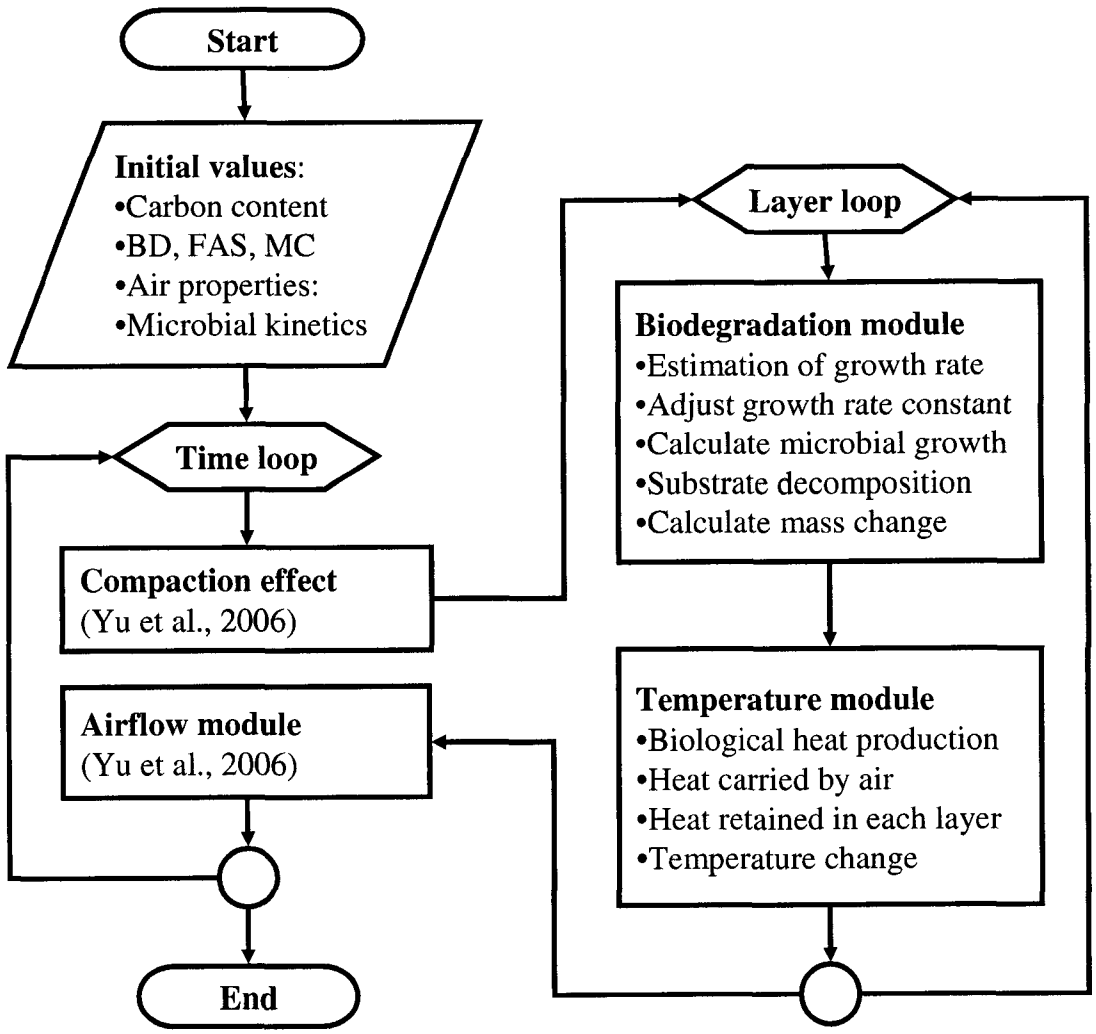

Figure 5-2. (a) Overall flow chart of the model

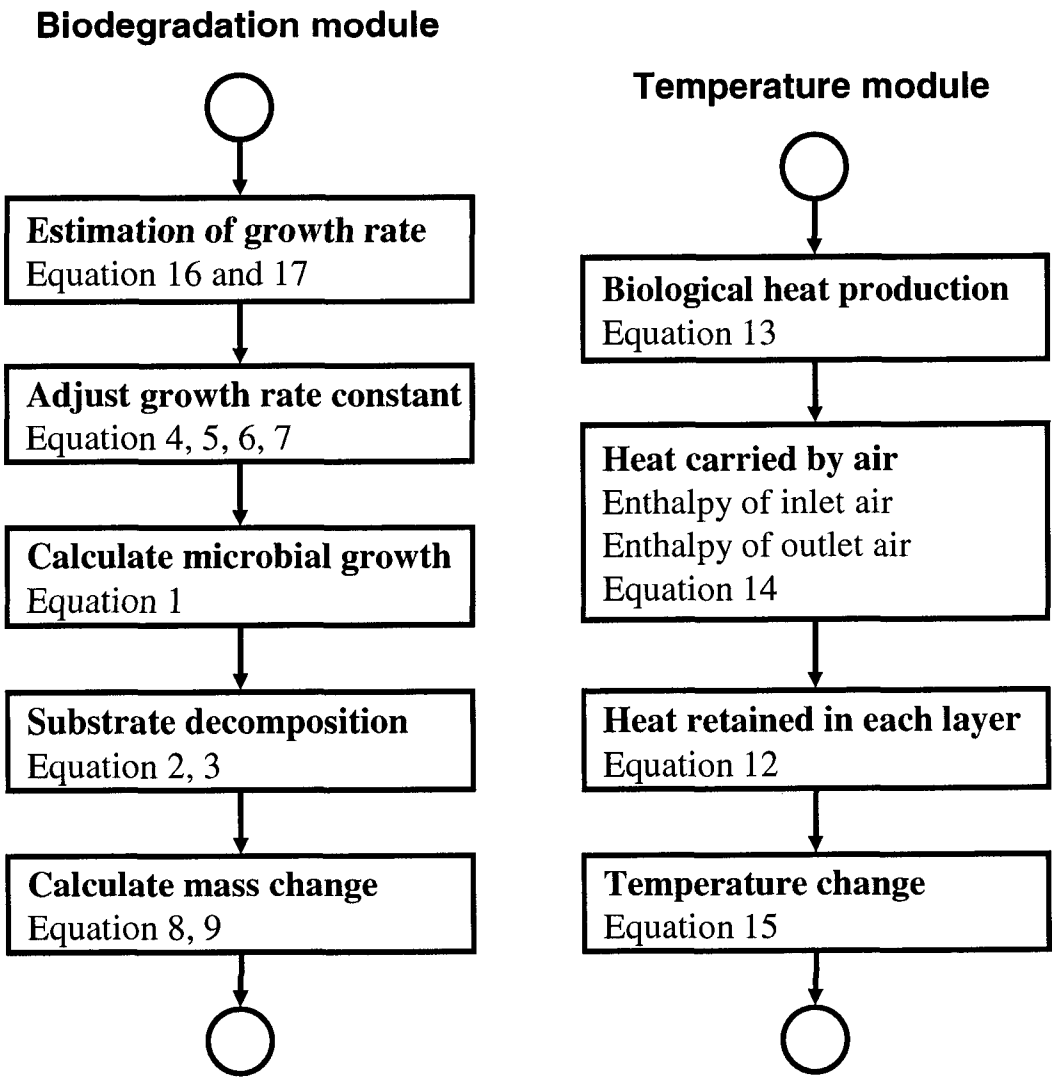

Figure 5-2. (b) Flow chart of biodegradation model and temperature model

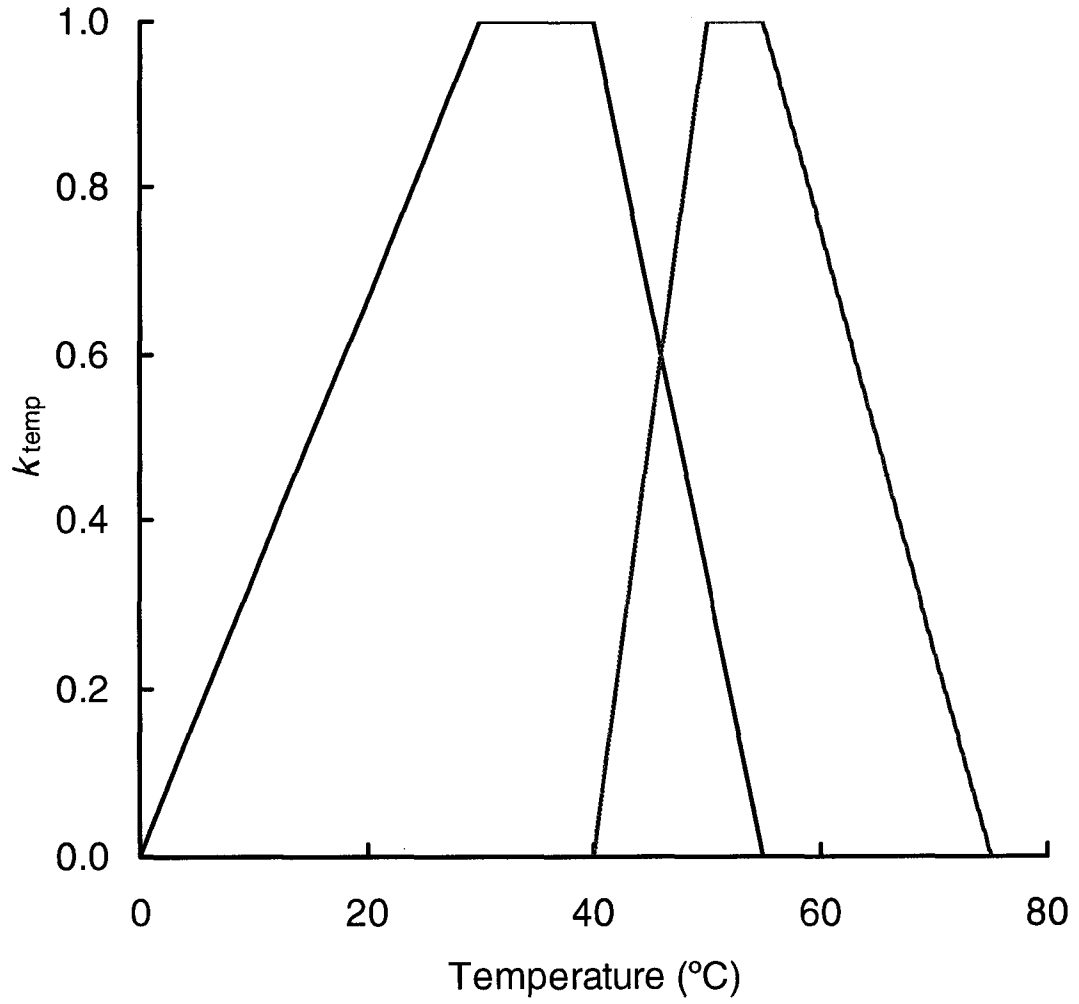

Figure 5-3. Assumed effect of temperature on decomposition rate, where k_{temp} is temperature correction coefficient for microbial growth

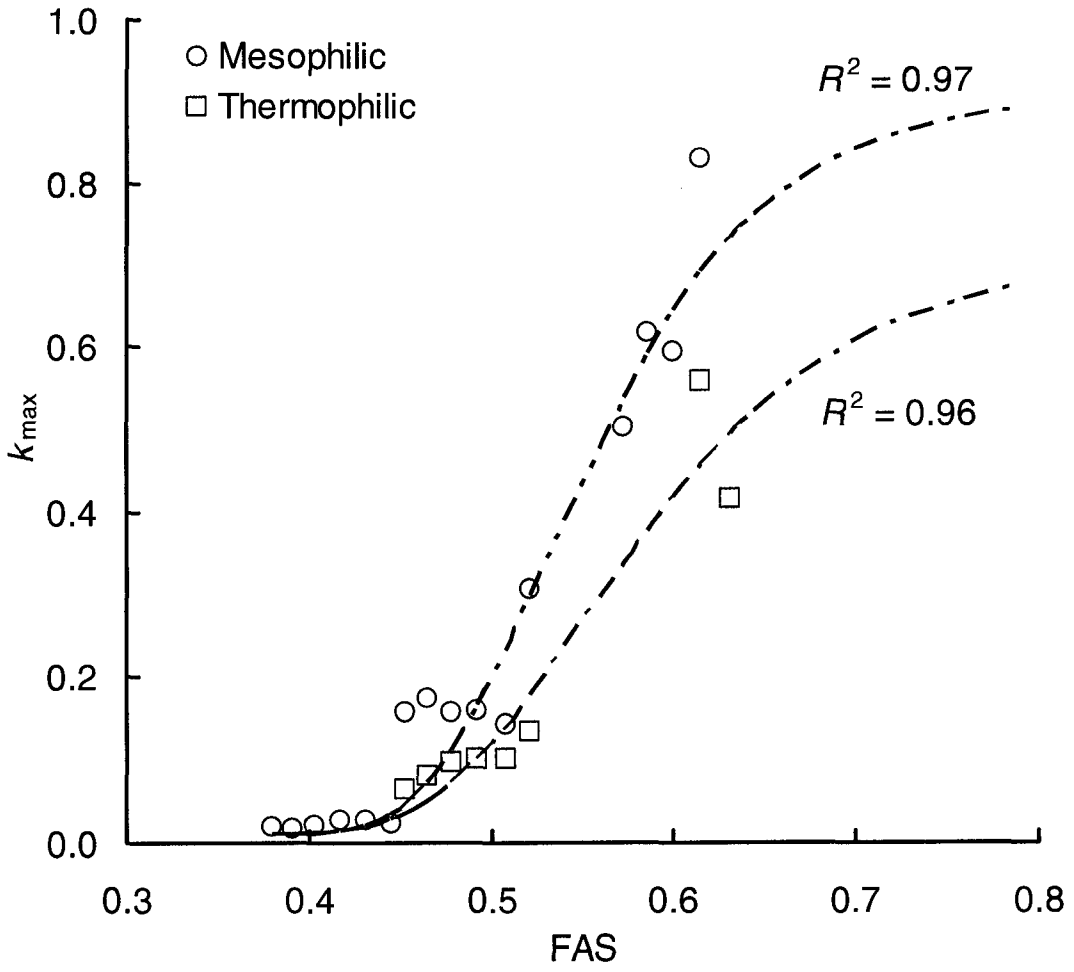

Figure 5-4. The maximum degradation rate at different stages of composting and different free air space (Equation 16 and 17)

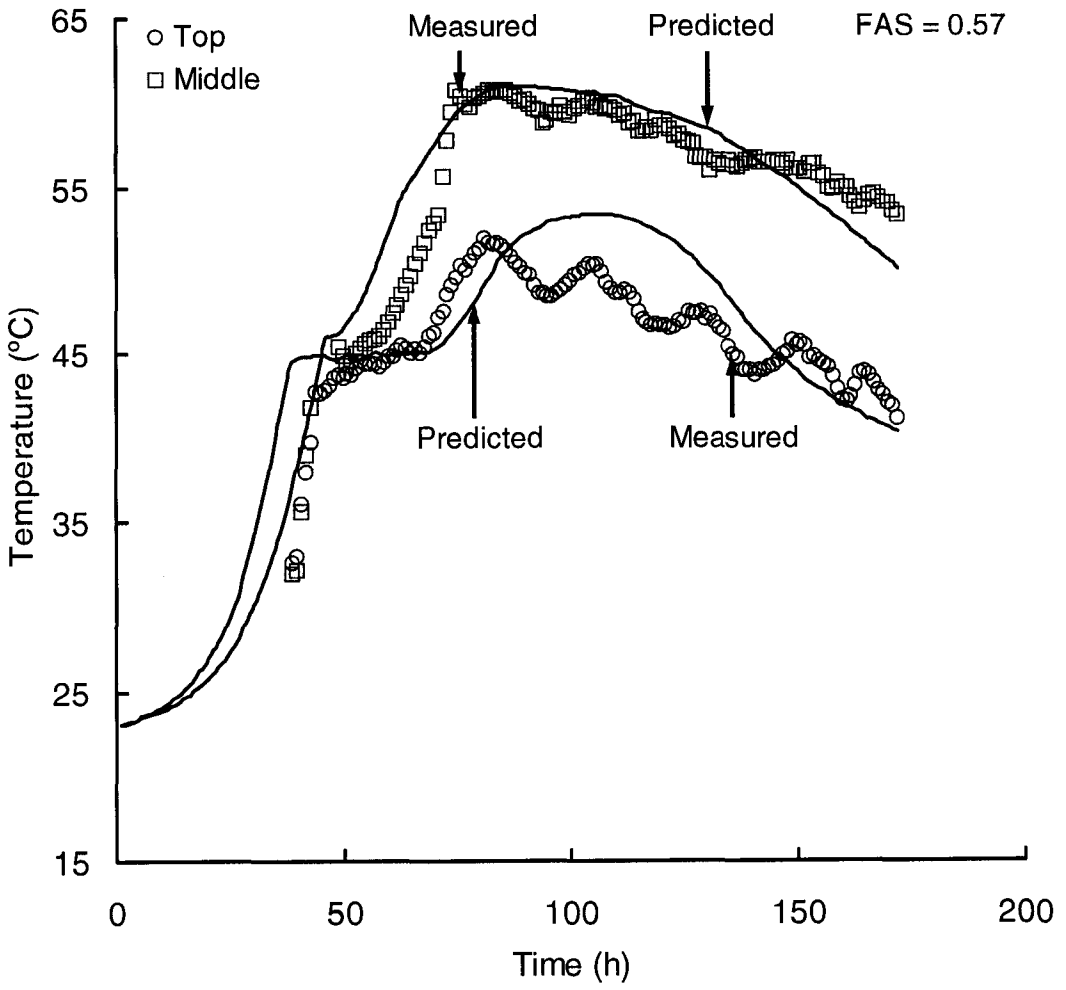

Figure 5-5. Measured and predicted temperature histories in the compost (initial FAS = 0.57)

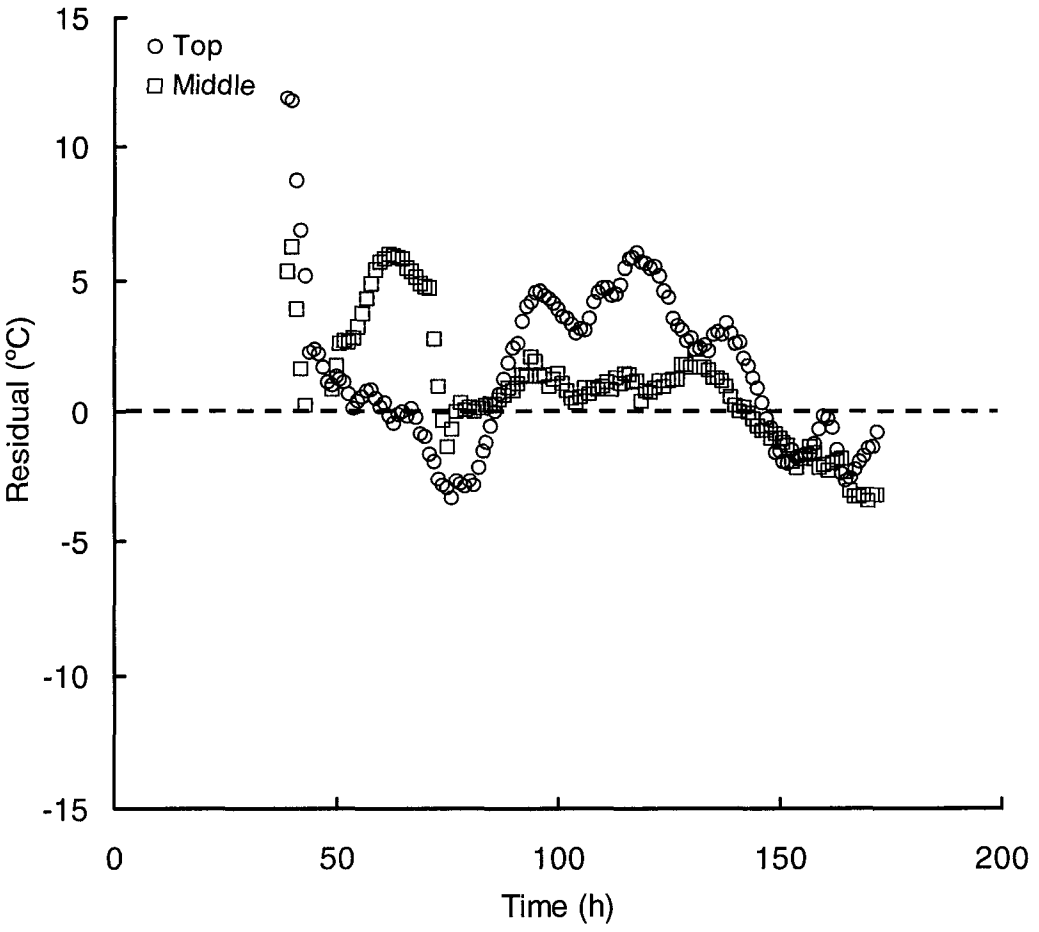

Figure 5-6. Residual plot of the predicted vs. measured temperature histories in the compost (initial FAS = 0.57)

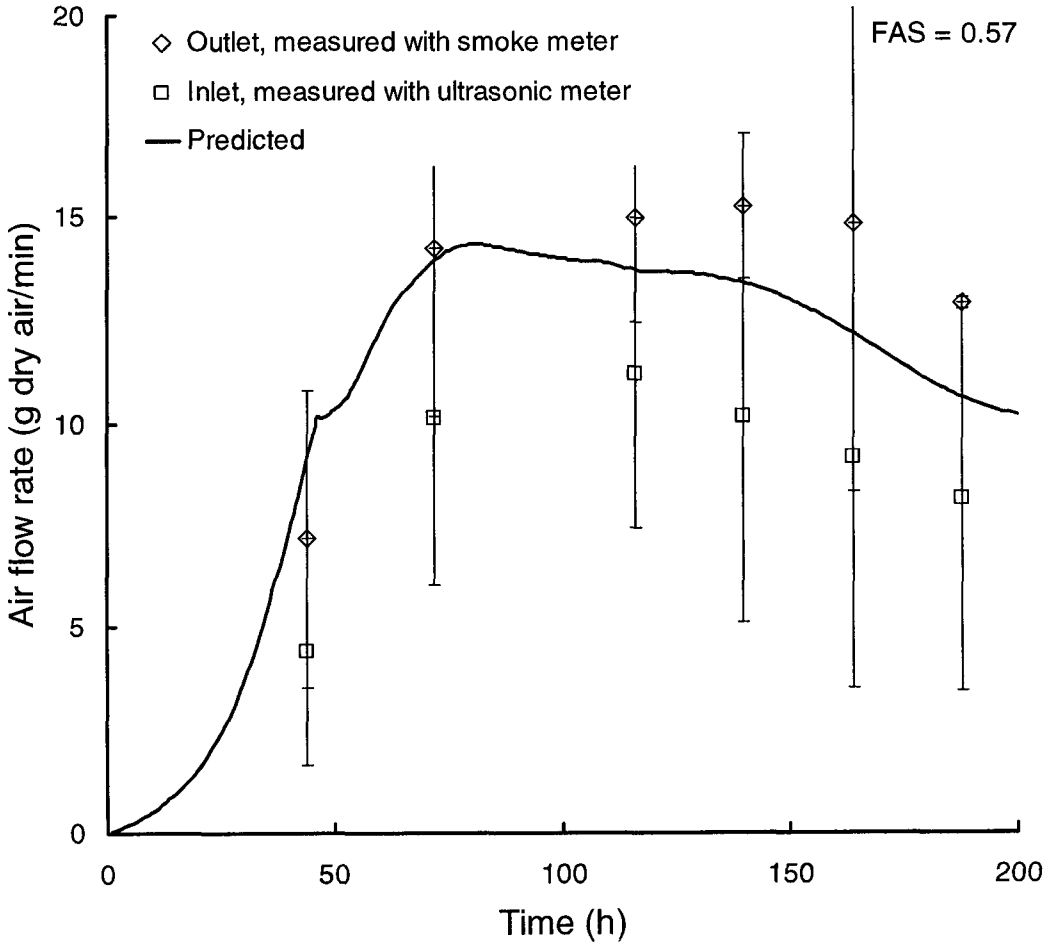

Figure 5-7. Measured and predicted air flow rates through the compost (initial FAS = 0.57)

Chapter 6 Synthesis

6.1 Summary and conclusions

The objectives set for this work were:

- Measurement of airflow in passively aerated compost systems
- Development of a practical model to predict airflow development
- Development of a rigorous significance test among treatments
- Determining an empirical relationship between FAS and biodegradation kinetics (k_{max})

For the measurement of airflow in passively aerated compost systems a smoke tracer flow meter was devised and evaluated in Chapter 2. Smoke from fuming sulphuric acid was used as a tracer and the tracer's passage was detected by two infrared emitter/detectors, separated by a known distance, installed on a straight air exhaust pipe. The total estimated pressure loss across the smoke tracer flow meter was 0.10 Pa, which had negligible influence on airflow measurement, and the responses of the flow meters were very linear in the calibration range ($R^2 = 0.98$). The smoke tracer flow meter exhibited greater variation at high airflow rates and the relatively low sampling rate (about 6 Hz), limited by the slow clock speed of the computer used in the trial, was considered a major contributor to this. Compared with other flow meters used in similar experiments, the smoke tracer flow meter had the advantages of very low pressure loss, low cost, and robust performance under humid conditions.

An analytical model for the prediction of airflow rate in passively aerated compost was developed based on Darcy's law:

$$v = -\frac{K}{\mu}\rho_0 g\left(1-\frac{T_0}{T_i}\right)$$

The model related the physical characteristics (permeability, K) and temperature of the compost (T_i) with the predicted air flow (v), and the compaction which occurs during composting was also taken into account in the application of the model. The model was implemented in a computer simulation, and verified by using temperature histories from the passively aerated composting experiment to predict airflow. The calculated airflow values were not significantly different from the measured values (p = 0.97).

Temperature, an important indicator of composting microbial activity, was recorded by an automatic data logger at different depths in the substrate, and the differences among the temperature histories were used as the basis for adjusting the microbial kinetic parameters in simulation. A novel mathematical model was proposed for the statistical comparison of temperature histories from composting trials, based on a modified Gompertz function that includes nonlinear, time-correlated effects.

$$T(t) = T_a + T_{hm}\cdot e^{-e^{-k_{hm}\cdot(t-t_{hm})}} + T_{ht}\cdot e^{-e^{-k_{ht}\cdot(t-t_{ht})}} - T_c\cdot e^{-e^{-k_c\cdot(t-t_c)}}$$

Methods were developed for the estimation of initial values for the model parameters, and algorithms in SAS® were used to fit the model to different sets of temperature data. A method was also developed for rigorously determining the significance of differences among the datasets as described using the proposed model. The model and methods were shown to be useful tools for the statistical comparison of time series temperature data in composting. The model cannot, however, accommodate

discontinuous data such as those from compost trials that involve turning and/or re-mixing.

Finally, microbial growth and the accompanying rate of substrate consumption were modeled using modified first-order kinetics. The kinetic parameters used in simulation were locally adjusted for different layers in the compost bed, based on an empirical description of the relationship between those parameters and the measured substrate FAS. Separate relationships were derived for the mesophilic and thermophilic regimes. The initial kinetic parameters used to define these relationships were based on temperature data from three preliminary trials (i.e., FAS values of 0.45, 0.52, and 0.65), and were estimated using the new statistical methods described previously. For mesophilic bacteria, active from about 0°C to 55 °C, the resulting empirical relationship between k_{max} and FAS developed in this study was:

$$k_{\max}^{meso} = 0.01 + 0.90 \cdot \exp(-\exp(-15.0 \cdot (FAS - 0.53))) \qquad R^2 = 0.97$$

For mesophilic bacteria, active from about 40°C to 75 °C, k_{max} was estimated by:

$$k_{\max}^{thermo} = 0.01 + 0.70 \cdot \exp(-\exp(-12.3 \cdot (FAS - 0.55))) \qquad R^2 = 0.96$$

Temperature histories and airflow measurements from an independent trial using compost with FAS of 0.57 were used to assess the model's performance. Simulation results indicate that the model could predict the general trend of temperature development. A plot of the residuals showed that the model was biased, however, possibly because many parameters in the model were not measured directly but instead were estimated from literature. The results from this study help to further develop the understanding of the relationships between various compost parameters,

and models similar to this one could eventually be useful in the design, optimization, and management of passively aerated composting facilities.

6.2 Contributions to knowledge

The following contributions to the composting literature arose out of the work discussed in this thesis:

- A smoke tracer flow meter was shown to be suitable for the measurement of the exhaust air velocity during passively aerated composting
- Airflow rate in passively aerated compost can be estimated by
  - $v = -\frac{K}{\mu}\rho_0 g\left(1-\frac{T_0}{T_i}\right)$
- For a given substrate, temperature time series can be represented by the sum of three functions representing mesophilic growth, thermophilic growth and decay:
  - $T(t) = T_a + T_{hm}\cdot e^{-e^{-k_{hm}\cdot(t-t_{hm})}} + T_{ht}\cdot e^{-e^{-k_{ht}\cdot(t-t_{ht})}} - T_c\cdot e^{-e^{-k_c\cdot(t-t_c)}}$
  - Methods were developed for the estimation of initial values for the model parameters
  - Rigorous statistical comparison of different data sets was demonstrated
- Microbial rate constants in composting can be determined by the analysis of temperature time series
  - Both mesophilic and thermophilic rate constants are well described using a sigmoid relationship with FAS
    - For mesophilic bacteria, active from about 0°C to 55 °C, the empirical relationship between k_{max} and FAS developed in this study was:

$$k_{max}^{meso} = 0.01 + 0.90 \cdot \exp(-\exp(-15.0 \cdot (FAS - 0.53))) \qquad R^2 = 0.97$$

- For mesophilic bacteria, active from about 40°C to 75 °C, k_{max} was estimated by:

$$k_{max}^{thermo} = 0.01 + 0.70 \cdot \exp(-\exp(-12.3 \cdot (FAS - 0.55))) \qquad R^2 = 0.96$$

- A biodegradation model using the above relationships can predict the general trend of temperature development

6.3 Recommendations

Airflow measurement for passively aerated composting processes is still challenging and deserves further study in order to effectively validate models such as the one presented here. Further work could be done to completely automate the smoke flow meter devised in this study to improve the accuracy and convenience of measurement. The airflow model proposed in this study was developed with highly idealized assumptions, which excluded phenomena such as the evaporation of moisture from the substrate and volatilization of the substrate, consumption of oxygen, and release of carbon dioxide by microbial activity. Further research could be done to quantify and model their effect on convective airflow development. Another possible improvement of the model would be to incorporate effects of drag on airflow, using an expression such as the Dupuit-Forcheimer relationship (Richard et al., 2004; Lage and Antohe, 2000).

The permeability of the substrate is another critical variable that must be accurately determined to improve the accuracy of airflow model. It has been pointed out that some void space in the composting substrate may not be available for air flow

development (Eftoda and McCartney, 2004). A model of such "unsaturated" air flow might therefore be considered in future research to improve the prediction of average air velocity through compost.

The maximum microbial growth rate was estimated in this study by the analysis of temperature histories from composting trials, which involved fitting the sum of two sigmoid, asymptotic growth curves to the temperature histories. The fitted parameters were thereafter used to estimate the microbial kinetic coefficients. Further research is required, however, to establish a rigorous theoretical underpinning for this relationship between temperature measurements and the values of the microbial growth parameters.

The 1-dimensional model developed in this thesis should be extended to 2-dimensional and 3-dimensional real world applications, i.e., in windrow composting, distribution of substrate FAS, air flow, and temperature in actual windrows need to be measured and corresponding mathematical descriptions developed. Computational fluid dynamics (CFD) and finite element analysis (FEM) can be thereafter employed to simulate and predict the composting process in windrow systems.

The complexity of the compost system limits the accuracy of deterministic models, since it challenges both the current understanding of the process and available measurement techniques (Hamelers, 2004, Mason 2006). Alternatives to deterministic modeling, such as the training of artificial neural networks, could be considered, since such models can sometimes usefully represent systems that are not well-understood in theory or in which intermediate or internal quantities are difficult to observe (Rabunal and Dorado, 2006).

6.4 References

Eftoda, G., and D. McCartney. 2004. Determining the critical bulking agent requirement for municipal biosolids composting. *Compost science & utilization.* 12 (3): 208-218

Hamelers, H.V.M. 2004. Modeling composting kinetics: A review of approaches. Reviews in Environmental Science & Bio/Technology. 3: 331–342

Lage, J.L., and B.V. Antohe. 2000. Darcy's experiments and the deviation to nonlinear flow regime. *ASME J. Fluids Eng.* 122: 619-625

Mason, I.G. 2006. Mathematical modelling of the composting process: A review. Waste Management 26 (1): 3-21

Rabunal, J. R., and J. Dorado. 2006. Artificial Neural Networks in Real-Life Applications. Hershey, PA.: Idea Group Pub. 391p

Richard, T.L., A.H.M. Veeken, V. de Wilde, and H.V.M. Hamelers. 2004. Air-filled porosity and permeability relationships during solid-state fermentation. Biotechnology progress 20 (5): 1372-1381

Appendix A Simulation C source code

```
/*************************************************************/
/* Func : main()                                             */
/*                                                           */
/* Use  : prediction of temp and airflow development in      */
/*        passively aerated compost                          */
/*                                                           */
/* In   : [C] BD FAS AmbientTemperature AmbientRH            */
/*                                                           */
/* Out  : temperature at each layer                          */
/*        arflow rate through the compost                    */
/* Date : 2005-May-4th                                       */
/*************************************************************/
#include <stdio.h>
#include <stdlib.h>
#include <conio.h>
#include <math.h>

/* Psychrometric estimation – developed by:          */
/*                              S.H. Zhang  R.S. Gates */
/*                              University of Kentucky */

#include "protof.h"     /* prototype file for PSYFUNC.H      */
#include "protop.h"     /* prototype file for PSYPROC.H      */
#include "psyfunc.h"    /* use psyfunc.h as INCLUDE file     */
#include "psyproc.h"    /* use psyproc.h as INCLUDE file     */

main()
{
/* Substrate chemical information */
  double iniC = 0.085;          /* kg/kg dm */

/* Substrate physical information */
  double Height = 0.5,          /* total height of the initial compost (m)        */
         Volume = 0.12,         /* volume of the initial compost (m3)             */
         BD0 = 520.,            /* initial bulk density, (kg/m3) - trt2           */
         iniDM0,                /* initial total dry matter (kg)                  */
         iniW0,                 /* initial water content (kg)                     */
         nvs,                   /* non-volatile-solid (kg)                        */
         FAS0;                  /* initial Free Air Sapce (FAS) (0~1)             */

  double FAS[6],        /* free air space values for each layer (0~1)             */
         BD[6],         /* bulk Density (kg/m3) at each layer                     */
         Pd[6],         /* compressive stress at each layer (Pa)                  */
         hi[6],         /* non-dimensional height of at stress Pi [Das & Keener]  */
         hm[6],         /* non-dimensional height of maximum compressed state     */
         dh0[6],        /* total compressible fraction of compost (m/m)           */
         beta[6],       /* rate of volume reduction                               */
```

```
        C[6],           /* Kozeny-Carman constant at each layer                */
        K[6],           /* substreat permeability at each layer                */

        height[6]={0.05,        /* height of layer 0 (m) - bottom      */
                   0.10,        /* height of layer 1 (m)               */
                   0.10,        /* height of layer 2 (m)               */
                   0.10,        /* height of layer 3 (m)               */
                   0.10,        /* height of layer 4 (m)               */
                   0.05};       /* height of layer 5 (m) - top         */

/* File handle for recording calculation results */
 FILE *fp;

/* Kinetic parameters - growth rate (1/hr), use growth_rate() to calculate*/
 double kd[6],                  /* actual overall degradation rate, 1/hr       */
        kmax,                   /* maximum overall degradation rate, 1/hr      */
        kmax_meso,              /* maximum mesophilic degradation rate, 1/hr   */
        kmax_thermo;            /* maximum thermophilic degradation rate, 1/hr */

 double km,     /* coefficients for effect of temperature (mesophilic range, 0 - 45)      */
        kt,     /* coefficients for effect of temperature (thermophilic range, 35 - 60)   */
        kw;     /* coefficients for effect of moisture content                            */

 /* conversion factor of biomass from carbon*/
 double fbc = 0.085;

 /* conversion factor of substrate from carbon*/
 double fsc = 0.085;

 /*Half velocity const for degradable (volatile) substrate */
 double Ksc = 0.30;     /* half saturation constant for Carbon: kg/kgdm  */

 /*Half velocity const for oxygen */
 /* - Modified from Stombaugh and Nokes, Liang - 0.00003 */
 double KO2 = 0.000002;

/* Yield coefficients */
 /* kg cells produced / kg substrate (volatile solid) consumed     */
 /* - Stombaugh and Nokes */
 double Yxs = 0.35;

 /* kg O2 used / kg substrate (volatile solid) consumed */
 /* - Stombaugh and Nokes 1.37 */
 double YO2s = 1.0 / 0.085;

 /* kg water produced / kg substrate (volatile solid) consumed */
 /* - Liang */
 double Yws = 0.631 / 0.085; /* 0.46 - 0.77 (Bach et la. 1987) kg/kg*/
```

```
 /* Joule of heat produced / kg substrate (volatile solid) consumed */
 /* - Modified from Stombaugh and Nokes */
 double Yhs = 1.8e7 ;

/* Bioreactor (vessel) physical parameters*/
 /* Diameter of the vessel (m) */
 double diameter = 0.5;

 /* Intersectional area (m2)*/
 double sectionArea = 0.25 * 3.14 * diameter * diameter;

/* Thermodynamic parameters*/
 double cvs = 1480.,    /* Specific heat of substrate (J/kg-C) at each layer      */
        cw = 4180.,     /* Specific heat of water (J/kg-C)                        */
        cnvs = 840.;    /* Specific heat of non-volatile substrate (J/kg-C)       */

/*Moist air properties*/
 /* Ambient air*/
 double ambientTemp = 23.0,  /* Unit: C            */
        ambientRH = 0.6,     /* Unit:              */
        airdensity = 1.286,  /* Unit: kg/m3        */
        airviscosity = 1.8e-5, /* Unit: Pa s       */
        O2conc = 0.2992;     /* Unit: kg / m3 air. */

/*********************************************************************/
/* Goal: Define variables used in calculation                        */
/*       Two-dimension arrays: one for layer number and the other time */
/*********************************************************************/

 double X[6][250],     /* Total microbial biomass concentration (kg cells / kgdm)  */
     dXdt[6][250],     /* Growth rate of microbes (dXdt) (kg cells / kg/hr)        */
     CDM[6][250],      /* Carbon content in each layer (kg/kgdm)                   */
     dCdt[6][250],     /* Rate of carbon consumption at each layer(kg/hr)          */
     dSdt[6][250],     /* Rate of substrate consumption at each layer(kgdm/hr)     */

     O2DM[6][250],     /* Oxygen amount in each layer (kgO2/kgdm)                  */
     dO2dt[6][250],    /* Oxygen concentration changing rate (kg/hr)               */
     Oin[6][250],      /* Oxygen content of air entering layer (kgO2/m3)           */
     Oout[6][250],     /* Oxygen content of air leaving layer (kgO2/m3)            */

     win[6][250],      /* Humidity ratio of air entering layer (kgH2O/kg da)       */
     wout[6][250],     /* Humidity ratio of air leaving layer (kgH2O/kg da)        */
     hin[6][250],      /* Enthalpy of the air entering layer (J/kg da)             */
     hout[6][250],     /* Enthalpy of the air leaving layer (J/kg da)              */

     dWdt[6][250],     /* Humidity ratio change at each layer (kgH2O/hr)           */
     MC[6][250],       /* Moisture content at each layer(kg/kg)                    */
     VS[6][250],       /* Volatile Solid (BVS) content at each layer(kg)           */
     NVS[6],           /* Non-Volatile Solid content at each layer(kg)             */
     W[6][250],        /* Water content at each layer(kg/kgdm)                     */
```

```
    w_change,       /* Average humidity ratio change at each layer                */

    dTdt[6][250],   /* Temperature change at each layer (C/hr)                    */
    dT[6],          /* Temperature differences between each layer and ambient (C) */
     sdT,           /* Sum of the all the temperature differences                 */
    Temp[6][250],   /* Temperature at each layer (C)                              */

    volflow,        /* Volumetric flow rate (m3/s)                                */
    flowrate[250];  /* Airflow rate going through the compost (kg/hr)             */

 int    Stage[6][250]; /* The stage status of the composting: meso or thermo      */

/*************************************************************************/
/* Psychrometrics:                                                       */
/*   By the use of dry-bulb temperature (C) and relative humidity (RH%), */
/*   find out all other psychrometric properties, such as, humidity ratio, w;  */
/*   wet-bulb temperature, twb; dwp point temperature, tdp; enthalpy, h;  */
/*   specific volume, spvol; and air density, dens.                      */
/*************************************************************************/

 double h0,     /* enthalpy of air/water vapor mixture [kg/kJ].*/
        w0;     /* humidity ratio of air/water vapor mixture.*/

 struct psyprops airflow;       /* declare name props for struct PSYPROPS */

 int i, j, l, t;                /* variables for loop control*/
 double depth = 0;

 iniDM0 = BD0 * Volume * 0.25;      /* Initial dry matter, kg; moisture content 75% */
 iniW0 = BD0 * Volume * 0.75;       /* Initial water, kg; moisture content 75%      */
 nvs = 0.05 * iniDM0;               /* Amount of non-volativle-solid, kg;           */
 FAS0 = 0.57;                       /* Initially measured, treatment 3              */

/*************************************************************************/
/* At inlet:                                                             */
/*   Dry-bulb temperature (C) was assumed to be the same as ambient (23C)*/
/*   Relative humidity (RH%) assumed to be the same as ambient (60%)     */
/*   As a result, humidity ratio, w0, and enthalpy, h0 were contant      */
/*************************************************************************/

 airflow.airp = 101.325;        /* kPa */

 /* call db_rh() in psyproc.h for the calculation */
 db_rh(ambientTemp, ambientRH, &airflow);

 w0 = airflow.w;        /* The H2O ratio of air entering bottom layer  */
 h0 = airflow.h;        /* The enthalpy of air entering bottom layer   */

/*************************************************************************/
```

```
/* Initial values of related parameters for each layer */
 for (i = 0; i < 6; i++)            /*i: layer number, counting from bottom*/
 {
  BD[i] = BD0;
  MC[i][0] = 0.75;

  depth = 0.0;                      /* calculate the height of compost on each layer*/
        for (j = 0; j < (6 - i); j++) depth += height[j];
  Pd[i] = BD[i] * 9.8 * depth;

  hm[i] = -0.0022 * MC[i][0] * 100 + 0.6887;
  dh0[i] = 0.0023 * MC[i][0] * 100 + 0.308;
  beta[i] = 0.0011 * MC[i][0]  * 100 + 0.0429;
  hi[i] = hm[i] + dh0[i] * exp(-beta[i] * Pd[i] / 1000.);    /* -Das and Keener*/
  FAS[i] = FAS0 * hi[i];
  BD[i] /= hi[i];

  X[i][0] = 0.00025;                                         /* -Liang */

        CDM[i][0] = iniC;

        VS[i][0] = (1 - MC[i][0]) * 0.95 * BD[i] * Volume * height[i] / Height;

        NVS[i] = (1 - MC[i][0]) * 0.05 * BD[i] * Volume * height[i] / Height;

  W[i][0] = MC[i][0] * BD[i] * Volume * height[i] / Height;

  C[i] = 13.244 * MC[i][0] * MC[i][0] - 1552.2 * MC[i][0] + 45950;
  K[i] = (FAS[i] * FAS[i] * FAS[i]) / (C[i] * (1 - FAS[i]) * (1 - FAS[i]));

  O2DM[i][0] = O2conc * FAS[i] * sectionArea * height[i] / (VS[i][0] + NVS[i]);
  Oin[i][0] = O2conc;
  Oout[i][0] = 0.0;

  Temp[i][0] = ambientTemp;
  dT[i] = 0.0;

  Stage[i][0] = 1;

  kd[i] = 0.0;

 }

 flowrate[0] = 0.0;

 if ( (fp = fopen("trt03-2.txt", "w")) == NULL )
 {
   printf("*** output.txt could not be opened for write. \n");
   exit(1);
 }
```

```
else

  fprintf(fp, " time   Pos0   Pos1   Pos2   Pos3   Middle Top   airflow   \n");


/*************************************************************************/

 /* Start the simulation process basing on time progress*/
 /* Time step is taken as 1 hour, as specified by "t++" */

 for (t = 1; t <= 200; t++)
 {
  win[0][t] = w0;              /* Humidity ratio entering the bottom (0) layer*/
  hin[0][t] = h0;              /* Enthaphy the bottom layer*/

  /*****************************************************************/
  /* At outlet                                                     */
  /*   Dry-bulb temperature: the same as that in the top layer     */
  /*   Relative humidity: 100%                                     */
  /*                                                               */
  /* Assume:                                                       */
  /*   Constant evaporation rate at each layer,                    */
  /*   That is, humidity ratio (kg H2O/kg dry air) changing rates  */
  /*   are the same at each layer                                  */
  /*****************************************************************/
  /* call db_rh() in psyproc.h */
  db_rh(Temp[5][t - 1], 1.0, &airflow);

  wout[5][t] = airflow.w;      /* Humidity ratio of air leaving layer (kgH2O/kg da)  */
  hout[5][t] = airflow.h;      /* Enthalpy of the air leaving layer (kJ/kg da)       */

  sdT = 0.0;                   /* Calculate all the sum of temperature differences   */
  for (l = 0; l <= 5; l++)
        sdT += dT[l];

  if (sdT > 0)
  {
    w_change = (wout[5][t] - w0) / sdT;

    for (l = 0; l < 5; l++)
    {
     wout[l][t] = win[l][t] + w_change * dT[l];
     win[l + 1][t] = wout[l][t];
    }
  }
  else
  {
    w_change = (wout[5][t] - w0) / 6;
    for (l = 0; l < 5; l++)
     {
```

```
    wout[l][t] = win[l][t] + w_change;
    win[l + 1][t] = wout[l][t];
    }
}

/*****************************************************************/
/* Calculation of changes at each layer:                         */
/*****************************************************************/

Oin[0][t] = O2conc;          /* O2 content entering the bottom layer*/

flowrate[t] = 0.0;

for (l = 0; l <= 5; l++)     /*l: layer*/
{
/*****************************************************************/
/* Use  : Calculation growth rate constant with give FAS         */
/* In   : Free Air Space (FAS): 0 ~ 1                            */
/*        volatile solid Concentration (Cvs): kg/kgdm            */
/*        Oxygen concentration (O2con): kg/kgdm                  */
/*****************************************************************/

 /* calculate kmax for both meso- and thermo-philic ranges*/
 kmax_meso = 0.01 + 0.9 * exp(- exp(-16.84 * (FAS[l] - 0.53)));

 kmax_thermo = 0.01 + 0.7 * exp(- exp(-12.33 * (FAS[l] - 0.55)));

 /* moisture correction factor kw */
 if (MC[l][t-1]>0. && MC[l][t-1]<.20)
  kw=0.;
 else
 {
  if (MC[l][t-1]>.20 && MC[l][t-1]<.40)
    kw = MC[l][t-1] /0.2 - 1;
  else
    kw = 1.;
 }

 /* temperature correction factor, meso- km, thermo- kt*/
 km = 0.01;  /* Assumed minimal activity */
 kt = 0.01;

 if ((Temp[l][t-1] >= 0.) && (Temp[l][t-1] <= 30.))
    km = Temp[l][t-1] / 30.;

 if ((Temp[l][t-1] >= 30.) && (Temp[l][t-1] <= 40.))
    km = 1.0;

 if ((Temp[l][t-1] >= 40.) && (Temp[l][t-1] <= 55.))
    km = (55. - Temp[l][t-1]) / 15.;
```

```
if ((Temp[l][t-1] >= 40.) && (Temp[l][t-1] <= 50.))
   kt = 0.1 * Temp[l][t-1] - 4.0;

if ((Temp[l][t-1] >= 50.) && (Temp[l][t-1] <= 55.))
   kt = 1.0;

if ((Temp[l][t-1] >= 55.) && (Temp[l][t-1] <= 75.))
    kt = 3.75 - 0.05 * Temp[l][t-1];

if (km <= 0.01) km = 0.01;
if (kt <= 0.01) kt = 0.01;

kmax = kmax_meso * km + kmax_thermo * kt;

kd[l] = kmax * (CDM[l][t-1]/(CDM[l][t-1] + Ksc)) *
                (O2DM[l][t-1]/(O2DM[l][t-1] + KO2));

dXdt[l][t] = kd[l] * X[l][t - 1] * VS[l][t-1];

dCdt[l][t] =  dXdt[l][t] / Yxs ;

VS[l][t] = VS[l][t-1] - dCdt[l][t] + dXdt[l][t];
/*          ----------    ----------    -----------          */
/*            start      consumed    produced biomass */

CDM[l][t] = (CDM[l][t - 1] * (VS[l][t-1] + NVS[l]) -
            (dCdt[l][t] - dXdt[l][t])) / (VS[l][t] + NVS[l]);

X[l][t] = (X[l][t - 1] * (VS[l][t-1] + NVS[l]) + dXdt[l][t]) / (VS[l][t] + NVS[l]);

/*****************************************************************/
/*For now, only the O2 content in the airflow is calculated      */
/*Assume the oxygen is consumed once obsorbed by the matrix      */
/*The oxygen mass in the matrix is therefore ignored             */
/*Also, the O2 consumption rate is a constant in each hour       */
/*****************************************************************/
db_w(Temp[l][t-1], win[l][t], &airflow);

dO2dt[l][t] = (flowrate[t-1] * airflow.spvol) * (Oin[l][t-1] - Oout[l][t-1]) -
              YO2s * dCdt[l][t];

Oout[l][t] = Oin[l][t] + dO2dt[l][t];

if (Oout[l][t] < 0) Oout[l][t] = 1e-3;

if (l < 5) Oin[l + 1][t] = Oout[l][t];

O2DM[l][t] = Oout[l][t] * FAS[l] * sectionArea * height[l] / (VS[l][t] + NVS[l]);
```

```
if (O2DM[l][t] < 0) O2DM[l][t] = .00001;

/*****************************************************************/
/*First part is the H2O generation from microbial decomposition  */
/*Second part is the H2O taken away by the airflow               */
/*Use the airflow rate from previous hour, assuming no           */
/*significant change of airflow rate between these two hours     */
/*****************************************************************/
dWdt[l][t] = Yws * dCdt[l][t] - flowrate[t - 1] * (wout[l][t] - win[l][t]);

W[l][t] = W[l][t - 1] + dWdt[l][t];

MC[l][t] = W[l][t] / (VS[l][t] + NVS[l] + W[l][t]);

BD[l] =  (VS[l][t] + NVS[l] + W[l][t]) /(Volume * (height[l] / Height));

if (BD[l] > 1000.)
{
  printf("\nThe bulk density was greater than 1000!\n");
  fclose(fp);
  exit(1);
}

/*****************************************************************/
/*Call db_w() in psyproc.h to calculate the enthalpy             */
/*Second part is the H2O taken away by the airflow               */
/*Use the temperature from previous hour, assuming no change     */
/*  The enthalpy of ambient air (entering the bottom layer) has  */
/*  been calculated at the beginning of the program - h0         */
/*  The enthalpy of exhaust air (leaving the top layer) has      */
/*  been calculated at the beginning of the loop - hout[5][t]    */
/*****************************************************************/
db_w(Temp[l][t - 1], wout[l][t], &airflow);
hout[l][t] = airflow.h;
if (l < 5) hin[l + 1][t] = hout[l][t];


/*****************************************************************/
/*First part in numerator is the Heat generation and the         */
/*  second part is the heat taken away by the airflow            */
/*Use the airflow rate from previous hour, assuming no           */
/*  significant change of airflow rate between these two hours   */
/*Note: the airflow rate at this hour has not been calculated    */
/*  since the temperature for this hour need to be calcualted    */
/*  firstly.                                                     */
/*****************************************************************/
dTdt[l][t] = (Yhs * dCdt[l][t] - (hout[l][t] - hin[l][t]) * 1000. *
              flowrate[t - 1] * airflow.spvol * airflow.dens) /
              (cvs * VS[l][t] + cnvs * NVS[l] + cw * W[l][t]);
```

```
    Temp[l][t] = Temp[l][t - 1] + dTdt[l][t];

    if (Temp[l][t] < ambientTemp) Temp[l][t] = ambientTemp;

    if (Temp[l][t] >= 45) Stage[l][t] = 2;
    if (Temp[l][t] < 45) Stage[l][t] = 1;
    if (Temp[l][t] >= 45 && dTdt[l][t] < 0 ) Stage[l][t] = 1;

    dT[l] = 1. / ambientTemp - 1. / Temp[l][t] ;

    if (l == 4 && Temp[l][t] > ambientTemp)
    {
      airviscosity = 1.458e-6 * pow((Temp[l][t] + 273), 1.5) / ((Temp[l][t] + 273) + 110.4);

      volflow = 0.001 * K[l] / airviscosity * airdensity * 9.8 *
                                              (1 - (ambientTemp + 273)/ (Temp[l][t] + 273));

      flowrate[t] = volflow * sectionArea / airflow.spvol * 3600.;

     }

    if (Stage[l][t] == 2 &&  Stage[l][t-1] == 1) X[l][t] = 0.003;

   }

   fprintf(fp, " %4d   ", t);
         for (l = 0; l < 6; l++)
         {
    fprintf(fp, " %3.1f  ", Temp[l][t]);
   }
   fprintf(fp, " %6.4f    %6.4f", flowrate[t], volflow);

  }

  printf("done!\n");
  fclose(fp);
  return 0;
}
```

Appendix B Airflow measurements

B.1 Measured and calculated data

Table A-1 Airflow rate data for treatment 1

Time (h)	Inlet				Outlet				
	Volumetric rate (L/min)	SD	Mass flow rate (g dry air/min)	SD	T (°C)	Volumetric rate (L/min)	SD	Mass flow rate (g dry air/min)	SD
48	3.33	2.85	3.85	3.30	27.0	7.92	2.86	8.99	3.25
53	4.28	3.25	4.95	3.76	28.3	9.79	1.97	11.04	2.22
72	6.27	3.00	7.26	3.47	28.2	12.34	3.19	13.94	3.60
92	7.07	2.90	8.18	3.35	31.0	13.36	4.87	14.82	5.40
116	8.55	2.45	9.90	2.84	37.4	13.98	2.45	14.89	2.60
140	7.60	3.47	8.80	4.02	37.6	13.00	1.74	13.82	1.85
164	7.13	2.39	8.25	2.77	37.2	11.39	1.51	12.15	1.61
188	6.81	2.70	7.88	3.12	36.2	11.44	1.80	12.27	1.93
212	6.65	2.45	7.70	2.84	34.8	10.92	1.07	11.83	1.16

Table A-2 Airflow rate data for treatment 2

Time (h)	Inlet				Outlet				
	Volumetric rate (L/min)	SD	Mass flow rate (g dry air/min)	SD	T (°C)	Volumetric rate (L/min)	SD	Mass flow rate (g dry air/min)	SD
48									
53	3.33	2.85	3.85	3.30	0.51	0.02	4.38	0.20	3.33
72	6.81	2.39	7.88	2.77	1.54	0.34	12.99	2.88	6.81
92	8.07	1.53	9.34	1.77	1.64	0.34	14.16	2.93	8.07
116	8.71	2.23	10.08	2.58	1.59	0.24	13.30	1.99	8.71
140	9.03	1.90	10.45	2.20	1.92	0.69	16.20	5.83	9.03
164	9.18	1.09	10.63	1.26	1.73	0.39	14.75	3.35	9.18
188	8.95	1.10	10.36	1.27	1.46	0.21	12.62	1.82	8.95
212	7.60	3.12	8.80	3.62	1.60	0.15	13.77	1.28	7.60

Table A-3 Airflow rate data for treatment 3

Time (h)	Inlet				Outlet				
	Volumetric rate (L/min)	SD	Mass flow rate (g dry air/min)	SD	T (°C)	Volumetric rate (L/min)	SD	Mass flow rate (g dry air/min)	SD
48	3.80	3.10	4.40	3.59	0.85	0.43	7.16	3.64	3.80
53									
72									
92	8.75	4.01	10.13	4.64	1.71	0.49	14.24	4.08	8.75
116									
140	9.67	1.36	11.19	1.57	1.87	0.32	14.99	2.57	9.67
164	8.79	1.76	10.18	2.04	1.87	0.22	15.27	1.78	8.79
188	7.92	2.10	9.16	2.43	1.78	0.78	14.84	6.50	7.92
212	7.04	1.32	8.15	1.53	1.52	0.02	12.88	0.15	7.04

Table A-4 Airflow rate data for treatment 4

Time (h)	Inlet				Outlet				
	Volumetric rate (L/min)	SD	Mass flow rate (g dry air/min)	SD	T (°C)	Volumetric rate (L/min)	SD	Mass flow rate (g dry air/min)	SD
48					2.08	0.39			
53	10.46	1.10	12.10	1.27	2.33	0.88	17.25	6.48	10.46
72	10.46	1.10	12.10	1.27					10.46
92	10.34	1.25	11.97	1.45	2.40	0.75	14.87	4.66	10.34
116	9.44	2.19	10.92	2.53	2.31	0.71	17.16	5.28	9.44

B.2 Figures of measured airflow

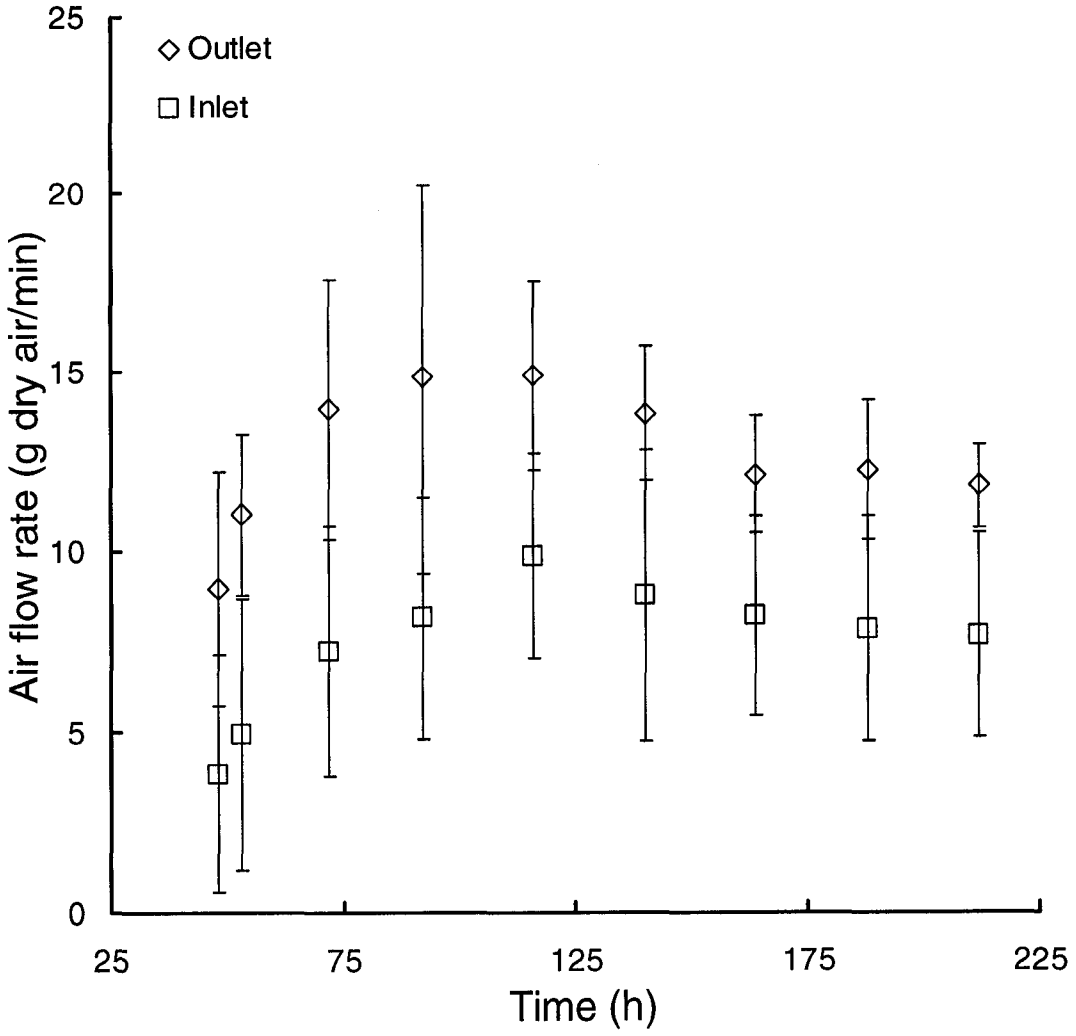

Figure B-1 Airflow rate for treatment 1

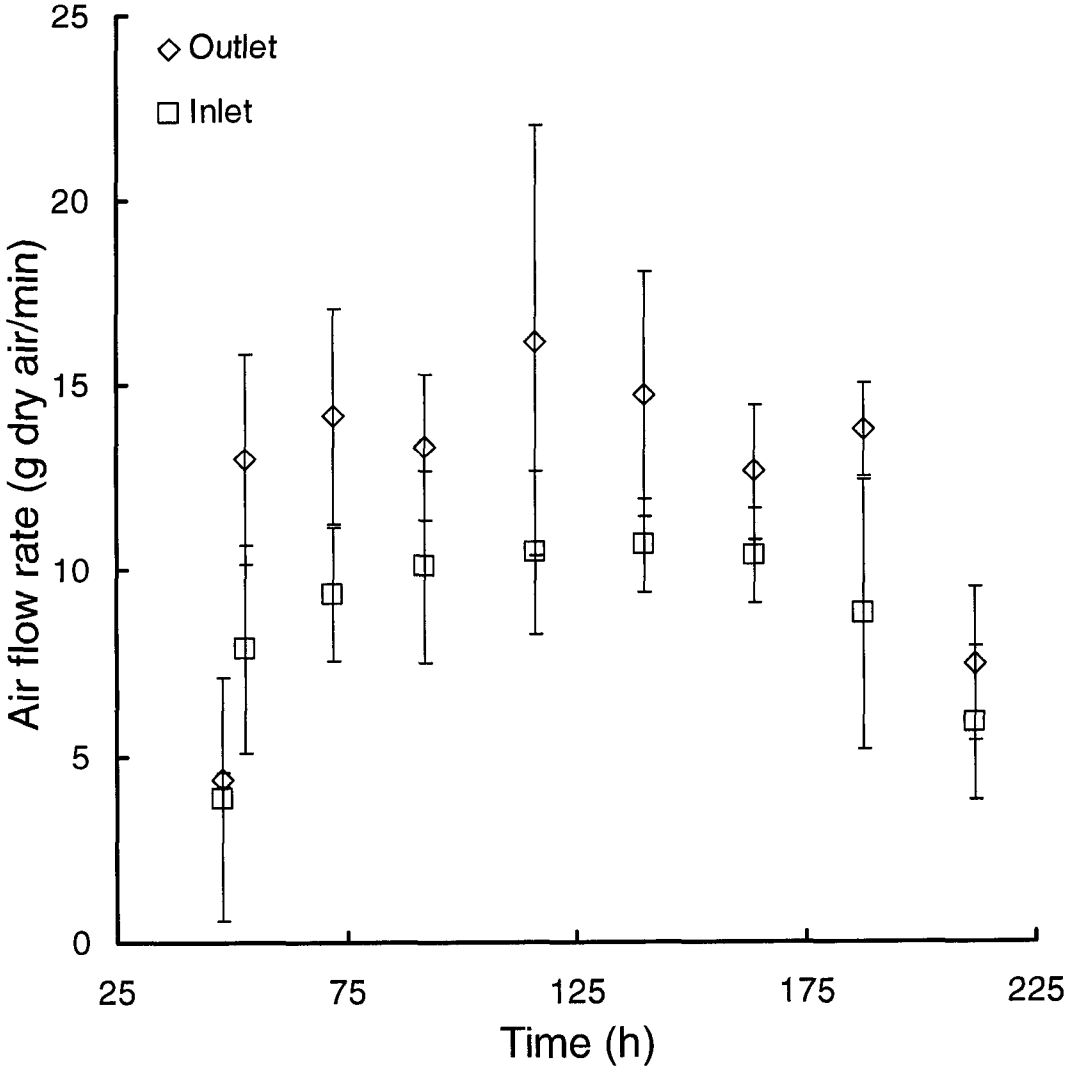

Figure B-2 Airflow rate for treatment 2

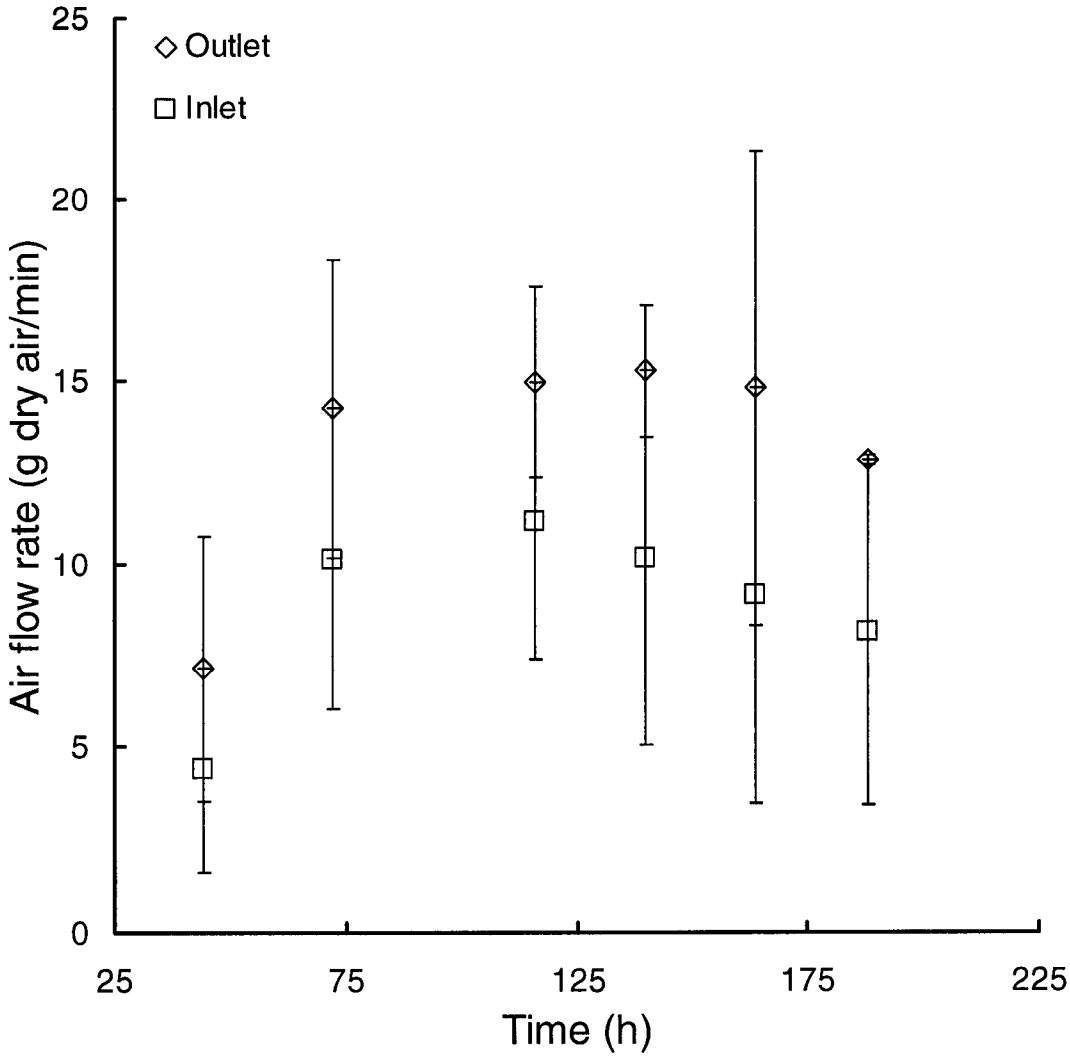

Figure B-3 Airflow rate for treatment 3

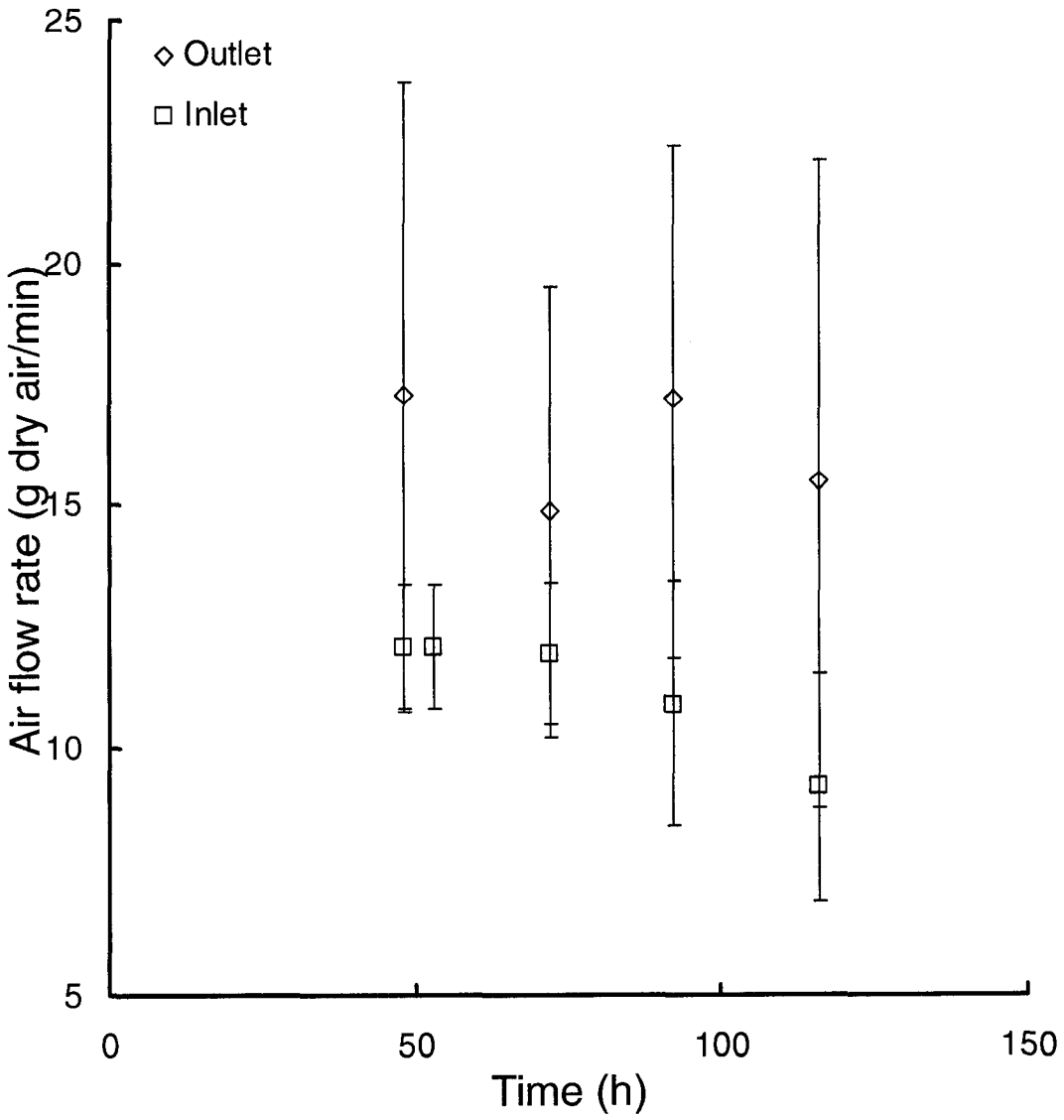

Figure B-4 Airflow rate for treatment 4

Appendix C SAS program for the analysis of temperature data

C.1 For curve fitting

```
Options ls=80 ps=40 formdlim='-' pageno=1;
Data trt3;
Input t bottom middle;
Cards;
39      28.5    32.0
.....
210     38.7    53.3
;
Run;
Proc nlin data=trt3 method=MARQUARDT NOITPRINT;
Parms ah=24 ac=24 bh=0.0754 bc=0.0073 th=21.5 tc=257.8;
        Lh = exp(-bh*(t-th));
        Lc = exp(-bc*(t-tc));
bounds 19 < ah < 29;
bounds bh bc th tc > 0;
Model bottom = 20 + ah*exp(-Lh) - ac*exp(-Lc);
        Der.ah = exp(-Lh);
        Der.ac = - exp(-Lc);
        Der.bh = ah*Lh*(t-th)*exp(-Lh);
        Der.th = -ah*Lh*bh*exp(-Lh);
        Der.bc = -ac*Lc*(t-tc)*exp(-Lc);
        Der.tc = ac*Lc*bc*exp(-Lc);
output out=set0 r=residual p=fitted;
Run;
proc univariate normal plot data = set0;
var residual;
; run
```

C.2 For the test of difference among datasets

```
Options ls=80 ps=40 formdlim='-' pageno=1;
Data trt3;
Input pos t temp d;
Cards;
0       39      28.5    0
......
0       210     38.7    0
3       39      32      1
......
3       210     53.3    1
;
Run;
/*The "combined" model*/
Proc nlin data=trt3 method=MARQUARDT NOITPRINT;
Parms ahm=21 aht=7.5 ac=31 bhm=0.3214 bht=0.1904 bc=0.0102 thm=42.6 tht=86.3
tc=267.1;
        Lhm = exp(-bhm*(t-thm));
        Lht = exp(-bht*(t-tht));
        Lc = exp(-bc*(t-tc));
bounds bhm bht bc thm tht tc > 0;
Model temp = 20 + ahm*exp(-Lhm) + aht*exp(-Lht) - ac*exp(-Lc);
        Der.ahm = exp(-Lhm);
        Der.aht = exp(-Lht);
        Der.ac = - exp(-Lc);
        Der.bht = aht*Lht*(t-tht)*exp(-Lht);
        Der.tht = -aht*Lht*bht*exp(-Lht);
        Der.bhm = ahm*Lhm*(t-thm)*exp(-Lhm);
        Der.thm = -ahm*Lhm*bhm*exp(-Lhm);
        Der.bc = -ac*Lc*(t-tc)*exp(-Lc);
        Der.tc = ac*Lc*bc*exp(-Lc);
output out=set0 r=residual p=fitted;
Run;

/*the "individual" model*/
Proc nlin data=trt3 method=MARQUARDT NOITPRINT;
Parms ahm=22 aht=2 ac=24 bhm=0.2606 bht=0.0949 bc=0.0069 thm=40.0 tht=75.3 tc=258.5
        dahm=3.5 daht=12.5 dac=16.0 dbhm=-0.0046 dbht=0.1528 dbc=0.0040 dthm=-2.2
        dtht=10.3 dtc=-6.8;
        Lhm = exp(-(bhm + d*dbhm)*(t-(thm + d*dthm)));
        Lht = exp(-(bht + d*dbht)*(t-(tht + d*dtht)));
        Lc = exp(-(bc + d*dbc)*(t-(tc + d*dtc)));
bounds bhm bht bc thm tht tc > 0;
Model temp = 20 + (ahm + d*dahm)*exp(-Lhm) + (aht + d*daht)*exp(-Lht) - (ac +
d*dac)*exp(-Lc);
        Der.ahm = exp(-Lhm);
        Der.aht = exp(-Lht);
        Der.ac = - exp(-Lc);
```

```
        Der.bht = (aht + d*daht)*Lht*(t-(tht + d*dtht))*exp(-Lht);
        Der.tht = -(aht + d*daht)*Lht*(bht + d*dbht)*exp(-Lht);
        Der.bhm = (ahm + d*dahm)*Lhm*(t-(thm + d*dthm))*exp(-Lhm);
        Der.thm = -(ahm + d*dahm)*Lhm*(bhm + d*dbhm)*exp(-Lhm);
        Der.bc = -(ac + d*dac)*Lc*(t-(tc + d*dtc))*exp(-Lc);
        Der.tc = (ac + d*dac)*Lc*(bc + d*dbc)*exp(-Lc);

        Der.dahm = d * exp(-Lhm);
        Der.daht = d * exp(-Lht);
        Der.dac = - d *  exp(-Lc);
        Der.dbht = d * (aht + d*daht)*Lht*(t-(tht + d*dtht))*exp(-Lht);
        Der.dtht = - d * (aht + d*daht)*Lht*(bht + d*dbht)*exp(-Lht);
        Der.dbhm = d * (ahm + d*dahm)*Lhm*(t-(thm + d*dthm))*exp(-Lhm);
        Der.dthm = - d * (ahm + d*dahm)*Lhm*(bhm + d*dbhm)*exp(-Lhm);
        Der.dbc = - d * (ac + d*dac)*Lc*(t-(tc + d*dtc))*exp(-Lc);
        Der.dtc = d * (ac + d*dac)*Lc*(bc + d*dbc)*exp(-Lc);
output out=set1 r=residual p=fitted;
Run;
```

Appendix D Analysis results of all temperature data

D.1 Regressed curves

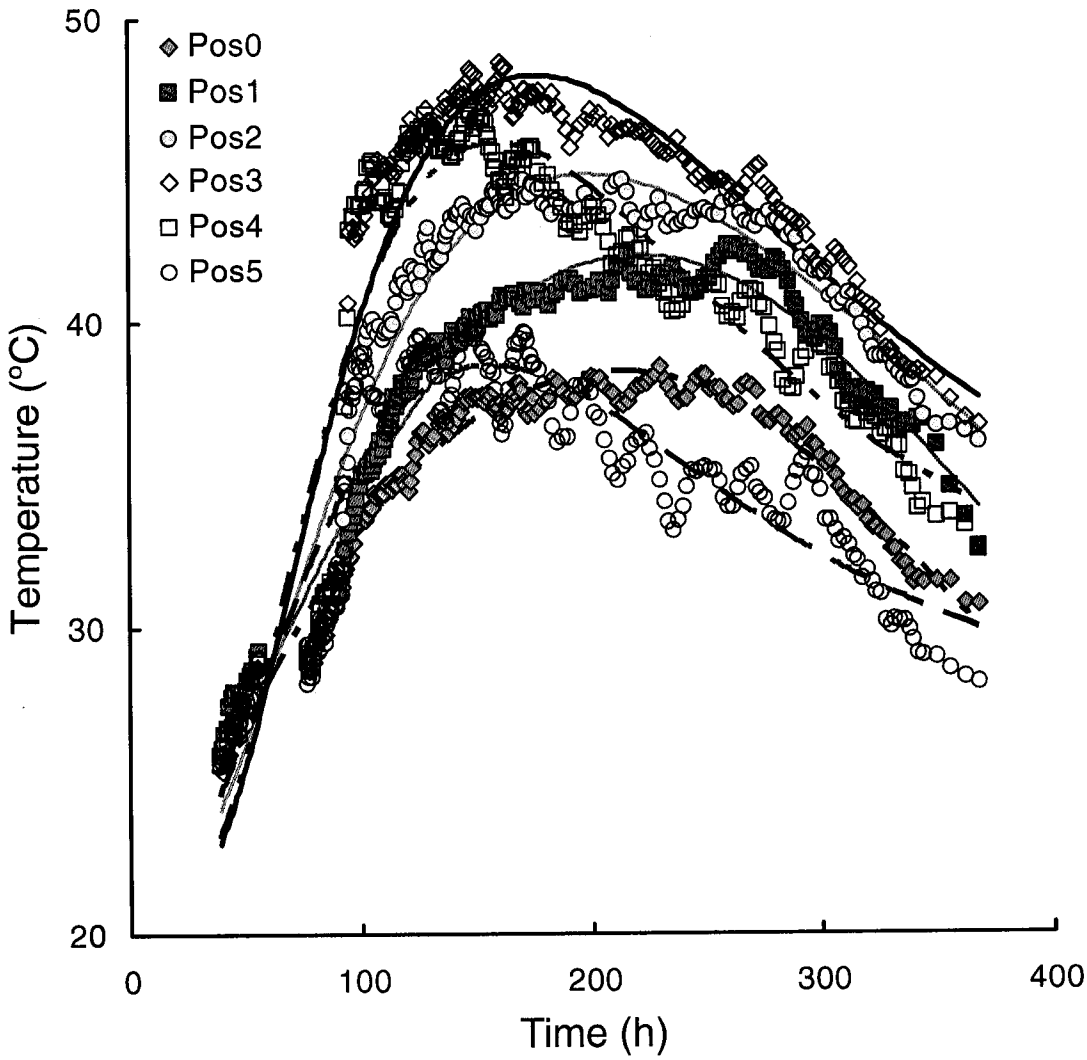

Figure D-1 Regressed curves for treatment 1

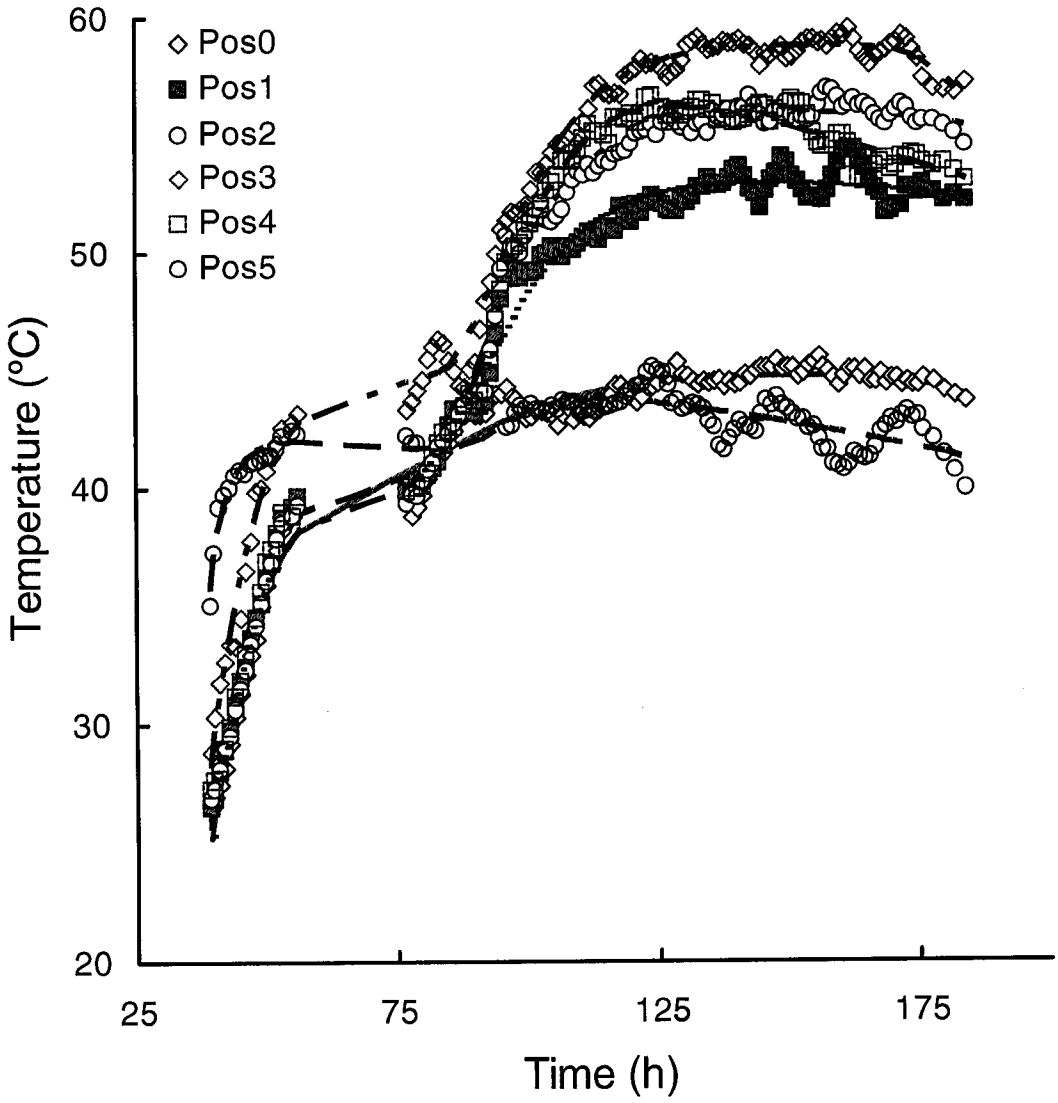

Figure D-2 Regressed curves for treatment 2

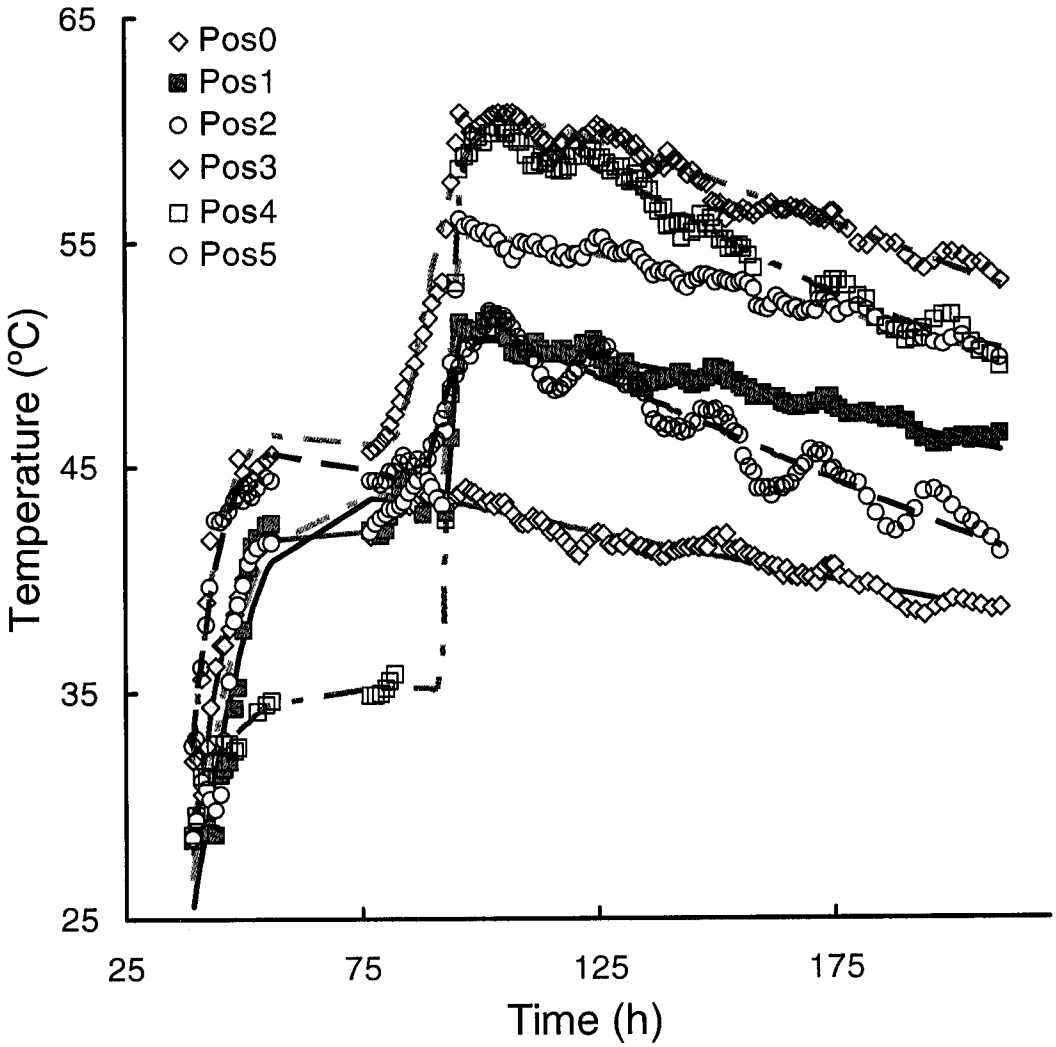

Figure D-3 Regressed curves for treatment 3

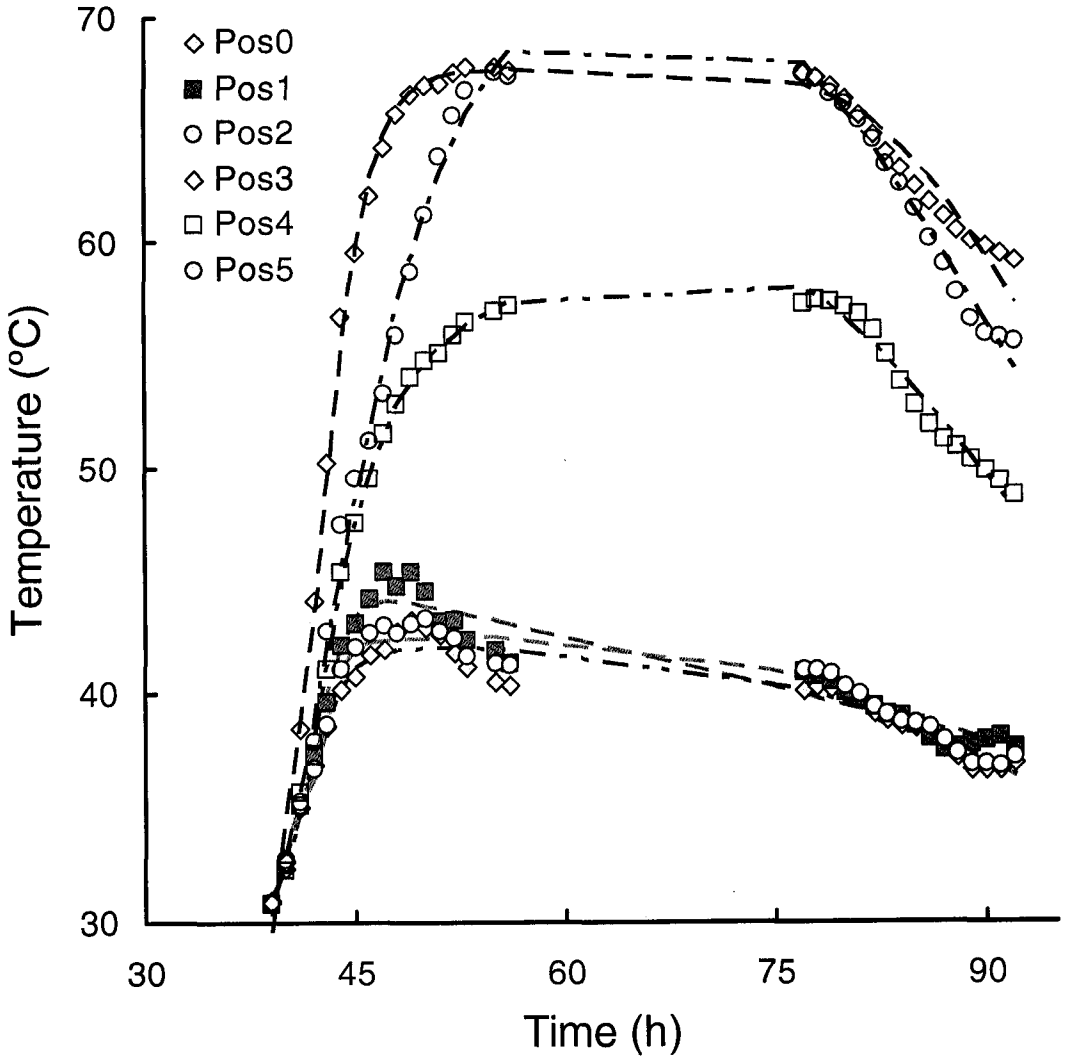

Figure D-4 Regressed curves for treatment 4

D.2 Regressed parameter values

Treatment	Parameter	Positions					
		0	1	2	3	4	5
1	T_{hm}	19.8	24.9	29.0	33.0	32.0	23.0
	T_c	23.0	28.0	29.0	23.0	22.0	15.5
	b_{hm}	0.0189	0.0167	0.0214	0.0266	0.0276	0.0238
	t_{hm}	52.7	63.4	70.2	71.7	69.4	59.2
	b_c	0.0099	0.0087	0.0065	0.0086	0.0106	0.0113
	t_c	352.2	362.4	341.8	261.1	217.2	215.0
2	T_{hm}	19.9	19.6	19.8	24.5	22.0	22.3
	T_{ht}	4.9	14.2	16.2	14.3	18.4	3.1
	T_c	30.0	29.0	41.0	34.0	32.0	19.0
	b_{hm}	0.1564	0.1739	0.1580	0.1587	0.1433	0.3055
	t_{hm}	40.9	40.5	40.5	39.5	40.3	35.5
	b_{ht}	0.0651	0.0814	0.0968	0.1020	0.1019	0.1350
	t_{ht}	85.6	90.6	91.7	95.5	93.4	94.4
	b_c	0.0242	0.0057	0.0186	0.0429	0.0068	0.0075
	t_c	235.9	379.6	260.4	207.5	239.5	239.4
3	T_{hm}	27.0	26.2	25.2	30.0	15.2	28.8
	T_{ht}	2.2	7.9	12.2	16.5	24.9	8.2
	T_c	19.0	26.0	31.0	35.0	12.0	26.0
	b_{hm}	0.1810	0.1290	0.1377	0.2113	0.1303	0.1993
	t_{hm}	38.1	41.2	40.5	37.6	33.4	37.2
	b_{ht}	0.3725	1.7622	1.0288	0.2001	0.7668	0.2947
	t_{ht}	79.3	94.0	93.4	87.9	93.3	91.3
	b_c	0.0063	0.0057	0.0060	0.0061	0.0267	0.0098
	t_c	121.0	230.4	265.3	202.4	147.3	141.7
4	T_{hm}	18.1	23.4	17.7	20.2	22.7	20.5
	T_{ht}	3.9	8.3	4.7	27.5	19.9	32.0
	T_c	30.0	30.0	18.0	43.0	32.0	42.0
	b_{hm}	0.5031	0.6171	0.5943	0.8602	0.0612	0.1552
	t_{hm}	37.8	37.2	37.9	38.7	34.2	38.6
	b_{ht}	0.9018	0.8354	1.4992	0.5584	0.4169	0.1999
	t_{ht}	42.7	42.6	43.0	43.1	42.5	43.8
	b_c	0.0333	0.0135	0.0534	0.0717	0.0678	0.0656
	t_c	107.5	71.1	93.5	96.8	89.4	89.3

Appendix E Temperature measurements

E.1 Averaged temperature measurements

Table E-1 Averaged temperature measurements for treatment 1

Time	Position 0	Position 1	Position 2	Position 3	Position 4	Position 5
– h –	°C					
39	25.9	25.9	25.9	25.6	25.6	25.5
40	26.1	26.1	25.8	25.4	25.9	25.7
41	26.3	26.5	26.2	25.7	26.1	25.9
42	26.3	26.8	26.3	25.8	26.6	26.0
43	26.6	27.5	26.5	25.9	26.7	26.5
44	26.7	27.7	26.6	26.4	26.8	26.5
45	26.9	27.9	26.8	27.0	27.0	26.5
46	26.7	27.8	27.1	27.2	27.0	26.5
47	26.5	27.8	26.7	27.4	27.0	26.9
48	26.7	27.8	26.9	27.6	27.3	27.0
49	27.1	27.8	27.0	27.7	27.6	27.2
50	27.2	27.7	26.9	28.0	27.9	27.4
51	27.8	27.8	27.4	28.4	28.3	27.6
52	27.8	28.4	27.7	28.5	28.5	28.3
53	28.2	28.6	28.3	28.6	28.6	28.3
55	28.4	29.1	28.6	28.8	28.8	28.7
56	28.5	29.2	29.0	29.0	28.9	28.4
77	28.8	28.9	29.4	29.2	29.2	28.2
78	28.6	28.6	29.5	29.2	28.9	28.4
79	28.9	28.7	29.4	29.4	28.9	28.4
80	28.9	29.1	29.3	29.5	29.4	29.0
81	29.2	29.4	29.4	29.7	29.6	29.5
82	29.7	29.9	29.2	30.1	30.3	29.7
83	29.7	30.0	29.4	30.0	30.8	30.3
84	30.1	30.1	29.5	29.8	31.1	30.2
85	30.6	30.4	29.5	29.8	31.1	30.1
86	30.5	30.6	30.1	30.3	31.2	30.4
87	31.2	31.2	30.5	30.8	31.5	30.3
88	31.3	31.0	31.2	31.5	31.3	30.6
89	31.0	31.1	31.7	31.9	31.5	30.7

Time	Position 0	Position 1	Position 2	Position 3	Position 4	Position 5
– h –	°C					
90	31.2	31.5	32.0	31.7	31.8	30.7
91	31.1	31.2	32.1	31.6	31.6	31.0
92	31.3	31.7	31.8	32.0	31.9	31.0
93	31.8	32.1	33.5	34.8	34.7	32.5
94	31.9	32.6	34.7	37.8	37.2	34.5
95	32.2	33.1	36.3	40.7	40.2	35.4
96	32.3	33.4	37.6	43.0	43.1	37.2
97	32.8	33.6	37.5	43.2	43.5	37.7
98	33.3	34.0	37.8	42.8	43.5	37.9
99	33.4	34.2	38.0	43.0	44.0	38.6
100	33.6	34.6	38.6	43.1	43.9	38.9
101	33.7	35.0	38.4	43.2	43.9	39.0
102	33.6	35.1	39.0	43.6	44.3	38.7
103	33.7	35.1	39.4	43.9	44.4	38.5
104	33.9	35.3	39.7	44.0	45.2	38.0
105	33.9	35.1	40.0	44.3	45.2	37.7
106	34.4	35.3	40.1	44.8	45.4	37.6
107	34.3	35.5	39.8	44.8	45.1	37.6
108	34.4	35.6	39.6	45.4	44.0	37.5
109	34.4	36.1	39.9	45.1	44.0	37.1
110	34.4	35.8	39.5	45.1	44.0	37.1
111	34.7	36.2	39.7	45.3	44.0	36.6
112	34.7	36.9	39.8	45.1	44.1	36.4
113	34.7	36.8	39.7	45.2	43.6	36.5
114	34.5	37.0	40.1	45.1	43.6	36.6
115	34.7	37.6	39.9	44.9	43.5	37.2
116	34.7	37.3	40.6	45.1	43.8	37.4
117	35.0	37.5	41.2	45.7	44.4	37.6
118	35.0	38.0	41.5	45.8	44.3	37.9
119	34.8	37.8	41.6	45.8	45.3	38.1
120	34.7	37.8	41.3	45.9	45.7	38.6
121	34.5	37.8	41.0	45.6	45.9	38.8
122	34.8	38.0	41.2	46.2	46.3	38.6
123	35.3	38.1	41.9	46.8	45.9	38.7
124	35.7	38.4	41.8	46.3	45.9	39.0

Time	Position 0	Position 1	Position 2	Position 3	Position 4	Position 5
– h –	°C					
125	36.1	38.7	41.5	46.0	45.9	39.4
126	36.4	38.7	41.2	46.1	46.4	39.5
127	36.4	39.0	41.7	45.7	46.2	39.5
128	36.5	38.9	42.4	46.4	46.5	39.1
129	36.1	38.8	42.9	47.1	46.8	38.9
130	36.0	39.1	43.2	46.7	46.2	38.8
131	36.3	38.9	42.5	46.7	46.5	39.2
132	36.3	39.3	42.2	46.6	46.2	38.6
133	37.0	39.3	41.9	46.4	46.3	38.2
134	36.7	39.4	42.1	46.4	46.1	38.3
135	36.8	39.0	42.2	46.6	45.7	37.1
136	36.8	38.9	42.2	47.0	45.7	37.1
137	36.5	38.8	42.5	47.1	45.7	36.9
138	36.7	38.8	42.9	47.4	45.8	36.8
139	36.4	39.1	43.1	47.2	45.9	37.4
140	36.7	39.3	43.5	47.0	45.5	37.6
141	36.7	39.7	43.3	47.0	45.5	38.0
142	36.9	39.6	43.6	47.4	45.6	38.4
143	37.1	39.4	43.6	47.7	46.0	38.9
144	37.1	39.4	43.7	47.5	46.1	39.3
145	37.4	39.6	43.9	47.8	46.2	39.9
146	37.6	39.8	43.4	47.5	46.8	39.9
147	37.5	39.9	43.7	47.9	46.5	39.5
148	37.7	40.2	43.2	48.4	47.0	39.6
149	37.5	39.7	43.6	48.2	46.9	39.6
150	37.6	39.8	43.5	48.2	46.4	39.5
151	37.5	40.1	43.0	47.8	46.6	39.6
152	37.6	40.2	43.6	47.5	46.8	39.7
153	37.6	40.3	43.5	47.6	46.8	39.1
154	37.4	40.3	43.8	47.4	46.7	39.0
155	37.7	40.4	43.9	47.4	46.6	38.9
156	37.4	40.4	43.7	47.5	46.2	38.4
157	37.6	40.1	43.9	47.2	45.8	38.6
158	37.2	40.3	44.3	47.4	45.6	38.4
159	37.3	40.3	44.4	47.8	45.1	37.8

Time	Position 0	Position 1	Position 2	Position 3	Position 4	Position 5
– h –	°C					
160	37.2	40.2	44.3	48.0	45.4	37.3
161	36.9	40.7	44.0	48.5	44.7	36.7
162	37.4	40.9	43.9	48.4	44.7	36.4
163	37.3	40.9	43.8	48.4	44.5	36.6
164	37.2	40.8	43.7	47.8	44.2	37.2
165	37.4	40.8	44.3	47.4	45.0	37.8
166	37.4	40.9	44.0	47.2	44.8	38.6
167	37.7	41.0	43.9	46.8	45.4	38.9
168	38.0	40.8	44.7	46.8	45.4	39.3
169	38.0	40.8	44.3	47.1	45.2	39.3
170	37.8	40.6	44.6	47.3	45.6	39.5
171	37.3	40.5	44.7	47.7	45.4	39.7
172	37.1	41.1	44.2	47.7	45.4	39.6
173	37.0	41.0	44.1	47.4	45.8	39.4
174	37.1	40.9	44.3	47.6	45.8	38.9
175	37.5	41.1	44.6	47.5	45.8	38.7
176	37.0	40.7	44.6	47.6	45.7	38.6
178	37.2	41.0	44.4	47.6	45.0	38.4
180	37.4	40.8	43.9	47.2	44.6	38.0
182	37.6	40.6	43.8	47.2	44.9	37.4
184	38.2	40.9	43.6	47.6	44.4	36.6
186	38.1	41.0	44.0	47.1	44.1	36.1
188	37.8	41.3	43.9	46.9	43.8	36.2
190	37.6	41.4	43.3	46.3	43.1	36.3
192	37.6	41.4	43.8	45.8	43.3	37.0
194	37.6	41.3	43.7	46.2	43.2	37.9
196	37.8	40.9	43.8	46.5	43.0	37.9
198	38.1	41.0	44.3	46.7	43.3	37.9
200	38.2	41.1	43.9	47.0	43.5	37.7
202	38.2	41.2	43.6	46.7	43.8	37.0
204	38.2	41.4	43.6	46.9	43.6	36.9
206	37.9	41.1	43.6	46.6	43.1	36.1
208	37.8	40.9	43.8	46.1	42.6	35.5
210	37.7	41.4	44.5	46.5	42.0	35.1
212	37.4	41.8	44.6	46.3	42.2	34.8

Time	Position 0	Position 1	Position 2	Position 3	Position 4	Position 5
– h –	°C					
214	37.3	41.9	44.7	46.4	42.3	35.2
216	37.4	42.2	44.3	46.4	42.8	35.4
218	37.7	41.6	43.7	46.4	42.9	36.0
220	37.9	41.3	43.5	46.3	42.4	36.1
222	38.0	41.4	43.0	46.3	42.4	36.2
224	38.0	41.0	43.3	46.3	41.8	36.4
226	38.2	41.3	43.6	46.1	41.6	35.9
228	38.3	41.1	43.6	45.9	41.8	35.5
230	38.5	41.5	44.1	45.7	41.3	34.8
232	38.1	41.6	43.7	45.6	40.9	34.1
234	37.9	41.5	43.2	45.6	40.6	33.5
236	37.7	41.8	43.4	45.7	40.3	33.2
238	37.4	41.5	43.2	46.1	40.4	33.5
240	37.5	41.4	43.3	45.5	40.6	33.9
242	37.5	41.1	43.4	45.4	41.1	34.6
244	37.9	41.2	43.3	45.1	40.9	35.1
246	38.2	41.0	43.7	44.7	41.1	35.1
248	38.3	41.2	43.7	44.8	41.2	35.2
250	38.3	41.5	43.8	44.5	41.3	35.2
252	37.8	41.5	43.6	44.6	41.4	35.1
254	37.9	42.0	43.6	44.7	41.3	35.1
256	37.9	42.2	43.6	44.7	41.2	34.8
258	37.5	42.3	43.9	44.7	40.5	34.2
260	37.5	42.6	44.4	44.6	40.2	33.9
262	37.3	42.6	44.0	44.1	40.3	33.9
264	37.3	42.3	44.0	44.3	40.1	34.5
266	37.9	42.5	43.6	44.3	40.6	35.0
268	38.0	42.2	43.3	44.6	41.0	35.1
270	37.9	42.3	43.3	45.0	41.1	35.3
272	37.7	42.0	43.2	45.1	41.0	34.5
274	37.0	41.7	43.4	45.2	40.6	34.4
276	36.8	41.8	43.4	44.5	40.4	34.2
278	36.7	41.7	43.7	44.4	39.9	33.7
280	36.9	42.1	43.3	44.1	39.3	33.5
282	37.0	42.0	43.4	43.8	39.0	33.4

Time	Position 0	Position 1	Position 2	Position 3	Position 4	Position 5
– h –	°C					
284	36.8	41.7	43.2	43.7	38.1	33.4
286	36.3	41.3	42.8	43.5	37.8	34.0
288	36.2	40.7	43.0	43.5	37.8	34.7
290	36.4	40.5	42.7	43.3	38.2	35.1
292	36.4	40.0	42.1	43.2	38.8	35.4
294	36.6	39.5	41.9	42.9	39.0	35.7
296	36.0	39.7	42.2	42.3	39.7	35.0
298	36.0	39.4	41.7	42.0	39.4	34.9
300	35.7	39.9	41.8	41.6	39.2	34.5
302	35.4	39.9	41.6	41.9	39.1	33.5
304	35.5	39.6	40.8	42.0	38.5	33.5
306	35.0	39.1	40.9	42.5	38.5	33.1
308	34.6	38.3	40.6	42.3	38.0	32.8
310	34.4	38.0	40.7	42.0	37.4	32.9
312	34.1	37.5	41.0	41.9	37.3	32.6
314	34.2	37.8	40.5	40.9	36.7	32.3
316	33.9	37.4	40.3	41.3	36.7	32.2
318	34.0	37.6	39.9	40.7	37.1	31.6
320	33.5	37.7	39.5	40.6	37.0	31.8
322	33.3	37.1	39.1	40.5	36.7	31.5
324	33.3	37.6	38.8	40.1	36.9	31.1
326	33.1	37.2	38.8	39.8	36.3	31.0
328	33.0	36.9	38.9	39.1	36.5	30.2
330	32.6	37.1	38.8	39.1	36.4	30.0
332	32.5	36.7	38.5	38.8	35.9	30.2
334	32.1	36.5	38.3	38.7	35.9	30.2
336	32.1	36.6	38.1	38.6	35.1	30.2
338	31.7	36.7	38.0	38.4	35.0	29.9
340	31.4	36.6	38.1	38.3	34.5	29.5
342	31.6	36.8	37.5	38.4	33.9	29.1
344	31.4	36.8	36.9	38.3	34.1	29.1
350	31.5	36.0	36.6	38.2	33.6	29.0
356	31.5	34.6	36.6	37.5	33.7	28.6
362	30.8	33.6	36.4	36.9	33.3	28.3
368	30.7	32.6	36.1	36.7	32.5	28.2

Table E-2 Averaged temperature measurements for treatment 2 (n.d.: no data)

Time	Position 0	Position 1	Position 2	Position 3	Position 4	Position 5
– h –	°C					
39	26.5	26.5	26.9	28.8	27.2	35.0
40	26.9	26.9	27.3	30.3	27.6	37.3
41	27.5	28.0	28.0	31.7	28.3	39.2
42	28.1	28.9	28.9	32.6	29.0	39.7
43	29.2	29.7	29.5	33.4	29.9	40.0
44	30.3	30.8	30.6	33.3	31.1	40.5
45	31.3	31.7	31.4	34.5	31.8	40.8
46	32.1	32.4	32.3	36.5	32.9	40.6
47	32.9	33.6	33.4	37.7	33.5	41.0
48	33.6	34.4	34.1	39.8	34.5	41.1
49	35.0	35.1	35.1	40.0	35.6	41.2
50	35.9	36.1	36.1	40.7	36.8	41.4
51	36.7	36.8	36.8	41.3	37.4	41.4
52	37.4	37.9	37.8	41.9	38.0	41.7
53	38.2	38.8	38.5	42.5	38.9	42.2
55	38.8	39.2	38.8	42.7	38.8	42.4
56	39.2	39.7	39.2	43.1	39.7	42.2
77	39.4	39.9	39.3	43.3	39.9	42.2
78	38.8	39.8	39.7	43.7	40.0	41.8
79	39.2	40.3	39.6	44.1	40.0	41.9
80	39.7	40.4	40.3	44.6	40.0	n.d.
81	40.4	40.5	40.8	45.4	40.6	n.d.
82	41.2	40.8	41.0	46.0	41.2	n.d.
83	41.3	41.1	41.7	46.3	41.9	n.d.
84	41.5	41.8	42.0	46.1	42.3	n.d.
85	41.9	42.6	42.3	45.4	42.4	n.d.
86	42.4	43.3	42.7	45.0	42.6	n.d.
87	42.9	43.2	43.0	44.3	43.0	n.d.
88	43.1	43.1	43.5	44.3	43.5	n.d.
89	43.2	43.2	43.8	45.0	43.9	n.d.
90	43.0	43.1	44.0	45.3	43.7	n.d.
91	43.0	43.4	44.1	46.7	44.1	n.d.
92	43.1	43.6	44.0	47.9	44.0	n.d.
93	43.8	44.9	45.8	48.7	45.4	n.d.

Time	Position 0	Position 1	Position 2	Position 3	Position 4	Position 5
– h –	°C					
94	44.0	46.5	47.3	49.9	47.1	n.d.
95	44.0	48.0	49.2	51.0	48.4	n.d.
96	44.3	49.0	50.7	51.3	49.6	42.6
97	43.8	49.5	50.2	51.7	50.1	42.6
98	43.8	49.3	50.1	51.7	50.3	43.1
99	43.3	48.9	50.0	51.8	50.3	43.4
100	42.9	49.2	50.7	52.0	50.9	43.3
101	43.0	49.1	51.4	52.7	51.2	43.5
102	43.2	49.2	51.8	53.4	51.5	43.3
103	43.2	49.9	52.1	53.4	51.8	43.3
104	43.1	49.9	51.3	53.8	52.6	43.2
105	43.1	50.2	51.3	54.2	53.0	43.4
106	42.6	50.1	51.5	54.7	53.3	43.3
107	43.0	49.8	51.8	54.7	53.9	43.7
108	43.3	50.2	52.6	55.0	53.9	43.6
109	42.9	50.1	53.1	54.4	53.9	43.6
110	43.1	50.4	53.4	54.7	54.4	43.3
111	43.0	50.6	53.3	55.6	54.8	43.2
112	42.9	50.8	53.7	56.2	55.5	43.3
113	43.2	50.7	53.4	57.1	55.1	43.2
114	43.3	50.5	53.7	57.2	55.1	43.6
115	43.5	50.9	53.9	56.8	55.0	43.3
116	43.9	51.0	53.8	56.8	54.7	43.4
117	44.4	50.9	54.2	56.8	55.7	43.5
118	44.3	51.9	54.3	56.7	55.8	43.6
119	44.1	51.5	54.3	57.6	55.7	43.8
120	43.8	51.3	54.6	57.7	55.9	44.1
121	43.6	52.0	55.0	57.8	55.5	44.3
122	43.8	51.6	55.1	58.2	55.9	44.4
123	44.3	52.1	55.2	58.0	56.6	44.9
124	44.3	52.4	55.5	58.0	56.7	45.0
125	44.4	52.3	55.0	58.0	56.0	44.9
126	44.8	52.0	55.5	57.8	56.1	44.8
127	44.7	51.8	55.9	57.5	55.8	44.4
128	45.0	51.8	55.8	57.6	55.5	43.5

Time	Position 0	Position 1	Position 2	Position 3	Position 4	Position 5
– h –	°C					
129	45.3	51.7	55.6	57.7	56.0	43.7
130	44.8	52.3	55.3	58.1	55.8	43.3
131	44.7	52.1	55.4	58.8	56.0	43.4
132	44.5	52.3	55.0	59.0	56.1	43.5
133	44.3	52.8	55.4	59.1	56.4	43.4
134	44.5	52.7	55.6	58.8	56.4	43.3
135	44.4	53.1	55.1	58.6	56.0	42.7
136	44.5	52.9	56.0	58.6	56.3	42.6
137	44.5	52.9	55.8	58.7	55.6	41.7
138	44.2	52.9	55.8	59.0	55.7	41.6
139	44.5	53.2	56.0	58.9	56.0	42.0
140	44.4	53.5	55.6	58.9	55.5	42.4
141	44.4	53.6	56.1	59.0	55.6	42.7
142	44.8	53.2	56.1	58.8	55.7	42.6
143	44.7	52.7	56.6	58.7	55.8	42.5
144	44.9	52.5	56.2	58.5	55.9	42.3
145	45.1	51.8	55.8	57.9	56.2	43.0
146	45.1	52.6	55.5	58.4	56.2	43.7
147	45.1	53.1	55.5	58.4	55.6	43.4
148	45.4	53.3	56.0	58.6	56.0	43.8
149	45.0	54.1	56.1	58.7	55.9	43.5
150	45.1	53.8	56.3	58.2	55.8	43.3
151	45.1	53.2	55.8	58.3	56.5	43.1
152	44.7	53.0	55.6	58.5	56.3	42.9
153	44.9	52.6	55.8	58.9	56.3	42.8
154	45.1	52.2	55.6	59.0	55.8	42.4
155	45.3	52.3	55.8	59.1	55.1	42.5
156	45.5	52.2	56.3	58.9	54.7	42.0
157	45.1	52.2	56.7	59.0	54.5	41.6
158	44.9	52.6	56.9	58.7	54.7	41.6
159	44.6	53.2	56.8	59.0	54.7	41.0
160	44.4	53.8	56.6	59.2	55.0	40.9
161	44.7	54.4	56.1	59.2	55.0	40.8
162	45.0	54.4	56.3	59.5	54.6	41.0
163	45.0	54.4	56.5	59.1	53.9	41.4

Time	Position 0	Position 1	Position 2	Position 3	Position 4	Position 5
– h –	°C					
164	44.7	54.0	56.2	58.5	53.2	41.2
165	45.0	53.6	56.3	58.2	53.0	41.2
166	44.5	53.1	56.1	58.0	53.4	41.3
167	44.5	52.7	55.8	58.3	53.7	41.6
168	44.8	52.5	55.6	58.4	53.8	42.3
169	44.4	51.6	55.5	58.6	54.0	42.6
170	44.6	51.7	55.8	58.8	53.5	42.8
171	44.7	52.0	56.1	58.9	53.7	42.7
172	44.3	52.0	56.3	59.2	54.0	43.0
173	44.5	52.8	56.1	59.1	54.0	43.2
174	44.3	52.7	55.7	58.6	54.2	42.9
175	44.3	52.5	55.5	58.2	54.1	43.0
176	44.7	52.9	55.6	57.4	53.8	42.4
178	44.5	52.5	55.6	57.0	53.7	42.0
180	44.1	52.2	55.4	56.9	53.8	41.4
182	43.9	52.4	55.1	56.8	53.4	40.7
184	43.6	52.2	54.5	57.3	53.1	40.0

Table E-3 Averaged temperature measurements for treatment 3 (n.d.: no data)

Time	Position 0	Position 1	Position 2	Position 3	Position 4	Position 5
– h –	°C					
39	28.5	28.5	28.5	32.0	28.7	32.6
40	29.2	29.3	29.3	32.2	29.5	33.0
41	30.5	28.9	31.0	35.6	31.3	36.1
42	32.7	29.0	30.8	39.0	31.3	37.9
43	34.4	28.8	30.3	41.7	31.9	39.6
44	36.1	28.7	29.8	n.d.	32.7	42.6
45	37.1	31.4	30.5	n.d.	32.0	42.5
46	37.1	31.6	32.9	n.d.	32.7	42.7
47	37.8	32.0	35.5	n.d.	32.7	43.0
48	38.4	34.3	38.1	n.d.	32.4	43.5
49	39.2	35.3	38.9	45.4	32.6	43.7
50	40.0	37.7	39.7	44.8	n.d.	43.5
51	40.5	40.5	40.7	44.2	n.d.	43.8
52	41.2	41.5	41.1	44.5	n.d.	43.7
53	41.3	41.8	41.4	45.0	34.1	44.0
55	41.7	42.4	41.6	45.3	34.4	44.5
56	41.8	42.5	41.6	45.5	34.6	44.3
77	41.9	42.1	42.1	45.7	34.8	44.3
78	42.3	42.1	42.5	45.8	34.8	44.3
79	42.6	41.9	42.7	46.0	34.9	44.2
80	42.9	42.2	42.8	46.4	35.2	44.4
81	43.2	42.8	43.1	46.8	35.5	44.7
82	43.4	43.4	43.1	47.3	35.8	44.8
83	43.2	44.0	43.2	47.9	n.d.	45.2
84	43.3	44.4	43.4	48.5	n.d.	45.4
85	43.2	44.4	43.8	49.1	n.d.	45.2
86	43.3	44.4	44.1	49.6	n.d.	45.0
87	43.7	44.5	44.4	50.4	n.d.	45.3
88	43.8	42.8	44.7	51.0	n.d.	45.0
89	43.7	n.d.	44.3	51.6	n.d.	45.3
90	43.9	n.d.	44.0	52.4	n.d.	45.9
91	43.6	n.d.	43.6	52.8	n.d.	46.2
92	43.6	n.d.	43.2	53.3	n.d.	47.1
93	43.4	42.9	46.6	55.7	42.6	47.5

Time	Position 0	Position 1	Position 2	Position 3	Position 4	Position 5
– h –	°C					
94	43.4	46.2	49.6	57.7	48.2	48.5
95	43.7	49.5	52.9	59.4	53.2	49.0
96	43.8	51.4	56.0	60.8	58.3	49.5
97	44.1	51.2	55.7	60.4	58.8	50.2
98	43.8	51.1	55.8	59.9	59.0	50.0
99	43.8	51.1	55.7	59.7	59.5	50.5
100	43.6	51.1	55.4	60.2	59.6	51.0
101	43.4	51.5	55.5	60.3	59.4	51.3
102	43.5	51.7	55.2	60.6	59.8	51.9
103	43.3	51.8	55.4	60.7	59.9	51.7
104	43.4	51.6	55.1	60.8	60.0	51.5
105	43.4	51.2	54.7	60.7	60.1	51.7
106	43.1	50.7	54.7	60.7	59.8	51.5
107	42.8	50.1	54.2	60.7	59.6	51.2
108	42.6	50.0	54.6	60.6	59.4	50.8
109	42.5	50.0	55.0	60.4	59.4	50.5
110	42.5	50.2	54.9	60.1	58.9	50.1
111	42.8	50.5	54.9	60.2	58.4	49.8
112	42.6	50.6	55.0	59.9	58.4	49.7
113	42.6	50.2	54.7	59.6	58.5	49.1
114	42.3	50.0	54.7	59.5	58.5	48.6
115	42.1	50.0	54.9	58.8	58.7	48.6
116	42.1	50.0	54.4	59.0	58.3	48.4
117	41.9	50.2	54.3	59.5	58.1	48.4
118	41.6	50.3	54.6	59.4	58.2	48.6
119	41.4	50.0	54.2	59.9	58.3	48.8
120	41.1	49.9	54.5	59.5	58.8	49.1
121	41.1	50.0	54.5	59.2	58.8	49.3
122	41.5	50.5	54.3	59.6	58.8	49.7
123	41.7	50.5	54.8	59.8	59.1	49.8
124	42.0	50.7	54.9	60.1	59.1	50.1
125	42.0	50.4	55.2	60.2	58.7	50.4
126	41.9	49.7	55.2	60.0	58.7	50.2
127	41.5	49.5	54.8	59.7	58.5	50.3
128	41.4	49.3	54.6	59.8	58.2	49.8

Time	Position 0	Position 1	Position 2	Position 3	Position 4	Position 5
– h –	°C					
129	41.6	49.4	54.5	59.6	58.3	49.2
130	41.5	49.5	54.4	59.7	58.3	48.9
131	41.8	49.6	54.5	59.6	57.8	48.6
132	41.7	49.2	54.7	59.3	57.7	48.6
133	41.5	48.7	54.7	59.3	58.0	48.8
134	41.4	48.4	54.4	58.8	57.8	48.6
135	41.3	48.4	54.1	58.8	57.5	48.2
136	41.2	48.6	53.9	58.3	57.3	47.5
137	41.2	48.8	53.5	58.3	56.7	47.0
138	41.0	48.8	53.7	58.5	56.4	46.9
139	41.0	48.8	53.6	58.3	56.5	46.6
140	41.2	48.9	53.7	59.0	55.7	46.8
141	41.2	48.9	53.6	58.6	55.8	46.6
142	41.3	49.1	53.4	58.6	55.9	46.7
143	41.4	49.2	53.2	58.4	55.2	46.4
144	41.3	48.7	53.0	58.0	55.8	46.6
145	41.4	48.6	53.3	58.1	55.4	46.9
146	41.4	48.9	53.4	57.8	55.6	46.8
147	41.4	48.7	53.6	57.7	56.2	47.5
148	41.4	48.9	53.5	57.6	55.8	47.4
149	41.9	49.4	53.4	56.9	56.0	47.4
150	41.9	49.4	53.2	56.8	55.6	47.5
151	41.7	49.3	53.4	56.8	55.1	47.1
152	41.9	49.2	53.3	56.0	55.1	47.3
153	41.3	48.8	53.2	56.5	54.7	46.9
154	41.3	48.7	53.1	56.4	54.8	46.4
155	41.3	48.6	53.2	56.3	54.9	46.3
156	41.1	48.4	53.3	56.5	54.7	45.4
157	41.0	48.4	53.1	56.3	54.4	44.9
158	41.0	48.1	52.9	56.2	53.9	44.7
159	40.7	48.0	52.2	56.3	n.d.	43.9
160	40.7	48.2	52.0	56.6	n.d.	43.9
161	40.5	48.0	52.0	56.7	n.d.	44.0
162	40.6	48.1	52.2	56.7	n.d.	43.7
163	40.5	48.1	52.6	56.5	n.d.	44.0

Time	Position 0	Position 1	Position 2	Position 3	Position 4	Position 5
– h –	°C					
164	40.1	47.8	52.4	56.5	n.d.	43.9
165	40.4	47.8	52.2	56.5	n.d.	44.1
166	40.1	47.6	51.9	56.6	n.d.	44.2
167	40.0	47.6	52.1	56.5	n.d.	44.5
168	40.2	47.7	51.8	56.4	n.d.	44.9
169	40.0	47.7	51.9	56.5	n.d.	45.0
170	40.0	47.6	51.9	56.1	n.d.	45.7
171	39.8	47.8	51.9	56.1	n.d.	45.4
172	40.3	47.8	52.5	56.1	52.7	45.6
173	40.5	48.1	52.4	55.9	53.1	45.4
174	40.6	48.0	52.2	56.3	53.0	44.7
175	40.6	47.6	52.0	56.4	53.3	44.8
176	40.1	47.5	51.8	55.8	53.3	44.5
178	39.9	47.3	51.9	55.6	53.0	44.3
180	39.6	47.3	52.2	55.0	52.6	44.1
182	39.7	47.3	52.0	54.9	52.4	43.6
184	39.6	47.1	51.5	55.3	51.6	42.8
186	39.3	47.0	51.2	55.0	51.2	42.2
188	39.0	47.2	51.1	54.9	51.0	42.1
190	38.6	46.9	50.9	54.4	50.5	42.4
192	38.5	46.4	50.9	54.1	50.7	43.0
194	38.4	46.2	50.6	53.8	51.1	43.8
196	38.7	45.9	50.5	54.1	51.5	43.9
198	38.9	45.9	50.4	54.5	51.7	43.6
200	39.1	46.2	50.6	54.6	51.7	43.2
202	39.0	46.2	50.7	54.4	51.2	42.7
204	38.8	46.0	50.3	54.0	50.5	42.4
206	38.8	46.2	50.2	54.1	50.1	42.0
208	38.6	46.2	49.9	53.6	49.9	41.8
210	38.7	46.4	49.7	53.3	49.4	41.1

Table E-4 Averaged temperature measurements for treatment 4

Time	Position 0	Position 1	Position 2	Position 3	Position 4	Position 5
– h –	°C					
39	30.9	30.8	30.9	30.9	30.8	30.8
40	32.4	32.6	32.7	32.7	32.4	32.8
41	35.0	35.1	35.1	38.5	35.6	35.2
42	36.8	37.4	36.7	44.0	37.3	37.9
43	38.5	39.5	38.6	50.3	41.0	42.7
44	40.2	42.0	41.0	56.6	45.3	47.5
45	40.7	43.0	42.0	59.5	47.5	49.5
46	41.7	44.1	42.6	62.0	49.5	51.2
47	41.9	45.3	42.9	64.2	51.5	53.3
48	42.7	44.6	42.6	65.7	52.8	55.8
49	43.2	45.3	43.0	66.6	54.0	58.6
50	42.8	44.4	43.2	67.0	54.7	61.2
51	42.5	43.1	42.7	67.1	55.0	63.8
52	41.7	43.1	42.3	67.6	55.8	65.6
53	41.1	42.3	41.6	67.8	56.4	66.7
55	40.4	41.8	41.2	67.8	56.8	67.5
56	40.3	41.3	41.2	67.6	57.1	67.4
77	40.0	40.8	40.9	67.4	57.1	67.4
78	40.2	40.6	41.0	67.3	57.4	67.2
79	40.1	40.4	40.8	66.9	57.3	66.6
80	39.9	40.0	40.2	66.3	57.0	66.1
81	39.7	39.7	39.9	65.6	56.7	65.4
82	39.1	39.4	39.4	64.8	56.0	64.5
83	38.8	39.0	39.0	63.9	55.0	63.4
84	38.5	39.0	38.7	63.2	53.8	62.5
85	38.5	38.6	38.6	62.5	52.7	61.4
86	38.1	38.0	38.4	61.7	51.9	60.0
87	37.8	37.5	37.9	61.1	51.2	59.0
88	37.2	37.6	37.3	60.4	50.8	57.7
89	36.7	37.7	36.9	60.0	50.3	56.5
90	36.7	37.9	36.8	59.7	49.8	55.9
91	36.7	38.1	36.8	59.4	49.4	55.6
92	36.9	37.6	37.2	59.1	48.7	55.5

E.2 Raw temperature data

Table E-5 Raw temperature data (°C) for all treatments

Time (h)	Position	Trt1		Trt2		Trt3		Trt4	
		Rep 1	Rep 2	Rep 1	Rep 2	Rep 1	Rep 2	Rep 1	Rep 2
29	0	25.9	24.7	25.1	26.2	27.4	27.1	27.8	28.7
29	1	25.6	26.0	24.4	27.0	26.9	26.9	28.0	27.0
29	2	26.3	25.2	25.7	27.2	27.5	26.7	27.9	27.0
29	3	26.9	25.2	25.1	27.0	30.8	26.5	27.3	26.7
29	4	25.6	24.7	26.3	26.1	27.5	26.2	27.7	27.6
29	5	26.2	26.0	29.0	30.3	30.5	27.3	27.2	27.7
31	0	25.4	24.4	24.9	26.6	28.6	27.4	28.2	28.2
31	1	25.1	25.2	25.4	25.5	28.5	26.9	28.0	27.9
31	2	24.8	24.7	26.2	26.4	27.9	27.5	28.7	28.4
31	3	24.9	24.5	26.8	32.4	34.1	27.5	27.8	29.6
31	4	24.5	26.2	25.8	27.1	28.0	27.7	28.3	28.6
31	5	25.2	25.7	32.2	32.0	34.0	26.8	29.0	28.9
38	0	28.3	27.0	26.8	28.4	29.7	28.6	33.0	32.9
38	1	27.1	26.7	27.9	26.9	29.7	28.4	32.7	33.5
38	2	26.8	27.0	27.5	27.0	30.2	29.0	32.0	33.8
38	3	25.3	26.3	26.7	28.4	38.7	29.0	33.4	33.7
38	4	26.3	24.5	25.9	28.5	29.8	29.7	31.9	34.7
38	5	25.7	26.3	39.2	40.2	43.1	28.3	31.7	33.3
39	0	25.4	26.3	25.1	28.7	30.4	28.7	33.1	35.6
39	1	24.8	26.3	25.4	29.3	30.6	29.8	33.2	35.9
39	2	26.6	26.0	26.9	28.2	30.5	28.8	34.2	34.9
39	3	26.4	25.6	25.4	38.4	40.2	29.1	34.3	34.0
39	4	27.1	25.8	27.2	30.8	30.7	30.1	33.0	34.7
39	5	24.7	24.3	39.4	37.8	42.6	28.2	33.6	35.2
40	0	25.3	26.5	26.0	29.0	30.3	29.7	33.0	35.4
40	1	26.7	26.7	25.5	29.0	31.0	29.3	35.3	34.0
40	2	25.3	25.3	26.0	29.8	30.5	30.0	35.1	34.2
40	3	24.8	25.1	26.7	37.7	30.1	28.6	33.7	35.4
40	4	26.6	25.8	27.1	28.5	30.2	30.0	33.0	34.6
40	5	27.1	26.2	38.4	38.9	30.9	29.7	35.0	35.9
41	0	25.6	25.9	26.9	28.7	34.2	32.4	39.1	38.2
41	1	27.1	26.8	29.5	30.4	26.7	25.4	37.5	38.5
41	2	26.5	26.3	28.9	29.9	36.2	33.0	38.0	38.3

Time (h)	Position	Trt1		Trt2		Trt3		Trt4	
		Rep 1	Rep 2	Rep 1	Rep 2	Rep 1	Rep 2	Rep 1	Rep 2
41	3	25.4	26.6	28.1	42.3	44.8	44.3	52.1	51.1
41	4	25.7	27.3	27.9	30.7	34.8	35.3	39.4	43.7
41	5	26.8	26.1	41.1	38.5	42.9	42.9	1.9	41.9
42	0	28.2	27.0	29.5	31.2	39.2	36.3	39.7	40.6
42	1	27.3	28.3	28.9	32.8	29.4	29.7	42.1	42.3
42	2	27.4	26.7	29.3	32.2	27.6	29.4	38.5	40.5
42	3	26.9	25.8	28.2	33.9	46.2	48.5	55.3	56.2
42	4	27.2	26.9	29.4	30.3	28.4	31.1	324.2	42.5
42	5	26.7	25.8	42.0	41.3	42.8	43.5	2.7	45.9
43	0	27.5	26.5	29.7	32.7	36.4	36.5	40.3	41.9
43	1	27.7	29.1	29.6	31.8	27.7	31.1	42.7	43.8
43	2	28.2	26.5	28.0	31.8	25.5	30.2	41.4	43.1
43	3	26.8	25.8	28.0	42.0	43.4	47.7	59.4	58.8
43	4	27.6	26.6	30.9	34.2	31.2	34.5	45.4	48.6
43	5	27.1	26.3	40.2	39.6	41.4	43.0	49.9	47.5
44	0	26.2	26.4	30.0	33.9	36.0	38.0	40.1	41.3
44	1	27.6	28.0	29.6	33.5	27.5	32.3	44.2	45.1
44	2	26.0	25.5	31.0	33.8	25.4	31.2	43.4	44.7
44	3	27.5	26.6	29.9	34.1	44.1	48.8	61.2	59.0
44	4	27.0	25.9	31.5	34.1	31.2	34.9	47.3	50.1
44	5	28.1	25.1	42.3	39.3	40.4	44.0	51.6	48.0
45	0	27.8	25.2	31.3	31.7	36.5	37.9	39.0	42.6
45	1	28.1	27.0	31.2	35.8	34.8	38.3	39.6	43.8
45	2	27.4	26.5	31.0	34.2	35.7	39.3	41.7	42.4
45	3	28.6	27.7	35.7	43.8	43.7	49.3	63.5	62.6
45	4	27.2	27.2	28.9	35.3	30.3	34.0	48.0	50.7
45	5	26.2	26.8	41.9	39.4	42.0	43.2	54.3	49.3
46	0	27.3	26.6	32.4	34.9	34.3	41.1	42.2	45.8
46	1	27.4	27.8	32.5	35.4	26.6	34.4	46.2	47.5
46	2	28.1	28.2	31.8	36.4	35.4	40.1	41.1	43.0
46	3	28.3	26.1	35.8	42.6	43.6	49.8	66.2	65.3
46	4	27.9	26.7	31.7	36.9	31.0	34.4	51.6	54.2
46	5	27.1	25.0	40.6	41.3	42.8	44.8	57.2	51.9
47	0	27.2	24.9	32.6	36.2	37.0	41.5	41.0	43.2
47	1	27.5	29.2	33.5	37.0	26.2	35.5	47.0	48.8

Time (h)	Position	Trt1		Trt2		Trt3		Trt4	
		Rep 1	Rep 2	Rep 1	Rep 2	Rep 1	Rep 2	Rep 1	Rep 2
47	2	26.5	25.5	32.5	36.4	34.9	41.6	42.6	44.1
47	3	27.0	27.1	37.1	42.8	43.7	50.3	68.3	67.3
47	4	28.2	25.7	33.9	35.9	31.4	34.5	53.9	56.4
47	5	29.2	27.9	42.8	40.6	42.3	44.3	58.1	55.6
48	0	28.2	26.5	32.3	37.3	36.2	42.8	41.7	45.9
48	1	26.8	28.2	32.5	37.3	35.9	42.3	40.0	44.2
48	2	27.5	25.8	33.1	37.5	34.9	43.1	41.9	43.9
48	3	28.5	27.7	37.8	43.0	40.5	47.4	66.5	65.7
48	4	28.0	27.7	34.9	38.3	29.1	34.4	52.0	55.8
48	5	27.6	26.0	41.7	40.5	44.1	44.3	61.9	58.4
49	0	27.1	28.6	33.5	40.6	37.2	43.7	40.8	44.6
49	1	27.9	27.8	33.8	38.6	36.6	44.5	42.9	45.9
49	2	26.8	27.6	33.7	39.0	36.3	44.5	42.7	44.5
49	3	28.4	28.3	37.3	43.8	39.8	47.7	67.2	65.9
49	4	28.8	27.7	34.3	38.6	29.4	36.2	51.9	56.2
49	5	28.2	26.9	41.8	40.2	43.0	44.0	65.2	60.6
50	0	27.1	28.0	35.4	39.5	36.7	45.1	41.4	43.8
50	1	27.6	26.9	35.2	40.8	34.9	45.7	43.5	42.8
50	2	27.3	28.2	34.7	41.5	36.1	46.3	39.8	46.1
50	3	28.8	28.5	39.3	44.7	40.0	48.6	68.1	66.9
50	4	29.5	27.9	36.8	42.0	29.6	37.5	53.4	57.8
50	5	27.0	26.4	42.0	41.4	42.6	43.0	66.5	62.9
51	0	29.3	27.9	34.8	39.8	36.8	45.3	40.5	41.6
51	1	28.3	28.6	35.8	40.6	35.9	48.3	40.8	44.6
51	2	26.9	28.9	34.9	40.1	36.5	47.5	39.8	42.9
51	3	29.0	28.2	38.6	46.0	40.3	49.3	68.6	67.5
51	4	30.4	26.4	34.2	40.3	29.2	38.3	54.4	58.5
51	5	28.9	29.9	41.2	42.2	44.2	45.0	70.4	64.3
52	0	27.6	26.7	35.0	40.3	36.8	47.8	39.1	41.8
52	1	30.8	29.3	36.4	41.8	37.2	48.6	39.8	44.7
52	2	29.0	27.1	36.9	41.7	35.2	46.0	39.7	43.2
52	3	29.1	27.8	38.9	46.5	40.4	49.8	68.6	67.6
52	4	29.6	27.4	36.4	41.6	29.3	39.0	54.8	59.4
52	5	30.9	28.0	41.0	43.5	44.3	43.2	69.3	65.7
53	0	30.5	28.8	37.1	44.0	35.2	46.6	38.6	41.6

Time (h)	Position	Trt1		Trt2		Trt3		Trt4	
		Rep 1	Rep 2	Rep 1	Rep 2	Rep 1	Rep 2	Rep 1	Rep 2
53	1	28.5	29.0	37.3	42.1	36.0	48.0	38.6	43.2
53	2	30.9	27.7	37.2	40.9	34.9	48.3	39.1	42.1
53	3	28.2	28.9	40.6	45.5	40.7	50.5	67.8	67.2
53	4	28.0	29.6	35.8	44.4	29.6	40.4	53.8	58.8
53	5	29.2	26.2	42.4	43.5	44.0	45.8	69.4	65.4
55	0	28.5	27.6	37.4	42.3	37.3	47.4	38.2	41.8
55	1	29.6	28.6	37.2	42.2	36.1	48.7	39.0	43.5
55	2	31.3	27.1	36.9	41.8	36.0	48.4	38.8	44.0
55	3	28.7	30.1	41.5	44.3	40.6	50.7	67.6	67.3
55	4	30.5	28.6	35.4	42.4	29.7	39.7	55.2	59.7
55	5	28.7	27.7	41.1	44.0	45.5	44.1	70.6	65.2
56	0	30.2	27.8	34.5	43.1	35.8	47.5	39.0	42.0
56	1	28.9	28.9	37.6	42.6	36.8	48.2	38.7	42.6
56	2	29.6	29.4	36.8	41.7	36.4	47.7	39.6	42.8
56	3	30.1	29.2	41.1	46.4	40.5	50.8	67.6	67.3
56	4	29.7	28.0	36.8	44.4	29.6	39.6	55.2	59.6
56	5	28.4	27.9	40.7	41.7	43.2	44.3	68.9	64.6
77	0	28.9	28.0	35.8	40.8	36.3	49.1	37.7	41.4
77	1	28.8	28.9	36.9	43.1	36.3	46.9	39.1	41.7
77	2	32.2	27.2	37.6	41.7	35.7	49.0	37.6	43.5
77	3	28.1	30.0	41.3	45.3	40.7	50.9	67.5	67.2
77	4	29.2	29.6	37.9	41.8	29.8	39.9	55.2	59.6
77	5	30.0	27.1	42.1	42.0	44.0	43.7	70.9	64.4
78	0	30.0	28.0	37.1	39.2	35.8	49.2	39.0	42.7
78	1	28.3	26.8	37.1	41.8	36.2	47.7	38.3	42.2
78	2	29.3	29.7	37.4	43.7	37.0	49.6	38.1	43.2
78	3	28.7	28.3	42.5	47.0	40.7	51.5	66.9	66.9
78	4	29.8	26.0	38.4	42.8	29.6	40.5	54.9	59.4
78	5	30.0	27.4	41.7	41.4	44.3	45.5	69.2	64.0
79	0	28.7	29.5	38.7	44.3	37.0	50.3	37.1	42.1
79	1	29.5	29.6	37.1	46.3	35.4	47.9	39.6	41.0
79	2	29.9	27.9	35.6	42.5	37.0	49.3	38.3	42.9
79	3	31.4	29.2	41.6	47.5	40.9	52.2	65.9	66.1
79	4	29.0	29.5	36.5	41.4	29.6	40.8	55.0	59.1
79	5	28.8	27.7	41.8	43.7	44.2	44.0	68.1	62.8

Time (h)	Position	Trt1		Trt2		Trt3		Trt4	
		Rep 1	Rep 2	Rep 1	Rep 2	Rep 1	Rep 2	Rep 1	Rep 2
80	0	30.7	27.5	39.5	42.5	35.6	49.7	37.5	41.4
80	1	31.6	29.2	38.1	42.8	35.3	51.6	35.9	42.1
80	2	29.8	28.6	40.9	43.2	35.3	49.7	36.6	41.4
80	3	29.8	30.1	44.0	47.2	40.9	53.0	65.1	65.1
80	4	31.2	30.6	39.7	41.8	30.0	41.1	54.1	58.8
80	5	32.1	29.0	40.8	39.2	43.5	45.7	66.2	63.2
81	0	30.9	28.4	39.1	42.6	36.1	51.8	37.4	40.6
81	1	31.2	28.6	38.2	42.9	36.6	51.4	36.4	41.9
81	2	30.1	30.2	40.0	42.7	36.2	50.7	37.0	41.7
81	3	30.1	30.1	46.3	47.3	41.1	54.2	64.2	64.5
81	4	30.6	29.7	39.2	45.1	29.9	42.2	53.9	58.4
81	5	32.2	29.0	39.8	41.2	43.7	47.0	67.1	62.5
82	0	32.2	29.5	40.1	42.5	36.5	50.3	36.2	40.4
82	1	31.6	28.1	38.8	42.4	37.3	51.4	37.5	40.5
82	2	29.7	27.6	38.8	44.4	35.5	51.2	35.8	41.1
82	3	29.7	30.2	45.0	49.1	41.1	55.3	63.5	63.6
82	4	32.9	28.8	40.5	45.7	29.9	42.8	51.7	56.9
82	5	29.9	28.8	40.3	40.6	44.8	45.1	64.9	61.3
83	0	30.8	27.8	40.7	43.2	35.1	50.4	36.8	39.9
83	1	30.9	28.6	42.8	43.1	36.0	52.6	36.9	40.8
83	2	29.5	29.4	39.5	44.4	35.8	51.4	37.2	41.1
83	3	29.7	30.5	43.9	47.3	41.0	56.3	62.6	62.7
83	4	32.6	30.0	41.7	41.2	29.6	43.6	50.7	55.3
83	5	31.7	29.5	39.7	38.9	43.5	47.9	62.2	59.9
84	0	31.4	30.0	40.6	43.4	34.6	51.5	36.1	40.7
84	1	31.8	30.0	41.7	44.6	38.5	51.5	36.6	41.1
84	2	31.1	28.4	41.6	44.3	36.6	49.8	36.1	39.8
84	3	28.9	29.1	42.4	47.8	41.1	57.9	62.1	62.4
84	4	34.2	29.8	40.1	44.9	29.5	44.1	48.6	54.6
84	5	31.2	29.0	40.5	41.4	44.7	46.8	62.3	59.6
85	0	32.0	31.1	41.8	42.8	36.0	51.3	36.8	40.7
85	1	31.7	30.5	42.1	45.2	35.6	52.6	36.0	39.0
85	2	30.8	29.6	41.7	43.3	36.3	53.4	36.8	40.9
85	3	30.6	29.7	42.5	44.9	41.0	59.0	61.3	61.5
85	4	31.9	28.9	43.3	41.5	29.1	44.0	49.7	54.2

Time (h)	Position	Trt1		Trt2		Trt3		Trt4	
		Rep 1	Rep 2	Rep 1	Rep 2	Rep 1	Rep 2	Rep 1	Rep 2
85	5	31.7	28.8	39.9	38.2	41.9	46.9	61.8	59.1
86	0	32.2	29.0	42.1	44.3	35.2	52.5	35.0	38.6
86	1	31.5	29.8	41.4	45.2	36.1	52.6	34.8	38.8
86	2	32.1	30.0	42.3	44.3	36.2	53.4	36.2	39.4
86	3	32.9	30.6	43.9	47.0	40.7	59.8	60.5	60.5
86	4	32.9	29.2	42.4	45.3	29.1	44.5	48.9	52.9
86	5	31.2	29.9	42.0	39.3	39.8	48.3	59.1	56.3
87	0	31.9	31.6	43.3	45.1	37.3	51.3	36.5	38.1
87	1	34.2	30.4	41.6	43.9	37.4	51.4	34.6	39.3
87	2	33.8	28.3	41.6	45.2	38.3	50.8	35.3	38.3
87	3	34.0	30.6	40.8	45.4	40.9	62.7	60.1	60.0
87	4	33.8	31.4	42.7	44.1	29.1	44.4	49.0	51.5
87	5	31.8	29.0	39.1	36.4	42.4	51.3	58.7	54.8
88	0	33.0	29.3	41.6	43.7	36.1	50.3	33.7	37.8
88	1	32.5	27.3	41.6	43.8	26.8	50.0	37.2	40.8
88	2	33.6	31.3	44.6	44.7	36.6	52.7	33.8	38.0
88	3	32.3	31.2	42.5	47.0	40.8	62.8	59.8	59.7
88	4	33.1	29.0	43.9	44.4	29.0	44.3	48.9	51.6
88	5	32.7	29.4	37.6	35.9	40.7	48.4	57.3	54.1
89	0	32.2	28.6	41.1	44.6	36.3	50.6	34.4	39.1
89	1	33.5	29.7	43.9	43.8	26.5	49.6	35.7	40.4
89	2	33.6	31.1	43.2	44.5	35.8	50.6	35.0	38.9
89	3	33.3	30.5	45.5	48.1	41.0	64.2	59.7	59.6
89	4	31.5	31.1	44.5	44.1	28.5	44.7	48.6	51.2
89	5	32.3	29.5	39.0	37.7	39.8	51.8	58.3	53.3
90	0	33.7	29.2	41.1	43.8	36.9	52.4	35.5	38.1
90	1	34.1	29.9	42.7	43.7	26.8	50.2	34.7	40.3
90	2	34.1	30.1	44.2	43.8	34.9	52.2	35.3	40.0
90	3	31.8	30.1	46.2	46.8	40.9	65.5	59.4	59.3
90	4	34.1	30.4	41.4	44.2	28.2	45.7	47.7	50.1
90	5	32.8	27.8	41.1	39.5	41.4	51.7	56.5	53.8
91	0	32.8	29.7	43.5	44.9	35.0	50.9	34.2	40.4
91	1	33.2	29.5	43.8	44.2	26.4	50.0	35.9	39.6
91	2	33.1	29.9	43.0	45.1	34.6	51.2	34.9	38.2
91	3	34.0	29.6	49.4	48.2	41.0	66.5	59.0	58.9

Time (h)	Position	Trt1		Trt2		Trt3		Trt4	
		Rep 1	Rep 2	Rep 1	Rep 2	Rep 1	Rep 2	Rep 1	Rep 2
91	4	32.0	31.3	45.5	44.7	28.2	47.0	47.2	49.5
91	5	33.5	30.2	39.9	39.4	41.3	54.3	57.3	54.4
92	0	34.0	30.4	42.8	43.2	34.4	52.1	34.6	38.9
92	1	34.4	29.3	43.7	43.1	34.9	51.6	36.4	37.4
92	2	33.7	28.9	43.6	44.8	35.8	50.5	35.6	39.5
92	3	35.4	31.0	50.1	49.2	40.5	67.0	58.4	58.1
92	4	34.6	30.2	43.8	43.4	28.6	48.8	45.7	49.7
92	5	33.5	28.6	41.2	37.9	42.4	53.8	56.5	53.8
93	0	33.9	30.3	45.2	45.5	35.0	50.8	36.6	41.6
93	1	34.4	32.1	49.3	48.4	38.6	64.7	48.7	50.9
93	2	43.0	35.3	54.5	47.7	41.7	71.5	57.6	58.8
93	3	44.9	41.4	54.0	45.7	48.2	75.6	63.5	60.2
93	4	42.0	42.8	53.7	46.4	47.3	66.9	62.7	65.5
93	5	36.8	36.8	42.3	41.2	41.3	53.9	56.6	52.5
94	0	33.3	30.9	44.7	42.0	35.4	53.7	37.2	40.6
94	1	35.3	32.2	51.7	47.5	39.6	63.7	50.4	53.2
94	2	37.7	36.1	54.0	45.5	41.2	70.1	54.9	56.0
94	3	44.3	41.6	53.6	49.0	47.1	75.9	61.7	61.6
94	4	43.2	41.7	54.8	44.7	47.1	71.4	63.4	65.6
94	5	39.1	37.3	45.1	41.1	43.0	58.0	55.4	52.6
95	0	35.7	29.4	43.1	45.3	36.4	51.9	35.9	40.7
95	1	35.1	32.0	54.7	45.5	38.5	64.3	48.0	49.2
95	2	39.7	36.0	55.9	47.8	40.1	72.5	57.9	58.6
95	3	44.4	42.3	56.3	50.0	46.6	74.6	61.0	60.2
95	4	44.2	42.5	53.4	46.8	46.1	69.5	63.6	63.9
95	5	34.7	36.4	43.0	40.7	43.0	56.8	54.2	52.8
96	0	33.8	31.1	44.0	44.2	34.8	52.4	37.4	40.1
96	1	35.8	30.4	48.9	46.2	38.3	63.8	50.3	52.7
96	2	38.5	34.1	52.9	47.3	40.7	70.3	55.6	59.0
96	3	42.7	42.6	52.2	49.9	45.1	73.0	61.5	62.6
96	4	44.4	43.9	53.0	43.9	47.8	69.9	59.4	65.1
96	5	37.5	38.6	45.6	41.5	42.6	57.1	53.3	53.3
97	0	34.7	33.4	45.5	41.7	35.3	52.5	38.4	39.7
97	1	35.9	32.4	54.6	46.5	38.2	63.0	51.5	51.3
97	2	40.9	37.3	54.4	44.1	39.8	71.0	56.2	59.7

Time (h)	Position	Trt1		Trt2		Trt3		Trt4	
		Rep 1	Rep 2	Rep 1	Rep 2	Rep 1	Rep 2	Rep 1	Rep 2
97	3	45.0	42.6	54.6	48.2	46.3	74.4	61.5	62.2
97	4	44.0	44.2	57.2	47.0	48.2	70.5	61.6	64.6
97	5	38.5	39.4	43.4	40.5	43.3	57.9	56.1	54.1
98	0	35.0	33.0	43.7	42.6	34.6	52.7	38.9	39.5
98	1	37.2	32.8	53.7	44.2	36.7	65.6	50.7	50.7
98	2	40.3	35.2	54.2	44.5	40.2	71.6	54.5	58.3
98	3	40.9	42.0	54.4	47.7	44.6	74.8	61.2	62.7
98	4	43.4	41.7	52.1	48.6	48.3	71.6	63.1	63.5
98	5	38.3	39.7	45.0	45.2	43.7	55.2	53.6	53.3
99	0	35.6	30.8	42.6	41.8	35.7	52.0	39.1	42.4
99	1	37.2	32.1	50.4	46.5	38.0	64.8	50.2	52.9
99	2	40.9	36.6	55.7	46.6	41.1	70.6	56.7	56.9
99	3	43.9	44.1	56.6	50.5	45.3	74.4	62.3	62.8
99	4	46.8	43.2	52.5	48.4	48.0	71.4	64.4	66.3
99	5	36.7	39.7	44.3	42.0	45.6	58.6	53.6	53.8
100	0	34.3	32.3	43.3	41.8	35.1	50.8	37.5	40.6
100	1	35.8	33.7	50.8	46.9	38.1	64.1	51.1	52.0
100	2	39.4	37.8	57.7	48.2	40.7	68.3	55.4	56.9
100	3	43.5	43.1	54.8	49.2	43.9	78.1	64.0	60.8
100	4	42.7	45.1	53.6	48.0	47.0	72.0	61.6	63.5
100	5	37.9	40.9	44.8	41.3	44.1	59.3	55.2	51.2
101	0	36.6	31.7	46.5	41.8	35.5	50.5	37.6	40.0
101	1	38.4	32.7	53.8	46.4	39.8	64.6	52.5	52.1
101	2	40.0	36.9	56.3	48.3	40.8	70.4	56.5	57.2
101	3	45.0	43.0	60.2	48.2	46.4	75.2	61.3	61.9
101	4	43.6	44.8	56.7	49.5	47.0	70.0	60.1	65.4
101	5	39.7	39.3	43.5	42.0	44.9	58.6	53.3	52.6
102	0	35.9	31.2	46.1	41.9	36.7	51.7	38.2	40.3
102	1	36.6	33.9	51.8	46.8	40.6	63.2	53.1	52.9
102	2	43.4	37.0	56.0	45.6	41.8	68.0	55.9	59.5
102	3	43.5	42.7	58.8	49.2	46.6	74.7	62.2	59.4
102	4	44.7	43.6	55.8	47.5	49.9	73.2	61.6	66.8
102	5	38.3	37.3	45.7	42.9	45.3	59.0	52.6	54.3
103	0	35.0	32.6	43.8	40.5	36.3	49.4	36.6	40.7
103	1	36.2	33.5	56.0	46.3	41.3	62.4	51.9	52.6

Time (h)	Position	Trt1		Trt2		Trt3		Trt4	
		Rep 1	Rep 2	Rep 1	Rep 2	Rep 1	Rep 2	Rep 1	Rep 2
103	2	43.1	37.9	55.6	48.8	40.7	72.7	55.0	59.2
103	3	45.2	45.2	56.4	50.4	44.3	76.4	64.0	60.8
103	4	44.9	45.9	56.3	47.2	47.2	72.5	63.5	62.8
103	5	36.4	38.4	44.5	41.3	44.2	57.9	53.7	50.5
104	0	35.3	32.9	45.2	39.3	36.6	50.2	37.8	40.6
104	1	36.1	34.9	53.6	44.5	38.5	62.3	50.5	51.8
104	2	41.2	38.4	53.7	46.3	40.1	66.4	57.0	57.4
104	3	44.4	42.6	58.5	48.9	48.0	74.5	62.8	60.2
104	4	50.2	43.5	58.1	49.7	47.2	73.1	62.3	61.9
104	5	35.6	39.0	43.8	41.8	43.1	59.2	54.9	51.9
105	0	35.2	33.4	45.1	42.7	37.5	48.5	36.6	41.6
105	1	35.8	34.1	55.7	46.9	39.8	61.7	48.4	52.0
105	2	42.3	36.7	57.9	46.1	41.7	66.4	54.8	57.9
105	3	45.3	45.4	61.4	50.2	47.0	73.8	61.3	62.3
105	4	44.2	44.8	58.9	50.5	46.4	70.9	62.3	64.1
105	5	37.8	38.8	44.4	42.9	44.9	59.9	53.1	53.1
106	0	37.0	34.0	44.4	40.1	36.6	49.6	37.4	39.4
106	1	37.9	34.1	52.3	45.4	37.8	61.5	48.8	50.5
106	2	42.6	38.9	55.8	47.7	40.8	68.7	55.5	58.3
106	3	44.4	45.6	60.5	50.9	47.3	74.5	64.1	60.6
106	4	45.7	43.7	56.0	49.6	48.0	72.9	62.1	64.9
106	5	36.4	38.0	46.3	41.5	41.8	60.8	53.2	50.2
107	0	33.5	33.3	46.8	40.7	36.0	47.4	36.9	39.8
107	1	36.6	34.5	54.7	45.2	39.1	60.1	51.5	51.5
107	2	38.7	39.6	59.5	47.5	41.5	68.2	55.8	57.3
107	3	46.5	44.5	59.5	48.0	47.7	73.0	63.6	61.5
107	4	45.5	43.0	59.3	48.7	47.3	71.0	61.3	63.6
107	5	36.8	38.6	46.4	42.3	43.3	56.6	55.2	52.6
108	0	34.7	34.0	46.4	40.5	36.4	48.4	35.6	40.5
108	1	36.0	36.0	55.9	45.8	40.2	59.6	48.7	51.4
108	2	41.6	36.7	58.0	47.9	43.2	66.6	53.5	57.2
108	3	47.9	43.7	59.9	49.3	47.4	73.8	63.5	61.3
108	4	42.0	43.1	58.2	50.0	47.2	71.7	62.4	62.4
108	5	36.2	37.7	43.8	41.0	42.0	57.2	54.3	51.4
109	0	34.8	34.2	42.9	41.1	37.3	48.1	37.4	39.9

Time (h)	Position	Trt1		Trt2		Trt3		Trt4	
		Rep 1	Rep 2	Rep 1	Rep 2	Rep 1	Rep 2	Rep 1	Rep 2
109	1	37.6	36.3	53.2	48.1	40.4	60.9	49.6	52.4
109	2	40.8	40.4	61.2	47.0	42.6	68.3	55.7	57.1
109	3	44.5	43.3	60.3	47.1	46.3	72.9	64.8	64.0
109	4	45.5	43.4	59.2	50.4	45.9	71.5	63.9	65.3
109	5	36.0	37.2	44.4	42.7	43.4	58.5	53.8	52.7
110	0	35.3	35.4	45.1	41.3	38.1	48.0	35.3	38.9
110	1	37.1	32.6	54.9	45.4	40.2	61.0	48.6	51.0
110	2	40.0	37.8	59.9	46.2	41.4	67.7	55.8	58.1
110	3	45.8	44.5	63.6	49.7	46.6	72.9	63.6	60.6
110	4	46.3	43.1	60.6	48.7	47.1	69.3	62.3	64.0
110	5	37.3	37.3	45.0	41.0	43.4	56.6	54.9	51.9
111	0	36.6	32.7	43.9	42.7	37.6	48.1	36.8	37.1
111	1	38.6	35.2	57.7	43.8	41.2	60.4	47.7	51.4
111	2	41.5	38.6	59.1	47.0	42.5	66.5	54.4	57.4
111	3	47.5	44.9	63.8	51.1	46.4	75.2	59.9	61.9
111	4	44.3	44.6	62.0	49.5	46.1	68.6	61.8	64.1
111	5	35.0	36.0	43.9	44.1	40.5	56.5	52.0	52.2
112	0	35.3	33.4	45.0	41.2	36.6	47.0	33.9	38.0
112	1	40.5	37.1	58.3	45.2	40.3	60.1	48.4	49.7
112	2	41.5	37.6	61.4	48.0	43.3	67.7	55.3	56.8
112	3	45.8	44.3	61.3	52.3	46.3	72.8	62.2	60.7
112	4	43.1	42.7	62.0	51.2	48.4	70.0	63.0	62.3
112	5	36.7	35.6	44.6	40.6	40.8	57.9	54.1	52.0
113	0	36.0	33.1	44.4	42.2	38.5	46.8	34.5	37.8
113	1	38.2	34.9	55.9	44.1	40.1	58.5	48.3	48.5
113	2	41.7	39.0	59.9	45.5	41.2	67.5	54.0	58.1
113	3	45.4	43.6	62.8	52.2	45.9	70.5	63.4	60.2
113	4	43.7	40.8	57.8	49.2	46.5	72.2	62.3	64.3
113	5	36.5	37.8	44.2	42.2	40.1	56.8	54.8	52.1
114	0	34.7	34.5	46.5	40.6	36.9	46.8	34.2	38.4
114	1	37.0	34.5	56.5	42.4	39.7	59.7	46.5	49.6
114	2	41.8	39.4	62.0	46.3	41.4	67.5	53.8	56.1
114	3	44.1	44.8	62.3	51.6	45.4	73.8	61.8	60.0
114	4	44.8	44.4	61.0	48.3	48.1	67.9	62.2	60.1
114	5	36.1	38.9	47.3	41.6	41.3	54.8	55.0	52.2

Time (h)	Position	Trt1		Trt2		Trt3		Trt4	
		Rep 1	Rep 2	Rep 1	Rep 2	Rep 1	Rep 2	Rep 1	Rep 2
115	0	36.4	34.0	46.6	41.1	36.9	47.1	34.3	38.6
115	1	41.2	37.0	59.0	45.9	40.4	60.9	46.6	50.2
115	2	42.8	35.6	62.3	45.6	43.8	66.9	53.2	58.0
115	3	46.6	44.3	62.8	48.9	44.1	71.8	60.2	59.5
115	4	43.6	44.5	60.6	49.8	47.7	68.9	61.3	63.3
115	5	36.9	38.9	45.5	40.6	41.6	55.5	54.9	49.9
116	0	35.1	33.6	46.7	43.1	36.9	47.0	34.9	38.0
116	1	39.7	35.6	58.2	46.1	40.7	60.1	47.9	48.6
116	2	44.4	40.4	62.3	46.3	41.8	65.2	56.5	57.9
116	3	47.1	44.5	63.8	49.6	47.6	72.8	61.8	59.9
116	4	44.1	44.3	62.2	48.4	45.6	69.1	60.9	63.1
116	5	35.8	38.5	46.8	39.3	41.0	55.9	53.4	52.0
117	0	37.3	34.6	47.9	42.4	36.7	46.8	35.5	38.0
117	1	39.9	35.3	55.9	43.2	40.4	59.7	47.9	49.3
117	2	45.4	40.1	63.0	45.9	41.6	66.5	54.8	56.4
117	3	46.9	47.0	65.0	50.1	46.4	73.7	60.8	59.1
117	4	44.4	44.8	65.9	49.7	47.1	70.7	61.0	64.5
117	5	37.6	37.7	46.3	40.8	40.9	56.5	53.9	50.4
118	0	35.4	33.9	47.4	39.4	35.8	45.8	34.5	36.6
118	1	39.7	35.8	60.2	47.0	40.1	59.8	47.6	49.7
118	2	42.8	40.3	63.2	45.7	42.7	67.9	52.6	56.7
118	3	45.4	44.2	65.8	47.9	46.3	72.4	60.3	58.6
118	4	45.2	43.7	61.3	48.3	46.4	70.0	61.8	63.3
118	5	39.6	38.3	45.7	43.5	41.2	56.2	54.5	50.7
119	0	34.9	33.5	45.8	39.9	35.8	46.7	35.9	39.6
119	1	41.2	35.2	56.9	44.3	38.7	60.5	47.7	48.2
119	2	41.6	37.9	61.2	46.9	43.0	65.1	54.7	55.7
119	3	45.4	45.9	68.9	49.3	47.6	72.0	60.0	59.5
119	4	48.8	46.9	61.2	48.3	47.4	70.1	61.4	62.5
119	5	38.0	39.1	46.6	41.2	42.4	56.3	55.5	50.8
120	0	34.0	34.1	47.9	39.9	35.3	46.0	34.6	38.2
120	1	41.5	33.6	59.6	43.0	40.2	59.4	48.0	49.2
120	2	43.0	39.3	64.1	46.9	40.9	68.0	52.6	55.0
120	3	46.6	46.0	64.2	50.1	44.9	72.3	61.3	60.1
120	4	45.3	46.2	60.7	51.8	47.5	71.2	61.4	64.1

Time (h)	Position	Trt1		Trt2		Trt3		Trt4	
		Rep 1	Rep 2	Rep 1	Rep 2	Rep 1	Rep 2	Rep 1	Rep 2
120	5	38.6	40.2	46.0	42.6	43.0	56.2	53.8	53.1
121	0	36.3	33.6	48.0	40.4	36.3	46.7	35.8	38.4
121	1	39.3	35.7	60.1	44.8	41.1	59.9	48.3	49.5
121	2	44.5	38.7	65.0	47.3	41.7	66.3	52.0	55.9
121	3	45.7	45.5	66.0	50.3	47.2	71.2	61.4	58.3
121	4	46.1	45.0	63.3	49.2	47.3	70.4	63.0	62.5
121	5	37.4	39.4	46.6	42.1	43.9	55.3	52.1	50.1
122	0	37.4	34.5	48.3	40.2	37.2	48.0	36.0	37.5
122	1	38.8	38.4	59.6	44.8	41.6	62.4	48.7	49.3
122	2	46.2	38.1	63.9	45.8	41.6	67.8	52.3	55.5
122	3	46.4	48.0	67.7	49.2	48.5	73.4	62.7	59.1
122	4	47.1	44.6	62.0	50.6	46.1	70.4	60.4	62.6
122	5	37.4	38.8	45.9	43.8	43.5	56.7	52.1	49.8
123	0	37.1	35.0	48.0	41.3	37.5	46.8	35.6	39.3
123	1	41.9	35.7	59.1	45.8	38.8	60.4	49.3	49.1
123	2	44.9	40.3	63.2	45.4	42.7	69.1	51.6	57.2
123	3	48.8	47.1	67.0	49.2	48.8	72.2	61.5	58.9
123	4	45.3	47.3	62.9	52.3	47.2	72.6	59.8	58.6
123	5	39.4	38.4	46.5	45.6	43.3	56.1	51.4	50.0
124	0	36.7	35.1	46.1	41.9	37.5	46.1	35.3	39.3
124	1	39.8	37.8	60.8	44.1	40.8	60.2	47.7	48.6
124	2	42.6	39.0	64.4	48.8	41.3	68.5	53.9	57.6
124	3	44.3	44.3	63.4	51.4	46.3	72.9	59.6	59.9
124	4	46.2	45.5	63.6	49.3	49.1	69.3	59.6	60.3
124	5	40.3	40.8	46.4	43.4	45.8	55.9	51.2	51.0
125	0	37.7	35.6	48.5	40.7	37.5	45.6	35.7	38.7
125	1	40.5	36.8	60.7	43.1	39.6	59.3	46.5	50.7
125	2	42.6	38.3	63.8	44.8	43.1	67.2	53.9	55.2
125	3	45.9	43.3	65.4	50.5	46.9	72.9	62.2	58.0
125	4	47.0	43.9	61.9	45.6	46.8	68.0	58.4	62.9
125	5	39.7	40.3	45.5	42.4	44.8	56.9	53.2	49.8
126	0	38.1	36.0	50.5	41.0	37.6	46.9	34.9	39.9
126	1	40.8	36.1	59.7	42.6	41.2	57.0	47.0	49.8
126	2	42.3	39.7	65.0	48.6	42.8	66.5	53.4	55.8
126	3	50.0	45.1	65.3	49.8	46.7	73.4	59.7	59.0

Time (h)	Position	Trt1		Trt2		Trt3		Trt4	
		Rep 1	Rep 2	Rep 1	Rep 2	Rep 1	Rep 2	Rep 1	Rep 2
126	4	47.9	47.9	63.4	49.7	48.7	67.7	59.3	61.4
126	5	36.8	40.6	45.2	43.6	44.4	54.6	51.4	49.6
127	0	36.1	36.2	48.0	41.2	35.7	45.2	36.1	39.0
127	1	42.4	37.6	58.3	45.2	39.4	58.2	48.6	51.0
127	2	45.4	43.8	65.3	46.6	42.3	66.3	53.3	55.0
127	3	47.6	45.4	66.2	47.8	46.7	71.9	59.9	59.8
127	4	46.0	45.4	63.4	49.7	48.5	70.0	60.7	60.0
127	5	37.6	40.1	45.5	42.9	44.1	56.0	52.9	49.4
128	0	37.4	34.8	49.9	40.0	37.4	45.6	35.0	37.5
128	1	39.9	36.9	60.4	44.0	41.4	58.4	48.4	50.2
128	2	46.5	40.9	64.6	47.3	41.7	66.8	52.2	56.5
128	3	47.5	46.5	66.5	49.5	46.5	73.5	59.7	59.3
128	4	46.5	47.2	63.4	46.8	46.8	69.0	60.3	60.4
128	5	37.8	40.2	42.0	41.2	43.0	54.9	51.1	48.3
129	0	37.6	32.2	51.7	39.8	37.6	46.5	35.6	37.2
129	1	40.4	36.5	59.1	44.4	40.1	59.6	48.2	50.4
129	2	43.6	40.9	62.5	45.1	42.8	66.6	51.2	55.9
129	3	47.8	46.5	66.9	49.8	46.1	71.9	59.1	57.7
129	4	45.8	47.9	62.5	49.4	48.0	67.6	57.6	60.7
129	5	40.0	38.3	45.9	43.2	41.3	55.3	53.9	49.2
130	0	38.3	35.6	49.4	38.3	37.7	45.9	34.4	37.7
130	1	40.9	37.8	61.9	45.0	40.6	58.0	46.1	49.0
130	2	44.1	40.2	64.2	47.0	42.3	66.7	52.2	57.7
130	3	47.3	45.1	66.9	51.3	48.3	72.5	59.8	57.3
130	4	45.6	45.4	61.3	49.9	47.4	69.0	58.7	61.0
130	5	39.1	37.2	43.3	42.3	40.5	55.9	52.1	47.8
131	0	37.3	36.9	49.4	38.9	38.2	45.7	34.5	38.5
131	1	40.7	38.4	59.5	42.3	40.2	58.6	47.1	50.0
131	2	43.7	40.1	67.1	45.6	42.3	66.9	53.3	54.9
131	3	46.2	46.6	67.1	52.4	46.1	71.5	55.5	56.6
131	4	46.8	46.4	63.6	50.8	47.3	67.6	59.5	60.9
131	5	40.9	40.3	46.8	42.1	42.6	55.4	53.0	50.0
132	0	36.9	35.4	50.7	37.7	36.2	45.6	35.7	37.6
132	1	41.0	38.3	62.8	43.5	40.3	56.5	47.8	48.2
132	2	42.9	41.7	64.8	44.0	44.2	65.9	50.9	57.0

Time (h)	Position	Trt1		Trt2		Trt3		Trt4	
		Rep 1	Rep 2	Rep 1	Rep 2	Rep 1	Rep 2	Rep 1	Rep 2
132	3	47.7	45.5	65.8	51.5	45.9	71.9	60.3	58.1
132	4	45.7	46.2	61.4	50.2	46.4	68.5	58.7	60.5
132	5	36.2	36.5	43.3	41.4	42.8	54.9	51.4	48.9
133	0	38.9	36.6	49.0	41.0	38.1	44.3	34.8	37.4
133	1	41.1	35.8	64.1	43.2	39.3	56.1	46.7	48.3
133	2	43.6	39.2	65.4	45.2	42.5	66.5	52.1	55.8
133	3	46.4	46.7	67.7	50.1	46.7	71.7	59.5	57.6
133	4	49.2	45.0	64.5	49.4	46.9	71.0	60.7	59.0
133	5	37.2	38.3	46.0	42.3	41.9	56.1	49.5	49.6
134	0	36.3	35.1	49.8	39.2	37.9	45.4	34.7	37.8
134	1	42.1	37.8	60.5	46.0	39.4	56.8	46.9	49.3
134	2	45.8	39.4	64.3	48.0	40.3	66.2	51.8	55.6
134	3	47.7	44.0	66.5	49.5	45.7	70.8	58.9	56.8
134	4	45.5	44.3	61.8	49.6	45.9	68.4	59.3	60.0
134	5	38.5	38.1	43.6	40.5	41.5	53.7	49.6	47.4
135	0	39.5	35.5	49.4	38.2	38.7	44.2	33.5	37.7
135	1	39.1	36.8	63.2	41.8	40.7	58.1	45.8	49.6
135	2	44.4	40.8	63.5	45.4	41.2	65.9	52.4	55.8
135	3	48.0	46.8	67.2	50.6	47.3	70.7	58.7	57.2
135	4	44.6	44.9	62.7	48.7	45.2	67.4	59.0	59.7
135	5	34.6	37.2	43.0	41.7	41.0	53.6	51.5	49.6
136	0	36.2	36.5	49.9	39.6	37.6	43.4	33.2	37.8
136	1	41.8	36.9	59.7	44.5	40.8	57.8	44.6	48.0
136	2	42.0	42.0	68.7	47.2	42.3	65.9	51.2	54.5
136	3	48.9	47.8	66.8	50.7	44.5	69.1	59.5	58.9
136	4	48.5	43.9	64.6	48.8	46.9	67.0	60.6	60.2
136	5	35.4	37.8	42.3	41.1	39.3	52.8	49.8	48.0
137	0	35.2	37.5	51.1	39.0	37.8	44.3	34.0	37.1
137	1	38.5	37.7	60.3	46.8	40.5	56.6	45.4	48.3
137	2	44.6	41.3	65.9	43.2	41.5	64.9	51.0	53.5
137	3	46.4	47.2	68.0	50.3	45.1	73.3	61.2	58.2
137	4	46.6	47.3	61.5	46.8	45.9	66.6	55.8	60.5
137	5	35.2	38.3	43.1	38.4	40.8	53.3	51.9	48.8
138	0	37.9	35.4	48.5	38.2	37.5	44.4	33.0	37.8
138	1	41.0	38.2	63.6	43.1	40.2	55.3	43.5	47.1

Time (h)	Position	Trt1		Trt2		Trt3		Trt4	
		Rep 1	Rep 2	Rep 1	Rep 2	Rep 1	Rep 2	Rep 1	Rep 2
138	2	45.4	42.3	65.6	47.2	43.2	64.8	52.1	54.7
138	3	50.0	44.2	67.5	50.6	44.8	72.9	57.1	56.5
138	4	46.8	44.0	63.5	49.0	45.5	66.3	57.4	60.9
138	5	38.6	37.0	42.7	40.5	40.5	53.5	49.2	47.9
139	0	35.5	36.9	50.0	39.5	38.1	44.6	34.5	37.1
139	1	41.6	37.3	62.8	44.5	40.9	58.2	43.7	48.8
139	2	44.6	42.3	66.0	44.4	41.7	64.8	51.1	53.7
139	3	47.9	45.2	66.8	50.1	45.9	70.7	56.1	57.9
139	4	45.8	44.3	64.9	49.0	48.4	65.5	57.7	61.3
139	5	38.8	38.4	44.7	43.2	40.2	52.5	50.6	47.9
140	0	39.1	36.4	49.7	38.8	37.2	46.0	33.6	37.8
140	1	40.4	39.5	61.5	45.3	41.5	58.1	44.1	48.0
140	2	44.6	42.9	66.4	45.9	42.4	66.6	51.4	55.6
140	3	50.0	45.2	67.9	49.7	46.6	72.8	58.9	58.1
140	4	45.1	44.1	61.3	47.9	44.4	63.0	56.2	59.3
140	5	37.0	37.5	43.7	42.7	41.1	52.2	50.3	47.6
141	0	37.9	34.1	50.3	40.5	37.6	44.4	34.0	36.5
141	1	42.5	37.4	63.8	44.5	41.2	56.0	45.1	48.4
141	2	44.6	39.4	67.0	46.3	40.7	64.4	52.2	53.8
141	3	47.2	46.3	69.4	50.0	46.4	68.7	56.9	57.2
141	4	46.8	46.8	61.4	47.8	46.6	66.7	56.6	62.4
141	5	37.0	39.3	44.3	40.1	39.7	53.0	49.7	47.1
142	0	40.2	34.9	49.7	39.6	37.7	44.4	33.9	37.7
142	1	39.7	38.1	61.2	42.3	40.9	55.9	45.8	47.6
142	2	49.3	40.9	67.1	45.7	41.9	64.5	51.1	54.7
142	3	49.2	48.1	68.1	48.6	46.6	70.8	60.3	58.8
142	4	46.9	45.3	65.3	48.0	47.1	65.6	57.2	59.5
142	5	40.7	38.6	43.8	38.0	42.6	52.0	50.1	47.4
143	0	38.9	35.4	50.3	39.0	38.4	45.1	33.5	36.6
143	1	40.7	37.0	60.4	42.5	41.0	58.6	46.0	46.6
143	2	45.6	41.3	69.7	44.9	41.5	63.3	48.5	52.9
143	3	47.5	47.7	67.6	48.5	45.8	69.4	56.3	56.8
143	4	47.0	46.2	63.9	50.9	46.4	61.6	56.5	57.4
143	5	40.6	40.6	43.4	43.9	39.1	51.8	49.0	47.1
144	0	39.0	36.1	51.3	38.7	38.6	44.5	34.3	39.1

Time (h)	Position	Trt1		Trt2		Trt3		Trt4	
		Rep 1	Rep 2	Rep 1	Rep 2	Rep 1	Rep 2	Rep 1	Rep 2
144	1	40.7	38.7	62.3	43.0	40.1	56.2	46.4	48.4
144	2	46.4	42.1	64.6	44.2	42.4	65.1	50.7	53.7
144	3	47.9	45.9	66.5	49.6	46.3	70.3	57.7	55.8
144	4	46.3	43.4	63.0	46.7	46.7	65.8	58.4	57.6
144	5	39.0	38.3	44.6	40.6	41.0	53.2	48.9	45.4
145	0	39.3	35.4	52.1	40.0	37.2	45.2	35.7	36.5
145	1	42.7	39.4	60.7	42.3	39.5	56.2	45.2	48.1
145	2	44.3	41.3	65.5	44.8	42.5	65.0	50.2	53.3
145	3	49.6	46.1	66.5	47.9	46.6	69.3	58.9	56.7
145	4	48.2	46.6	66.2	45.9	46.2	64.0	56.9	55.1
145	5	41.6	39.9	47.7	42.2	42.0	53.5	49.8	49.1
146	0	40.0	36.5	50.2	39.2	37.6	44.3	34.3	38.4
146	1	40.4	38.7	65.9	43.6	42.1	57.1	47.1	47.7
146	2	45.4	40.6	64.8	45.3	42.1	65.3	51.9	53.3
146	3	49.2	46.0	69.2	51.6	46.5	68.2	58.9	56.0
146	4	48.0	48.4	65.0	48.2	49.1	64.7	57.1	56.9
146	5	38.1	41.1	44.1	42.9	43.2	50.8	49.0	46.7
147	0	37.3	36.2	50.4	38.6	38.3	45.8	33.9	38.5
147	1	41.5	37.2	62.4	44.3	40.9	57.2	46.0	48.1
147	2	46.8	42.9	70.0	45.0	43.1	63.0	51.0	53.9
147	3	48.8	49.5	68.3	47.5	46.4	67.7	57.6	55.7
147	4	45.2	45.9	60.8	48.6	47.4	65.4	57.4	58.5
147	5	37.9	39.8	43.8	41.6	42.7	53.2	49.0	46.6
148	0	39.5	37.0	52.5	39.8	37.2	45.3	34.3	38.9
148	1	41.4	39.9	65.0	42.5	40.3	57.6	47.1	48.3
148	2	44.0	40.5	69.0	43.5	43.0	64.2	50.3	54.6
148	3	49.1	48.5	68.2	49.5	45.2	70.7	57.6	54.9
148	4	48.4	45.2	63.8	49.6	46.2	63.5	56.2	57.3
148	5	38.8	39.5	45.8	42.3	41.4	52.5	49.7	46.7
149	0	37.1	36.6	50.1	39.4	39.5	46.8	35.4	36.3
149	1	41.0	37.6	65.4	43.4	43.0	57.0	44.1	47.8
149	2	47.1	41.2	66.8	44.1	43.3	63.5	48.7	54.3
149	3	48.8	46.0	67.3	48.3	42.9	67.3	58.6	55.9
149	4	47.9	46.0	64.2	46.9	45.7	66.1	54.7	58.7
149	5	40.8	40.7	46.3	40.9	42.7	52.8	48.9	47.3

Time (h)	Position	Trt1		Trt2		Trt3		Trt4	
		Rep 1	Rep 2	Rep 1	Rep 2	Rep 1	Rep 2	Rep 1	Rep 2
150	0	40.3	36.7	50.9	38.8	37.0	45.2	35.6	38.3
150	1	40.5	39.2	63.9	43.3	40.8	58.0	46.5	48.7
150	2	44.4	40.9	66.8	45.3	43.2	62.6	50.8	53.1
150	3	48.3	46.6	68.5	48.3	47.2	66.8	58.6	55.3
150	4	47.9	44.8	62.1	50.2	47.0	63.2	57.3	57.3
150	5	38.9	39.3	44.2	41.3	42.7	51.8	47.2	44.9
151	0	37.7	35.1	51.8	37.5	37.3	45.6	35.1	38.0
151	1	42.3	39.2	60.7	41.2	41.2	56.6	46.9	46.9
151	2	46.1	39.9	66.0	44.9	41.6	65.6	51.9	51.4
151	3	46.6	48.2	67.1	49.1	45.9	68.2	56.5	55.8
151	4	46.4	46.5	65.4	50.0	45.5	63.4	54.6	57.1
151	5	39.3	39.7	44.0	39.7	40.8	51.7	47.2	44.8
152	0	37.1	39.8	49.5	39.4	38.1	46.0	34.9	39.1
152	1	42.6	38.9	63.2	42.6	41.0	56.1	44.9	46.7
152	2	48.3	40.9	65.9	45.2	42.3	64.1	50.2	53.0
152	3	48.3	46.9	68.5	50.8	45.3	64.6	54.4	55.9
152	4	47.7	46.9	61.7	50.1	45.6	64.0	53.5	54.0
152	5	39.8	39.3	43.8	42.7	42.3	53.2	47.4	45.0
153	0	37.9	36.4	50.5	40.4	37.2	44.0	36.5	38.8
153	1	42.2	37.1	63.8	42.3	41.6	54.8	45.8	48.0
153	2	47.0	40.4	68.2	43.7	41.9	64.6	51.2	52.0
153	3	49.9	45.9	67.5	51.2	46.1	68.1	55.0	56.0
153	4	47.2	46.9	64.6	46.1	46.2	62.8	55.4	57.8
153	5	38.9	37.6	43.7	43.0	41.6	50.7	47.1	45.6
154	0	37.4	38.0	52.3	39.5	37.6	44.3	34.5	38.1
154	1	42.8	37.5	60.3	43.7	41.9	56.6	45.3	47.0
154	2	46.3	41.4	66.4	44.2	41.7	63.2	50.7	51.7
154	3	47.9	45.4	66.8	51.0	45.4	67.4	56.8	53.9
154	4	48.1	44.1	62.3	46.1	48.7	61.8	53.8	56.0
154	5	39.1	38.5	42.6	40.0	40.2	50.9	47.0	44.2
155	0	37.0	37.7	51.2	39.6	39.4	44.1	35.4	37.9
155	1	41.2	40.7	60.8	41.9	40.3	56.1	44.5	45.9
155	2	44.4	42.4	68.3	44.2	43.2	64.7	50.3	50.2
155	3	49.7	44.8	67.3	49.3	45.0	68.5	56.7	54.5
155	4	46.3	45.3	65.3	44.4	46.8	63.2	54.0	55.5

Time (h)	Position	Trt1		Trt2		Trt3		Trt4	
		Rep 1	Rep 2	Rep 1	Rep 2	Rep 1	Rep 2	Rep 1	Rep 2
155	5	39.0	38.6	43.3	41.1	40.0	51.2	46.0	45.4
156	0	38.6	36.5	50.9	39.9	37.8	44.1	35.8	36.7
156	1	42.9	38.7	62.7	42.3	39.6	56.4	45.6	45.7
156	2	45.6	42.4	66.5	48.8	42.4	64.5	50.1	52.0
156	3	48.7	47.9	69.6	48.5	45.0	66.7	57.5	54.1
156	4	45.6	46.0	61.9	46.5	43.2	65.0	55.3	55.7
156	5	36.8	38.7	42.1	40.4	39.2	49.0	45.8	45.2
157	0	39.6	36.0	49.8	37.6	37.6	43.1	34.5	39.2
157	1	40.5	36.7	63.4	42.5	40.6	55.6	45.5	48.0
157	2	46.0	42.5	69.4	45.7	42.2	63.0	49.3	52.0
157	3	46.5	46.3	68.0	51.1	44.8	67.8	55.6	54.1
157	4	45.1	45.7	62.7	46.6	44.7	61.8	53.7	53.6
157	5	38.5	39.4	44.1	38.8	39.8	48.5	44.5	43.3
158	0	37.2	34.6	50.9	39.4	37.2	44.4	34.0	39.1
158	1	40.8	40.8	62.7	44.8	40.0	55.9	45.6	45.6
158	2	49.2	41.9	68.2	44.4	40.4	62.8	50.0	51.9
158	3	47.7	47.7	67.9	48.2	45.7	66.2	55.4	53.7
158	4	45.2	45.8	62.5	47.5	45.4	60.7	54.0	56.8
158	5	37.9	38.0	43.3	39.4	38.6	51.0	45.4	44.1
159	0	39.5	36.2	50.4	37.9	37.1	44.6	34.0	36.6
159	1	42.3	39.4	63.3	43.8	40.2	55.9	44.5	47.3
159	2	44.0	43.8	65.6	46.1	40.8	61.1	49.9	50.5
159	3	50.3	47.5	69.5	49.3	46.1	68.4	54.4	54.8
159	4	43.0	44.4	63.3	46.7	42.2	59.1	53.5	54.9
159	5	34.9	38.2	41.8	37.8	37.1	48.2	43.2	42.0
160	0	38.7	35.6	50.2	38.7	38.4	43.1	34.0	36.2
160	1	41.6	39.5	65.1	44.8	41.0	56.3	45.2	47.4
160	2	46.4	40.6	66.8	46.6	42.6	63.1	49.8	52.8
160	3	50.3	47.3	68.5	51.3	45.1	68.3	57.1	54.0
160	4	47.1	46.6	63.2	47.7	43.2	62.1	54.2	53.1
160	5	35.9	35.5	42.1	39.7	37.3	50.9	45.2	43.8
161	0	38.1	35.5	50.6	39.5	37.0	42.1	33.6	36.1
161	1	41.4	39.7	65.3	45.0	40.1	54.8	45.4	46.8
161	2	44.6	41.3	66.3	45.0	42.2	62.8	48.6	52.8
161	3	51.2	46.3	69.8	49.2	45.4	68.1	54.5	53.7

Time (h)	Position	Trt1		Trt2		Trt3		Trt4	
		Rep 1	Rep 2	Rep 1	Rep 2	Rep 1	Rep 2	Rep 1	Rep 2
161	4	41.9	43.7	61.9	47.3	46.3	60.2	52.3	53.1
161	5	36.5	36.7	43.1	38.8	37.9	50.8	44.4	43.1
162	0	38.9	36.6	52.5	40.3	38.7	43.7	35.3	37.7
162	1	42.5	40.7	61.6	45.9	39.8	56.3	44.4	46.0
162	2	46.8	43.4	67.0	47.0	42.1	63.1	50.0	53.2
162	3	47.3	47.1	68.2	50.2	44.6	67.7	55.1	54.2
162	4	47.7	42.9	62.1	44.9	43.8	60.9	51.6	52.0
162	5	35.8	37.4	44.4	40.1	36.0	51.0	44.1	41.5
163	0	37.2	37.7	48.6	39.5	36.9	43.8	34.4	38.5
163	1	42.6	38.9	62.3	45.0	41.3	54.8	45.4	45.9
163	2	45.8	41.7	67.7	45.3	41.8	62.9	50.4	52.7
163	3	46.6	51.0	68.1	47.1	44.7	67.7	54.0	54.4
163	4	43.6	42.2	59.8	44.1	43.2	60.8	53.0	55.1
163	5	38.0	37.3	44.1	39.0	38.2	49.8	46.1	42.0
164	0	36.6	36.9	49.7	37.1	35.9	42.9	35.6	38.5
164	1	42.3	38.5	64.2	42.3	40.3	54.7	45.6	46.9
164	2	43.6	42.4	67.2	44.3	41.3	62.6	47.9	50.6
164	3	47.1	45.9	67.9	47.8	45.7	67.8	54.2	53.6
164	4	46.0	45.2	58.6	46.6	42.9	61.5	53.6	54.8
164	5	36.8	38.7	43.0	37.4	37.4	50.3	44.6	43.1
165	0	39.0	36.6	51.7	40.4	38.2	42.9	36.2	37.5
165	1	41.8	38.8	63.7	43.7	40.4	54.4	45.9	47.0
165	2	47.9	43.1	66.3	45.5	41.3	62.3	49.7	51.2
165	3	49.3	44.7	67.2	49.1	44.9	68.6	53.5	52.3
165	4	44.8	47.4	62.5	45.4	45.1	60.6	52.6	53.8
165	5	40.5	38.0	43.7	37.7	39.0	51.0	42.9	42.6
166	0	39.2	36.1	49.1	39.5	36.6	43.5	35.2	37.9
166	1	43.4	40.8	61.8	41.4	38.6	56.3	43.6	46.8
166	2	44.6	43.1	65.1	47.3	40.0	63.2	49.3	50.0
166	3	48.7	44.1	69.4	47.4	45.5	67.7	55.4	54.6
166	4	45.4	44.0	62.1	47.9	45.8	59.5	51.3	52.2
166	5	39.8	39.5	45.8	39.6	38.5	49.3	43.8	42.5
167	0	38.1	38.8	49.9	38.5	37.4	42.9	35.5	37.4
167	1	41.9	40.1	61.5	42.8	41.0	54.8	45.4	46.4
167	2	44.7	41.7	67.9	42.7	42.6	63.1	48.6	52.3

Time (h)	Position	Trt1		Trt2		Trt3		Trt4	
		Rep 1	Rep 2	Rep 1	Rep 2	Rep 1	Rep 2	Rep 1	Rep 2
167	3	48.0	46.4	69.2	48.6	44.4	67.6	55.0	54.2
167	4	46.0	44.4	61.9	44.2	44.5	60.3	53.2	52.8
167	5	38.7	39.0	43.9	42.0	40.0	50.8	43.1	42.0
168	0	38.1	38.0	51.2	38.3	36.2	43.7	35.2	38.5
168	1	39.2	40.2	63.4	41.5	41.3	54.7	45.6	47.8
168	2	47.5	44.9	65.2	44.8	42.7	59.0	48.1	50.0
168	3	47.6	45.9	69.7	46.8	45.8	66.8	52.6	52.1
168	4	45.2	45.7	60.4	46.1	44.0	59.7	49.9	54.7
168	5	39.1	39.7	44.7	40.9	39.8	50.5	43.7	44.3
169	0	37.9	37.9	50.4	38.2	36.3	43.2	35.5	38.2
169	1	41.3	39.4	58.9	41.7	40.0	55.1	45.9	48.6
169	2	46.2	41.9	66.6	44.2	42.5	61.7	50.8	51.7
169	3	49.3	46.6	70.2	47.3	45.3	69.0	56.1	53.5
169	4	45.1	45.7	63.3	46.0	43.6	60.6	51.7	55.0
169	5	39.1	39.5	43.6	40.0	40.5	50.8	45.3	43.6
170	0	36.7	36.8	51.3	39.2	36.5	43.7	37.3	39.1
170	1	43.6	39.0	61.4	42.3	40.3	53.9	46.9	47.5
170	2	47.5	42.2	68.5	46.4	41.0	62.8	49.2	50.7
170	3	47.7	47.0	68.8	50.1	43.1	67.0	53.8	52.6
170	4	47.4	45.4	61.1	45.2	45.7	60.4	50.7	54.0
170	5	40.9	39.8	45.7	41.6	41.6	51.4	44.5	44.0
171	0	37.3	35.4	49.7	39.0	36.1	42.8	37.5	39.1
171	1	40.9	40.4	63.0	43.4	41.5	55.4	45.3	46.8
171	2	45.3	42.0	67.5	45.4	42.5	63.0	49.9	51.7
171	3	50.5	46.7	70.3	47.7	45.2	66.8	55.4	52.6
171	4	44.9	43.9	60.9	46.4	45.7	58.8	51.1	54.5
171	5	39.0	40.4	44.7	40.5	39.9	48.9	44.4	43.8
172	0	38.1	36.5	48.0	38.7	38.4	45.0	37.4	40.2
172	1	43.1	40.7	61.4	43.5	39.2	57.1	48.3	46.3
172	2	47.0	41.8	67.9	43.8	41.9	64.2	50.9	50.6
172	3	49.0	44.6	69.7	49.1	45.5	66.7	55.2	52.2
172	4	46.4	44.1	62.8	46.4	45.1	61.4	50.1	52.9
172	5	39.2	38.9	45.1	42.4	41.3	50.5	45.1	43.8
173	0	37.0	38.0	52.2	37.9	37.2	44.3	37.2	39.9
173	1	42.1	38.1	64.2	42.9	41.7	55.4	46.7	48.2

Time (h)	Position	Trt1		Trt2		Trt3		Trt4	
		Rep 1	Rep 2	Rep 1	Rep 2	Rep 1	Rep 2	Rep 1	Rep 2
173	2	45.6	41.7	64.9	44.7	41.3	62.6	49.5	49.8
173	3	47.7	45.9	66.7	50.1	45.6	67.5	54.3	52.8
173	4	47.4	46.6	63.0	45.8	46.3	61.1	53.0	51.0
173	5	37.8	39.3	43.8	42.0	39.7	49.9	44.0	42.2
174	0	38.7	35.8	49.9	39.1	37.0	43.6	37.2	39.5
174	1	42.5	39.2	61.9	41.6	38.8	55.2	49.5	48.2
174	2	48.1	42.6	66.0	45.4	41.6	60.8	47.9	52.1
174	3	50.1	46.2	67.2	48.1	45.6	67.8	54.3	52.3
174	4	48.9	44.3	62.0	46.4	45.3	60.5	50.6	52.2
174	5	38.3	38.2	45.6	39.0	39.1	48.2	44.5	42.7
175	0	39.6	36.4	50.1	38.6	36.5	42.6	37.8	40.1
175	1	43.3	39.5	63.4	41.3	39.0	54.5	46.9	47.4
175	2	46.8	43.1	66.0	45.1	40.7	63.0	50.5	52.0
175	3	48.3	47.8	67.9	47.0	45.3	66.8	54.5	52.2
175	4	45.6	43.0	60.1	46.3	45.8	60.6	50.2	54.0
175	5	38.6	39.1	44.9	40.8	40.0	49.5	42.1	41.7
176	0	36.6	34.1	50.3	39.2	36.4	43.0	36.7	41.8
176	1	41.8	39.4	65.1	42.9	40.7	54.7	48.2	47.9
176	2	46.6	41.9	68.2	44.5	41.8	62.2	49.4	52.4
176	3	48.1	46.6	65.0	47.2	44.4	63.7	55.5	53.6
176	4	46.1	43.5	58.7	48.1	45.2	61.7	49.7	51.0
176	5	37.9	39.7	44.2	38.8	39.5	50.1	43.6	43.0
178	0	39.0	37.1	50.6	38.2	37.7	42.6	39.0	39.5
178	1	42.6	39.6	61.8	42.1	39.6	55.7	49.3	47.7
178	2	44.9	41.2	65.2	44.1	41.4	63.9	49.8	52.9
178	3	48.9	45.0	65.9	47.3	44.4	66.8	54.3	51.7
178	4	43.5	44.7	63.8	43.9	44.1	61.1	50.0	52.8
178	5	38.8	36.9	44.4	38.5	39.2	49.1	43.8	41.7
180	0	39.2	37.2	48.3	37.6	36.4	41.6	37.6	39.2
180	1	41.1	38.7	59.1	41.6	41.1	52.7	49.1	46.6
180	2	46.0	41.0	64.2	45.6	41.8	62.4	50.7	54.6
180	3	47.8	45.1	66.3	48.4	43.2	65.1	54.1	53.8
180	4	46.3	44.2	62.9	46.7	41.7	60.6	50.8	53.1
180	5	36.1	36.5	43.1	36.3	38.2	47.5	42.5	42.6
182	0	39.3	38.1	48.1	38.6	37.3	42.9	37.2	38.4

Time (h)	Position	Trt1		Trt2		Trt3		Trt4	
		Rep 1	Rep 2	Rep 1	Rep 2	Rep 1	Rep 2	Rep 1	Rep 2
182	1	42.4	39.0	61.6	45.2	40.5	53.4	49.7	50.0
182	2	46.8	42.1	65.4	43.5	41.4	61.0	50.7	51.6
182	3	50.3	46.1	68.3	45.7	45.4	65.9	56.6	53.5
182	4	44.8	45.9	58.6	44.7	45.4	59.7	49.9	53.4
182	5	35.4	38.1	42.2	37.8	36.2	48.6	41.5	40.7
184	0	38.2	37.1	48.0	39.6	38.1	40.3	38.4	39.1
184	1	44.6	39.0	63.4	42.6	40.7	53.3	47.9	47.6
184	2	44.9	41.7	63.6	44.6	39.8	60.5	50.6	51.8
184	3	48.9	48.6	68.7	47.5	44.5	66.7	54.1	52.3
184	4	44.6	41.0	59.2	44.6	41.3	58.6	51.5	51.4
184	5	35.8	35.0	42.1	35.2	36.2	47.4	41.2	40.0
186	0	38.7	36.6	49.2	39.7	36.6	41.5	38.1	39.4
186	1	44.4	38.6	63.9	43.8	41.9	52.3	47.6	48.0
186	2	46.1	43.7	65.6	47.7	42.3	60.6	51.1	52.1
186	3	45.5	44.6	65.1	48.4	43.7	65.2	54.8	54.3
186	4	42.8	43.3	59.1	44.1	41.5	60.6	51.2	51.7
186	5	34.5	37.0	42.0	37.4	35.8	47.5	40.2	41.5
188	0	36.0	38.0	48.4	40.1	35.9	39.3	38.6	39.6
188	1	42.0	40.7	62.4	42.5	40.1	55.0	49.4	47.1
188	2	46.4	39.6	63.8	45.1	41.2	61.8	51.6	51.2
188	3	46.3	44.6	68.1	49.9	43.6	64.5	55.2	52.8
188	4	46.2	42.0	60.0	43.1	42.3	58.4	48.6	49.7
188	5	36.2	37.9	43.3	37.9	36.8	48.0	43.0	40.9
190	0	37.9	38.1	47.7	39.8	34.8	42.2	40.1	39.9
190	1	40.3	41.8	62.5	46.9	40.2	51.6	49.3	48.4
190	2	43.4	40.3	64.4	46.1	40.7	60.4	50.4	50.5
190	3	47.7	44.5	66.4	47.3	43.4	63.6	55.9	53.8
190	4	43.2	41.7	59.5	42.6	43.8	57.8	52.2	51.0
190	5	36.4	37.3	41.9	39.5	37.7	49.4	42.4	41.6
192	0	38.6	36.9	48.6	40.5	35.5	42.1	41.4	41.9
192	1	42.2	41.4	63.8	44.7	37.7	52.6	49.0	47.4
192	2	48.0	42.5	64.4	46.7	39.4	60.9	51.4	51.4
192	3	47.4	45.6	70.2	48.4	43.8	64.6	54.6	51.9
192	4	43.9	43.2	59.5	44.1	43.5	57.3	52.5	51.9
192	5	36.6	40.4	44.8	35.7	38.3	50.3	43.4	42.3

Time (h)	Position	Trt1		Trt2		Trt3		Trt4	
		Rep 1	Rep 2	Rep 1	Rep 2	Rep 1	Rep 2	Rep 1	Rep 2
194	0	38.1	37.1	47.9	40.8	36.4	40.6	40.4	40.5
194	1	40.7	41.2	63.3	45.5	39.7	52.5	51.3	48.1
194	2	48.6	40.9	64.3	46.5	41.3	59.3	51.6	52.0
194	3	47.2	46.3	66.7	48.3	43.1	63.9	56.2	52.4
194	4	44.5	41.1	59.7	43.3	44.0	61.4	51.7	52.8
194	5	39.5	38.9	43.6	40.1	39.6	50.0	44.6	41.8
196	0	37.2	38.4	47.9	41.1	36.8	40.9	41.5	42.6
196	1	42.7	37.0	59.2	49.2	41.2	51.6	51.7	48.6
196	2	46.3	40.1	65.7	47.6	41.4	60.4	52.3	51.5
196	3	47.0	46.6	64.8	46.4	45.2	65.4	57.1	53.8
196	4	43.8	42.6	58.0	45.2	43.2	60.8	50.1	51.5
196	5	37.3	36.8	45.8	36.7	37.9	47.7	44.2	42.5
198	0	41.5	36.8	48.9	41.5	37.1	41.4	42.0	43.3
198	1	43.9	39.1	62.6	46.7	40.1	52.1	49.5	50.2
198	2	45.3	42.4	67.1	47.7	42.4	58.0	53.2	52.3
198	3	47.8	45.7	65.8	49.1	44.8	65.5	57.9	53.2
198	4	44.5	42.9	58.4	44.5	45.1	58.2	52.2	49.1
198	5	37.4	36.4	41.0	36.8	38.1	47.1	44.4	41.3
200	0	38.0	38.6	47.8	41.5	37.5	41.7	40.6	42.5
200	1	44.7	39.2	61.1	48.4	39.1	53.1	51.2	49.3
200	2	47.0	40.8	66.6	46.9	41.1	61.0	53.7	54.0
200	3	47.9	47.7	64.2	48.5	44.9	63.8	58.0	51.6
200	4	45.8	43.0	60.0	45.3	43.5	57.5	51.8	51.8
200	5	37.6	37.4	43.7	37.7	39.3	45.8	43.4	41.2
202	0	37.7	37.0	49.2	44.7	35.0	41.5	40.9	43.3
202	1	42.4	40.2	62.7	49.4	39.6	52.8	49.8	48.1
202	2	46.0	40.5	65.3	49.2	41.3	60.3	52.4	51.9
202	3	46.2	44.9	63.2	50.0	43.7	61.7	57.2	52.2
202	4	42.9	45.1	55.9	47.8	42.8	58.2	51.0	49.6
202	5	37.0	36.1	43.2	38.4	38.3	47.5	44.1	41.3
204	0	38.9	37.1	45.7	42.6	36.1	40.4	39.9	41.6
204	1	43.2	38.4	59.7	48.9	40.2	51.2	49.5	48.7
204	2	45.8	40.6	64.2	49.4	40.7	57.8	53.6	52.3
204	3	48.0	47.0	67.6	50.9	43.7	64.2	55.2	52.5
204	4	42.7	41.6	57.4	45.6	40.7	57.7	52.0	51.3

Time (h)	Position	Trt1		Trt2		Trt3		Trt4	
		Rep 1	Rep 2	Rep 1	Rep 2	Rep 1	Rep 2	Rep 1	Rep 2
204	5	37.3	35.7	41.8	37.3	36.5	46.7	45.1	39.9
206	0	38.5	37.6	47.0	44.9	35.9	42.1	40.2	43.4
206	1	41.2	39.6	62.0	50.3	40.5	53.4	50.9	48.9
206	2	45.6	42.2	66.6	48.0	40.2	59.4	54.0	52.7
206	3	46.5	44.4	66.5	50.3	44.8	65.6	56.1	53.6
206	4	42.5	41.5	56.3	43.1	43.6	56.8	52.2	50.1
206	5	34.6	33.4	42.1	35.8	36.4	45.7	42.8	39.6
208	0	38.7	36.5	47.6	46.3	36.6	41.0	38.3	41.4
208	1	42.5	39.8	58.3	51.3	39.5	52.0	49.8	51.3
208	2	46.7	43.1	64.4	52.0	41.1	58.7	54.4	53.2
208	3	46.3	45.8	65.7	50.4	43.0	62.3	58.1	52.5
208	4	42.3	42.4	57.1	44.0	42.8	56.4	53.1	50.7
208	5	35.4	34.6	40.6	34.7	36.9	46.2	42.9	38.5
210	0	35.9	38.4	48.1	45.6	37.4	40.1	38.3	41.5
210	1	43.8	42.6	60.4	51.7	40.5	53.9	48.3	50.5
210	2	46.7	45.0	63.7	53.3	41.2	58.8	54.0	53.8
210	3	49.4	44.7	64.5	51.9	42.1	60.7	54.8	53.8
210	4	42.4	40.2	56.1	44.5	42.0	54.8	52.8	51.5
210	5	34.0	35.4	41.3	36.9	34.0	46.5	44.8	40.1
212	0	37.2	36.2	46.3	44.5	36.5	40.3	38.0	42.1
212	1	45.8	39.1	59.1	51.9	40.5	52.0	48.5	49.2
212	2	46.1	41.6	63.8	50.0	39.4	56.2	54.1	53.6
212	3	47.0	46.5	65.6	50.5	42.8	63.5	56.6	52.0
212	4	44.3	41.9	55.4	45.1	42.6	56.3	54.5	50.2
212	5	34.7	36.2	41.4	38.2	35.6	44.8	43.1	39.8
214	0	37.2	38.3	47.0	43.9	35.4	38.2	38.0	42.5
214	1	42.5	38.8	63.6	52.4	38.7	50.5	49.9	51.2
214	2	45.6	42.9	63.8	52.5	41.7	57.0	52.8	54.6
214	3	46.4	44.8	62.1	51.3	42.7	60.5	55.9	53.8
214	4	42.9	42.0	55.9	44.4	41.4	55.8	51.6	51.9
214	5	35.4	36.1	41.4	39.2	37.0	47.4	43.1	41.3
216	0	37.0	39.0	47.5	44.7	35.2	40.0	39.3	42.0
216	1	42.8	42.3	60.6	53.7	37.4	48.9	48.9	50.0
216	2	43.6	42.9	63.2	53.5	40.1	54.9	51.6	52.5
216	3	46.6	45.8	65.2	49.7	43.4	62.5	56.9	52.4

Time (h)	Position	Trt1		Trt2		Trt3		Trt4	
		Rep 1	Rep 2	Rep 1	Rep 2	Rep 1	Rep 2	Rep 1	Rep 2
216	4	44.4	43.9	56.5	45.7	42.9	54.5	51.1	51.3
216	5	36.9	34.5	39.9	37.9	37.8	47.5	44.1	41.9
218	0	37.5	39.1	45.8	44.6	36.4	38.1	39.4	39.5
218	1	42.2	39.2	59.4	53.7	39.3	47.7	46.9	48.8
218	2	44.4	42.3	62.9	54.9	41.0	56.2	51.7	51.5
218	3	48.2	45.8	64.7	51.8	43.9	59.9	56.6	53.2
218	4	41.5	42.0	53.1	44.6	43.4	56.6	53.4	50.8
218	5	36.8	37.1	41.7	39.7	39.0	46.8	44.9	40.0
220	0	38.3	37.0	47.2	45.8	34.8	38.4	38.0	42.8
220	1	43.5	39.4	60.1	55.7	40.0	50.1	47.5	52.2
220	2	42.3	43.6	62.8	53.5	40.7	58.0	53.2	53.4
220	3	45.9	46.8	64.0	52.7	43.2	60.8	57.4	52.1
220	4	41.8	40.3	56.5	44.0	42.9	53.2	52.5	50.9
220	5	36.2	36.1	41.1	38.8	37.4	47.2	43.2	39.8
222	0	37.7	38.0	47.5	43.4	36.9	39.3	38.7	41.8
222	1	43.1	38.7	61.5	53.2	39.6	50.0	48.3	50.1
222	2	43.7	41.4	62.5	54.4	41.7	57.9	51.6	52.7
222	3	46.4	44.9	65.8	54.5	42.8	60.6	56.5	54.1
222	4	43.2	42.2	55.2	45.9	43.7	54.6	52.4	49.8
222	5	35.9	36.0	40.8	40.1	37.5	45.7	44.7	41.2
224	0	37.5	39.0	49.0	45.3	36.3	39.6	38.7	41.2
224	1	42.3	39.9	56.5	51.9	39.8	50.1	48.9	50.7
224	2	45.2	43.1	63.3	57.1	42.3	55.2	52.4	52.3
224	3	45.8	46.8	63.8	51.3	43.7	60.7	55.7	52.9
224	4	41.8	41.6	52.9	45.9	42.7	53.3	50.0	49.9
224	5	36.0	36.8	41.1	38.9	38.2	45.2	43.0	40.7
226	0	39.4	38.5	46.9	48.2	35.4	40.1	37.8	42.2
226	1	43.7	40.0	58.2	54.6	39.1	50.0	48.6	50.5
226	2	44.6	45.0	60.5	54.0	40.9	56.8	51.4	53.1
226	3	47.1	44.9	63.2	51.8	42.6	58.9	54.2	50.7
226	4	42.5	39.5	53.9	43.2	43.3	51.9	49.8	49.5
226	5	35.5	34.3	41.7	39.7	37.0	44.8	42.2	38.9
228	0	38.9	37.5	47.4	46.7	35.8	38.5	38.1	41.3
228	1	41.3	40.0	61.6	55.2	39.0	47.5	49.2	50.8
228	2	44.0	42.0	63.2	54.2	40.5	57.7	49.6	52.4

Time (h)	Position	Trt1		Trt2		Trt3		Trt4	
		Rep 1	Rep 2	Rep 1	Rep 2	Rep 1	Rep 2	Rep 1	Rep 2
228	3	44.9	46.3	61.7	55.7	44.8	58.6	56.0	51.9
228	4	42.3	41.1	53.1	46.6	42.7	53.3	51.5	47.0
228	5	33.7	35.4	41.3	39.8	37.3	44.0	41.9	38.4
230	0	39.0	38.5	47.5	48.3	36.3	38.7	37.4	38.9
230	1	43.3	41.6	60.4	58.1	40.3	49.9	48.0	50.4
230	2	46.4	42.3	62.5	56.0	41.8	56.6	52.3	52.5
230	3	45.3	44.5	63.8	54.7	42.5	58.3	55.2	51.3
230	4	40.0	41.2	52.8	47.5	41.6	52.2	51.4	48.4
230	5	32.8	34.1	40.3	38.4	35.3	41.8	42.3	39.8
232	0	37.4	35.7	44.3	44.5	35.4	37.0	34.8	38.7
232	1	41.2	41.5	58.8	52.7	40.1	47.9	46.9	49.1
232	2	43.2	41.9	64.3	57.8	40.4	54.2	51.1	52.1
232	3	44.7	47.2	62.5	55.3	44.2	58.6	53.4	51.0
232	4	40.3	40.5	54.9	48.2	42.5	49.9	49.4	47.1
232	5	32.4	34.5	40.2	35.2	34.4	40.2	39.3	37.4
234	0	37.8	38.4	45.2	48.4	35.8	39.3	35.1	39.5
234	1	42.5	40.2	58.3	57.1	40.9	49.1	46.5	48.3
234	2	42.8	42.7	62.1	55.7	39.4	55.1	50.7	51.5
234	3	47.9	43.7	61.6	55.4	43.2	57.9	54.1	49.8
234	4	38.8	40.4	53.5	46.0	41.5	48.8	47.5	47.9
234	5	31.7	33.0	38.3	36.6	34.7	40.1	40.3	37.4
236	0	37.7	36.7	45.2	49.4	34.7	38.2	35.8	39.3
236	1	42.6	41.3	60.6	61.3	39.2	48.9	46.5	49.9
236	2	44.2	43.4	62.9	58.6	39.5	55.0	47.1	51.1
236	3	45.8	46.5	62.0	54.4	42.5	56.4	52.8	51.3
236	4	42.3	39.2	53.5	46.5	38.9	50.6	48.4	47.0
236	5	33.2	33.6	38.6	38.1	33.6	41.4	39.3	37.2
238	0	37.7	37.7	44.7	48.0	34.5	39.2	34.7	39.4
238	1	40.7	41.7	58.9	54.9	39.0	48.2	46.3	49.6
238	2	43.4	43.9	60.2	58.2	40.0	53.4	50.4	50.8
238	3	46.8	46.2	62.9	55.6	42.6	57.2	52.6	50.4
238	4	40.9	40.8	53.2	47.4	41.7	49.1	49.8	46.5
238	5	34.2	35.4	40.7	38.5	34.4	41.9	41.0	38.9
240	0	36.7	37.2	45.4	45.0	32.3	39.0	35.2	40.1
240	1	42.7	39.4	60.8	60.0	38.7	47.2	46.2	47.9

Time (h)	Position	Trt1		Trt2		Trt3		Trt4	
		Rep 1	Rep 2	Rep 1	Rep 2	Rep 1	Rep 2	Rep 1	Rep 2
240	2	45.5	40.7	65.1	59.5	40.4	56.1	49.0	50.2
240	3	43.2	44.2	63.1	55.5	42.3	57.9	52.4	50.3
240	4	43.1	38.9	52.5	48.6	40.7	48.9	47.8	45.6
240	5	35.5	34.7	43.1	40.4	36.0	41.9	40.1	39.0
242	0	37.9	38.7	45.7	50.0	35.4	38.7	35.4	39.1
242	1	40.2	40.2	59.7	57.6	39.3	47.9	45.6	47.3
242	2	44.7	41.5	61.2	59.0	40.1	54.9	49.7	52.3
242	3	46.6	44.1	66.5	55.7	44.2	56.3	49.9	48.1
242	4	40.8	42.9	55.0	49.8	41.8	50.2	46.9	46.4
242	5	35.0	35.3	39.8	38.6	34.6	41.5	38.1	37.3
244	0	38.9	38.5	46.8	48.9	35.5	40.7	36.0	40.0
244	1	42.8	41.7	60.4	59.0	37.8	49.6	46.4	47.0
244	2	43.4	43.6	61.7	59.5	40.7	55.0	48.4	50.3
244	3	47.1	42.8	63.0	58.1	44.9	54.5	51.7	48.6
244	4	40.2	39.8	54.5	52.1	41.9	47.3	46.0	46.1
244	5	35.5	35.4	42.9	43.1	36.7	41.1	39.7	38.9
246	0	37.9	39.6	47.5	46.4	35.9	40.8	35.2	41.1
246	1	40.4	40.6	58.8	57.0	37.5	48.3	46.6	47.5
246	2	46.0	43.9	60.7	59.3	40.2	54.0	48.2	50.4
246	3	45.5	44.4	63.6	58.4	41.8	56.3	51.5	48.5
246	4	40.9	42.1	55.2	49.3	42.4	47.5	46.9	44.9
246	5	34.4	35.0	41.0	40.6	35.7	42.1	40.5	38.8
248	0	36.7	38.2	46.5	46.5	34.2	40.8	36.7	41.3
248	1	41.7	42.2	60.1	56.6	38.5	48.2	45.7	48.9
248	2	44.4	42.1	59.4	60.5	39.8	53.7	48.5	49.3
248	3	44.8	43.4	64.7	59.6	43.4	57.2	51.0	49.7
248	4	41.9	41.0	53.8	51.4	41.8	48.8	45.5	46.3
248	5	35.5	35.3	39.7	42.0	36.4	39.9	38.7	37.2
250	0	35.9	40.4	46.7	47.8	35.0	41.3	35.9	40.1
250	1	40.8	41.4	57.3	58.4	37.3	48.5	46.5	49.5
250	2	44.0	42.8	64.1	60.8	39.8	53.6	48.3	49.3
250	3	45.4	42.8	62.5	59.0	41.8	55.6	49.9	47.2
250	4	41.3	42.9	52.5	49.3	43.2	47.4	45.6	45.5
250	5	36.1	34.7	40.9	41.8	34.8	40.4	38.5	37.5
252	0	35.6	38.0	45.6	47.1	35.5	40.2	36.8	38.8

Time (h)	Position	Trt1		Trt2		Trt3		Trt4	
		Rep 1	Rep 2	Rep 1	Rep 2	Rep 1	Rep 2	Rep 1	Rep 2
252	1	42.4	42.5	58.6	58.6	37.3	47.9	47.2	47.8
252	2	44.4	41.5	61.3	59.9	39.6	53.8	46.7	50.0
252	3	46.3	44.5	63.9	58.8	42.4	57.0	51.0	49.5
252	4	40.9	40.5	54.4	51.1	39.6	46.8	44.6	45.2
252	5	35.9	34.0	40.1	41.9	37.5	39.3	38.2	35.9
254	0	38.1	39.9	45.4	49.0	35.3	39.2	35.9	39.8
254	1	42.0	42.6	57.7	56.5	40.5	49.2	44.7	48.5
254	2	45.9	43.4	59.0	59.3	39.6	54.0	48.2	50.9
254	3	43.7	46.4	62.2	59.8	42.5	53.2	48.7	47.6
254	4	39.7	42.1	52.0	52.9	42.5	48.9	45.0	43.7
254	5	34.7	34.8	37.9	39.4	36.2	38.5	36.0	37.3
256	0	36.2	38.7	45.8	47.1	34.5	39.0	34.5	38.3
256	1	42.4	43.3	59.7	60.6	37.9	48.1	45.1	47.0
256	2	42.5	43.9	60.2	60.2	40.8	53.9	47.1	48.9
256	3	45.9	42.5	60.6	58.0	42.9	54.3	48.4	46.8
256	4	42.1	40.1	51.8	52.9	39.8	47.1	43.4	44.2
256	5	33.3	34.7	39.7	38.5	35.6	39.0	37.6	35.8
258	0	36.7	36.5	44.0	49.2	34.6	40.3	33.9	38.9
258	1	41.1	42.1	60.3	60.2	38.8	50.5	45.2	48.5
258	2	44.7	44.9	59.1	64.0	39.8	53.2	48.6	50.1
258	3	44.5	43.8	60.3	62.3	42.7	53.2	48.4	46.3
258	4	38.7	39.8	53.5	49.0	40.5	44.5	44.1	44.9
258	5	33.5	32.6	38.7	39.2	33.5	38.4	37.6	35.9
260	0	36.5	37.0	43.7	47.7	34.6	39.2	35.9	39.9
260	1	41.9	45.0	58.0	58.7	37.9	48.1	45.0	46.8
260	2	43.6	46.2	60.7	61.6	39.2	51.8	46.4	47.8
260	3	46.5	43.4	60.1	61.8	43.6	53.6	48.7	47.1
260	4	39.0	39.9	50.7	50.9	39.8	44.9	43.1	45.0
260	5	33.2	34.7	40.4	41.5	33.9	37.7	35.9	36.0
262	0	36.4	40.0	42.9	49.1	35.0	40.5	34.5	39.2
262	1	41.5	43.2	59.4	60.5	39.3	50.4	44.9	47.4
262	2	45.1	41.4	61.2	62.3	40.9	52.4	47.1	48.9
262	3	43.1	43.3	61.5	57.3	42.9	54.5	49.6	47.4
262	4	41.7	40.7	49.6	48.4	38.6	43.4	43.3	43.6
262	5	36.6	32.8	39.4	39.5	35.6	37.9	37.2	35.5

Time (h)	Position	Trt1		Trt2		Trt3		Trt4	
		Rep 1	Rep 2	Rep 1	Rep 2	Rep 1	Rep 2	Rep 1	Rep 2
264	0	36.1	39.3	45.8	47.1	34.8	40.2	36.1	40.5
264	1	41.9	41.9	60.6	61.6	38.3	49.9	44.5	48.2
264	2	41.9	44.1	60.0	65.0	39.0	53.2	46.8	48.7
264	3	45.7	43.7	61.4	58.9	43.3	52.4	49.6	49.4
264	4	42.1	39.2	52.6	49.1	42.0	45.5	42.1	43.2
264	5	37.2	35.6	38.9	43.3	35.0	37.9	37.1	36.3
266	0	39.4	38.5	45.0	48.5	34.9	42.8	37.3	40.0
266	1	41.3	43.1	56.9	60.3	37.4	50.2	46.1	48.0
266	2	42.7	43.6	62.3	60.6	40.2	53.4	47.1	47.0
266	3	44.2	44.7	61.4	59.0	43.3	54.0	46.5	46.7
266	4	41.7	40.8	51.7	50.9	42.7	44.9	43.4	43.9
266	5	34.8	34.7	38.0	41.1	36.2	38.6	37.7	38.1
268	0	34.6	39.9	48.0	48.8	35.0	40.5	35.9	40.5
268	1	42.0	42.6	61.8	59.9	37.6	49.7	44.7	47.4
268	2	44.0	43.9	61.2	61.7	39.5	53.2	46.9	49.9
268	3	46.0	46.0	61.7	59.2	42.8	53.0	47.1	46.7
268	4	40.0	41.7	54.1	53.1	40.8	45.7	42.6	43.1
268	5	34.4	34.8	39.9	41.8	36.5	37.8	37.4	37.1
270	0	35.4	39.8	45.5	45.9	35.4	40.5	36.8	41.7
270	1	40.1	45.1	56.8	56.3	37.9	49.9	45.7	46.6
270	2	43.1	42.8	58.6	62.7	40.0	53.2	45.0	48.1
270	3	45.2	44.4	63.0	62.6	44.0	53.9	47.9	46.1
270	4	42.7	40.4	53.8	52.9	40.0	45.4	42.4	43.9
270	5	34.8	35.9	40.1	40.7	35.5	39.0	36.3	37.3
272	0	36.1	38.0	44.3	48.4	33.3	41.5	35.8	40.9
272	1	39.2	42.2	59.9	61.0	39.3	51.2	46.8	48.5
272	2	40.3	44.8	60.6	61.3	40.4	50.8	46.4	49.3
272	3	45.7	44.9	61.7	62.8	43.8	52.1	47.7	45.9
272	4	40.5	40.0	54.8	52.8	41.4	44.9	41.6	42.3
272	5	32.5	34.4	38.5	44.1	36.2	37.9	37.3	34.9
274	0	35.1	36.7	44.9	48.3	33.8	41.2	36.8	40.2
274	1	41.1	41.3	55.8	59.0	38.7	49.3	44.4	48.6
274	2	43.5	45.0	62.8	60.5	38.3	51.4	45.3	48.7
274	3	45.7	43.7	60.2	62.2	44.0	52.7	46.3	47.0
274	4	40.4	38.7	54.2	53.1	40.6	45.7	42.6	42.9

Time (h)	Position	Trt1		Trt2		Trt3		Trt4	
		Rep 1	Rep 2	Rep 1	Rep 2	Rep 1	Rep 2	Rep 1	Rep 2
274	5	32.8	35.4	39.1	41.3	35.0	36.7	36.6	35.2
276	0	36.9	36.3	45.9	46.5	33.8	42.1	36.2	41.0
276	1	41.8	43.5	58.4	59.0	38.3	49.4	46.8	47.0
276	2	43.1	44.5	59.7	63.1	39.8	53.0	45.8	48.0
276	3	43.4	43.2	60.9	63.5	42.6	51.8	45.3	46.1
276	4	40.7	40.1	52.8	49.8	42.0	44.6	42.0	41.6
276	5	35.4	32.2	38.0	42.2	36.1	38.1	36.2	34.7
278	0	37.3	37.5	47.4	49.8	33.9	41.9	37.0	40.7
278	1	41.3	43.0	58.4	58.9	36.9	50.2	45.8	47.7
278	2	43.7	44.4	61.8	62.8	39.0	52.4	47.3	49.3
278	3	43.1	45.3	60.6	62.4	42.9	51.9	45.8	45.5
278	4	38.0	40.4	53.7	50.1	41.0	43.5	41.1	41.7
278	5	33.8	32.8	38.6	39.2	35.3	36.7	36.9	34.3
280	0	37.4	38.0	45.7	47.5	34.3	41.1	35.3	37.9
280	1	43.2	41.5	57.9	59.3	38.1	49.5	45.5	46.8
280	2	42.2	40.1	60.8	61.5	38.2	53.8	45.3	47.4
280	3	44.8	43.7	60.7	61.4	42.3	49.7	46.4	45.9
280	4	38.6	37.4	52.4	51.3	40.2	43.5	41.2	40.6
280	5	32.8	32.8	37.4	40.0	34.9	36.0	33.8	34.1
282	0	36.6	35.6	46.1	47.3	34.3	41.0	35.9	39.8
282	1	40.5	40.9	57.7	58.2	37.7	49.5	44.7	46.4
282	2	45.6	43.2	60.2	62.9	38.0	52.6	46.2	48.0
282	3	43.4	43.3	59.6	59.9	40.1	52.9	46.4	44.5
282	4	39.4	37.5	52.0	51.3	40.2	42.9	40.5	42.7
282	5	34.2	33.4	36.8	39.8	33.6	35.7	34.4	32.9
284	0	36.0	35.9	46.0	48.0	33.0	42.1	35.2	39.2
284	1	40.8	42.6	57.3	60.7	37.3	49.3	45.3	47.3
284	2	44.9	41.6	60.4	62.5	40.1	53.2	46.3	49.4
284	3	44.0	41.6	61.6	60.0	41.4	51.6	44.4	44.9
284	4	36.2	37.2	51.4	50.4	39.0	43.0	39.7	42.8
284	5	33.0	34.4	35.4	41.9	33.6	34.8	34.6	34.2
286	0	36.3	34.9	44.4	48.3	34.3	42.0	36.4	40.0
286	1	40.6	40.6	58.6	59.7	39.3	50.5	45.0	46.8
286	2	41.9	42.9	60.0	65.4	38.7	51.8	46.5	47.8
286	3	43.2	44.2	60.3	60.9	41.2	51.5	45.3	45.9

Time (h)	Position	Trt1		Trt2		Trt3		Trt4	
		Rep 1	Rep 2	Rep 1	Rep 2	Rep 1	Rep 2	Rep 1	Rep 2
286	4	39.8	36.6	52.5	49.3	39.9	42.3	39.5	43.0
286	5	35.1	36.4	39.3	41.9	35.7	37.7	34.6	36.0
288	0	37.2	37.3	45.2	49.5	32.9	41.5	38.9	40.7
288	1	39.1	40.5	58.9	58.2	35.9	49.6	46.2	47.6
288	2	43.9	39.7	60.6	63.3	39.8	51.5	45.1	49.8
288	3	45.9	42.0	59.5	58.9	43.2	51.0	45.9	46.1
288	4	37.6	38.1	52.4	54.9	39.7	42.8	40.7	41.8
288	5	35.6	35.5	40.0	41.1	35.5	37.0	37.1	36.0
290	0	36.4	36.8	44.1	47.6	33.4	42.5	38.0	41.3
290	1	40.5	39.2	57.9	59.0	37.8	51.5	44.0	47.8
290	2	43.7	43.3	60.0	62.8	39.5	50.7	46.5	49.3
290	3	42.2	42.9	60.0	63.9	44.1	50.3	44.8	44.7
290	4	39.3	40.6	51.2	52.5	41.3	43.0	40.6	42.8
290	5	34.1	36.5	41.3	43.2	36.6	38.9	34.4	35.9
292	0	35.5	36.8	47.4	48.7	33.1	43.2	37.1	40.7
292	1	40.7	39.0	57.5	59.0	37.2	52.3	47.2	49.5
292	2	39.8	41.5	60.3	59.5	38.6	52.3	45.3	47.0
292	3	43.4	42.1	60.0	58.4	42.5	51.3	46.0	45.4
292	4	40.1	38.0	52.8	50.1	44.0	44.6	39.5	43.0
292	5	35.1	34.9	41.5	44.0	37.2	38.5	34.3	36.0
294	0	35.9	36.7	45.7	47.5	32.9	43.1	37.0	42.2
294	1	38.7	38.5	58.4	63.4	37.1	48.7	46.5	48.2
294	2	40.7	42.6	57.5	64.3	39.5	51.4	46.8	48.2
294	3	42.4	42.3	59.0	60.6	43.5	50.8	44.7	45.4
294	4	39.3	39.2	53.5	52.0	41.1	44.8	39.9	41.8
294	5	37.1	36.8	40.1	42.7	36.0	35.8	35.3	33.7
296	0	34.7	35.2	45.5	47.5	34.7	42.6	40.2	42.5
296	1	40.8	39.8	58.6	60.0	38.2	49.2	48.7	49.1
296	2	42.5	43.3	60.7	66.5	41.0	49.9	47.0	48.9
296	3	40.7	42.0	58.2	61.0	43.9	48.2	44.7	44.9
296	4	42.4	38.5	51.8	49.2	42.1	42.5	40.5	43.0
296	5	31.6	33.5	40.5	39.6	36.8	35.6	33.8	34.7
298	0	35.7	37.3	45.5	48.7	33.3	43.5	38.3	42.6
298	1	39.9	38.0	57.8	60.4	38.7	49.3	47.7	47.6
298	2	40.8	42.0	59.3	64.5	39.6	51.8	46.4	48.2

Time (h)	Position	Trt1		Trt2		Trt3		Trt4	
		Rep 1	Rep 2	Rep 1	Rep 2	Rep 1	Rep 2	Rep 1	Rep 2
298	3	40.8	42.4	60.7	61.2	43.7	49.5	46.3	46.7
298	4	38.6	39.0	51.8	53.9	40.7	42.3	40.4	41.9
298	5	35.6	34.8	38.8	42.4	36.3	37.1	34.2	34.7
300	0	34.7	35.1	46.7	46.2	34.6	42.0	39.3	42.8
300	1	42.6	40.8	56.8	57.3	37.3	49.9	47.8	50.6
300	2	41.5	41.3	56.7	63.3	39.8	50.8	47.3	48.8
300	3	40.8	41.6	60.5	60.2	42.6	51.1	46.4	45.6
300	4	37.4	39.5	50.5	52.2	40.9	43.4	39.6	42.4
300	5	32.6	33.7	40.3	42.9	37.7	36.4	33.7	34.2
302	0	35.8	34.4	45.3	47.1	33.1	42.2	37.4	40.9
302	1	38.4	38.7	57.3	61.0	38.9	49.6	46.7	49.1
302	2	40.3	41.2	60.5	62.8	40.5	51.2	46.5	49.8
302	3	42.4	44.1	62.8	60.8	43.6	48.8	46.7	44.8
302	4	38.7	38.9	50.5	52.6	40.8	42.9	39.3	41.5
302	5	32.9	33.1	38.2	40.7	35.6	35.4	35.0	32.8
304	0	36.4	34.4	45.0	48.8	34.4	43.2	38.0	39.9
304	1	38.7	39.6	58.9	61.1	36.5	49.9	47.7	49.1
304	2	39.7	39.7	58.1	64.6	38.7	52.3	45.9	49.9
304	3	41.8	42.2	58.0	62.6	41.8	47.1	47.8	45.8
304	4	37.5	38.0	49.8	49.4	42.7	43.2	39.3	42.0
304	5	33.4	31.6	37.5	42.4	36.1	34.6	34.0	35.2
306	0	35.6	33.5	44.7	47.6	34.8	43.5	38.4	40.9
306	1	37.3	36.7	55.6	60.0	37.6	49.5	47.4	47.6
306	2	41.9	41.9	61.1	63.8	37.9	51.9	47.9	49.2
306	3	41.0	45.7	58.6	64.8	43.3	49.5	46.2	44.4
306	4	39.8	38.1	51.6	51.1	40.7	42.1	39.1	40.8
306	5	33.6	34.1	40.0	40.4	34.7	35.4	35.5	34.0
308	0	32.7	34.1	44.7	47.0	34.3	43.6	37.2	42.2
308	1	37.3	39.9	52.2	60.7	36.6	50.1	46.2	49.3
308	2	40.1	39.7	59.9	62.7	39.4	50.7	48.0	49.9
308	3	38.7	42.3	58.9	63.5	43.1	49.2	47.2	46.3
308	4	37.1	35.9	52.0	52.0	40.7	41.3	40.2	42.1
308	5	31.1	32.3	38.2	40.6	33.5	34.8	34.0	33.5
310	0	35.2	33.1	45.6	48.2	34.4	41.8	39.0	43.1
310	1	36.8	38.0	56.3	60.6	37.3	48.9	46.8	50.0

Time (h)	Position	Trt1		Trt2		Trt3		Trt4	
		Rep 1	Rep 2	Rep 1	Rep 2	Rep 1	Rep 2	Rep 1	Rep 2
310	2	42.3	40.5	60.8	63.4	39.7	50.2	46.8	50.4
310	3	40.4	44.1	59.1	64.4	41.2	49.6	47.0	46.4
310	4	35.5	37.1	49.0	49.6	40.1	41.8	39.7	41.8
310	5	33.6	33.4	40.0	40.5	33.9	34.4	33.7	33.6
312	0	35.6	33.3	44.6	47.9	33.3	42.7	37.6	41.5
312	1	38.8	35.5	57.5	60.0	37.5	49.2	48.2	48.2
312	2	41.1	40.1	60.0	64.0	40.7	50.7	46.9	49.0
312	3	42.1	40.5	57.9	62.0	40.5	46.6	45.8	44.9
312	4	36.3	38.2	50.1	49.9	39.5	40.5	39.2	40.8
312	5	31.9	31.1	37.2	39.5	34.4	34.7	33.6	33.1
314	0	34.6	34.7	44.2	47.2	34.7	42.0	37.6	41.4
314	1	36.7	39.4	55.4	56.8	38.4	49.9	46.6	49.4
314	2	39.6	40.2	56.2	61.7	39.4	49.7	47.3	49.4
314	3	38.8	40.5	61.0	62.4	41.4	48.6	46.5	46.4
314	4	36.1	37.6	51.3	51.9	39.3	38.8	39.5	40.6
314	5	31.0	33.9	37.7	42.5	34.0	33.3	32.7	32.2
316	0	33.1	31.5	44.2	48.8	33.6	41.6	37.7	41.9
316	1	36.6	37.0	55.3	61.8	38.2	49.3	48.0	48.2
316	2	39.3	39.6	58.8	62.6	37.4	50.6	46.7	49.0
316	3	41.5	42.6	60.2	62.9	43.4	49.8	46.8	46.1
316	4	36.6	36.1	50.4	49.7	38.0	40.2	39.4	40.6
316	5	31.2	31.1	36.2	41.6	33.6	33.7	33.7	33.9
318	0	34.4	34.5	43.1	49.5	34.0	42.8	38.0	40.2
318	1	37.5	38.9	51.4	60.9	37.5	49.7	47.5	49.0
318	2	38.6	40.4	57.5	63.6	38.4	50.7	48.6	49.1
318	3	40.9	38.9	55.9	62.5	42.2	48.7	47.2	46.0
318	4	38.1	37.9	48.7	49.8	38.6	39.2	39.3	41.1
318	5	30.7	31.6	37.8	40.9	33.5	34.1	34.7	34.0
320	0	33.3	31.7	43.0	47.7	32.3	40.8	37.2	40.9
320	1	38.6	36.8	54.8	58.3	39.3	48.2	46.2	47.9
320	2	39.3	39.0	61.2	64.4	39.6	50.3	47.6	49.1
320	3	38.9	42.7	57.9	62.7	42.3	47.9	47.2	45.4
320	4	37.6	35.9	49.4	50.8	39.9	40.8	40.6	42.0
320	5	32.5	32.5	37.4	40.0	34.1	32.5	33.0	33.8
322	0	32.8	34.7	42.7	46.5	33.8	40.9	37.2	41.2

Time (h)	Position	Trt1		Trt2		Trt3		Trt4	
		Rep 1	Rep 2	Rep 1	Rep 2	Rep 1	Rep 2	Rep 1	Rep 2
322	1	36.1	34.9	55.0	61.3	37.1	48.3	46.3	48.7
322	2	39.1	37.7	60.1	62.9	38.7	50.0	47.9	49.9
322	3	37.5	41.1	57.1	61.8	40.5	45.6	45.7	45.7
322	4	36.0	35.5	51.8	50.0	39.3	40.1	40.4	39.4
322	5	30.7	31.4	35.3	39.2	33.2	32.4	33.4	32.1
324	0	33.3	31.5	43.0	45.4	33.7	41.0	37.2	40.9
324	1	39.6	38.0	54.9	60.1	37.1	51.1	47.2	47.3
324	2	39.6	36.9	60.5	64.3	38.9	48.1	48.0	49.2
324	3	39.2	41.8	59.2	62.3	38.5	46.9	47.1	45.1
324	4	37.3	36.5	47.4	51.4	38.1	38.8	40.3	40.9
324	5	29.1	30.5	36.8	37.7	32.2	32.4	32.0	32.9
326	0	33.9	33.4	45.1	46.0	32.5	40.5	38.0	39.2
326	1	38.0	35.2	53.7	59.1	37.5	48.0	46.1	48.6
326	2	38.6	40.3	58.9	63.0	39.0	48.9	47.5	48.2
326	3	38.7	38.1	57.6	63.0	39.5	46.5	46.7	44.1
326	4	34.6	37.1	49.7	52.6	36.9	37.9	38.4	39.1
326	5	29.3	32.3	36.7	40.2	32.5	33.0	31.9	32.6
328	0	31.5	32.6	43.6	44.5	32.0	40.1	37.8	40.1
328	1	37.7	35.5	56.1	59.8	36.4	48.6	47.3	47.4
328	2	40.9	37.8	58.2	61.6	39.2	48.6	47.2	48.8
328	3	38.1	38.4	58.5	61.3	41.8	45.6	44.4	46.0
328	4	37.0	37.8	48.9	46.9	38.5	38.1	39.6	41.2
328	5	29.6	28.4	34.8	39.8	32.0	32.4	32.5	34.0
330	0	33.6	30.7	42.3	45.6	30.8	41.7	37.7	40.9
330	1	38.0	35.0	56.6	58.0	37.0	47.2	47.8	47.2
330	2	38.7	37.4	57.3	64.9	37.7	49.4	48.5	49.6
330	3	37.9	40.4	55.9	61.2	41.1	45.6	46.3	44.5
330	4	35.5	35.7	49.0	49.0	38.3	38.6	39.5	40.2
330	5	30.3	30.5	36.3	40.7	33.0	32.2	32.5	33.1
332	0	32.5	32.0	45.2	47.5	33.0	41.3	36.9	39.7
332	1	38.1	36.0	56.6	61.7	36.8	47.5	47.1	47.3
332	2	37.8	36.4	59.6	63.5	37.6	47.4	47.7	49.6
332	3	38.7	40.4	59.2	61.4	40.3	44.5	45.6	44.2
332	4	33.4	36.0	49.4	50.2	37.6	36.5	39.5	41.0
332	5	30.4	31.1	35.7	39.1	31.3	31.8	31.8	32.7

Time (h)	Position	Trt1		Trt2		Trt3		Trt4	
		Rep 1	Rep 2	Rep 1	Rep 2	Rep 1	Rep 2	Rep 1	Rep 2
334	0	32.3	31.6	42.9	45.9	32.9	39.6	36.3	37.9
334	1	36.3	35.3	55.6	58.5	38.0	47.6	46.9	46.8
334	2	39.5	37.7	57.9	64.0	37.9	47.6	45.2	48.0
334	3	37.3	38.3	56.9	59.5	40.5	44.3	46.7	44.4
334	4	36.6	35.3	45.2	52.1	36.3	36.6	39.2	39.0
334	5	29.8	31.2	36.7	37.9	31.1	31.7	31.8	31.9
336	0	32.1	31.7	43.6	45.4	32.6	40.0	37.8	39.6
336	1	38.4	35.4	55.0	60.8	36.3	47.6	45.8	47.1
336	2	39.4	38.0	56.4	60.9	37.6	47.2	48.8	49.3
336	3	36.9	38.6	57.0	58.8	41.1	44.3	46.8	44.9
336	4	33.7	34.4	50.0	48.4	36.3	36.2	39.2	39.5
336	5	28.7	29.3	36.1	39.8	31.0	31.3	32.4	32.7
338	0	31.3	30.2	43.5	46.4	31.9	38.8	37.3	38.4
338	1	37.8	36.1	56.6	57.2	36.5	47.3	47.0	46.4
338	2	39.3	35.8	58.4	64.2	36.8	47.5	46.8	48.2
338	3	39.2	37.9	56.8	60.4	40.0	44.8	48.3	44.9
338	4	34.9	35.3	49.5	46.5	38.1	34.9	39.7	38.8
338	5	30.1	28.5	35.5	38.1	31.2	31.8	32.7	31.8
340	0	32.3	30.0	41.0	45.5	30.1	40.3	36.7	38.1
340	1	36.5	36.9	54.9	60.8	36.5	47.0	46.6	46.3
340	2	37.7	37.1	57.0	62.8	37.0	48.9	47.3	48.5
340	3	39.3	39.2	57.3	62.0	39.9	43.7	47.5	43.6
340	4	32.5	33.6	45.8	48.9	36.8	37.1	40.9	39.3
340	5	28.2	30.5	36.0	36.6	30.6	30.3	32.9	31.5
342	0	31.8	33.1	43.6	43.6	32.7	38.4	35.5	37.3
342	1	35.7	37.4	52.6	61.4	36.5	46.5	46.1	46.9
342	2	36.7	35.8	55.6	59.5	37.6	48.2	47.6	49.3
342	3	37.9	38.4	55.3	61.2	39.6	43.8	47.9	43.1
342	4	32.3	34.1	47.1	48.7	36.9	36.3	39.3	39.0
342	5	28.9	28.9	34.1	38.5	31.6	30.9	31.5	31.4
344	0	30.3	32.5	43.3	45.7	31.2	38.8	36.7	36.4
344	1	38.0	35.8	55.2	58.1	35.2	45.6	46.6	46.3
344	2	37.5	35.5	55.2	60.6	37.1	45.8	46.3	49.1
344	3	36.5	37.9	57.0	58.8	39.8	42.5	44.4	45.4
344	4	35.0	34.7	46.5	49.1	37.3	35.8	39.3	39.1

Time (h)	Position	Trt1		Trt2		Trt3		Trt4	
		Rep 1	Rep 2	Rep 1	Rep 2	Rep 1	Rep 2	Rep 1	Rep 2
344	5	30.1	27.2	36.7	37.5	31.6	29.8	32.8	30.6
350	0	32.0	29.9	41.6	44.8	32.7	40.6	35.7	36.8
350	1	34.3	33.3	54.5	56.0	37.0	45.2	44.5	44.4
350	2	37.5	34.8	55.6	61.3	37.5	45.6	46.4	47.4
350	3	39.2	37.2	54.2	57.6	39.7	42.8	45.6	43.7
350	4	32.3	34.3	46.4	47.1	36.5	35.1	38.7	38.8
350	5	29.1	29.0	35.1	38.2	30.5	30.5	31.4	31.7
356	0	31.8	30.4	42.4	47.0	31.6	39.3	35.8	36.6
356	1	30.0	32.4	51.8	57.0	35.3	45.3	46.0	43.7
356	2	38.1	37.0	57.7	61.6	36.1	43.5	46.5	46.7
356	3	35.6	37.1	56.3	57.4	40.2	40.8	45.8	42.5
356	4	33.6	33.4	46.5	45.0	35.5	35.2	39.5	38.9
356	5	27.5	28.4	35.2	36.2	30.9	30.6	32.0	31.4
362	0	29.6	29.7	41.4	43.2	31.4	37.9	34.6	35.0
362	1	33.4	31.5	51.6	59.8	34.1	44.7	46.1	42.0
362	2	36.9	33.8	55.9	63.3	37.3	43.7	45.3	44.7
362	3	34.9	36.4	52.5	56.0	39.2	40.6	45.4	43.4
362	4	30.9	32.2	45.0	47.7	36.5	34.3	39.2	39.3
362	5	27.4	27.9	33.6	36.3	30.0	29.7	31.9	30.8
368	0	32.6	29.6	42.1	44.9	30.1	38.4	34.1	33.7
368	1	33.3	32.7	50.1	56.5	33.8	43.6	43.2	41.7
368	2	34.4	35.9	55.9	60.5	35.7	43.9	46.9	44.7
368	3	35.2	37.6	55.4	59.9	39.2	40.1	45.5	42.6
368	4	30.6	32.7	43.5	45.9	35.8	33.0	38.6	38.1
368	5	28.9	27.3	32.7	39.9	30.1	29.7	31.8	30.8